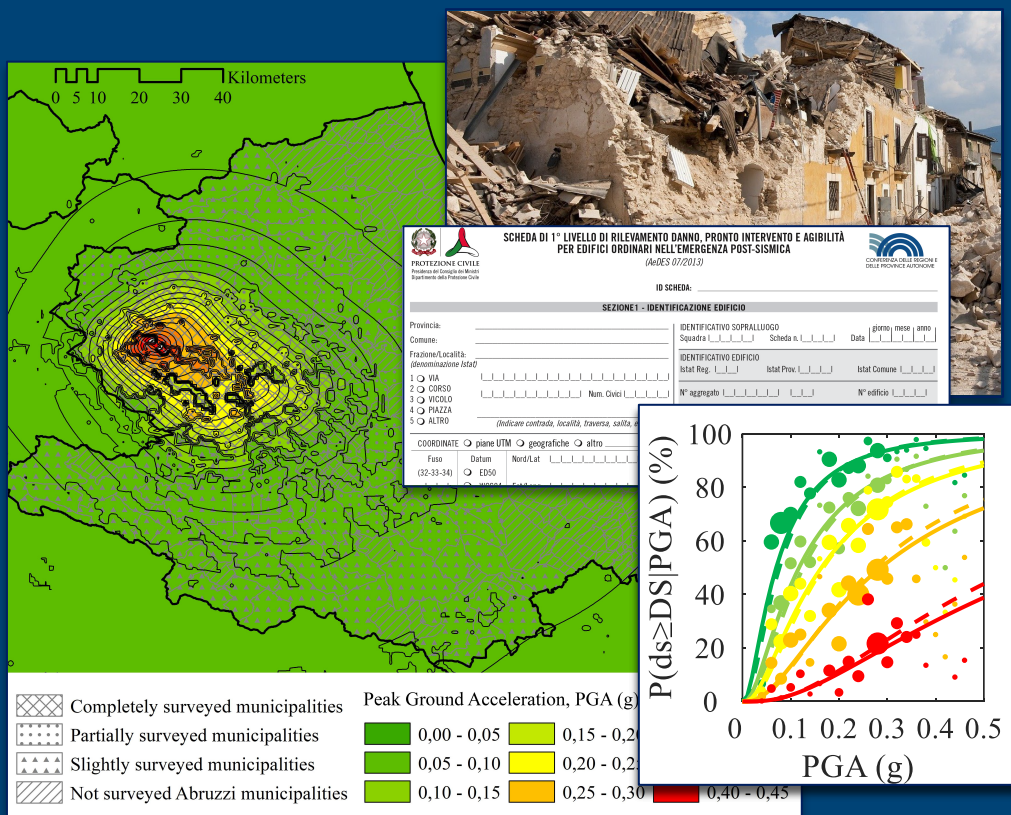




SEISMIC VULNERABILITY OF MASONRY BUILDINGS DAMAGED AFTER L'AQUILA 2009 EARTHQUAKE ACCOUNTING FOR THE EFFECT OF CONSTRUCTION AGE

XXXIV Ph.D. Programme in Structural, Geotechnical Engineering and Seismic Risk



2022



UNIVERSITÀ DEGLI STUDI DI NAPOLI
FEDERICO II Scuola Politecnica e
delle Scienze di Base



Università degli Studi di Napoli Federico II

Dottorato di Ricerca in
Ingegneria Strutturale, Geotecnica e Rischio Sismico

THESIS FOR THE DEGREE OF DOCTOR OF PHILOSOPHY

**Seismic vulnerability of masonry buildings
damaged after L'Aquila 2009 earthquake
accounting for the effect of construction age**

by
SANTA ANNA SCALA

Advisor: Prof. Ing. Gerardo M. Verderame

Co-advisor: Prof. Ing. Carlo Del Gaudio



SCUOLA POLITECNICA E DELLE SCIENZE DI BASE
DIPARTIMENTO DI STRUTTURE PER L'INGEGNERIA E L'ARCHITETTURA

*Sempre devi avere in mente Itaca -
raggiungerla sia il pensiero costante.
Soprattutto, non affrettare il viaggio;
fa che duri a lungo, per anni, e che da vecchio
metta piede sull'isola, tu, ricco
dei tesori accumulati per strada
senza aspettarti ricchezze da Itaca.
Itaca ti ha dato il bel viaggio,
senza di lei mai ti saresti messo
sulla strada: che cos'altro ti aspetti?*

Costantino Kavafis, *Itaca*. 1911

Seismic vulnerability of masonry buildings damaged after L'Aquila 2009 earthquake accounting for the effect of construction age

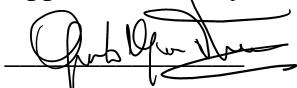
Ph.D. Thesis presented
for the fulfillment of the Degree of Doctor of Philosophy
in Ingegneria Strutturale, Geotecnica e Rischio Sismico

by
SANTA ANNA SCALA

March 2022



Approved as to style and content by

A handwritten signature in black ink, likely belonging to Prof. Gerardo Mario Verderame.

Prof. Gerardo Mario Verderame, Advisor

A handwritten signature in black ink, likely belonging to Prof. Carlo Del Gaudio.

Prof. Carlo Del Gaudio, Co-advisor

Università degli Studi di Napoli Federico II

Ph.D. Program in Ingegneria Strutturale, Geotecnica e Rischio Sismico
XXXIV cycle - Chairman: Prof. Iunio Iervolino



www.dist.unina.it/dottorati-di-ricerca/dottorati

CANDIDATE'S DECLARATION

I hereby declare that this thesis submitted to obtain the academic degree of Philosophiæ Doctor (Ph.D.) in Ingegneria Strutturale, Geotecnica e Rischio Sismico is my own unaided work, that I have not used other than the sources indicated, and that all direct and indirect sources are acknowledged as references. Parts of this dissertation have been published in international journals and/or conference articles (see list of the author's publications at the end of the thesis).

Napoli, March 9, 2022

Sante Anna Sede

ABSTRACT

The aim of this study is the analysis of seismic vulnerability of residential masonry buildings, with particular emphasis to the evolution of seismic behaviour over the years. To this purpose, first an in-dept analysis of the Italian building's codes enacted over the years have been done, focusing on the evolution of seismic classification and normative contents related to masonry buildings. Then, an empirical analysis has been performed, based on data collected shortly afterwards the L'Aquila 2009 earthquake and recently released by the Italian Department of Civil Protection (DPC) through the Da.D.O. (*Database di Danno Osservato, Database of Observed Damage*) platform (Dolce et al., 2019).

The building taxonomy has been defined reflecting the need to consider all the parameters available from post-earthquake inspections and the obtainment of reliable and homogeneous sample. A time-consuming data processing has been performed to obtain a generalized version of the original database, which has been integrated with census data to avoid bias in vulnerability and fragility analysis. Then, damage analysis has been done considering 5+1 damage grades defined for the whole building based on the conversion of damage for vertical

structures in sight of the classification of European Macroseismic Scale. The analysis of mean damage values reveals the general trends as a function of the main influential parameters, i.e. construction age, structural types, and presence of retrofit intervention.

Such vulnerability trends have been further investigated, introducing an intensity measure for the ground motion characterization. Thus, vulnerability curves have been derived assuming a lognormal statistical model and peak ground acceleration as intensity measure, through a minimization procedure of the distance between predicted and observed mean damage. So-obtained curves provide for each building class belonging to the defined taxonomy the relation between seismic intensity and mean damage, leading to the definition of a hierarchy in terms of damage attitude between classes.

Moreover, two regression models (*nonlinear weighted least squared estimation* and *maximum likelihood technique*) have been adopted to determine the parameters of lognormal fragility curves, measuring their goodness of fit with the observed damage probability matrices (DPMs). Starting from the *unconditioned* model, further regression constraints (i.e., the respect of the hierarchy of median PGA with the building class and a common value for logarithmic standard deviation) have been introduced, thus leading to the definition of the *conditioned* model. The benefits in the introduction of further regression constraints are counterposed to the effectiveness of conditioned curves to model observational data through the comparison of the goodness of fit between the unconditioned and conditioned models.

Keywords: Fragility curves, residential masonry buildings; AeDES form, post-earthquake damage data; construction age.

SINTESI

Lo scopo del presente studio è la valutazione della vulnerabilità sismica di edifici residenziali in muratura, con particolare attenzione all'evoluzione del comportamento sismico di tali edifici al variare dell'epoca di costruzione.

A tale scopo, è stata condotta innanzitutto un'attenta analisi dei Codici sismici italiani emanati nel secolo scorso, focalizzando l'attenzione sull'evoluzione della classificazione sismica italiana e sull'evoluzione delle prescrizioni di norma relative agli edifici in muratura.

In secondo luogo, è stata condotta un'analisi empirica partendo dai dati di danno raccolti a valle del terremoto de L'Aquila del 2009 e resi disponibili dal Dipartimento della Protezione Civile tramite la piattaforma Da.D.O. (Dolce et al., 2019). La tassonomia introdotta nasce come compromesso tra l'esigenza di considerare un elevato numero di parametri descrittivi dell'edificio e il bisogno di disporre di sample omogeni e ben popolati. Al fine di garantire la completezza del dato esaminato, si è fissata una soglia minima a livello comunale, scartando dall'analisi tutti gli edifici siti nei comuni sottosoglia ed integrando successivamente quelli ispezionati in maniera molto limitata con i dati derivanti dal censimento ISTAT 2011.

L'analisi del danno è stata condotta traducendo il danno alle strutture verticali in 5+1 livelli di danno dell'intero edificio, consistenti con la Scala Macrosismica Europea. Una prima valutazione dell'attitudine al danno è stata condotta tramite la valutazione del danno medio, ottenendo trend di vulnerabilità al variare dei principali parametri descrittivi dell'edificio in muratura (come la tessitura muraria, il tipo di struttura orizzontale, la presenza di interventi di retrofit, l'epoca di costruzione). Tali tendenze sono state ulteriormente approfondite, introducendo una misura di intensità sismica per la caratterizzazione dello scuotimento al suolo. La relazione tra danno medio e PGA, assunta quale misura di intensità, è stata ottenuta minimizzando la somma dei quadrati delle distanze tra punti osservati e punti predetti da una distribuzione lognormale, portando alla definizione di una gerarchia in termini di attitudine al danno tra le classi considerate.

Le curve di fragilità sono state invece derivate adottando due modelli di regressione (minimizzazione dei quadrati e massima verosimiglianza), quantificandone la bontà predittiva mediante il confronto con le matrici di probabilità di danno osservate. Inoltre, partendo dal modello *incondizionato*, sono stati introdotti ulteriori vincoli di regressione (in particolare, il rispetto della gerarchia ricavata dall'analisi di vulnerabilità in termini di PGA mediana e una deviazione standard logaritmica costante), giungendo alla definizione di modelli *condizionati*, la cui bontà di fitting è stata valutata nuovamente mediante il confronto tra DPM predette ed osservate.

Parole chiave: curve di fragilità, edifici residenziali in muratura, scheda AeDES, dato empirico, epoca di costruzione.

TABLE OF CONTENTS

ABSTRACT	I
SINTESI IN LINGUA ITALIANA	III
TABLE OF CONTENTS	V
ACKNOWLEDGEMENTS	IX
LIST OF FIGURES	XI
LIST OF TABLES	XXI
 CHAPTER 1. INTRODUCTION.....	 1
1.1 MOTIVATIONS.....	1
1.2 AIM AND SCOPE.....	5
1.3 ORGANIZATION.....	7
1.4 REFERENCES	9
 CHAPTER 2. STATE OF ART	 15
2.1 INTRODUCTION	15
2.2 BUILDING'S TAXONOMY	19
2.3 DATA COMPLETENESS	26

2.4	EMPIRICAL METHODS	30
2.4.1	<i>Damage Probability Matrix (DPM)</i>	32
2.4.2	<i>Vulnerability curves</i>	37
2.4.3	<i>Fragility curves</i>	43
2.5	REFERENCES	49
 CHAPTER 3. EVOLUTION OF THE ITALIAN SEISMIC		
CLASSIFICATION AND SEISMIC CODES.....		63
3.1	INTRODUCTION	63
3.2	ITALIAN EARTHQUAKES IN THE LAST CENTURY.....	64
3.2.1	<i>Strong earthquakes occurred between 1900 and 1940</i>	65
3.2.2	<i>Strong earthquakes occurred between 1940 and 1980</i>	70
3.2.3	<i>Strong earthquakes occurred between 1980 and 2020</i>	72
3.3	EVOLUTION OF THE ITALIAN SEISMIC CLASSIFICATION	75
3.4	EVOLUTION OF CODE PRESCRIPTIONS ABOUT MASONRY BUILDINGS	86
3.4.1	<i>Code prescriptions related to seismic loads</i>	87
3.4.2	<i>Code prescriptions related to masonry buildings</i>	90
3.4.3	<i>Code prescriptions related to retrofit intervention on masonry buildings</i>	93
3.5	REFERENCES	95
 CHAPTER 4. DATABASE OF OBSERVED DAMAGE OF PAST		
ITALIAN EARTHQUAKES		101
4.1	INTRODUCTION	101
4.2	DA.D.O. PLATFORM: MOTIVATIONS, PURPOSES AND CONTENTS.....	102
4.3	POST-EARTHQUAKE SURVEYS: EVOLUTION OF THE SURVEY FORM.....	106
4.4	CRITICAL REVIEW OF DA.D.O. POST-EARTHQUAKE DATA.....	115
4.5	REFERENCES	122
 CHAPTER 5. CRITICAL REVIEW OF DATA COLLECTED		
AFTER L'AQUILA 2009 EARTHQUAKE		125
5.1	INTRODUCTION	125
5.2	POST-EARTHQUAKE SURVEY AND COLLECTED DATA	126
5.2.1	<i>Completely inspected municipalities</i>	130
5.2.2	<i>Partially inspected municipalities</i>	145
5.2.3	<i>Slightly inspected municipalities</i>	146
5.3	BUILDING'S TAXONOMY	150

Table of contents

5.3.1	<i>Building's features according to AeDES form</i>	151
5.3.2	<i>Proposed building's taxonomy</i>	160
5.4	REFERENCES	164

CHAPTER 6. DAMAGE ANALYSIS AND VULNERABILITY

CURVES169

6.1	INTRODUCTION	169
6.2	ANALYSIS OF DAMAGE DATA PROVIDED BY AeDES FORM	170
6.3	DAMAGE DISTRIBUTION AND MEAN DAMAGE	174
6.3.1	<i>Mean damage for as-built classes</i>	178
6.3.2	<i>Mean damage for retrofitted classes</i>	181
6.4	VULNERABILITY CURVES.....	185
6.4.1	<i>Intensity measure</i>	187
6.4.2	<i>Functional form and fitting procedure</i>	189
6.4.3	<i>Vulnerability curves for as-built classes</i>	191
6.4.4	<i>Vulnerability curves for retrofitted classes</i>	197
6.4.5	<i>Vulnerability trends in terms of median PGA: common β case</i>	203
6.4.6	<i>Influence of seismic input: ShakeMap of Michelini et al., 2008</i>	206
6.5	REFERENCES	214

CHAPTER 7. FRAGILITY CURVES219

7.1	INTRODUCTION	219
7.2	FRAGILITY CURVES ACCORDING OBSERVED DPM	220
7.2.1	<i>LSE regression procedure</i>	223
7.2.2	<i>MLE regression procedure</i>	224
7.3	FRAGILITY CURVES FOR AS-BUILT CLASSES	226
7.3.1	<i>Comparison between observed and predicted DPMs</i>	233
7.3.2	<i>Critical review of obtained fragility trends</i>	236
7.3.3	<i>Conditioned MLE regression model</i>	239
7.3.4	<i>Conditioned(β) MLE regression model</i>	249
7.3.5	<i>Mean error evaluation</i>	254
7.3.6	<i>Influence of damage conversion rules</i>	257
7.4	FRAGILITY CURVES FOR RETROFITTED CLASSES.....	267
7.4.1	<i>Fragility curves according to Unconditioned, Conditioned and Conditioned(β) models</i>	269
7.4.2	<i>Mean error evaluation</i>	273
7.4.3	<i>Analysis on effectiveness of retrofit intervention</i>	275

Table of contents

7.5	REFERENCES	279
CONCLUSIONS		283
AUTHOR'S PUBLICATIONS		294
APPENDIX A		296

ACKNOWLEDGEMENTS

I would like to thank my scientific guide Professor Gerardo Mario Verderame for the constant support and for the opportunity given to me to be part of his brilliant research group and of the Department of Structures for Engineering and Architecture of the University of Naples Federico II. No words can explain how grateful and proud I am.

Sincere gratitude to the Professor Carlo Del Gaudio for being a constant reference in these years and for sharing with me his experience and knowledge, essential for the success of this study.

Special thanks also to all the other research team members; in these years, they provided, in different ways, a great support to my cultural and personal growth. Among them, I would like to thank the Professor Maria Teresa De Risi; her dedication to scientific research is a constant source of inspiration for me.

I am grateful to the reviewers of my thesis. Their suggestions and comments were very helpful to improve the present study.

Thanks to Antonio and to my family, for their understanding and support, without which I would not have reached my objective today.

Naples, March 2022

Santa Anna Scala

LIST OF FIGURES

Figure 1. Main strong earthquakes ($I_{MCS} \geq IV$) occurred in Italy in the twentieth century (Rovida et al., 2021).....	65
Figure 2. <i>Messina Earthquake, 28 December 1908</i> . Description: Street in Messina, Sicily, showing damage caused by the earthquake. Photographed in January 1909. Collection of Lieutenant Commander Richard Wainwright, 1928. U.S. Naval History and Heritage Command Photograph. (Catalog #: NH 1447)	66
Figure 3. Avezzano 1915, Palazzo Torlonia after the earthquake. Photo retrieved from http://marsica1915.rm.ingv.it/it/79/il-terremoto-del-1915	67
Figure 4. Italien, Erdbeben-Katastrophe. Description: houses collapsed due to the catastrophic earthquake of Vulture, 23 July 1930. This image was provided to Wikimedia Commons by the German Federal Archive (Deutsches Bundesarchiv). ...	69
Figure 5. View of the destroyed city of Conza della Campania after the earthquake of November 1980. Photographed by Giuseppe Maria Galasso.	71
Figure 6. Global collapse of the L'Aquila's Prefecture.	73
Figure 7. Seismically classified municipalities until 1915.....	76
Figure 8. Evolution of the Italian seismic classification between R.D. 29/04/1915 n.573 and R.D. 13/03/1927 n.431 with the indication of the stronger earthquakes occurred until the enactment of the two Codes.	77

Figure 9. Evolution of the Italian seismic classification between R.D. 13/03/1927 n.431 and R.D. 25/03/1935 n.640 with the indication of the stronger earthquakes occurred until the enactment of the two Codes.	78
Figure 10. Evolution of the Italian seismic classification between R.D. 25/03/1935 n.640 and R.D. 22/11/1937 n.2105 with the indication of the stronger earthquakes occurred until the enactment of the two Codes.	79
Figure 11. Evolution of the Italian seismic classification between R.D. 22/11/1937 n.2105 and L. 25/11/1962 n.1684 with the indication of the stronger earthquakes occurred until the enactment of the two Codes.	80
Figure 12 Evolution of the Italian seismic classification between L. 25/11/1962 n.1684 and D.M. 10/03/1969 with the indication of the stronger earthquakes occurred until the enactment of the two Codes.	81
Figure 13. (a) Cover of the Publication n.277 (ESA Editor), containing the preliminary maps of shakeability (CNR, 1979). (b) Map of seismic hazard in Italy (Petrini, 1981).	82
Figure 14. Italian seismic classification at the end of 1984.	84
Figure 15. Evolution of the Italian seismic classification between 1984 and 2003 (according to O.P.C.M. 20/03/2003 n.3274).	85
Figure 16. Percentage distribution of Da.D.O. data among the nine seismic events.	105
Figure 17. Building's description according to (a) 1976 Friuli, (b) 1980 Irpinia, and (c) 1984 Abruzzi form.	108
Figure 18. Building's description according to AeDES 09/1997 form.	109
Figure 19. Building's description according to AeDES 06/2008 form.	110
Figure 20. Damage description according to (a) 1976 Friuli, (b) 1980 Irpinia, and (c) 1984 Abruzzi form.	113
Figure 21. Damage description according to (a) AeDES 09/1997, and (b) AeDES 06/2008 form.	114

Figure 22. Structural typology distribution for residential buildings of Da.D.O. platform.	116
Figure 23. Completeness Ratio, C.R., for all municipalities of each considered database.	119
Figure 24. Survey level of detail (as a function of the completeness ratio, CR) for all Abruzzi municipalities.	129
Figure 25. Period of construction versus (a) number of storeys, (b) horizontal structures and (c) masonry layout distributions for residential masonry buildings....	130
Figure 26. Abaci of masonry layouts (first level of knowledge according to AeDES manual). (a) Rounded stones or pebbles; (b) raw stones or rubble; (c) plate-shaped elements; (d) pseudo-regular elements; (e) natural hewn stones; (f) artificial stones.	132
Figure 27. Abaci of flat horizontal structures (retrieved from AeDES Manual). Wooden slab with (a) brick elements (“mezzane”); (b) single layer of wood planks; (d) double layers of wood planks; iron beams with (c) shallow arch vaults; (e) hollow flat blocks; (f) prefabricated slab (SAP type); (g) R.C. slab; R.C. joists with hollow clay brick, either (i) cast-in-place or (h) prefabricated	134
Figure 28. Period of construction versus (a) number of storeys and (b) horizontal structures percentage distributions for BQ residential masonry building.	136
Figure 29. Period of construction versus (a) number of storeys and (b) horizontal structures percentage distributions for GQ residential masonry.	136
Figure 30. Seismic classification of Abruzzi municipalities, detecting the completely surveyed municipalities.	139
Figure 31. Percentage of buildings belonging to the two considered design classes for all 36 completely inspected municipalities.	139
Figure 32. Presence/absence of retrofit intervention (a); masonry quality for not-retrofitted buildings (b); horizontal structure for as-built GQ (c) and BQ (d) buildings, given the construction age.	141

Figure 33. Period of retrofit intervention for buildings built before 1919 (a), between 1919 and 1945 (b), and between 1946 and 1961 (c).	142
Figure 34. Masonry quality for retrofitted buildings constructed before 1919 (a), between 1919 and 1946 (b) and before 1946 and 1961 (c); horizontal structures for GQ and BQ retrofitted buildings built in <1919 (d-g), 1919-1946 (e-h) and 1946-1961 (f-i) time periods.	144
Figure 35. Seismic classification of Abruzzi municipalities, detecting the slightly surveyed and the not inspected municipalities.	146
Figure 36. (a) Number of buildings (i.e., masonry, R.C. and other material) and (b) distribution of construction age for masonry ones, provided by ISTAT 2011 for all slightly surveyed and not inspected Abruzzi municipalities.	147
Figure 37. (a) Damaged and (b) undamaged DBs, varying the construction age.	149
Figure 38. Distributions of number of storeys, given the horizontal structural type and the construction age (<i>damaged</i> database) for considered as-built GQ typologies.	155
Figure 39. Distributions of number of storeys, given the horizontal structural type and the construction age (<i>damaged</i> database) for considered as-built BQ typologies.	156
Figure 40. Distributions of number of storeys, given the horizontal structural type and the retrofit age (<i>damaged</i> database) for considered retrofitted BQ typologies....	157
Figure 41. Distributions of presence/absence of tie rods/beams, given the horizontal structural type and the construction age (<i>damaged</i> database) for as-built GQ buildings.	158
Figure 42. Distributions of presence/absence of tie rods/beams, given the horizontal structural type and the construction age (<i>damaged</i> database) for as-built BQ buildings.	159

List of figures

Figure 43. Distributions of presence/absence of tie rods/beams, given the horizontal structural type and the retrofit age (<i>damaged</i> database) for retrofitted BQ typologies.	160
Figure 44. Proposed building's taxonomy based on presence of retrofit interventions, masonry's quality, construction age and horizontal structural type.	161
Figure 45. Proposed building's taxonomy for retrofitted buildings.	162
Figure 46. Number of buildings for each considered class, deriving from damaged and undamaged DBs, for (a) as-built and (b) retrofitted typologies.....	164
Figure 47. Section 4 (damage description) of AeDES 06/2008 form.	171
Figure 48. Maximum damage observed among vertical, horizontal and roof structures, given the building's class for (a) as-built and (b) retrofitted typologies...	172
Figure 49. Presence of pre-existing damage equal or greater than the maximum damage among all structural components, given the building's class for (a) as-built and (b) retrofitted typologies.....	173
Figure 50. Damage distributions, given the building's class for (a) as-built and (b) retrofitted typologies.	177
Figure 51. Number of as-built buildings with GQ and BQ, given the horizontal structural type and the construction age (<i>damaged</i> database).	179
Figure 52. Mean damage for as-built classes	180
Figure 53. Number of retrofitted buildings with GQ and BQ built before 1919, given the horizontal structural type and the retrofit age (<i>damaged</i> database).....	181
Figure 54. Mean damage: influence of structural interventions for masonry buildings constructed before 1919, given the period of retrofit, for each horizontal structural type.	182
Figure 55. Number of retrofitted buildings with GQ and BQ built before 1919 (a), between 1919 and 1945 (b), between 1946 and 1961 (c), given the horizontal structural type (<i>damaged</i> database).....	183

Figure 56. Mean damage: influence of structural interventions for masonry buildings constructed in (<1919), (1919-1945), (1946-1961) periods, given the horizontal structural type for BQ (a) and GQ (b) typologies.	184
Figure 57. ShakeMap in terms of Peak Ground Acceleration (PGA) derived by means of procedure proposed by in Michellini et al. 2020.....	188
Figure 58. Vulnerability curves for as-built masonry buildings built up to 1962-1971 timespan, as a function of construction age and structural types.	192
Figure 59. Vulnerability curves for as-built masonry buildings built starting from 1972-1981 timespan, as a function of construction age and structural types.	193
Figure 60. Vulnerability curves for GQ as-built typologies. Comparison in terms of horizontal structure, given the construction age.....	195
Figure 61. Vulnerability curves for BQ as-built typologies. Comparison in terms of horizontal structure, given the construction age.....	195
Figure 62. Vulnerability curves for as-built typologies. Comparison in terms of construction age (<i>EC</i>), given the structural type.	196
Figure 63. Vulnerability curves for BQ typologies built before 1919. Comparison in terms of presence/absence of retrofit interventions, given the structural type.	198
Figure 64. Vulnerability curves for BQ typologies. Comparison in terms of presence/absence of retrofit interventions, given the structural type.	201
Figure 65. Vulnerability curves for GQ typologies. Comparison in terms of presence/absence of retrofit interventions, given the structural type.	202
Figure 66. Median PGA (a) and mean damage (b) values for as-built classes as a function of construction age and (horizontal + vertical) structural typologies.	204
Figure 67. Median PGA (a) and mean damage (b) values for retrofitted BQ classes built before 1919 as a function of retrofit age and horizontal type.	205
Figure 68. ShakeMap in terms of peak ground acceleration according to the procedure of Michellini et al., 2008.	207

Figure 69. Vulnerability curves for as-built masonry buildings built up to 1962-1971 timespan, as a function of construction age and structural types. ShakeMap of Michelini et al., 2008.	208
Figure 70. Vulnerability curves for as-built masonry buildings built starting from 1972-1981 timespan, as a function of construction age and structural types. ShakeMap of Michelini et al., 2008.	209
Figure 71. Median PGA (a) and mean damage (b) distributions for each horizontal structural type given the construction age, for both GQ and BQ non-retrofitted masonry buildings. ShakeMap of Michelini et al., 2008.	211
Figure 72. PGA distribution according the two considered procedures (Michelini et al., 2008 and Michelini et al., 2020).....	211
Figure 73. Vulnerability curves for BQ typologies built before 1919. Comparison in terms of presence/absence of retrofit interventions, given the structural type. ShakeMap of Michelini et al., 2008.	213
Figure 74. Median PGA values for retrofitted BQ buildings constructed before 1919, according to Michelini et al., 2008 (a) and Michelini et al. 2020 (b) ShakeMap.....	213
Figure 75. From observed damage distribution to probability of exceeding of a given DS for each PGA value (BQ-V-PRE1919 class).	221
Figure 76. Fragility curves for all BQ classes given the construction age and the horizontal structures. Comparison between LSE (solid line) and MLE (dashed line) technique.	227
Figure 77. Fragility curves for GQ classes (built until 1971) given the construction age and the horizontal structures. Comparison between LSE (solid line) and MLE (dashed line) technique.....	228
Figure 78. Fragility curves for GQ classes (built after 1971) given the construction age and the horizontal structures. Comparison between LSE (solid line) and MLE (dashed line) technique.....	229

Figure 79. From fragility curves to corresponding DPMs (BQ-V-PRE1919 class).	233
Figure 80. Comparison between LSE and MLE regression models in terms of error given the DS.	234
Figure 81. Lognormal parameters for as-built classes.	237
Figure 82. Lognormal parameters for as-built BQ classes, according to <i>unconditioned</i> and <i>conditioned</i> models.	240
Figure 83. Lognormal parameters for as-built GQ classes, according to <i>unconditioned</i> and <i>conditioned</i> models.	241
Figure 84. Comparison between fragility curves of BQ classes, given the DS and the construction age, as a function of horizontal structure.	245
Figure 85. Comparison between fragility curves of BQ classes, given the DS and the horizontal structure, as a function of construction age.	246
Figure 86. Comparison between fragility curves of GQ classes, given the DS and the construction age, as a function of horizontal structure.	247
Figure 87. Comparison between fragility curves of GQ classes, given the DS and the horizontal structure, as a function of construction age.	248
Figure 88. Fragility curves for all BQ classes given the construction age and the horizontal structures, according to the three considered models.	250
Figure 89. Fragility curves for GQ classes (built until 1971) given the construction age and the horizontal structures, according to the three considered models.	251
Figure 90. Fragility curves for GQ classes (built after 1971) given the construction age and the horizontal structures, according to the three considered models.	252
Figure 91. Observed (a) DPMs of BQ-V(<1919) class and those predicted by (b) <i>unconditioned</i> , (c) <i>conditioned</i> , and (d) <i>conditioned</i> (β) MLE models.	255
Figure 92. Mean error for BQ-V(<1919) class, according to the three considered regression models.	256

Figure 93. EMS'98 scale damage levels (Grünthal, 1998) for masonry buildings.	257
Figure 94. Number of buildings in each damage states according to Rota et al., 2008 and Dolce et al., 2019 conversion rules.	260
Figure 95. Mean damage of as-built classes (a- vaults; b- flexible slabs; c- semi-rigid slabs; d- rigid slabs) according to Rota et al., 2008 and Dolce et al., 2019 conversion rules.	261
Figure 96. Fragility curves for all BQ classes given the construction age and the horizontal structures, according to Rota et al., 2008 and Dolce et al., 2019 conversion rules.	263
Figure 97. Fragility curves for GQ classes (built until 1971) given the construction age and the horizontal structures, according to Rota et al., 2008 and Dolce et al., 2019 conversion rules.	264
Figure 98. Fragility curves for GQ classes (built after 1971) given the construction age and the horizontal structures, according to Rota et al., 2008 and Dolce et al., 2019 conversion rules.	265
Figure 96. Median PGA (a) and mean damage (b) values for retrofitted BQ classes built before 1919 as a function of retrofit age and horizontal type (see Chapter 6 for more details).	267
Figure 97. Number of retrofitted buildings (sited in the municipality where a building-by-building survey has been done after 2009 L'Aquila earthquake) varying the period of retrofit.	268
Figure 98. Fragility curves for BQ retrofitted classes built before 1919, given the retrofit age and the horizontal structures, according to the three considered models.	269
Figure 99. Lognormal parameters for retrofitted BQ classes built before 1919, according to <i>Unconditioned</i> model.	272
Figure 100. Mean error for retrofitted classes, according to the three considered regression models.	274

Figure 101. Median PGA values for each as-built and retrofitted classes, according to <i>Conditioned(β)</i> model.	276
Figure 102. Mean error given the DS (going to DS0 to DS2) for BQ as-built classes varying the period of construction.	298
Figure 103. Mean error given the DS (going to DS3 to DS5) for BQ as-built classes varying the period of construction.	299
Figure 104. Mean error given the DS (going to DS0 to DS2) for GQ as-built classes varying the period of construction.	300
Figure 105. Mean error given the DS (going to DS3 to DS5) for GQ as-built classes varying the period of construction.	301

LIST OF TABLES

Table 1. Main functional forms used in the literature to express the fragility curves.	46
Table 2. Ministerial Decree for the seismic classification at regional scale enacted between 1980 and 1984.	83
Table 3. Range of ground acceleration according to O.P.C.M. 28/04/2006 n.3519.....	86
Table 4. Code prescriptions related to structural-geometric details in masonry buildings between 1909 and 1935.....	92
Table 5. Code prescriptions related to structural-geometric details in masonry buildings between 1937 and 1975.....	93
Table 6. Survey form adopted after each considered seismic event.	106
Table 7. Brief review of parameters needed to the building's description according to the different survey forms.	111
Table 8. Brief review of parameters needed to the structural typology definition according to the different survey forms.....	112
Table 9. Brief review of parameters needed to the damage description according to the different survey forms.	115
Table 10. Structural typologies of buildings reported in Da.D.O. platform for each available database.	115

Table 11. Number of masonry buildings sited in the <i>completely</i> surveyed municipalities for each database of Da.D.O. platform.....	120
Table 12. Number of Abruzzi municipalities as a function of the Completeness Ratio (C.R.).	128
Table 13. Classification of masonry structures based on material features	133
Table 14. Number of as-built masonry buildings belonging to <i>damaged</i> DB for each structural type given the construction age.....	152
Table 15. Number of retrofitted buildings belonging to <i>damaged</i> DB for each construction and retrofit age.	153
Table 16. Number of retrofitted buildings built before 1919 belonging to <i>damaged</i> database.	154
Table 17. Number of retrofitted buildings built between 1919 and 1945 belonging to <i>damaged</i> database.	154
Table 18. Number of retrofitted buildings built between 1946 and 1961 belonging to <i>damaged</i> database.	154
Table 19. Conversion's rule of the damage levels in Damage State consistent with the EMS-98.	175
Table 20. Log-normal parameters for as-built buildings with bad quality (BQ) texture as a function of horizontal structural typology and construction age.	197
Table 21. Log-normal parameters for as-built buildings with good quality (GQ) texture as a function of horizontal structural typology and construction age.	197
Table 22. Lognormal parameters of vulnerability curves for BQ retrofitted masonry buildings built before 1919 as a function of horizontal structural typology and period of retrofit.	200
Table 23. Lognormal parameters of vulnerability curves for retrofitted BQ masonry buildings as a function of horizontal structural typology and period of construction.	203
Table 24. Lognormal parameters of vulnerability curves for retrofitted GQ masonry buildings as a function of horizontal structural typology and period of construction.	203

Table 25. Log-normal parameters for as-built BQ buildings as a function of horizontal structural typology and construction age. ShakeMap of Michelini et al., 2008.....	210
Table 26. Log-normal parameters for as-built GQ buildings with as a function of horizontal structural typology and construction age. ShakeMap of Michelini et al., 2008.....	210
Table 27. Lognormal parameters for BQ retrofitted masonry buildings built before 1919. ShakeMap of Michelini et al., 2008.....	212
Table 28. Lognormal parameters (median and logarithmic standard deviation) for each as-built building class, according to LSE technique.....	231
Table 29. Lognormal parameters (median and logarithmic standard deviation) for each as-built building class, according to MLE technique.....	232
Table 30. Lognormal parameters (median and logarithmic standard deviation) for each as-built BQ building class, according to <i>conditioned</i> MLE approach.....	243
Table 31. Lognormal parameters (median and logarithmic standard deviation) for each as-built GQ building class, according to <i>conditioned</i> MLE approach.....	244
Table 32. Lognormal parameters (median and logarithmic standard deviation) for each as-built building class, according to <i>Conditioned</i> (β) MLE model...	253
Table 33. Damage conversion rules by Rota et al., 2008 and Dolce et al., 2019.....	259
Table 34. Lognormal parameters (median and logarithmic standard deviation) for each as-built building class, according to damage conversion rules of Dolce et al., 2019.....	266
Table 35. Lognormal parameters (median and logarithmic standard deviation) for each retrofitted (BQ built before 1919) building class, according to <i>unconditioned</i> model.....	271
Table 36. Lognormal parameters (median and logarithmic standard deviation) for each retrofitted (BQ built before 1919) building class, according to <i>conditioned</i> model.....	271

Table 37. Lognormal parameters (median and logarithmic standard deviation) for each retrofitted (BQ built before 1919) building class, according to <i>conditioned(β)</i> model.	271
--	-----

Chapter 1.

INTRODUCTION

1.1 MOTIVATIONS

Among natural hazards, earthquakes represent one of the most unpredictable phenomena, able to cause significantly lethal and devastating effects from the economic and social standpoint.

The considerable economic losses due to earthquakes in conjunction with social impact and indirect economic losses have prompted a great interest in performance assessment of existing building's stock to future seismic events. In the last 50 years, seismic-induced fatalities and economic losses have been reached dramatic values. In Italy, an amount of about 100 victims per year has been caused by seismic events, starting from the catastrophic Belice 1968 earthquake (Di Ludovico et al., 2017a). Economic losses related to the emergency management and reconstruction process amount to over 200 billion Euro, about half of which related to the events of the last 15 years (namely, Molise 2002, L'Aquila 2009, Emilia Romagna 2012, Central Italy 2016–2017 earthquakes) (Dolce et al., 2021).

Obviously, the consequences in terms of casualties and in terms of damage to the structures and infrastructures are functions of the degree of urbanization and the demographic level of the affected areas, as well as the quality and type of

housing, which is connected substantially to the presence or absence of seismic codes for constructions.

The recent seismic events have been a unique occasion to collect a huge amount of data about existing building stock, highlighting its general weaknesses. In fact, until the beginning of the 2000s, only 37% of the Italian municipalities had been seismically classified (according to ECS-it tool, Del Gaudio et al., 2015). Only after Molise 2002 earthquake, the entire Italian territory was classified as seismic, making compulsory anywhere the design for seismic loads. Conversely, the Italian building's stock is mainly composed of ancient buildings: suffice to say that about 30% of current masonry buildings has been constructed before 1919 (ISTAT 2011). It means that the greater proportion of the Italian building's stock was designed only for gravity loads, namely without any seismic criteria. Thus, the age of buildings on the one hand and the recent seismic classification on the other have contributed to the high vulnerability of the Italian existing buildings, making it a worthy of study argument. In fact, an in-depth knowledge of the building's features able to affect the damage attitude under seismic loads is the base for the consequent actions of prevention and mitigation, or also actions of response in the emergency's phase.

In fact, seismic vulnerability models can be used just after an earthquake to estimate losses in the affected area, but also to manage the decision process involved in policies of disaster prevention, detecting the most prone areas or to guide prioritization of financial interventions by means of cost/benefit studies.

In this view, a very powerful tool to know and characterize in terms of seismic vulnerability the Italian building's portfolio is the great amount of data collected after the earthquake, namely during the post-earthquake surveys. In fact, such data allow identifying the main building's features, and assigning a certain damage attitude due to such features. In Italy, several studies based on empirical data collected after seismic events have been conducted, starting from the catastrophic Irpinia 1980 earthquake. Actually, several approaches (numerical, empirical, hybrid) have been used in the literature to perform the vulnerability assessment of Italian existing buildings. Many of them (for example, Braga et al., 1982; Sabetta et al., 1998; Orsini, 1999; Lagomarsino and Giovinazzi, 2006;

Rota et al., 2008; Zuccaro and Cacace, 2009; Dolce and Goretti, 2015; Del Gaudio et al., 2017; Rosti et al., 2018; Del Gaudio et al., 2019; Del Gaudio et al., 2020; Del Gaudio et al., 2021) are based on the use of post-earthquake data, aiming at vulnerability assessment (typically in terms of damage or usability) for homogeneous building's classes. This need is particularly felt in the Italian building's stock for the numerous features, whose it is characterized, due to the different combination of structural typologies, building types, classes of height, construction age and building's materials. Clearly, some of these features are somehow cross-related (for example, moment resisting frame structures are typically the higher ones) or depend on the regional context (for example, the availability of a certain material can explain their widespread use in certain areas).

Thus, several studies (e.g., Rota et al, 2008; Dolce and Goretti, 2015; Rosti et al., 2020a), grouped the Italian building's stock in a limited number of typological building's classes. In Rota et al, 2008, starting from the data collected after several earthquakes occurred in different Italian zones, 23 building's typologies have been identified based on the vertical structures (masonry, reinforced concrete R.C., steel and mixed structures), the number of stories, the type of design (seismic or not, in case of R.C. buildings) and the horizontal structures (in case of masonry buildings).

Recently, the Italian Department of Civil Protection (DPC, *Dipartimento della Protezione Civile*) issued a framework for National Risk Assessment (ICPD 2018) and its periodically updating (Dolce et al., 2021; Dolce and Prota, 2021; Masi et al., 2021), coherently with EU decision 1313/2013 and to the specific requirement of the “Sendai Framework for Disaster Risk Reduction 2015–2030”. As part of these activities, an expert elicitation approach to comparative fragility analysis (da Porto et al., 2021) was developed, collecting together all the approaches (Borzi et al., 2020; Del Gaudio et al., 2020; Donà et al., 2020; Lagomarsino et al., 2021; Rosti et al., 2020b; Rosti et al., 2020c.; Zuccaro et al., 2020) adopted for the definition of fragility curves for 10 typological classes (for both unreinforced masonry – URM - and Reinforced Concrete – RC - buildings) representative of Italian building environment.

Actually, among all the disastrous earthquakes occurred in Italy in recent time, the one that produced an intense bibliography on seismic vulnerability topic, as a result also of the numerous and detailed post-earthquake survey campaigns carried out by DPC and other institutions, is certainly the seismic event of 6th of April 2009 in the Abruzzi region. Thus, in the studies of D'Ayala and Paganoni, 2011, Del Gaudio et al., 2019, Zucconi et al., 2018, D'Amato et al., 2020, Del Gaudio et al., 2021, empirical approaches are provided, aimed to investigate building behaviour and vulnerability factors after Abruzzi earthquake. Many of these works are focused on masonry buildings, that represent a greater part (about 65%, according to ISTAT 2011 census) of the Abruzzi building's portfolio. In D'Ayala and Paganoni, 2011, two recurrent building typologies (the mansion and the common dwelling) have been analysed, most widespread in the historic city centre of L'Aquila and in the villages of Paganica and Onna, emphasizing the role of the masonry's quality and strengthening interventions. In Del Gaudio et al., 2019 fragility curves for several building's typologies are provided, defined as a function of the quality (good and bad) of masonry walls, the horizontal structure (vaults, flexible-, semi rigid- and rigid slabs) and the presence of tie rods/beams. Nearly the same taxonomy has been proposed in Rosti et al., 2020c, where only two horizontal structural types (flexible and rigid) have been considered. Also, in Zucconi et al., 2018 several vulnerability factors have been considered, i.e. the quality of masonry walls, the number of storeys, the period of construction, the presence of strengthening interventions, analysing their influence on usability trends. The study of Dolce and Goretti, 2015 proposed a taxonomy for masonry buildings based on three building's classes (from A to C), depending on the types of vertical and horizontal structures. The Authors also point out that this primary classification, which is considered true on average, could undergo variations based on several relevant factors (such as the type of roof, the number of floors and the time of construction). A major part of these factors (structural typology, material characteristics, structural details) could be related to the building location and to the period of construction. In fact, a general improvement in construction practices and to the enhancement of building

materials over the years, also related to the subsequent enactment of seismic prescriptions, is already observed in previous study (Del Gaudio et al, 2021).

1.2 AIM AND SCOPE

The purpose of this study is the analysis of vulnerability trends, with particular emphasis on the evolution of the seismic behaviour of masonry buildings over the years due to the improvements in construction practices and to the enhancement of building materials over the years, also related to the subsequent enactment of seismic prescriptions. To this aim, residential masonry buildings damaged after the 2009 L'Aquila earthquake are considered, coming from the online platform Da.D.O. (*Database di Danno Osservato*, Database of Observed Damage) (Dolce et al., 2019) recently released from the Italian Department of Civil Protection.

A time-consuming data processing has been performed to obtain a generalized version of the original database, which has been integrated with census data to avoid bias in vulnerability analysis and ensure data completeness (Rossetto et al., 2013). The adopted building's taxonomy has been defined reflecting the need to consider all the parameters available from post-earthquake inspections, safeguarding the reliability and homogeneity of the sample, nonetheless. General features of all the parameters available from the original database have been thoroughly analysed, a selection of which is used for vulnerability analysis, namely the period of construction and the design type, the presence of structural interventions, the type of horizontal structure, the quality for masonry layout. Then, damage analysis has been done considering 5+1 damage grades defined for the whole building based on the conversion (Rota et al., 2008) of damage to vertical structures in sight of the classification of European Macroseismic Scale (Grunthal, 1998). The analysis of mean damage values reveals the general trends as a function of the main influential parameters, i.e., construction age, (if any) period of retrofit and horizontal structural types, having fixed the vertical structural type and the quality layout. Beyond mean damage analysis, vulnerability assessment has been performed by means of vulnerability curves, that provide a relationship between mean damage and seismic intensity measure.

Such curves were derived assuming a lognormal statistical model and peak ground acceleration as intensity measure, through a minimization procedure of the distance between predicted and observed mean damage. The curves are firstly obtained as a function of period of construction and structural types, highlighting their clear influence on seismic behaviour. Lastly, the effectiveness of retrofit intervention is evaluated comparing the vulnerability curves for strengthened masonry buildings with those not subjected to any retrofit interventions.

As above mentioned, L'Aquila 2009 earthquake is one of the most studied seismic events in Italy and, over the years, an extensive literature (among the others, D'Ayala et al., 2011; Del Gaudio et al., 2017; Del Gaudio et al., 2017; Di Ludovico et al., 2017a; Di Ludovico et al., 2017b; Zucconi et al., 2018; Del Gaudio et al., 2019; Donà et al., 2020; Rosti et al., 2020c; D'Amato et al., 2020; Zuccaro et al., 2020; Borzi et al., 2020; Lagomarsino et al., 2021; Masi et al., 2021) has been produced based on data collected after this earthquake. Many of these studies provide fragility curves to understand the building's response with reference to different levels of damage. In fact, fragility curves describe, for a given building or building's class, the probability of experiencing or exceeding a particular level of damage, given the seismic intensity measure value.

Also in the present Thesis work, fragility curves have been derived to identify fragility trends of a given structural typology as a function of the construction and the retrofit ages. Thus, the main aim of this study is to understand how the seismic fragility of a specific structural class (defined in terms of vertical and horizontal structures) changes varying the construction age and how the fragility of a given retrofitted class (defined in terms of structural typology and construction age) changes, varying the retrofit age.

Moreover, based on the most recent literature, two regression models to develop empirical fragility curves can be identified: the nonlinear *least squared estimation*, i.e. LSE technique (adopted, among the others, by Zuccaro et al., 2020) and the *maximum likelihood estimation*, i.e. MLE technique (adopted, for example, by Rosti et al., 2020c). The parameters of fragility curves have been obtained, in the first case (LSE) minimizing the distance between the observed and the expected cumulative damage distributions. In the second case (MLE),

the same parameters have been derived, maximizing a bi- or multinomial likelihood function. In this work, both the regression models have been adopted deriving lognormal fragility curves, to quantify possible differences and to understand if the obtained fragility trends is influenced by the regression procedure. Secondly, starting from such fitting approaches, further two regression models have been considered, first constraining the median PGA values and then, also the logarithmic standard deviation.

Basically, the constraint on median PGA values allows obtaining the optimum solution of the fitting procedure that also complies the trends derived in terms of mean damage and vulnerability curves. Conversely, constant logarithmic standard deviation (Kircher et al., 2006; FEMA 2012; Karababa and Pomonis 2011; Coburn and Spence 2003; Del Gaudio et al., 2019) has been introduced to overcome the presence of crossing curves.

Lastly, in order to quantify the difference between the three considered models and then the influence of each assumption, observed DPMs (i.e., damage probability matrices) have been compared with those “predicted”, deriving from the obtained fragility curves.

1.3 ORGANIZATION

The present research work focuses on the seismic behaviour of masonry buildings, based on data collected after the Abruzzi 2009 earthquake. The main scope is clarifying the evolution over the time of damage attitude of masonry buildings, by means of the derivation of vulnerability and fragility curves.

The dissertation is organized into seven chapters with the following contents:

- Chapter 2 – *State of Art*: existing vulnerability and fragility functions are summarized, highlighting how the main issues (such as data completeness, the building's taxonomy, sample size) are addressed to avoiding any bias in the assessment.
- Chapter 3 – *Evolution of the Italian seismic classification and seismic codes*: in this Chapter, the focus is on the evolution of the seismic classification of the Italian municipalities, following the occurrence of the strongest earthquakes and analysing the corresponding normative

contents. Thus, a timeline of the major Italian earthquakes of the last century is firstly provided. Then, the seismic classification of the entire national territory adopted after these events is described, detecting the most relevant normative contents about the definition of seismic loads, structural details and retrofit interventions on masonry buildings.

- Chapter 4 – *Database of observed damage of past Italian earthquakes*: in this Chapter, the focus is on the Da.D.O. platform, emphasizing the motivations and purposes of such valuable project, and deeply describing the available data collected after each earthquake. Obviously, the data resulting from different seismic events (namely, adopting different survey forms developed over the years) are not immediately comparable with each other. Moreover, the survey campaign could be conducted following different criteria, reaching different degree of completeness, especially between the areas farthest and nearest to the epicenter. All these issues (together with other ones) could affect the data's use. Therefore, the last paragraph of the present Chapter is dedicated to the description of such issues, with particular emphasis on numerousness and completeness of the available data.
- Chapter 5 – *Critical review of data collected after 2009 L'Aquila earthquake*: in this Chapter, starting from the raw data collected after 2009 L'Aquila event and provided by the Da.D.O. platform (Dolce et al., 2019), the adopted database has been defined based on two main requirements, namely the building taxonomy's detail and the data's completeness.
- Chapter 6 – *Damage analysis and vulnerability curves*: in this Chapter, the damage analysis has been performed, converting damage data collected in the post-earthquake survey by means of the AeDES form (Baggio et al., 2007) in damage states consistent with the European Macroseismic Scale, *EMS98* (Grunthal, 1998). The seismic vulnerability of each building class has been investigated first by means of mean damage (mean of damage distribution), deriving vulnerability trends. Then, the same trends have been analysed in terms of vulnerability curves, introducing as intensity measure the *peak ground acceleration*, PGA,

derived from the ShakeMap by Italian National Institute of Geophysics and Volcanology (INGV) (Michellini et al., 2020). Lastly, a comparison between building's classes in terms of median PGA values has been shown, assuming a common logarithmic standard deviation.

- Chapter 7 – *Fragility curves*: the aim of this Chapter is to derive fragility curves according to the considered very detailed taxonomy, to identify fragility trends of a given structural typology as a function of construction and, if any, retrofit ages. Fragility curves have been derived according to two regression procedures (namely, LSE and MLE) and under different assumptions on output lognormal parameters. Lastly, in order to quantify the difference between models and then the influence of each assumption, the comparison between observed and predicted DPMs has been done, using an error measure.

1.4 REFERENCES

- [1] Baggio, C., Bernardini, A., Colozza, R., Corazza, L., Della Bella, M., Di Pasquale, G., Papa, F., 2007. Field manual for post-earthquake damage and safety assessment and short term countermeasures (AeDES). European Commission—Joint Research Centre—Institute for the Protection and Security of the Citizen, EUR, 22868.
- [2] Borzi B, Faravelli M, Di Meo A (2020) Application of the SP-BELA methodology to RC residential buildings in Italy to produce seismic risk maps for the national risk assessment. Bull Earthq Eng. <https://doi.org/10.1007/s10518-020-00953-6>
- [3] Braga F., Dolce M., Liberatore D., 1982. A statistical study on damaged buildings and an ensuing review of the MSK-76 scale. Proceedings of the seventh European conference on earthquake engineering, Athens, Greece, 431-450.
- [4] Coburn, A., & Spence, R. (2003). Earthquake protection. John Wiley & Sons.
- [5] D'Ayala D.F., Paganoni S., 2011. Assessment and analysis of damage in L'Aquila historic city centre after 6th April 2009. Bulletin of Earthquake Engineering, 9(1), 81-104.
- [6] da Porto F, Donà M, Rosti A, Rota M, Lagomarsino S, Cattari S, Borzi B, Onida M, De Gregorio D, Perelli FL, Del Gaudio C, Ricci P, Speranza E (2021) Comparative analysis of the fragility curves for Italian masonry and RC buildings. Bull Earthq Eng 19(7):219–231

- [7] D'Amato M, Laguardia R, Di Trocchio G, Coltellacci M, Gigliotti R. Seismic Risk Assessment for Masonry Buildings Typologies from L'Aquila 2009 Earthquake Damage Data. *Journal of Earthquake Engineering* 2020; 00(00): 1-35. DOI: 0.1080/13632469.2020.1835750.
- [8] Del Gaudio C., De Martino G., Di Ludovico M., Manfredi G., Prota A., Ricci P. and Verderame G.M.; 2017: Empirical fragility curves from damage data on RC buildings after the 2009 L'Aquila earthquake. *Bull. Earthquake Eng.*, 15, 1425-1450.
- [9] Del Gaudio C., De Martino G., Di Ludovico M., Manfredi G., Prota A., Ricci P., Verderame G.M., 2019. Empirical fragility curves for masonry buildings after the 2009 L'Aquila, Italy, earthquake. *Bulletin of Earthquake Engineering*. <https://doi.org/10.1007/s10518-019-00683-4>.
- [10] Del Gaudio C., Ricci P., Verderame G.M., 2015. ECS-it – Evoluzione della classificazione sismica in Italia. ReLUIS, Naples, Italy. Available at <http://www.reluis.it>.
- [11] Del Gaudio, C., Di Ludovico, M., Polese, M. et al. Seismic fragility for Italian RC buildings based on damage data of the last 50 years. *Bull Earthquake Eng* 18, 2023–2059 (2020). <https://doi.org/10.1007/s10518-019-00762-6>
- [12] Del Gaudio, C., Scala, S.A., Ricci, P., Verderame G.M., 2021. Evolution of the seismic vulnerability of masonry buildings based on the damage data from L'Aquila 2009 event. *Bull Earthquake Eng* (2021). <https://doi.org/10.1007/s10518-021-01132-x>
- [13] Di Ludovico M, Prota A, Moroni C, Manfredi G, Dolce M (2017a) Reconstruction process of damaged residential buildings outside the historical centres after L'Aquila earthquake-part I: “light damage” reconstruction. *Bull Earthq Eng*. <https://doi.org/10.1007/s10518-016-9877-8>
- [14] Di Ludovico M, Prota A, Moroni C, Manfredi G, Dolce M (2017b) Reconstruction process of damaged residential buildings outside historical centres after the L'Aquila earthquake-part II: “heavy damage” reconstruction. *Bull Earthq Eng*. <https://doi.org/10.1007/s10518-016-9979-3>
- [15] Dolce M, Prota A, Borzi B, da Porto F, Lagomarsino S, Magenes G, Moroni C, Penna A, Polese M, Speranza E, Verderame GM, Zuccaro G (2021) Seismic Risk Assessment of residential buildings in Italy. *Bull Earthq Eng*. <https://doi.org/10.1007/s10518-020-01009-5>

- [16] Dolce M., Goretti A., 2015. Building damage assessment after the 2009 Abruzzi earthquake. *Bulletin of Earthquake Engineering* 13, 2241–2264 (2015). <https://doi.org/10.1007/s10518-015-9723-4>.
- [17] Dolce M., Speranza E., Giordano F., Borzi B., Bocchi F., Conte C., Di Meo A., Faravelli M. and Pascale V.; 2019: Observed damage database of past Italian earthquakes: the Da.D.O. Webgis. *Boll. Geof. Teor. Appl.*, 60, 141-164.
- [18] Dolce, M., & Prota, A. (2021). Guest editorial to the special issue—Seismic risk assessment in Italy. *Bulletin of Earthquake Engineering*, 1-4.
- [19] Donà M, Carpanese P, Follador V, Sbrogiò L, da Porto F (2020) Mechanics-based fragility curves for Italian residential URM buildings. *Bull Earthq Eng* 19(7):256. <https://doi.org/10.1007/s10518-020-00928-7>
- [20] Federal Emergency Management Agency (FEMA) (2012) Hazus-MH 2.1 technical manual: earthquake model
- [21] Grünthal M., 1998. European Macro-seismic Scale. *Cahiers du Centre Européen de Géodynamique et de Séismologie*, Vol. 15. European Macro-seismic Scale 1998. European Center for Geodynamics and Seismology. (in French)
- [22] ISTAT 2011. Istituto Nazionale di Statistica (National Institute of Statistics). 15° Censimento generale della popolazione e delle abitazioni. Dati sulle caratteristiche strutturali della popolazione, delle abitazioni e variabili. (in Italian) <http://www.istat.it/it/archivio/104317>
- [23] Karababa, F.S., Pomonis, A., 2011. Damage data analysis and vulnerability estimation following the August 14, 2003 Lefkada Island, Greece, Earthquake. *Bull Earthquake Eng* 9, 1015–1046. <https://doi.org/10.1007/s10518-010-9231-5>
- [24] Kircher, Charles A., Robert V. Whitman, and William T. Holmes. "HAZUS earthquake loss estimation methods." *Natural Hazards Review* 7.2 (2006): 45-59.
- [25] Lagomarsino G. and Giovinazzi S.; 2006: Macroseismic and mechanical models for the vulnerability and damage assessment of current buildings. *Bull. Earthquake Eng.*, 4, 415-443.
- [26] Lagomarsino S, Cattari S, Ottonelli D (2021) The heuristic vulnerability model: fragility curves for masonry buildings. *Bull Earthq Eng*. <https://doi.org/10.1007/s10518-021-01063-7>
- [27] Masi A, Lagomarsino S, Dolce M, Manfredi V, Ottonelli D (2021) Towards the updated Italian seismic risk assessment: exposure and vulnerability modelling. *Bull Earthq Eng*. <https://doi.org/10.1007/s10518-021-01065-5>

- [28] Michelini, A., Faenza, L., Lanzano, G., Lauciani, V., Jozinović, D., Puglia, R., & Luzi, L. (2020). The new ShakeMap in Italy: Progress and advances in the last 10 yr. *Seismological Research Letters*, 91(1), 317-333.
- [29] Orsini G., 1999. A model for buildings' vulnerability assessment using the Parameterless Scale of Seismic Intensity (PSI). *Earthquake Spectra*, 15(3), 463-483.
- [30] Rossetto T., Ioannou I., Grant D.N., 2013. Existing empirical fragility and vulnerability functions: Compendium and guide for selection, GEM Technical Report 2013-X, GEM Foundation, Pavia, Italy.
- [31] Rosti A., Del Gaudio C., Di Ludovico M., Magenes G., Penna A., Polese M., Verderame G.M., 2020a. Empirical vulnerability curves for Italian residential buildings. *Bollettino di Geofisica Teorica ed Applicata*, 61(3).
- [32] Rosti A., Del Gaudio C., Rota M., Ricci P., Di Ludovico M., Penna A., Verderame G.M., 2020b. Empirical fragility curves for Italian residential RC buildings. *Bull Earthquake Eng* (2020). <https://doi.org/10.1007/s10518-020-00971-4>.
- [33] Rosti A., Rota M., Penna A., 2020c. Empirical fragility curves for Italian URM buildings. *Bulletin of Earthquake Engineering*.
- [34] Rosti, A., Rota, M., & Penna, A. (2018). Damage classification and derivation of damage probability matrices from L'Aquila (2009) post-earthquake survey data. *Bulletin of Earthquake Engineering*, 16(9), 3687-3720.
- [35] Rota M., Penna A., Strobbia C.L., 2008. Processing italian damage data to derive typological fragility curves. *Soil Dynamics and Earthquake Engineering*, 933-947.
- [36] Sabetta F., Goretti A., Lucantoni A., 1998. Empirical Fragility Curves from Damage Surveys and Estimated. 11th European Conference on Earthquake Engineering © 1998 Balkema, Rotterdam, ISBN 90 5410 982 3.
- [37] Zuccaro G, Perelli FL, De Gregorio D, Cacace F (2020) Empirical vulnerability curves for Italian masonry buildings: evolution of vulnerability model from the DPM to curves as a function of acceleration. *Bull Earthq Eng*. <https://doi.org/10.1007/s10518-020-00954-5>
- [38] Zuccaro G., Cacace F., 2009. Revisione dell'inventario a scala nazionale delle classi tipologiche di vulnerabilità ed aggiornamento delle mappe nazionali di rischio sismico. Atti del XIII Convegno ANIDIS "L'ingegneria sismica in Italia", June 28–July 2, Bologna, Italy. Paper S14.39 (in Italian)

- [39] Zucconi M., Ferlito R., Sorrentino L., 2018. Simplified survey form of unreinforced masonry buildings calibrated on data from the 2009 L'Aquila earthquake. *Bulletin of Earthquake Engineering*, 16(7), 2877-2911.

Chapter 2.

STATE OF ART

2.1 INTRODUCTION

In the last 50 years, seismic-induced fatalities and economic losses have been reached dramatic values. In Italy, an amount of about 100 victims per year has been caused by seismic events, starting from the catastrophic Belice 1968 earthquake. Economic losses related to the emergency management and reconstruction process amount to over 200 billion Euro, about half of which related to the events of the last 15 years (namely, Molise 2002, L'Aquila 2009, Emilia Romagna 2012, Central Italy 2016–2017 earthquakes).

The recent seismic events have been a unique occasion to collect a huge amount of data about existing building stock, highlighting its general weaknesses. In fact, until the beginning of the 2000s, only 37% of the Italian municipalities had been seismically classified (Del Gaudio et al., 2015). Thus, only in a few numbers of municipalities the need of protect the building against the possible consequences of the seismic event had been recognized, making compulsory the seismic design. Only after Molise 2002 earthquake, the entire Italian territory was classified as seismic, making compulsory anywhere the design for seismic loads. Conversely, the Italian building's stock is mainly composed by ancient buildings: suffice to say that about 30% of current masonry buildings has been constructed before 1919 (ISTAT 2011). It means that most of

the Italian building's stock was designed only for gravity loads, namely without any seismic criteria. Thus, the age of buildings on the one hand and the recent seismic classification on the other one have contributed to the high vulnerability of the Italian existing buildings, making it a worthy of study argument. In fact, an in-depth knowledge of the building's features able to affect the damage attitude under seismic loads is the base for the consequent actions of prevention and mitigation, or also actions of response in the emergency's phase.

In this view, a very powerful tool to know and characterize in terms of seismic vulnerability the Italian building's portfolio is the great amount of data collected after the earthquake, namely during the post-earthquake surveys. In fact, such data allows one side to identify the main building's features and, on the other side, to assign a certain damage attitude due to these features. In Italy, several studies based on empirical data collected after seismic events have been conducted, starting from the catastrophic Irpinia 1980 earthquake. For example, Braga et al., 1982 provided damage probability matrices (DPMs) for 13 building's classes, based on about 36.000 buildings inspected after the Irpinia 1980 earthquake. The building's classes were defined as a function of the structural typology (namely, reinforced concrete and masonry buildings): in particular the 12 classes of masonry buildings were defined, combining three kinds of vertical structures (i.e., field, hewn and brick stone) with four horizontal structures (i.e., vaults, wooden, steel and reinforced concrete floors). Of course, a crucial issue in the vulnerability studies is just the definition of a reliable building's taxonomy. In fact, as deeply investigated in literature, the building's seismic behaviour could be affected not only by the structural characteristics, but also by many other features (Zuccaro et al., 2015) such as the building's height or the period of construction or the presence of retrofit interventions.

Of course, each mentioned building's feature plays a role in the seismic response of a buildings. Nevertheless, also the combination of these factors could increase or reduce the vulnerability. Thus, a building's taxonomy able to consider all together several building's features (such as structural typology, building's material, the presence of retrofit intervention, the construction age, the number of stories, ...) leads to the most accurate vulnerability's analysis, avoiding any

cross-correlation between the building's features. However, such high level of detail could result in small sample sizes. For this reason, the adopted taxonomy should be the better compromise between the level of detail in the building classification and the sample size of each defined class (Rossetto et al., 2013). Thus, different degrees of refinement are reached by existing studies, in which typically only some features (among all possible building's features) are considered as vulnerability factors.

A further crucial aspect in the empirical studies is about the data's completeness, that is a direct result of the survey campaign, often more focused on the areas most affected by the earthquake. Typically, after an earthquake, a major part of the inspections is done in municipalities near to the epicenter, planning a building-by-building survey (Dolce and Goretti, 2015; Zucconi et al., 2018; Rosti et al., 2018; Del Gaudio et al., 2019). Conversely, in the municipalities farthest from the epicenter, where shaking was light, the inspection is performed only under request of the building's owner, thus likely only in case of damaged building. Such rule allows a faster survey campaign but may introduce a systematic overestimation of the damage at low seismic intensities (Rossetto et al., 2013). To prevent this bias, in several studies (Colombi et al., 2008; Zucconi et al., 2018; D'Amato et al., 2020) the underestimation of the total number of buildings is overcome, integrating the original database by means of census data. In other works (Sabetta et al., 1998; Goretti and Di Pasquale, 2004; Rota et al., 2008; Del Gaudio et al., 2019), the fragility assessment is performed discarding from the original database all buildings located in the less inspected municipalities. Lastly, a two-step mixed approach is adopted in still other studies (Del Gaudio et al., 2021; Scala et al., 2022), combining the first two solutions. Such approaches are based on the evaluation of a completeness ratio (namely the ratio between the number of inspected buildings and the total one) for each municipality, setting a minimum completeness threshold.

Fragility functions correlate damage to ground motion intensity and their form is found to be either discrete or continuous. Most existing functions are expressed either in terms of damage probability matrices (e.g., Whitman et al., 1973; Güllan

et al, 1992; Decanini et al, 2004; Eleftheriadou and Karampinis, 2008) or fragility curves (e.g., Rossetto and Elnashai, 2003; Colombi et al, 2008; Rota et al, 2008). Damage probability matrices (DPM) are composed of sets of values defining the probability of a level of damage being reached in each building class at specified intensity measure levels. By contrast, fragility curves express the probability of a level of damage being reached or exceeded given a range of intensity measure levels. Moreover, a simple parameter to evaluate the damage attitude is the weighted mean of the damage distribution (Del Gaudio et al., 2021; Scala et al., 2022) regardless to the intensity measure values. The same definition can be applied to evaluate the mean damage at specified intensity measure levels, leading to the definition of vulnerability curves (Dolce and Goretti 2015; Rosti et al., 2018; Del Gaudio et al., 2019; Del Gaudio et al., 2021; Scala et al., 2022), i.e., relationship between mean damage and seismic intensity measure. This measure should be determined from earthquake ground motion records. However, due to the scarcity of strong ground motion recording stations, in practice seismic intensity measure values are obtained from ground motion prediction equations (GMPE). Given the large availability of GMPE in terms of peak ground acceleration (PGA), this latter is the main parameter used to represent ground motion intensity in empirical fragility studies (among the others, Sabetta et al, 1998; Rota et al, 2008).

Moreover, almost all mentioned works investigate the damage (so the dependent variable is typically a damage measure, as well as mean damage given the IM value), but also the building's usability is a relevant performance indicator (Stannard et al. 2014; Zucconi et al., 2018; Bertelli et al., 2018), especially in the post-earthquake emergency. More in general, fragility functions can be drawn in terms of a Damage Index, related to the cost of repair, or of some Performance Indicators, which are related to the conditions of use (Lagomarsino and Cattari, 2014).

In some empirical studies, discrete damage functions (i.e., observed DPMs) are transformed into parametric probability distributions. In several studies (Braga et al., 1982, Sabetta et al., 1998, Di Pasquale et al., 2005 and Lagomarsino and Giovinazzi, 2006) discrete binomial distributions (fully described by a single

parameter) is used to fit the “actual” DPM. Instead, other studies (Rossetto and Elnashai, 2003; Lallemand et al., 2015) adopt continuous beta distributions, which are fully described by two parameters. Conversely, when the seismic fragility is represented by means of empirical fragility curves, the majority of studies adopt lognormal cumulative distribution functions, due to their properties (Rossetto et al., 2013). The normal cumulative distribution function is the second most popular shape for empirical curves (e.g., Spence et al, 1992; Orsini, 1999; Karababa and Pomonis, 2010). Lastly, also exponential function is used in several studies (Rossetto and Elnashai 2003; Amiri et al 2007; Rosti et al., 2018).

As already mentioned in the previous Chapter, the present study is based on the analysis of the damage data collected after the catastrophic L’Aquila 2009 earthquake, focusing on residential masonry buildings that represent most of the current Italian building’s stock (about 57% according to ISTAT 2011 census). Of course, L’Aquila 2009 earthquake is one of the most studied seismic events in Italy and, over the years, an extensive literature (among the others, D’Ayala et al., 2011; Del Gaudio et al., 2017; Di Ludovico et al., 2017a; Di Ludovico et al., 2017b; Zucconi et al., 2018; Del Gaudio et al., 2019; Donà et al., 2020; Rosti et al., 2020c; D’Amato et al., 2020; Zuccaro et al., 2020; Borzi et al., 2020; Lagomarsino et al., 2021; Masi et al., 2021) has been produced based on data collected after such earthquake.

In this Chapter, starting from the above-mentioned studies, a review of existing methodologies for constructing empirical vulnerability and fragility functions is done. The review is organised in terms of the aspects of the fragility or vulnerability functions deemed important, such as the choice of the building’s taxonomy, data completeness (i.e., data quality), sample size (i.e., data quantity), the choice of the result’s representation (namely, discrete or continuous), of the functional form or the intensity measure.

2.2 BUILDING’S TAXONOMY

Different structural-geometric features could cause wide differences in building performance despite subjected to similar seismic intensities. Therefore, in empirical vulnerability studies typically building classes with a similar seismic

behaviour need to be defined to derive corresponding vulnerability/fragility functions. Clearly, the more detailed the building class the more homogenous the group of buildings belonging to the same class and the smaller the variation in the seismic response of such buildings.

However, more detailed building's taxonomies often result in small sample sizes. Thus, a careful balance should be struck between the level of detail in the definition of building taxonomy and the resulting sample size of each class (Rossetto et al., 2013).

Different types of taxonomies have been proposed in the last decades (European Macroseismic Scale, EMS-98 (Grünthal, 1998), HAZUS (Kircher et al., 2006), PAGER-STR (Jaiswal et al., 2010), GEM (Brzev et al., 2012)) and several approaches available in the literature have dealt with the introduction of taxonomies. Among those, EMS-98 (Grünthal, 1998) is aimed at describing the observable seismic effects, introducing 15 different classes of buildings, accounting for wall materials and seismic design level. Each class, representative of the building stock in Europe, is associated to an *expected* vulnerability, defined on a six level-scale (going from “A” to “F”, with decreasing seismic vulnerability).

The HAZUS taxonomy (Barthel et al., 1998; Graber et al., 1999; Kircher et al., 2006) has been originally proposed by the Federal Emergency Management Agency (FEMA) with the aim of evaluating the performance level of life safety and immediate occupancy. Such taxonomy that has been optimized to describe the USA building stock classifies structures by building code, type and height, for a total of 36 structural types and 4 design code levels (High-Code, Moderate-Code, Low-Code, and Pre-Code). For each of these building classes fragility models have been provided (Council et al., 1999).

The PAGER-STR taxonomy (Jaiswal et al., 2010) is the most comprehensive risk-oriented classification at global scale, featuring a total of 103 building's classes. This taxonomy of global building types for post-earthquake loss estimation and pre-earthquake risk analysis was developed for the U.S. Geological Survey's Prompt Assessment of Global Earthquakes for Response (PAGER) program. It is the result of a time-consuming process aiming to join

already existing taxonomies, complementing it with further building typologies collected by means of surveys in several countries. The main features considered in the PAGER taxonomy are lateral load resisting system, material, height and seismic code compliance.

All these taxonomies (PAGER-STR taxonomy (Jaiswal et al., 2010), HAZUS taxonomy (Kircher et al., 2006) or European Macroseismic Scale (Grünthal, 1998)) are usually employed for large-scale applications, being risk-oriented taxonomies. Actually, two different taxonomy typologies can be used in order to describe a building classification, namely *risk-oriented* or *faceted* taxonomies (Pittore et al., 2018). These latter are independent by the fragility component and, hence, they cannot be directly employed to perform seismic risk assessment. An example of faceted taxonomy has been proposed within the framework of the SYNER-G project with the aim of describing European buildings (Pitilakis et al., 2014), based on 15 facets.

A comprehensive faceted taxonomy has been proposed also by the Global Earthquake Model (GEM v.2.0, Brzev et al., 2013), based upon these past applications (in particular, EERI and IAEE World Housing Encyclopedia, PAGER-STR, and HAZUS) and allowing a building's description independent from the specific geographical contest. This taxonomy is based on 13 different types of attributes: (1) building's direction, (2) material of the lateral load-resisting system and (3) lateral load-resisting system; (4) height, (5) construction or retrofit age and (6) occupancy; (7) exterior walls, (8) building position within aggregate constructions, (9) shape of the building plan and (10) structural irregularity; (11) roof, (12) floor and (13) foundation system, grouped in four areas (structural system, building's information, exterior attributes, roof/floor/foundation structures). Moreover, each attribute can be characterized by several possible refinements with increasing level of detail. For example, in the case of the (2) attribute, the material is described by means of type (*level 1*), technology (*level 2*) and material's properties (*level 3*).

Despite the existence of various building classification systems (such as those adopted by HAZUS (Kircher et al., 2006) or GEM (Brzev et al., 2012)), these are not commonly adhered to by existing studies; rather, bespoke building classes

are defined, based on the available data (mainly deriving from census data or post-earthquake survey).

For example, fragility models for Italian URM residential buildings (Donà et al., 2020; Lagomarsino et al., 2021; Rosti et al., 2020c.; Zuccaro et al., 2020) developed in the framework of National Risk Assessment (ICPD 2018), consider inventory of the residential buildings from ISTAT 2001 census. This latter consists of information on the number of buildings, number of flats, flat surface and resident people, aggregated in each town by considering: the building material (masonry and reinforced concrete), periods of construction and the number of stories. According to this classification, 15 subtypes of masonry buildings have been identified, having considered 5 periods of construction (i.e., <1919; 1919-1945; 1946-1961; 1962-1981; >1981) and three height class (i.e., low, medium and high rise).

In the same project, also fragility models for Italian R.C. residential buildings (Borzi et al., 2020; Rosti et al., 2020c) have been developed, defining building's classes based on height classes and design type (i.e., for gravity loads or seismic design). The assignment of a design types to buildings is related to their age of construction and to the year of first seismic classification of the municipality to which they belong.

Several other Italian works (Dolce and Goretti, 2015; Del Gaudio et al., 2019; Del Gaudio et al., 2021; Scala et al., 2022) exploit information collected with the AeDES (Baggio et al., 2007) survey form (or previous ones), whose level of knowledge is less informative (especially if compared with GEM or PAGER-STR taxonomies) of course. In fact, although the information on masonry layer (level 1), the analysis of the mortar's quality (level 2) and also of the section of the masonry's wall (level 3) are required for the technician to typify the masonry layout, the final outcome reported in the AeDES form is synthesized in only two possible attribute's values (i.e., good and bad quality) with consequent building classification based on only two types of masonry quality.

Evidently, the collection of observed data from post-earthquake survey is extremely valuable not only for the seismic assessment of buildings, but also for the definition of suitable building taxonomies. Thus, significant efforts have been

made in recent years to compile national and international databases and make them available to the scientific community, e.g., the Italian Database of the Observed Damage (DaDO) discussed in Dolce et al., 2009, the Cambridge Earthquake Impacts Database (CEQID) compiled by Spence et al., 2009, GEM Consequence database (So et al., 2012), the Cambridge Earthquake Damage and Casualty Database (Spence et al., 2011), the international CATDAT database (Daniell et al., 2011), amongst others.

Overall, different degrees of refinement are reached by taxonomies adopted in the existing studies, in which typically only some features (among all possible building's features) are considered as vulnerability factors. As above mentioned, in the first DPMs developed in Europe (Braga et al., 1982), 13 building classes were defined based on data collected after the dramatic Irpinia (southern Italy) 1980 earthquake. Basically, such classification was related to the structural typology, grouping together all R.C. buildings and defining 12 masonry typologies based on vertical and horizontal structural types. Among the same building's features were considered to define the taxonomy of Dolce and Goretti, 2015, based on 6 classes. In particular, the first three classes (from A to C) were related to masonry buildings, whereas the remaining ones to R.C., mixed and steel structures. The assignment of a building class to masonry buildings depended on the types of vertical and horizontal structures. The Authors also point out that this primary classification, which is considered true on average, could undergo variations based on several relevant factors (such as the type of roof, the number of floors and the time of construction). The relevance of such further building's features was confirmed by following studies. For example, Zuccaro et al., 2015 pointed out that the only vertical structural system could be not sufficient to assign accurately the vulnerability class because wide variations in the seismic behaviour could be caused by several factors (among the others, the building's height, the period of construction, the roof type, site topography, ...). Similarly, in Zucconi et al., 2018 several vulnerability factors (i.e., the quality of masonry walls, the number of storeys, the period of construction, the presence of strengthening interventions) have been considered, analysing their influence on usability trends.

In particular, the height of the building can influence the seismic response of a structure, because directly related to its period of vibration. It has been shown that the building's height (i.e., the number of storeys) can modify the seismic fragility of classes defined based on construction material (Colombi et al., 2008). In addition, the presence of seismic strengthening interventions may modify the seismic behaviour of a given structural typology (among the others, Dolce et al., 2006; D'Ayala and Paganoni, 2011; Gaudio et al., 2021).

However, classifying buildings based purely on structural-geometric features could lead to group together buildings with very different seismic performances (Karababa and Pomonis, 2010), due for example to changes in the in force normative contents or to different degree of building's decay.

In this view, a crucial building's feature is of course the period of construction. For example, in Rota et al., 2008 the presence of tie rods/beams in Italian masonry structures has been indirectly attributed distinguishing between buildings constructed before and after the disastrous Messina 1908 earthquake (Royal Decree 18/04/1909 n.193). In Rosti et al., 2020c, the same building's classification used by Rota et al., 2008 has been adopted for masonry structures, considering 6 periods of construction (i.e., <1919; 1919-1945; 1946-1961; 1962-1971; 1972-1981; >1981) and 2 height's classes (i.e., low and mid/high rise buildings). In Del Gaudio et al., 2021 the information about the construction age and the Italian seismic classification has been both considered, to obtain homogeneous classes also in terms of normative contents in force at the period of the building's construction. About the same approach has been used by several Greece studies. For example, Pnevmatikos et al., 2020 for buildings sited in Cephalonia and Ithaca islands, adopted a building taxonomy based on the period of construction (i.e., <1960; 1960-1986; 1986-1995; >1995), building material (namely, masonry and R.C. buildings), type of design (i.e., buildings designed according to no code or according to Greek Code enacted in 1959, 1984, and 2000), and structural form. Similarly, Karababa and Pomonis, 2010 to classify buildings in Lefkada island, have considered four relevant building features: the vertical load-bearing structure, the horizontal structures, the roof, and the period

of construction, highlighting the relevance of this latter due to changes in design philosophy, quality of construction materials and workmanship.

Also, Japanese studies (Torisawa et al., 2020; Yamazaki et al., 2019) highlighted the great variability of seismic fragility varying the construction period, given the structural typology (i.e., wooden buildings).

To date, no general consensus exists in the building classification, despite as above mentioned the relevance of several building features on seismic vulnerability/fragility has been demonstrated in past works. Basically, the adopted taxonomies reflect the need to consider a major part of available parameters, safeguarding the reliability (i.e., the size) of the sample, nonetheless. In fact, sample size of a given class determines the reliability of the obtained vulnerability or fragility functions. Such size basically depends on the data source (post-earthquake survey, census data, single building inspections) and the adopted building taxonomy (a high level of detail could result in small sample sizes). According to Rossetto et al., 2013 most existing functions are based on samples of 200 buildings; however, wide range of sample sizes, with a minimum equal to 20 buildings (Sarabandi et al. 2004; Karababa and Pomonis, 2010), are used in literature.

Moreover, almost all mentioned studies are about residential buildings, that represent most of available post-earthquake data, as well as of the existing building stock. Thus, the above-mentioned taxonomies basically were designed to describe residential buildings. Nevertheless, non-negligible part of the existing building stock is composed by construction belonging to the so-called cultural heritage (such as churches, historical palaces, tower, ...), especially in countries such as Italy. In the last years, an increasing interest on such typologies has been observed, likely due to the recent availability of data. In particular, after Umbria-Marche (Italy) earthquake, an extensive damage survey was done, leading to the derivation of vulnerability models (Lagomarsino and Podestà, 2004).

Within the 2019–2021 research agreement between the Civil Protection Department (DPC) and the Network of University Laboratories for Earthquake Engineering (ReLUIIS), several vulnerability models related to the Italian churches (such as Guerreiro et al., 2000; da Porto et al., 2012; Leite et al., 2013;

Sorrentino et al., 2014; De Matteis et al., 2016; Marotta et al., 2018; Penna et al., 2019; Lagomarsino et al., 2019; Canuti et al., 2019; Cescatti et al., 2020) have to be implemented in the new version of IRMA platform for risk calculation.

Similar studies carried out on churches of other countries may be found, for instance in Jorquera et al., 2017, Palazzi et al., 2018, Fuentes et al., 2019, where emphasis has been placed on ancient churches in Chile, in Fuentes et al., 2021 for Mexican churches, or in Goded et al., 2018 for unreinforced masonry churches in New Zeland.

However, the need to develop specific vulnerability models for churches is basically due to the distinctive features with respect to residential buildings. In several studies (Cescatti et al., 2020), the type of plan shape is used as key parameter to develop a suitable classification. Clearly, some features (such as plan shape, roof type, building material, constructive quality) can be correlated with the period of construction (De Matteis et al., 2019), because related to different architectonic styles.

A similar argument is for school buildings, for which recently a dedicated platform (IRMA School, Masi et al., 2021), containing an inventory of georeferenced Italian buildings, has been created. The taxonomy adopted in such database is highly detailed, considering not only the ISTAT census types (i.e., material, period of construction and number of storeys), but also other building's features (such as horizontal diaphragms, roof structure, plan area).

2.3 DATA COMPLETENESS

A crucial aspect in the empirical studies is about the data's completeness, that is typically a direct result of the survey campaign, often more focused on the areas most affected by the earthquake. Such issue, well-known in literature, requires suitable elaborations, aiming to ensure the data representativeness and to avoid any bias in the vulnerability/fragility assessment.

The degree of completeness is usually evaluated at municipal scale (Goretti and Di Pasquale, 2004; Rota et al., 2008; Zucconi et al., 2018), comparing the number of inspected buildings in a given municipality with the corresponding one provided by the census data.

Obviously, the lowest is such completeness ratio the highest is the number of not inspected buildings; conversely when completeness ratio approaches to 1 (or sometimes overcomes 1 – because of difference in the estimation of the total number of buildings between census and survey data (Rota et al., 2008)), it means that all the buildings sited in that municipality have been inspected.

It can occur that in the area near the epicenter a complete (building-by-building) survey was done, whereas in the area farthest from the epicenter the inspections were done only under building owner's request.

This represent a critical circumstance, since in this area (farthest from the epicenter) mainly damaged buildings were inspected, systematically neglecting undamaged ones. In other words, data collected in such way, if without further suitable elaborations, could introduce biases in the vulnerability or fragility assessments (Rossetto et al., 2013; Rossetto et al., 2018), overestimating the actual number of damaged buildings sited in municipalities less affected by earthquake, where a partial survey was done, systematically neglecting a great part or even the totality of un-damaged buildings.

In this regard, Rossetto et al., 2013 summarizes the possible solutions adopted in literature to overcome this problem. The first solution deals with the removal of all the data regarding to buildings sited in municipalities where a minimum proportion of buildings has not been surveyed (namely, municipalities characterized by a completeness ratio value below a predefined threshold).

Values of completeness threshold reported in previous studies are of the order of 0.75 (Sabetta et al., 1998), 0.80 (Goretti and Di Pasquale, 2004), 0.60 (Rota et al., 2008), 0.91 (Del Gaudio et al., 2020; Rosti et al, 2020a, Rosti et al, 2020b; Del Gaudio et al., 2021; Scala et al., 2022).

Moreover, as highlighted in previous studies (Zuconni et al., 2018; Rosti et al., 2018; Del Gaudio et al., 2019), the completeness of survey for a given municipality can be correlated to the observed macro-seismic intensity. For example, after L'Aquila 2009 event, the greatest part of inspected buildings was in municipalities subjected to a macro-seismic intensity value equal or greater than VI. In fact, the reconnaissance field trips were done through building-by-building survey only for these municipalities, whereas in the remaining area hit

by the earthquake the inspection was performed only if required by the building's owners, therefore likely only or mostly on damaged buildings. A similar circumstance occurred also after Molise 2002 earthquake (Goretti e Di Pasquale, 2004), inspecting almost all buildings only in epicentral area.

The second solution (Colombi et al., 2008; Eleftheriadou and Karampinis, 2008; Karababa and Pomonis, 2010; Eleftheriadou and Karampinis, 2011; Zucconi et al, 2018; Zucconi et al, 2020; D'Amato et al, 2020) consists of the identification of incomplete subsets and their integration using census data, considering this additional source as characterized by no-damage to any structural components. Thus, such approach commonly relies on the assumption that not surveyed buildings were undamaged during the seismic event. Clearly, such integration is only possible when census data is available. However, it can be occurred that census data is not available in the considered country or is not coeval with the earthquake.

To overcome such issue, the number of buildings located in a given area could be obtained by means of data projections. For example, in Iran such approach was used by Tavakoli and Tavakoli, 1993, projecting the population recorded in the 1976 census to 1986.

Lastly, in Del Gaudio et al., 2021 a two-step mixed approach was adopted, firstly discarding those municipalities partially surveyed and secondly integrating the original database with an addition source, accounting for the negative evidence of damage, i.e. those buildings not reported in damage database since not affected by damage although a slight ground shaking.

Incomplete datasets could be due not only to the fact that survey has not been conducted on all affected areas (incomplete sample) but could be due also to the omission of key information from fields of interest within a portion of the survey forms. It is quite commonly in existing databases that some forms do not have complete entries across all fields, due to errors in the completion of the survey forms or errors in transcription from the forms to the databases (Rossetto and Ioannou, 2018).

The most adopted approach in fragility/vulnerability literature (among the others, Rota et al., 2008; Del Gaudio et al., 2021) is to remove from the analysis

any partial data (such as buildings of unknown material or unknown damage) or at least to discard all survey forms that do not report the data crucial for the study (typically, damage data and structural-geometric description of the building).

It should be noted that missing data could have a specific meaning. For example, systemic lack of damage data could be due to the fact that such information is provided only for damaged buildings. Thus, discarding all buildings without damage data could mean to overestimate the actual damage. Therefore, it is crucial an in-dept knowledge of the data and of the source of data, to avoiding any bias introduction.

In the other hand, missing data could be random. In such cases, as above mentioned, one can discard all or almost all incomplete survey forms.

Only few studies (Macabuag et al., 2016) estimate missing data from other attributes (reported in the survey form) by means of multiple imputation technique. Such approach involves replacing missing observed data (for example, building material) with values estimated based on other building features (for example, surface area, building use, observed damage), assumed as explanatory variables.

Moreover, the assignment of a given building feature as a function of the period of construction is quite common in literature. For example, as highlighted in previous studies (Zucconi et al., 2018; Del Gaudio et al., 2021), the presence of tie rods/beams in masonry structures results very difficult to detect by means of a rapid visual inspection, during the emergency phases right after the earthquake, without the aid of invasive inspections (such as plaster scarifying). Thus, such information, despite able to modify the building's behaviour under seismic actions (Sorrentino et al., 2017), quite often is not reported in the survey form. So, in Rota et al., 2008 the presence of such structural details has been indirectly attributed distinguishing between Italian buildings constructed before and after the disastrous Messina 1908 earthquake (Royal Decree 18/04/1909 n.193).

Another example could be related to the design type since all survey forms adopted in Italy over the time do not clarify if the building has been designed only for gravity loads or also considering seismic actions. In several studies

(among the others, Del Gaudio et al., 2020; Del Gaudio et al., 2021), design class is assigned comparing the period of construction with the year of first seismic classification of municipality where the building is sited. About the same approach was used by Eleftheriadou and Karampinis, 2011, for R.C. and mixed structures in Greece.

Among all described approaches aiming to “complete” the available database, one should prefer those based on the data integration, rather than data discarding. In fact, as highlighted in the previous paragraph, a crucial issue in empirical studies is the amount of data of course. Thus, approaches that discard incomplete and/or missing data could be result in a small sample size.

In general, the data treatment should take into consideration both quality (i.e., completeness of data) and quantity (i.e., sample size) aspects, to ensure high reliability of the obtained assessment.

2.4 EMPIRICAL METHODS

Empirical seismic vulnerability assessment of buildings at large scale has been for the first time carried out in the early 70’s (Whitman et al., 1973), using discrete intensity measures (i.e., macroseismic intensity).

At that time in fact, only hazard maps based on a discrete description, were available. Thus, the first results of empirical methods were provided in terms of damage probability matrices (DPM), which express in a discrete form the conditional probability of obtaining a given damage level ds_i , under a certain intensity measure (IM_j).

$$P(DS = ds_i | IM_j; \theta)$$

Nowadays, a convenient and widely adopted way for defining seismic vulnerability is the use of fragility curves (among the many others, Rota et al., 2008; Rosti et al., 2020; Del Gaudio et al., 2019), which are continuous functions expressing the probability of exceeding a given damage state threshold (ds_i), as a function of a selected seismic input parameter IM_j (often continuous seismic intensity measures, such as the peak ground acceleration PGA).

Thus, if damage is described by n damage states DS , the link between DPMs and fragility curves is:

$$P(DS = ds_i | IM_j) = \begin{cases} 1 - P(DS \geq ds_1 | IM_j) & i = 0 \\ P(DS \geq ds_i | IM_j) - P(DS \geq ds_{i+1} | IM_j) & i \in [1; n-1] \\ P(DS \geq ds_i | IM_j) & i = n \end{cases}$$

A difficult task in vulnerability/fragility assessment is the definition of consequences that are evaluated by the fragility functions. Usually Damage States (DS) are considered, which are referred to physical damage to structural and non-structural elements, but fragility functions can be also drawn in terms of a Damage Index (DI) or Performance Indicators (PIs).

In such cases, seismic vulnerability is expressed by a function (so-called vulnerability curves) linking a mean damage/loss/performance measure (L) with seismic intensity values IM_j (i.e., Dolce and Goretti, 2015; D'Amato et al., 2020; Del Gaudio et al., 2021).

The link between DPMs and vulnerability function is provided by the following equation:

$$E(L | IM_j) = \sum_{i=0}^n E(L | ds_i) P(DS = ds_i | IM_j)$$

$E(L | IM_j)$ is the mean or expected value of the selected damage/loss measure (L), given the intensity measure IM_j . Similarly, $E(L | ds_i)$ is the expected loss value, given the damage state ds_i . Lastly, $P(DS = ds_i | IM_j)$ is exactly the probability provided by the DPMs.

A huge amount of existing studies investigates the damage due to the seismic event, for given building classes. However, recent works have highlighted that the building usability is a relevant performance indicator (Stannard et al. 2014; Bertelli et al., 2018; Sisti et al., 2018; Zucconi et al., 2017; Zucconi et al., 2020)

of the building's behaviour under seismic loads. Thus, vulnerability assessments in terms of building's usability have been recently derived, by means of DPMs (Zucconi et al., 2020), fragility curves (Bertelli et al., 2018) and vulnerability curves (Zucconi et al., 2017).

In the following sub-sections, an in-dept review of existing empirical studies is provided, focusing on models based on DPM, fragility and vulnerability curves.

2.4.1 Damage Probability Matrix (DPM)

As in detail explained in Calvi et al., 2006, first DPMs have been proposed by Whitman et al., 1973, based on the damage observed in over 1600 buildings after the 1971 San Fernando earthquake. For a given structural typology, the probability of being in a given state of structural and non-structural damage is provided, together with the damage ratio (representing the ratio between the cost of repair and the cost of replacement) for each damage state.

The first European version of DPMs (Braga et al., 1982) were based on the damage observed after the 1980 Irpinia earthquake. These were derived under the assumption of binomial damage distribution, considering three vulnerability classes (see 2.2) and the macroseismic intensity based on the Medvedev-Sponheuer-Karnik (MSK, Medvedev 1977) scale as intensity measure.

Later, such DPMs were improved by Di Pasquale et al., 2005, changing the seismic intensity measure from the MSK to the Mercalli-Cancani-Sieberg (MCS) scale and dividing the vulnerability class C into two sub-classes to differentiate between good masonry (C1) and R.C. (C2) buildings. Furthermore, the number of buildings was replaced by the number of dwellings to use the census inventory provided by the Italian National Institute of Statistics (ISTAT 1991).

A further improvement was gained by Dolce et al., 2003, adapting these DPMs to the town of Potenza. In particular, an additional vulnerability class (i.e., D class) was introduced for buildings constructed after 1980 (clearly not considered by Braga et al., 1982), expressing the seismic intensity according to the European Macroseismic Scale (Grünthal, 1998).

This latter implicitly provides DPMs, since introduces six vulnerability building classes (A to F) and for each of them a qualitative description of the proportion of buildings suffering a given level of damage is provided as a function of the seismic intensity level. Nevertheless, such DPMs are incomplete, because the proportion of buildings suffering a given damage level (ranging from 1 to 5) for a given seismic intensity (ranging from V to XII) is not provided for all possible combinations of damage levels and seismic intensities). Moreover, such DPMs are quite vague, since the proportion of buildings is provided only in qualitative terms (“few”, “many” and “most”).

Such issues were addressed by Lagomarsino and Giovinazzi, 2004, assuming a beta damage distribution (Spence 1990) to overcome the lack of information related to some damage states and intensity measure values.

Furthermore, the qualitative description based on the attributes “few”, “many” and “most” was replaced with a quantitative description, by means of Fuzzy Set theorem (Dubois and Prade, 1980). Such approach has been further developed in the European RISK-UE project for a larger number of building typologies and vulnerability classes (Lagomarsino and Giovinazzi, 2006), assuming a binomial distribution.

To improve the assignment of vulnerability classes, in several works (Bernardini et al., 2004; Lagomarsino and Giovinazzi, 2006; Preciado et al., 2020) typological building features (such as age, number of storeys, construction details, position in the aggregate, ...) are considered as “modifier” vulnerability factors (ranging from 0 to 100, according to vulnerability index of Benedetti and Petrini, 1984), assigned by expert judgment.

To overcome the possible arbitrariness of an expert judgment method, Zuccaro et al., 2015 propose the SAVE method in which the weight of each vulnerability factor is derived directly by the analysis of actually observed damage.

As above mentioned, two parametric damage distribution models predominantly are used in literature: (1) binomial distribution (among the others., Braga et al., 1982; Corsanego et al. 1993; Augusti et al. 2001; Lagomarsino and

Podesta, 2004; Pasquale et al., 2005; Lagomarsino and Giovinazzi, 2006; Roca et al. 2006), and (2) the beta distribution model (i.e., Spence 1990; Omidvar et al., 2012; Lallemand et al., 2015).

The first one is the most used, basically since binomial distribution has the advantage of needing one parameter (ranging between 0 and 1) only. In the binomial distribution model, the probability of being in the damage state k is defined as (Ang and Tang, 2007):

$$P(DS = DS_k) = \binom{k_{max}}{k} p^k (1 - p)^{k_{max}-k}$$

The model results in a discrete probability mass function, with one prediction for each k damage state, ranging from 0 to k_{max} (i.e., the highest damage state). The parameter p , the single unknown parameter in the model, represents the central value (i.e., mean of the distribution).

In Braga et al., 1982, such parameter is the normalized sample mean deriving from observed data. Thus, in binomial distribution, the sample mean μ_D can be defined as the mean number of successes out of the total number of trials, according to the following equation:

$$p = \mu_D = \frac{\sum_{k=0}^{k_{max}} n_k k}{k_{max} \sum_{k=0}^{k_{max}} n_k}$$

with n_k , number of buildings in each k damage state.

Conversely, beta distribution is a family of two-parameter continuous probability distributions. The main advantages in using such distribution are (Lallemand et al., 2015): (1) the finite domain, constrained between 0 and 1, used to represent the damage ranging from no-damage to collapse; (2) beta distribution can flexibly model a broad variety of shapes, differently from binomial one; (3) it is fully characterized by only two shape parameters (α, β).

$$f(x; \alpha, \beta) = \frac{\Gamma(\alpha + \beta)}{\Gamma(\alpha)\Gamma(\beta)} x^{\alpha-1} (1-x)^{\beta-1}$$

The shape parameters (α, β) are function of two parameters, namely the mean μ_D and the variance σ_D^2 , defined according to the following expressions:

$$\begin{cases} \alpha = \mu_D \left(\frac{\mu_D(1 - \mu_D)}{\sigma_D^2} - 1 \right) \\ \beta = (1 - \mu_D) \left(\frac{\mu_D(1 - \mu_D)}{\sigma_D^2} - 1 \right) \end{cases}$$

Several studies (Lagomarsino and Giovinazzi, 2006; Lallemand et al., 2015; Rosti et al., 2020; Vicente et al., 2011) have highlighted that limited flexibility of binomial distribution in some cases does not permit to well reproduce observed damage repartition in damage states.

Despite the greater flexibility of beta distribution, the advantage of the binomial one is, however, the fact that damage repartition in different damage states is described through a unique parameter, representing the mean damage μ_D of the discrete distribution.

Such issue is the reason why binomial distribution is most widely used in literature.

Thus, assuming such distribution to describe the occurrence of a given damage state under a given intensity measure, the only unknown parameter is the mean damage μ_D . Among the above-mentioned works, Lagomarsino and Giovinazzi, 2006 use the following equation (originally proposed by Sandi and Floricel, 1994) to evaluate the mean damage:

$$\mu_D = 2.5 \left[1 + \tanh \left(\frac{I + 6.25V - 13.1}{Q} \right) \right]$$

where I is the seismic input provided in terms of a macroseismic intensity, V is the vulnerability index, and Q is the ductility index (conventionally assumed equal to 2.3 for residential buildings, according to Lantada et al., 2010).

Several following studies (Omidvar et al., 2012; Ferreira et al., 2014; Ferreira et al., 2017; Brando et al., 2017; Rapone et al., 2018), starting from such definition of μ_D , have proposed modifications of parameters and/or coefficients in the formula, based on different sources of data or building typologies.

Moreover, the same definition has been used to characterize the expected damage, using the Vulnerability Index Method (VIM) in the Risk-UE project (Lagomarsino and Giovinazzi, 2002). The method has been initially applied to assess the seismic risk for seven European cities (Barcelona, Bitola, Bucharest, Catania, Nice, Sofia and Thessaloniki) (Mouroux et al. 2004; Pitilakis et al. 2006; Lantada et al. 2010) around the Mediterranean Sea. Then, it has been adapted and applied also to constructions of other Countries. By way of example, the Risk-UE VIM was used to assess the seismic vulnerability of Moroccan constructions in the city of Al Hoceima (e.g., Cherif et al., 2016).

As above mentioned, vulnerability assessment based on vulnerability indices was proposed for the first time by Benedetti and Petrini, 1984. Such method groups together structures with similar seismic performance, applying behaviour modifiers to evaluate the vulnerability index of a given building, according to the following equation:

$$V_I^{building} = V_I^{class} + \Delta M_R + \sum_{j=1}^n Vm_j$$

where V_I^{class} is the vulnerability index related to a given class of buildings (with similar seismic behaviour). ΔM_R and Vm_j are modifier indices that modify the seismic vulnerability of a given class, based on building characteristics related to a specific geographical region and on further building features (able to affect the seismic performance), respectively.

In the Risk-UE project, so-obtained vulnerability index has been used to evaluate the mean damage through the formula originally proposed by Sandi and Floricel, 1994.

2.4.2 Vulnerability curves

In literature, a simple vulnerability parameter is the mean damage, seen as the mean of the damage distribution for a given intensity measure.

By way an example, in the vulnerability model introduced by Braga et al., 1982, such parameter is the mean p of a damage distribution, assumed as binomial in each IM value. Thus, DPMs were evaluated by Braga et al., 1982, applying for each IM value the following equation:

$$P(p, ds, N_{DS}) = \binom{N_{DS}}{ds} p^{ds} (1 - p)^{N_{DS}-ds}$$

Clearly, $P(p, ds, N_{DS})$ is the probability of occurrence of a certain damage state ds in a given IM value, being N_{DS} the total number of damage levels and p the mean of the distribution. Starting from the same assumption of binomial DPMs, Sabetta et al., 1998 provided a relationship between the seismic intensity measure and such mean value p . In particular, linear and weighted polynomial regression models were adopted, linking the considered IMs (i.e., PGA, Arias Intensity and effective peak ground acceleration) to the mean damage. This latter was calculated for each municipality and for each vulnerability class, as:

$$p = \frac{1}{N_{DS}} \sum_{ds=0}^{N_{DS}} \frac{N_{ds}}{N} ds$$

where N_{DS} is the number of damage states; N is the number of buildings belonging to a given vulnerability class in each municipality. Lastly, N_{ds} is the portion of N with a degree of damage equal to ds . Such curves basically provide for each IM value the expected mean value of the damage distribution, describing in a continuous form the mean seismic behaviour of a given building class, as a function of the seismic intensity.

Later, the same definition of p was used by Dolce et al., 2003, providing in a discrete form a relation between mean damage and the macroseismic intensity

according to Medvedev-Sponheuer-Karnik (Medvedev 1977) scale, based on data related to the city of Potenza. Clearly,

Conversely, Del Gaudio et al., 2019 provided continuous vulnerability curves for masonry buildings as a function of PGA, using the ShakeMap of Italian National Institute of Geophysics and Volcanology (INGV) (Michellini et al., 2008) and data collected after L'Aquila 2009 earthquake. In particular, the mean damage has been calculated in five PGA bins ranging from 0.05 to 0.50 g with a step of 0.10 g (except for the first one, which has a step of 0.05 g). Vulnerability curves have been obtained fitting the observed data, assuming a power function characterized by an exponent term generally less than 1.

Such approach was improved by Del Gaudio et al., 2020, where mean damage has been used to derive vulnerability curves related to R.C. buildings, distinguishing in several building's classes (as a function of the level of design and the number of storeys) and considering data collected after several Italian earthquakes. Vulnerability curves have been obtained, fitting the observed data (i.e., mean damage – PGA points) by means of an optimization technique. This latter minimizes the sum of squared differences between the observed data points and those predicted by lognormal cumulative functions, assuming a constant logarithmic standard deviation for all considered building classes. Moreover, the number of buildings in each PGA bin has been used as weight in the fitting procedure. The novelty of the approach is mainly about to the definition of a *generalized* database, adding to the available database (positive evidence of the damage) not-damaged buildings (negative evidence of the damage). Such integration, as explained in Section 2.3, allows to overcome the underestimation of undamaged buildings, caused by the presence of not completely surveyed municipalities.

The same approach was used by Rosti et al., 2020, deriving vulnerability curves both for R.C. and masonry buildings. In this study, in addition to cumulative lognormal functions, also exponential ones were used, in order to identify the best functional form. In particular, the goodness-of-fit (i.e., the accuracy of each selected model to reproduce the observed mean damage) was quantified in terms of the coefficient of efficiency, E (Nash and Sutcliffe, 1970):

$$E = 1 - \frac{\sum_{i=1}^m (y_i - \hat{y}_i)^2}{\sum_{i=1}^m (y_i - \bar{y})^2}$$

where y_i are the observations, \hat{y}_i indicate the predictions, \bar{y} is the mean of the observations and m is the total number of observations. Results show that, despite the suitability of both the lognormal and exponential models to reproduce the observational data, higher efficiency is globally attained when the lognormal model is adopted.

Conversely, an iterative approach was used by Dolce and Goretti., 2015, since the frequency $f_{c,ds}$ of each ds for buildings belonging to a given class depends on the mean damage p . This latter was defined as:

$$p = \frac{1}{N_{DS}} \sum_{ds=0}^{N_{DS}} f_{c,ds} ds$$

whereas the frequency $f_{c,ds}$ was calculated averaging the observed damage distribution related to the N buildings of a considered class, according to the following equation:

$$f_{c,ds} = \frac{1}{N} \sum_{b=0}^N f_{b,ds}$$

$f_{b,ds}$ provides the damage distribution for a single building belonging to the considered building's class, being the subscript “ ds ” related to a given damage state. Thus, for each building the sum of $f_{b,ds}$ (with ds ranging between 0 and N_{DS}) have to be equal to 1.

$$\sum_{ds=0}^{N_{DS}} f_{b,ds} = 1$$

Moreover, $f_{b,ds}$ were defined as a function of the observed damage provided by the survey form (AeDES, Baggio et al., 2007), according to the following conversion rules:

$$\left\{ \begin{array}{l} DS0 \rightarrow f_{b,DS0} = 1 \\ DS1 \rightarrow f_{b,DS1} = 1 \\ DS2 \rightarrow f_{b,DS2} = \alpha_{DS2} \\ DS3 \rightarrow f_{b,DS3} = 1 - \alpha_{DS2} \\ DS4 \rightarrow f_{b,DS4} = \alpha_{DS4} \\ DS5 \rightarrow f_{b,DS5} = 1 - \alpha_{DS4} \end{array} \right.$$

Parameters α_{DS2} and α_{DS4} have been related to the mean damage p of the class and to constant values k_{DS2} and k_{DS4} , since defined as follow:

$$\alpha_{ds} = (1 - p)^{k_{ds}}$$

Since p depends on $f_{c,ds}$, $f_{c,ds}$ depends on $f_{b,ds}$, $f_{b,ds}$ depends on α_{ds} and α_{ds} depends on p , an iterative procedure is required. Such procedure was developed to derive the so-called mean non dimensional damage p for 4 vulnerability classes related to 3 seismic events (Irpinia 1980, L'Aquila 2009, and Molise 2002), obtaining a relation between p and the macroseismic intensity consistent with the European Macroseismic Scale (Grünthal, 1998).

Different definition was used by (Dolce et al., 2001; Di Pasquale and Goretti 2001; Goretti and Di Pasquale 2004), where the sum of all the possible damage levels to vertical bearing components ds , times their damage extension e_{ds} , was considered.

As mentioned in Section 2.4.1, Lagomarsino and Giovinazzi, 2006 use the following equation (originally proposed by Sandi and Floricel, 1994) to evaluate the mean damage p and then, vulnerability curves as a function of the *EMS*-98 macroseismic intensity (Grünthal, 1998):

$$p = \mu_D = 2.5 \left[1 + \tanh \left(\frac{I + 6.25V - 13.1}{Q} \right) \right]$$

where I is the seismic input provided in terms of a macroseismic intensity, V is the vulnerability index, and Q is the ductility index (conventionally assumed equal to 2.3). Such definition has been recently re-calibrated (Lagomarsino et al., 2020) based on a large database of observed vulnerability (Da.D.O., Dolce et al., 2019), leading to the following expression:

$$p = \mu_D = \begin{cases} 2.5 \left[1 + \tanh \left(\frac{I + 3.45V - 11.7}{0.9 + 2.8V} \right) \right] & \text{for } V \geq 0.32 \\ 2.5 \left[1 + \tanh \left(\frac{I + 6.25V - 12.6}{1.8} \right) \right] & \text{for } V < 0.32 \end{cases}$$

This latter is based on the statement that the ductility index Q is not constant varying the period of construction of the building. Thus, a correlation (calibrated on Italian masonry buildings) with the vulnerability index V has been derived, since Q decreases when V decreases (modern buildings).

As above mentioned, vulnerability functions can be drawn not only in terms of a Damage Index (such as the mean damage p), but also in terms of Performance Indicators (such as the building's usability). For example, Zucconi et al., 2018 provided the frequency distribution of unusable buildings given the macroseismic intensity of the Mercalli–Cancani–Sieberg (MCS) scale, as a function of several building features (number of storeys, period of construction, roof type, presence of isolated columns, presence of mixed structures, presence of retrofit interventions, ...). The aim was to detect the features that mostly affect the building's usability under seismic loads, leading to the definition of a simplified form for a faster usability assessment of unreinforced masonry buildings.

The number of unusable buildings, together with the number of collapsed ones and the number of homeless, are relevant post-earthquake indicators, since affecting the indirect costs (related to temporary shelters for homeless) and the social impact of earthquakes.

Also, in the latest Italian National Risk Assessment (Dolce et al., 2020; da Porto et al., 2021) building's usability has been considered as relevant

consequence of the earthquake, together with direct economic losses and casualties (injury and death). Damage-to-impact models have been used to derive consequences due to the earthquake, starting from the damage assessment. In particular, sets of coefficients to convert damage estimates into predictions of usable, unusable (in the short- and long-term) and collapsed buildings, direct economic loss, death and injury, have been used.

To estimate the number of unusable buildings in the short and the long term, respectively UB_{st} and UB_{lt} , equations similar to those proposed by Zuccaro and Cacace, 2011 have been used:

$$\begin{cases} UB_{st} = \sum_{ds=1}^{N_{DS}} (N_{M,ds} u_{st,ds}) + \sum_{ds=1}^{N_{DS}} (N_{RC,ds} u_{st,ds}) \\ UB_{lt} = \sum_{ds=1}^{N_{DS}} (N_{M,ds} u_{lt,ds}) + \sum_{ds=1}^{N_{DS}} (N_{RC,ds} u_{lt,ds}) \end{cases}$$

In the equations, $N_{M,ds}$ and $N_{RC,ds}$ are respectively the number of masonry or R.C. buildings in damage level ds ; whereas $u_{st,ds}$ ($u_{lt,ds}$) are the percentage of unsafe buildings in the short (long) term for each structural damage level ds .

Furthermore, to calculate the expected number of deaths N_d and injured N_i , it is assumed that the ratio of injured and victims with respect to occupant numbers is determined only by the most severe damage levels, DS4-DS5, (Lucantoni et al. 2001; Bramerini and Di Pasquale, 2008), using the equations originally proposed by Zuccaro and Cacace, 2011:

$$\begin{cases} N_d = \sum_{j=1}^{N_{masonry}} [(O_{M_j,DS4} p_{d,DS4} + O_{M_j,DS5} p_{d,DS5})] + \sum_{j=1}^{N_{RC}} [(O_{RC_j,DS4} p_{d,DS4} + O_{RC_j,DS5} p_{d,DS5})] \\ N_i = \sum_{j=1}^{N_{masonry}} [(O_{M_j,DS4} p_{i,DS4} + O_{M_j,DS5} p_{i,DS5})] + \sum_{j=1}^{N_{RC}} [(O_{RC_j,DS4} p_{i,DS4} + O_{RC_j,DS5} p_{i,DS5})] \end{cases}$$

In the equations, $O_{M/RC_j,DS4/DS5}$ is the number of occupants in masonry/R.C. buildings, which experienced a damage level DS4/DS5. $p_{d/i,DS4/DS5}$ is the percentage of deaths/injured with respect to the occupants in buildings with D4/D5 damage level.

Lastly, direct economic losses L have been computed based on damage repair cost (FEMA, 2003; Karaman et al., 2008; Molina et al., 2010), according to the following equation:

$$L = CU \left(\sum_{j=1}^{N_{masonry}} \sum_{ds=1}^{N_{DS}} A_{M_j} p_{M_j,ds} c_{ds} + \sum_{j=1}^{N_{RC}} \sum_{ds=1}^{N_{DS}} A_{RC_j} p_{RC_j,ds} c_{ds} \right)$$

CU is the Unit Cost of a building (including technical expenses and VAT); A_{M/RC_j} is the built area of the j^{th} masonry/R.C. building typology; $p_{M/RC_j,ds}$ is the probability, in the considered time range, for the j^{th} masonry/R.C. building typology to show a ds damage state Dk. Lastly, c_{ds} is the percentage cost of repair or replacement with respect to CU , given the ds damage state.

2.4.3 Fragility curves

Continuous functions for seismic vulnerability assessment were introduced slightly later than DPMs, since macroseismic intensity is not a continuous variable basically. A first attempt at deriving vulnerability as continuous information has been done by (Spence et al., 1991; Spence et al., 1992), using the Martin Centre database (which comprises about 70.000 buildings surveyed in 13 different earthquakes).

To overcome the discontinuity of macroseismic scales, a continuous variable (Parameterless Scale Intensity, PSI) to describe the seismic intensity was introduced. Later, a similar approach was used by Orsini et al., 1999, based on the data collected after the Irpinia 1980 seismic event.

PSI model is based on the main assumption that the structures belonging to a given vulnerability class overcome a given damage threshold for an intensity distributed according to Gaussian model. Thus, the use of PSI allowed the

definition of continuous functions depending on a macroseismic intensity parameter, tackling the problem that macroseismic intensity is not a continuous variable. However, both studies (Spence et al., 1992; Orsini et al., 1999) subsequently converted the PSI to PGA using empirical correlation functions.

Sabetta et al., 1998 derive fragility curves as a function of PGA, Arias Intensity and effective peak acceleration, based on a database of about 50000 buildings damaged after 1980 Irpinia and 1984 Abruzzi earthquakes. For each surveyed municipality (where at least 75% of buildings were inspected) and for each considered building class, a mean damage index was calculated as weighted average of the frequencies of each damage level. Then, empirical fragility curves were derived, assuming a binomial distribution for damage distribution.

Later, Rota et al., 2006 proposed fragility functions for typical building classes (e.g., seismically designed reinforced concrete buildings of 1-3 storeys) based on Italian post-earthquake damage data collected over the previous 30 years. PGA, obtained by means the ground motion prediction equation of Sabetta and Pugliese, 1987, was used as intensity measure, considering the same PGA value for all buildings located in the same municipality.

This approach was updated in Rota et al., 2008, based on about 91000 (out of the initial 164000 ones) damage survey forms. In fact, a preliminary data selection was done, disregarding survey forms with significant missing data, and including only data related to municipalities surveyed for at least 60%.

The Authors subdivided these data into 23 different building typologies and 10 ground motion intervals, using PGA as ground motion parameters. The adopted damage scale is similar to the EMS-98 scale (Grünthal, 1998), consisting of five levels of damage, plus the case of no damage. Hence, fragility curves were obtained by fitting the data with cumulative lognormal distributions, using an optimization technique (*Least square estimation*).

This latter is a procedure that minimizes the sum of squared differences (ε_j) between observed percentiles (y_j) and those predicted ($m(x_j)$) by means of a cumulative lognormal curve with unknown parameters (θ^{opt}).

$$\theta^{opt} = \underset{\theta}{\operatorname{argmin}} \sum_{j=1}^M \varepsilon_j^2 = \underset{\theta}{\operatorname{argmin}} \sum_{j=1}^M w_j (y_j - m(x_j))^2$$

In the above equation, M is the number of bins obtained by grouping the post-earthquake damage data in bins of similar ground motion intensities. x_j is the seismic intensity measure value in the j^{th} bin. Moreover, the inverse of standard deviation estimated in a bootstrap re-sampling technique (Efron et al., 1994) was used as weight w_j in the fitting procedure to account for the heteroskedasticity (non-constant variance) of the data.

Later, Ioannou et al., 2012 proposed fragility curves, derived by means of a different fitting/optimization technique, namely the MLE (i.e., *Maximum Likelihood Estimation*; Baker, 2015) method. Basically, whilst LSE searches for the parameter values that provide the most accurate description of the data, MLE searches for the parameter values that are most likely to have produced the same data, maximizing a certain likelihood function. In Ioannou et al., 2012, MLE technique was implemented, assuming a binomial likelihood function according to the following equation:

$$\begin{aligned} \theta^{opt} &= \underset{\theta}{\operatorname{argmax}} L(\theta) \\ &= \underset{\theta}{\operatorname{argmax}} \log \left\{ \prod_{j=1}^M \left[\binom{y_j}{m_j} P(DS \geq ds_i | x_j; \theta)^{y_j} [1 - P(DS \geq ds_i | x_j; \theta)]^{m_j - y_j} \right] \right\} \end{aligned}$$

$P(DS \geq ds_i | x_j; \theta)$ is the probability of reaching or exceeding a given (ds_i) damage state, being the intensity measure equal to x_j and the curve's parameters equal to θ .

In Ioannou et al., 2012, cumulative lognormal distribution (see Eq.(a) of Table 1), fully described by two parameters (i.e., the median θ and the logarithmic standard deviation β), has been considered as functional form.

Moreover, the possible overlapping of the obtained curves, which leads to meaningless results, was avoided by performing ordinal regression (Shinozuka

et al, 2000) analysis, which recognises the ordered categorical nature of the damage data.

Table 1. Main functional forms used in the literature to express the fragility curves.

Eq.	$P(DS \geq ds_i IM = x)$	References
(a)	$\Phi\left(\frac{\ln(x) - \vartheta}{\beta}\right)$	Shinozuka et al, 2000; Rota et al., 2008; Colombi et al., 2008; Liel and Lynch, 2009; Ioannou et al., 2012; Del Gaudio et al., 2017; Del Gaudio et al., 2019; Rosti et al., 2020; D'Amato et al., 2020; Zuccaro et al., 2020
(b)	$\Phi\left(\frac{x - \mu}{\sigma}\right)$	Spence et al, 1992; Orsini, 1999; Karababa and Pomonis, 2010
(c)	$\frac{1}{1 + \exp(-(\vartheta_0 + \vartheta_1 x))}$	Basöz et al, 1999; O' Rourke et al., 2000
(d)	$1 - \exp(-\vartheta_0 x^{\vartheta_1})$	Rossetto and Elnashai, 2003; Amiri et al., 2007; Del Gaudio et al., 2017

Del Gaudio et al., 2017 provided fragility curves, based on a database of 7597 private Reinforced Concrete buildings located in the city and the province of L'Aquila surveyed after the 2009 earthquake. In this study, both MLE and LSE techniques were used, assuming as functional form cumulative lognormal distributions. Differently from Rota et al., 2008, the weight used in the fitting LSE procedure was the number of buildings (Sabetta et al., 1998) in each isoseismic unit. Furthermore, in addition to lognormal distribution (Eq.(a) in Table 1), also exponential one (Eq.(d) in Table 1; Rossetto and Elnashai, 2003; Amiri et al., 2007) has been considered as functional form, overall resulting in 4 (2 functional forms x 2 regression models) set of fragility curves.

The study highlighted that the use of the exponential distribution yields slightly better results, i.e., lower weighted sum of the square of the errors or higher Likelihood, respectively if LSE or MLE model is used.

Despite that, lognormal distribution is the most widely used functional form in the fragility evaluations. Its popularity is due essentially to three properties (Rossetto et al., 2013): (1) y-axis is defined in the range [0, 1], that is particularly suitable for expressing probabilities; (2) x-axis is defined in the range [0, +∞], as

well as almost all the ground motion intensity measures; (3) this distribution appears to be skewed to the left, and can thus better reflect the frequency of the observations (mostly clustered at low ground motion intensities). Conversely, the normal cumulative (e.g., Spence et al, 1992; Orsini, 1999; Karababa and Pomonis, 2010) distribution function and logistic one (Basöz et al, 1999; O’Rourke et al., 2000), respectively reported as Eq.(b) and Eq.(c) in Table 1, are mostly preferred by studies that use intensity measures defined in the range $[-\infty, +\infty]$, such as the PSI.

In previous studies, beyond the binomial (e.g., Ioannou et al., 2012; Del Gaudio et al., 2017; Del Gaudio et al., 2019) likelihood function, also multinomial one (e.g., Charvet et al. 2014; Macabuag et al. 2016; Del Gaudio et al., 2020; Rosti et al., 2020; D’Amato et al., 2020) has been adopted. Such distribution is basically a generalization of the binomial one, and the assumption of multinomial likelihood function means that the repartition of buildings in the different damage states, for a given intensity measure, is described by the multinomial distribution.

For example, Rosti et al., 2020 has proposed fragility curves for six classes of R.C. buildings (as a function of the design type and of the number of storeys), based on data collected after several Italian earthquakes (available on Da.D.O. platform, Dolce et al., 2019). Such fragility curves have been derived, assuming the cumulative lognormal distribution as functional form and a common logarithmic standard deviation (for all damage states) to avoid crossing curves (Lallemant et al. 2015; Porter, 2018). The MLE fitting procedure has based on the assumption of multinomial likelihood function, according to the following equation:

$$\theta^{opt} = \operatorname{argmax} L(\theta) = \operatorname{argmax} \log \left(\prod_{j=1}^M \prod_{i=0}^{N_{DS}} \frac{N_j!}{n_{ij}!} P(DS = ds_i | x_j; \theta)^{n_{ij}} \right)$$

N_{DS} is the number of damage states, equal to 5+1 (null damage) according to the EMS-98 scale (Grünthal, 1998). $P(DS = ds_i | x_j; \theta)$ is the probability of occurrence of ds_i , given the j^{th} value of the intensity measure (x_j).

Clearly, such probability can be written as a function of the corresponding probability of exceeding, herein assumed as a lognormal cumulative function.

$$P(DS = ds_i | x_j; \theta) = \begin{cases} 1 - P(DS \geq ds_1 | x_j; \theta_1 \beta) & i = 0 \\ P(DS \geq ds_i | x_j; \theta_i \beta) - P(DS \geq ds_{i+1} | x_j; \theta_{i+1} \beta) & i \in [1; 4] \\ P(DS \geq ds_5 | x_j | PGA_j; \theta_5 \beta) & i = 5 \end{cases}$$

In vulnerability and fragility evaluations, the choice of the intensity measure (IM) is a critical point: in fact, some uncertainty partly depends on the capacity of chosen IM to describe the potential damage and consequent losses (Rossetto et al., 2013).

In previous studies, most frequently adopted IMs are macroseismic intensity and peak ground acceleration (PGA). The first one correlates well with observed damage but is a subjective and discrete measure. Furthermore, macroseismic intensity can also introduce an inter-dependence with predicted vulnerability or fragility, being determined itself through the direct observation of damage in a given building stock.

Instead, PGA is an objective and continuous measure, but could be worse correlated with observed damage, especially for ductile structures (Rossetto and Elnashai, 2003). It is to be noted that when the seismic intensity is measured by means of a parameter related to the spectral acceleration or spectral displacement at the fundamental period of vibration (e.g., Scawthorn et al. 1981; Shinozuka et al. 1997; Rossetto and Elnashai, 2003; Colombi et al., 2008; Yamazaki et al., 2019; Zucconi et al., 2020; D'Amato et al., 2020), different from macroseismic intensity or PGA, the vulnerability curves show a better prediction capacity, taking into consideration the relationship between the frequency content of the ground motion and the dynamic characteristics of the building stock. In such

cases, usually the seismic “demand” derives from a ground-motion prediction equation, using an estimated mean period of vibration for each building type.

2.5 REFERENCES

- [1] Amiri G.G., Jalalian M., Amrei S.A.R. (2007). Derivation of vulnerability functions based on observational data for Iran. Proceedings of International Symposium on Innovation & Sustainability of Structures in Civil Engineering.
- [2] Ang A.H., & TANG W. H. (2007). Probability concepts in engineering. Wiley. (ISBN: 978-0-471-72064-5)
- [3] Augusti, Giuliano, Marcello Ciampoli, and Paolo Giovenale. "Seismic vulnerability of monumental buildings." *Structural Safety* 23.3 (2001): 253-274.
- [4] Baggio, C., Bernardini, A., Colozza, R., Corazza, L., Della Bella, M., Di Pasquale, G., Papa, F., 2007. Field manual for post-earthquake damage and safety assessment and short term countermeasures (AeDES). European Commission—Joint Research Centre—Institute for the Protection and Security of the Citizen, EUR, 22868.
- [5] Baker JW (2015) Introduction to Probabilistic Seismic Hazard Analysis. White Paper Version 2.1, 77 pp
- [6] Barthel, R., Agency, U. S. F. E. M., and Reclamation, U. S. B. o. (1998). FEMA 178, Seismic Evaluation of Existing Building: Supplemental Class Notes. U.S. Department of the Interior, Bureau of Reclamation.
- [7] Basöz, Nesrin, and Anne S. Kiremidjian. "Development of empirical fragility curves for bridges." *Optimizing post-earthquake lifeline system reliability*. ASCE, 1999.
- [8] Benedetti, D., and V. Petrini. "On seismic vulnerability of masonry buildings: proposal of an evaluation procedure." *L'industria delle Costruzioni* 18.2 (1984): 66-74.
- [9] Bernardini A. Classi macrosismiche di vulnerabilità degli edifici in area veneto-friulana. Atti XI Congresso nazionale “L’ingegneria sismica in Italia”, Genova, CD_Rom;2004. **(in Italian)**
- [10] Bertelli, Silvia, Tiziana Rossetto, and Ioanna Ioannou. "Derivation of empirical fragility functions from the 2009 l'aquila earthquake." *Proceedings 16th European Conference on Earthquake Engineering*. Vol. 16. European Association of Earthquake Engineering, 2018.
- [11] Borzi B, Onida M, Faravelli M, Polli D, Pagano M, Quaroni D, Cantoni A (2020) IRMA platform for the calculation of damages and risks of residential buildings, *Bulletin of Earthquake Engineering*.

- [12] Braga F., Dolce M., Liberatore D., 1982. A statistical study on damaged buildings and an ensuing review of the MSK-76 scale. Proceedings of the seventh European conference on earthquake engineering, Athens, Greece, 431-450.
- [13] Bramerini F, Di Pasquale G (2008) Updated seismic risk maps for Italy. Ing Sismica XXV (2):5–23 (in Italian)
- [14] Brando, Giuseppe, Gianfranco De Matteis, and Enrico Spacone. "Predictive model for the seismic vulnerability assessment of small historic centres: application to the inner Abruzzi Region in Italy." *Engineering Structures* 153 (2017): 81-96.
- [15] Brzev S., Scawthorn C., Charleson A.W., Allen L., Greene M., Jaiswal K.S., et al., GEM Building Taxonomy, Version 2.0, GEM Technical Report, GEM Foundation, Pavia, Italy, 2013-02, p. 188, <https://doi.org/10.13117/GEM.EXP-MOD>.
- [16] Calvi, G. M., Pinho, R., Magenes, G., Bommer, J. J., Restrepo-Vélez, L. F., & Crowley, H. (2006). Development of seismic vulnerability assessment methodologies over the past 30 years. *ISET journal of Earthquake Technology*, 43(3), 75-104.
- [17] Canuti C, Carbonari S, Dall’asta A, Dezi L, Gara F, Leoni G, Morici M, Petrucci E, Prota A, Zona A (2019) Post-earthquake damage and vulnerability assessment of churches in the Marche region struck by the 2016 Central Italy Seismic Sequence. *Int J Archit Heritage*. <https://doi.org/10.1080/15583058.2019.1653403>
- [18] Cescatti E, Salzano P, Casapulla C, Ceroni F, da Porto F, Prota A (2020) Damages to masonry churches after 2016–2017 Central Italy seismic sequence and definition of fragility curves. *Bull Earthq Eng* 18(1):297–329
- [19] Charvet I, Ioannou I, Rossetto T, Suppasri A, Imamura F (2014) Empirical fragility assessment of buildings affected by the 2011 Great East Japan tsunami using improved statistical models. *Nat Hazards* 73:951–973.
- [20] Colombi, M., Borzi, B., Crowley, H. et al., 2008. Deriving vulnerability curves using Italian earthquake damage data. *Bull Earthquake Eng* 6, 485–504. <https://doi.org/10.1007/s10518-008-9073-6>
- [21] Corsanego, Alfredo, Giancarlo Giorgini, and Giovanni Roggeri. "Rapid evaluation of an indicator of seismic vulnerability in small urban nuclei." *Natural hazards* 8.2 (1993): 109-120.
- [22] Council, A. T., Response, P. f., Recovery, and Agency, U. S. F. E. M. (1999). *Evaluation of Earthquake Damaged Concrete and Masonry Wall Buildings: Basic Procedures Manual*. The Agency.

- [23] D'Ayala D.F., Paganoni S., 2011. Assessment and analysis of damage in L'Aquila historic city centre after 6th April 2009. *Bulletin of Earthquake Engineering*, 9(1), 81-104.
- [24] da Porto F, Donà M, Rosti A, Rota M, Lagomarsino S, Cattari S, Borzi B, Onida M, De Gregorio D, Perelli FL, Del Gaudio C, Ricci P, Speranza E (2021) Comparative analysis of the fragility curves for Italian masonry and RC buildings. *Bull Earthq Eng* 19(7):219–231
- [25] da Porto F, Silva B, Costa C, Modena C (2012) Macro-scale analysis of damage to churches after earthquake in Abruzzo (Italy) on April 6, 2009. *J Earthq Eng* 16(6):739–758
- [26] D'Amato M, Laguardia R, Di Trocchio G, Coltellacci M, Gigliotti R. Seismic Risk Assessment for Masonry Buildings Typologies from L'Aquila 2009 Earthquake Damage Data. *Journal of Earthquake Engineering* 2020; 00(00): 1-35. DOI: 0.1080/13632469.2020.1835750.
- [27] De Matteis G, Criber E, Brando G (2016) Damage probability matrices for Three-Nave Masonry Churches in Abruzzi after the 2009 L'Aquila Earthquake. *Int J Archit Heritage* 10(2–3):120–145
- [28] Decanini L.D., De Sortis A., Goretti A., Liberatore L., Mollaioli F., Bazzurro P. [2004] "Performance of Reinforced Concrete Buildings During the 2002 Molise, Italy, Earthquake", *Earthquake Spectra*, Vol. 20, No. S1, pp. S221-S255.
- [29] Del Gaudio C., De Martino G., Di Ludovico M., Manfredi G., Prota A., Ricci P. and Verderame G.M.; 2017: Empirical fragility curves from damage data on RC buildings after the 2009 L'Aquila earthquake. *Bull. Earthquake Eng.*, 15, 1425-1450.
- [30] Del Gaudio C., De Martino G., Di Ludovico M., Manfredi G., Prota A., Ricci P., Verderame G.M., 2019. Empirical fragility curves for masonry buildings after the 2009 L'Aquila, Italy, earthquake. *Bulletin of Earthquake Engineering*. <https://doi.org/10.1007/s10518-019-00683-4>.
- [31] Del Gaudio C., Ricci P., Verderame G.M., 2015. ECS-it – Evoluzione della classificazione sismica in Italia. ReLUIS, Naples, Italy. Available at <http://www.reluis.it>.
- [32] Del Gaudio, C., Di Ludovico, M., Polese, M. et al. Seismic fragility for Italian RC buildings based on damage data of the last 50 years. *Bull Earthquake Eng* 18, 2023–2059 (2020). <https://doi.org/10.1007/s10518-019-00762-6>

- [33] Del Gaudio, C., Scala, S.A., Ricci, P., Verderame G.M., 2021. Evolution of the seismic vulnerability of masonry buildings based on the damage data from L'Aquila 2009 event. *Bull Earthquake Eng* (2021). <https://doi.org/10.1007/s10518-021-01132-x>
- [34] Di Ludovico M, Prota A, Moroni C, Manfredi G, Dolce M (2017a) Reconstruction process of damaged residential buildings outside the historical centres after L'Aquila earthquake-part I: "light damage" reconstruction. *Bull Earthq Eng*. <https://doi.org/10.1007/s10518-016-9877-8>
- [35] Di Ludovico M, Prota A, Moroni C, Manfredi G, Dolce M (2017b) Reconstruction process of damaged residential buildings outside historical centres after the L'Aquila earthquake-part II: "heavy damage" reconstruction. *Bull Earthq Eng*. <https://doi.org/10.1007/s10518-016-9979-3>
- [36] Di Pasquale G, Goretti A (2001) Functional and economic vulnerability of residential buildings affected by recent Italian earthquakes. In: *Proceedings of the 10th national conference of seismic engineering in Italy, Potenza-Matera, Italy (in Italian)*.
- [37] Di Pasquale, Giacomo, Giampiero Orsini, and Roberto W. Romeo. "New developments in seismic risk assessment in Italy." *Bulletin of Earthquake Engineering* 3.1 (2005): 101-128.
- [38] Dolce M, Moroni C, Samela C, et al. (2001) Una Procedura di Normalizzazione del Danno per la Valutazione degli Effetti di Amplificazione Locale. In: *Proceedings of the X national conference of seismic engineering, Potenza-Matera, 9–13 September (in Italian)*.
- [39] Dolce M, Prota A, Borzi B, da Porto F, Lagomarsino S, Magenes G, Moroni C, Penna A, Polese M, Speranza E, Verderame GM, Zuccaro G (2020) Seismic Risk Assessment of residential buildings in Italy. *Bull Earthq Eng*. <https://doi.org/10.1007/s10518-020-01009-5>
- [40] Dolce M., Goretti A., 2015. Building damage assessment after the 2009 Abruzzi earthquake. *Bulletin of Earthquake Engineering* 13, 2241–2264 (2015). <https://doi.org/10.1007/s10518-015-9723-4>.
- [41] Dolce M., Masi A., Marino M. and Vona M.; 2003: Earthquake damage scenarios of the building stock of Potenza (southern Italy) including site effects. *Bull. Earthquake Eng.*, 1, 115-140.

- [42] Dolce M., Speranza E., Giordano F., Borzi B., Bocchi F., Conte C., Di Meo A., Faravelli M. and Pascale V.; 2019: Observed damage database of past Italian earthquakes: the Da.D.O. Webgis. *Boll. Geof. Teor. Appl.*, 60, 141-164.
- [43] Dolce, M., Kappos, A., Masi, A., Penelis, G., & Vona, M. (2006). Vulnerability assessment and earthquake damage scenarios of the building stock of Potenza (Southern Italy) using Italian and Greek methodologies. *Engineering Structures*, 28(3), 357-371.
- [44] Donà M, Carpanese P, Follador V, Sbrogiò L, da Porto F (2020) Mechanics-based fragility curves for Italian residential URM buildings. *Bull Earthq Eng* 19(7):256. [https:// doi. org/ 10. 1007/ s10518- 020- 00928-7](https://doi.org/10.1007/s10518-020-00928-7)
- [45] Dubois, Didier, and Henri Prade. "Systems of linear fuzzy constraints." *Fuzzy sets and systems* 3.1 (1980): 37-48.
- [46] Efron B, Tibshirani RJ. An introduction to the bootstrap. London: Chapman & Hall/CRC; 1994.
- [47] Eleftheriadou A.K., Karabinis A.I. [2008] "Damage probability matrices derived from earthquake statistical data", *Proceedings of 14th World Conference on Earthquake Engineering*, Beijing, China.
- [48] Federal Emergency Management Agency (FEMA) (2003) multi-hazard loss estimation methodology earthquake model, HAZUS-MH MR3 Technical Manual
- [49] Federal Emergency Management Agency (FEMA) (2012) Hazus-MH 2.1 technical manual: earthquake model
- [50] Ferreira, Tiago M., Romeu Vicente, and Humberto Varum. "Seismic vulnerability assessment of masonry facade walls: development, application and validation of a new scoring method." *Structural Engineering and Mechanics* 50.4 (2014): 541-561.
- [51] Ferreira, Tiago Miguel, et al. "Seismic vulnerability assessment of stone masonry façade walls: Calibration using fragility-based results and observed damage." *Soil Dynamics and Earthquake Engineering* 103 (2017): 21-37.
- [52] Fuentes, D. D., M. Laterza, and M. D'Amato, 2019. Seismic vulnerability and risk assessment of historic constructions: The case of Masonry and Adobe Churches in Italy and Chile. *Conference: SAHC - 11th International Conference on Structural Analysis of Historical Constructions*, Cusco (Perù). *RILEM Bookseries* 18, pp. 1127–1137, Paper n. 122.

- [53] Fuentes, D. D., Baquedano Julià, P. A., D'Amato, M., & Laterza, M. (2021). Preliminary seismic damage assessment of Mexican churches after September 2017 earthquakes. *International Journal of Architectural Heritage*, 15(4), 505-525.
- [54] Giovinazzi S, Lagomarsino S (2002) Wp04: guidelines for the implementation of the level I methodology for the vulnerability assessment of current buildings. RISK-UE project: an advanced approach to earthquake risk scenarios with applications to different European towns. Contract No. EVK4-CT-2000-00014, Genoa.
- [55] Giovinazzi, Sonia, and Sergio Lagomarsino. "A macroseismic method for the vulnerability assessment of buildings." 13th World Conference on Earthquake Engineering. Vol. 896. 2004.
- [56] Goded, T., Lewis, A., & Stirling, M. (2018). Seismic vulnerability scenarios of Unreinforced Masonry churches in New Zealand. *Bulletin of Earthquake Engineering*, 16(9), 3957-3999.
- [57] Goretti, A., & Di Pasquale, G. (2004). Building inspection and damage data for the 2002 Molise, Italy, earthquake. *Earthquake Spectra*, 20(1_suppl), 167-190.
- [58] Graber, T., Management, U. S. B. o. L., and Reclamation, U. S. B. o. (1999). FEMA 310, Seismic Evaluation of Buildings, Boise District Office Building, Boise, Ada County, Idaho. U.S. Department of the Interior, Bureau of Reclamation.
- [59] Grünthal M., 1998. European Macro-seismic Scale. *Cahiers du Centre Européen de Géodynamique et de Séismologie*, Vol. 15. European Macro-seismic Scale 1998. European Center for Geodynamics and Seismology. **(in French)**.
- [60] Guerreiro L, Azevedo J, Proença J, Bento R, Lopes M (2000) Damage in ancient churches during the 9th of July 1998 Azores earthquake. *Proceedings of XII World Conference on Earthquake Engineering*. January 30-February 4, 2000, Auckland, New Zealand.
- [61] Güllkan P., Sucuoğlu H., Ergüney O. [1992] "Earthquake vulnerability, loss and risk assessment in Turkey", *Proceedings of 1th World Conference on Earthquake Engineering Madrid, Spain*
- [62] H. Sandi, I. Floricel. Analysis of seismic risk affecting the existing building stock. *Proceedings of the 10th European conference on earthquake engineering*, Vienna, vol. 2, A. A. Balkema, Rotterdam (1994), pp. 1105-1110

- [63] Ioannou, I., Rossetto, T., & Grant, D. N. (2012, September). Use of regression analysis for the construction of empirical fragility curves. In Proceedings of the 15th world conference on earthquake engineering, September.
- [64] ISTAT 1991. Istituto Nazionale di Statistica (National Institute of Statistics). 13° Censimento generale della popolazione e delle abitazioni. **(in Italian)**
- [65] ISTAT 2001. Istituto Nazionale di Statistica (National Institute of Statistics). 14° Censimento generale della popolazione e delle abitazioni. **(in Italian)**
- [66] ISTAT 2011. Istituto Nazionale di Statistica (National Institute of Statistics). 15° Censimento generale della popolazione e delle abitazioni. Dati sulle caratteristiche strutturali della popolazione, delle abitazioni e variabili. **(in Italian)** <http://www.istat.it/it/archivio/104317>
- [67] Italian Civil Protection Department (2018) National Risk Assessment 2018. Overview of the potential major disasters in Italy. Updated December 2018
- [68] Jaiswal K., Wald D., Porter K., A global building inventory for earthquake loss estimation and risk management, *Earthq. Spectra* 26 (2010) 731–748, <https://doi.org/10.1193/1.3450316>.
- [69] Jorquera, N., G. Misseri, N. Palazzi, L. Rovero, and U. Tonietti. 2017. Structural characterization and seismic performance of San Francisco church, the most ancient monument in Santiago, Chile. *International Journal of Architectural Heritage* 11 (8):1061–85.
- [70] Karababa, F.S., Pomonis, A., 2011. Damage data analysis and vulnerability estimation following the August 14, 2003 Lefkada Island, Greece, Earthquake. *Bull Earthquake Eng* 9, 1015–1046. <https://doi.org/10.1007/s10518-010-9231-5>
- [71] Karaman H, Şahin M, Elnashai AS (2008) Earthquake Loss Assessment Features of Maeviz-Istanbul (Hazturk). *J Earthq Eng* 12(S2):175–186
- [72] Kircher, Charles A., Robert V. Whitman, and William T. Holmes. "HAZUS earthquake loss estimation methods." *Natural Hazards Review* 7.2 (2006): 45-59.
- [73] Lagomarsino G. and Giovinazzi S.; 2006: Macroseismic and mechanical models for the vulnerability and damage assessment of current buildings. *Bull. Earthquake Eng.*, 4, 415-443.
- [74] Lagomarsino S, Cattari S (2014) Fragility functions of masonry buildings. In: Pitilakis K, Crowley H, Kaynia AM (eds) SYNER-G: typology definition and fragility functions for physical elements at seismic risk: elements at seismic risk, geotechnical, geological and earthquake engineering. Springer

- [75] Lagomarsino, S., Cattari, S. & Ottonelli, D. The heuristic vulnerability model: fragility curves for masonry buildings. *Bull Earthquake Eng* 19, 3129–3163 (2021). <https://doi.org/10.1007/s10518-021-01063-7>
- [76] Lagomarsino, Sergio, and Stefano Podestà. "Seismic vulnerability of ancient churches: II. Statistical analysis of surveyed data and methods for risk analysis." *Earthquake Spectra* 20.2 (2004): 395-412.
- [77] Lagomarsino, Sergio, et al. "Earthquake damage assessment of masonry churches: proposal for rapid and detailed forms and derivation of empirical vulnerability curves." *Bulletin of earthquake engineering* 17.6 (2019): 3327-3364.
- [78] Lallemand, D., Kiremidjian, A., & Burton, H. (2015). Statistical procedures for developing earthquake damage fragility curves. *Earthquake Engineering & Structural Dynamics*, 44(9), 1373-1389.
- [79] Lantada, N., Irizarry, J., Barbat, A. H., Goula, X., Roca, A., Susagna, T., & Pujades, L. G. (2010). Seismic hazard and risk scenarios for Barcelona, Spain, using the Risk-UE vulnerability index method. *Bulletin of earthquake engineering*, 8(2), 201-229. doi:10.1007/s10518-009-9148-z
- [80] Leite J, Lourenco PB, Ingham JM (2013) Statistical assessment of damage to churches affected by the 2010–2011 canterbury (New Zealand) earthquake sequence. *J Earthq Eng* 17(1):73–97
- [81] Liel A.B., Lynch K.P. [2009] "Vulnerability of reinforced concrete frame buildings and their occupants in the 2009 L'Aquila", *Natural Hazards Review*, Vol. In press.
- [82] Lucantoni A, Bosi V, Bramerini F, De Marco R, Lo Presti T, Naso G, Sabetta F (2001) Seismic risk in Italy. *Ing Sismica XVI* I(1):5–36 (in Italian)
- [83] Macabuag, Joshua, et al. "A proposed methodology for deriving tsunami fragility functions for buildings using optimum intensity measures." *Natural Hazards* 84.2 (2016): 1257-1285.
- [84] Marotta A, Sorrentino L, Liberatore D, Ingham JM (2018) Seismic risk assessment of New Zealand unreinforced Masonry Churches using statistical procedures. *Int J Archit Heritage* 12(3):448–464
- [85] Masi, A., Lagomarsino, S., Dolce, M. et al. Towards the updated Italian seismic risk assessment: exposure and vulnerability modelling. *Bull Earthquake Eng* 19, 3253–3286 (2021). <https://doi.org/10.1007/s10518-021-01065-5>
- [86] Medvedev SV (1977) Seismic Intensity Scale M.S.K.-76, Publ. Inst. Geophysics. Pol. Acad. Sc., A-6 (117), Varsavia.

- [87] Michelini A., Faenza L., Lauciani V., Malagnini L., 2008. ShakeMap implementation in Italy. *Seismological research letters*, 79(5); 2008, 688–697.
- [88] Molina Palacios S, Lang DH, Lindholm C (2010) SELENA: an open-source tool for seismic risk and loss assessment using a logic tree computation procedure. *Comput Geosci* 36(2010):257–269
- [89] Mouroux P, Bertrand M, Bour M, Brun BL, Depinois S, Masure P, Risk-UE Team (2004) The European Risk-UE project: an advanced approach to earthquake risk scenarios. In: *Proceedings of the 13th world conference earthquake engineering, Vancouver (CD-ROM, paper no. 3329)*
- [90] Nash J.E. and Sutcliffe J.V.; 1970: River flow forecasting through conceptual models: Part I, a discussion of principles. *J. Hydrol.*, 10, 282-290.
- [91] Omidvar, Babak, Behrouz Gatmiri, and Sahar Derakhshan. "Experimental vulnerability curves for the residential buildings of Iran." *Natural Hazards* 60.2 (2012): 345-365.
- [92] O'Rourke, Michael J., and Pak So. "Seismic fragility curves for on-grade steel tanks." *Earthquake spectra* 16.4 (2000): 801-815.
- [93] Orsini G., 1999. A model for buildings' vulnerability assessment using the Parameterless Scale of Seismic Intensity (PSI). *Earthquake Spectra*, 15(3), 463-483.
- [94] Palazzi, N., L. Rovero, U. Tonietti, J. C. de la Llera, and C. Sandoval. 2018. Seismic vulnerability assessment of Basilica del Salvador, a significant example of neo-gothic architecture in Santiago, Chile. *Proceedings of 16th European Conference on Earthquake Engineering at Thessalonica, Greece*.
- [95] Penna A, Calderini C, Sorrentino L, Carocci CF, Cescatti E, Sisti R, Borri A, Modena C, Prota A (2019) Damage to churches in the 2016 central Italy earthquakes. *Bull Earthq Eng* 17(10):5763–5790
- [96] Pitilakis K, Alexoudi M, Argyroudis S, Anastasiadis A (2006) Seismic risk scenarios for an efficient seismic risk management: the case of Thessaloniki (Greece). *Adv Earthq Eng Urban Risk Reduct*. doi:10.1007/ 1-4020-4571-9_15
- [97] Pitilakis K, Crowley H, Kaynia AM (2014) Introduction in: *SYNER-G: Typology Definition and Fragility Functions for Physical Elements at Seismic Risk, Buildings, Lifelines, Transportation Networks and Critical Facilities*, Pitilakis K, Crowley H, Kaynia AM (editors) Springer Science+Business Media Dordrecht 2014
- [98] Pittore M, Haas M and Megalooikonomou KG (2018) Risk-Oriented, Bottom-Up Modeling of Building Portfolios with Faceted Taxonomies. *Front. Built Environ*. 4:41. doi: 10.3389/fbuil.2018.00041

- [99] Porter K (2018) A beginner's guide to fragility, vulnerability, and risk. University of Colorado Boulder. <http://spot.colorado.edu/~porterka/Porter-beginnersguide.pdf>
- [100] Rapone, Davide, et al. "Seismic vulnerability assessment of historic centers: description of a predictive method and application to the case study of Scanno (Abruzzi, Italy)." *International Journal of Architectural Heritage* 12.7-8 (2018): 1171-1195.
- [101] Regio Decreto 18 Aprile 1909. Provvedimenti e disposizioni in seguito al terremoto del 28 dicembre 1908. **(in Italian)**
- [102] Pnevmatikos, N., Konstandakopoulou, F., & Koumoutsos, N. (2020). Seismic vulnerability assessment and loss estimation in Cephalonia and Ithaca islands, Greece, due to earthquake events: A case study. *Soil Dynamics and Earthquake Engineering*, 136, 106252.
- [103] Roca A., Goula X., Susagna T., Chávez J., González M., Reinoso E. [2006] "A simplified method for vulnerability assessment of dwelling buildings and estimation of damage scenarios in Catalonia, Spain", *Bulletin of Earthquake Engineering*, Vol. 4, No. 2, pp. 141-158
- [104] Rossetto T., Ioannou I., Grant D.N., 2013. Existing empirical fragility and vulnerability functions: Compendium and guide for selection, GEM Technical Report 2013-X, GEM Foundation, Pavia, Italy.
- [105] Rossetto, T. and Elnashai, A. (2003) Derivation of Vulnerability Functions for European-Type RC Structures Based on Observational Data. *Engineering Structures*, 25, 1241-1263. [http://dx.doi.org/10.1016/S0141-0296\(03\)00060-9](http://dx.doi.org/10.1016/S0141-0296(03)00060-9)
- [106] Rossetto, Tiziana, and Ioanna Ioannou. "Empirical fragility and vulnerability assessment: not just a regression." *Risk Modeling for Hazards and Disasters*. Elsevier, 2018. 79-103.
- [107] Rossetto, Tiziana, et al. "Advances in the assessment of buildings subjected to earthquakes and tsunamis." *European Conference on Earthquake Engineering Thessaloniki, Greece*. Springer, Cham, 2018.
- [108] Rosti A., Del Gaudio C., Di Ludovico M., Magenes G., Penna A., Polese M., Verderame G.M., 2020a. Empirical vulnerability curves for Italian residential buildings. *Bollettino di Geofisica Teorica ed Applicata*, 61(3).
- [109] Rosti A., Del Gaudio C., Rota M., Ricci P., Di Ludovico M., Penna A., Verderame G.M., 2020b. Empirical fragility curves for Italian residential RC

- buildings. *Bull Earthquake Eng* (2020). <https://doi.org/10.1007/s10518-020-00971-4>.
- [110] Rosti A., Rota M., Penna A., 2020c. Empirical fragility curves for Italian URM buildings. *Bulletin of Earthquake Engineering*.
- [111] Rosti, A., Rota, M., & Penna, A. (2018). Damage classification and derivation of damage probability matrices from L'Aquila (2009) post-earthquake survey data. *Bulletin of Earthquake Engineering*, 16(9), 3687-3720.
- [112] Rota M., Penna A., Strobbia C.L., 2008. Processing italian damage data to derive typological fragility curves. *Soil Dynamics and Earthquake Engineering*, 933-947.
- [113] Rota, Maria, Andrea Penna, and Claudio Strobbia. "Typological fragility curves from Italian earthquake damage data." *Proceedings of the First European Conference on Earthquake Engineering and Seismology*, Geneva, Switzerland, Paper. No. 386. 2006.
- [114] Sabetta F., Goretti A., Lucantoni A., 1998. Empirical Fragility Curves from Damage Surveys and Estimated. 11th European Conference on Earthquake Engineering © 1998 Balkema, Rotterdam, ISBN 90 5410 982 3.
- [115] Sabetta, Fabio, and Antonio Pugliese. "Attenuation of peak horizontal acceleration and velocity from Italian strong-motion records." *Bulletin of the Seismological Society of America* 77.5 (1987): 1491-1513.
- [116] Sarabandi P., Pachakis D., King S., Kiremidjian A. [2004] "Empirical fragility functions from recent earthquakes", *Proceedings of 13th World Conference on Earthquake Engineering*, Vancouver, Canada.
- [117] Scala S.A., Del Gaudio C., Verderame G.M., 2022. Influence of construction age on seismic vulnerability of masonry buildings damaged after 2009 L'Aquila Earthquake (**under review**)
- [118] Scawthorn C., Iemura H., Yamada Y. [1981] "Seismic damage estimation for low- and mid-rise buildings in Japan", *Earthquake Engineering & Structural Dynamics*, Vol. 9, No. 2, pp. 93-115.
- [119] Shinozuka, Masanobu, et al. "Statistical analysis of fragility curves." *Journal of engineering mechanics* 126.12 (2000): 1224-1231.
- [120] Sisti R., Di Ludovico M., Borri A., Protà A., 2018. Damage assessment and the effectiveness of prevention: the response of ordinary unreinforced masonry buildings in Norcia during the Central Italy 2016–2017 seismic sequence. *Bulletin of Earthquake Engineering*, 1-21. <https://doi.org/10.1007/s10518-018-0448-z>.

- [121] Sorrentino L, Liberatore L, Decanini LD, Liberatore D (2014) The performance of churches in the 2012 Emilia earthquakes. *Bull Earthq Eng* 12(5):2299–2331
- [122] Sorrentino L., D'Ayala D., de Felice G. et al., 2017. Review of out-of-plane seismic assessment techniques applied to existing masonry buildings. *Int J Archit Herit* 11:2–21. <https://doi.org/10.1080/15583058.2016.1237586>.
- [123] So, E.K.M., Pomonis, A., Below, R., Cardona, O., King, A., Zulfikar, C., Koyama, M., Scawthorn, C., Ruffle, S., Garcia, D., 2012. An introduction to the global earthquake consequences database (GEMECD). In: *The Proceedings of the 15th World Conference on Earthquake Engineering 2012*, Lisbon, 10 pp.
- [124] Spence, R., So, E., Jenkins, S., Coburn, A., Ruffle, S., 2011. A global earthquake building damage and casualty database. In: *Human Casualties in Earthquakes*. Springer, Netherlands, pp. 65e79.
- [125] Spence R, Coburn A, Pomonis A, So E, Jenkins S, Saito K, Lee V, Tuck H, Furukawa A (2009) Cambridge university earthquake damage database. <http://www.arct.cam.ac.uk/EQ>.
- [126] Spence R.J.S., Coburn A.W., Pomonis A. 1992. "Correlation of ground motion with building damage: The definition of a new damage-based seismic intensity scale", *Proceedings of 10th World Conference on Earthquake Engineering*, Balkema, Rotterdam.
- [127] Spence, R. J. S., et al. "A Parameterless scale of seismic intensity for use in seismic risk analysis and vulnerability assessment." *Earthquake, Blast and Impact* (1991): 19.
- [128] Spence, R., 1990. A Note on the Beta Distribution in Vulnerability Analysis, Martin Centre Working Paper, Department of Architecture, University of Cambridge.
- [129] Stannard M, Galloway B, Brunsdon D et al (2014) Field guide: rapid post disaster building usability assessment—earthquakes. Ministry of Business, Innovation and Employment, Wellington
- [130] TORISAWA, K., HORIE, K., KAWABE, K., MATSUOKA, M., INOUCHI, M., & YAMAZAKI, F. (2020) Fragility Curves for Buildings Based on Damage Data in Uki City due the 2016 Kumamoto Earthquake.
- [131] Whitman R.V., Reed U.W., Hong S.T. [1973] "Earthquake damage probability matrices", *Proceedings of 5th World Conference on Earthquake Engineering*, Rome, Italy.

- [132] Yamazaki, F., Suto, T., Liu, W., Matsuoka, M., Horie, K., Kawabe, K., ... & Inoguchi, M. (2019, April). Development of fragility curves of Japanese buildings based on the 2016 Kumamoto earthquake. In 17th Pacific Conference on Earthquake Engineering and Annual NZSEE Conference, Auckland, New Zealand.
- [133] Zuccaro G, Cacace F (2011) Seismic casualty evaluation: the Italian model, an application to the L'Aquila 2009 event. In: Spence R, So E, Scawthorn C (eds) Human casualties in earthquakes. Advances in natural and technological hazards research. Springer, Netherlands, pp 171–184
- [134] Zuccaro G, Perelli FL, De Gregorio D, Cacace F (2020) Empirical vulnerability curves for Italian masonry buildings: evolution of vulnerability model from the DPM to curves as a function of acceleration. Bull Earthq Eng. [https:// doi. org/ 10. 1007/ s10518- 020- 00954-5](https://doi.org/10.1007/s10518-020-00954-5)
- [135] Zuccaro G., Cacace F., 2015. Seismic vulnerability assessment based on typological characteristics. The first level procedure “SAVE”. Soil Dynamics and Earthquake Engineering 69 (2015) 262–269.
- [136] Zucconi M, Ferlito R, Sorrentino L. Validation and extension of a statistical usability model for unreinforced masonry buildings with different ground motion intensity measures. Bulletin of Earthquake Engineering 2020. DOI: 10.1007/s10518-019-00669-2.
- [137] Zucconi M., Ferlito R., Sorrentino L., 2018. Simplified survey form of unreinforced masonry buildings calibrated on data from the 2009 L'Aquila earthquake. Bulletin of Earthquake Engineering, 16(7), 2877-2911.
- [138] Zucconi M., Sorrentino L., Ferlito R., 2017. Principal component analysis for a seismic usability model of unreinforced masonry buildings. Soil Dynamics and Earthquake Engineering 96 (2017): 64-75.

Chapter 3.

EVOLUTION OF THE ITALIAN SEISMIC CLASSIFICATION AND SEISMIC CODES

3.1 INTRODUCTION

In the last century, several strong earthquakes have been affected the Italian territory, causing relevant losses both in terms of human lives and damage to the constructions. For example, at the beginning of the twentieth century, two of the most powerful and devastating earthquakes ever occurred in Italy, struck several areas of southern and central Italy. The 1908 Messina earthquake caused about 80.000 victims in Sicilia Region and about 40.000 in Calabria Region, completely devastating several municipalities of southern Italy. Avezzano and Sora earthquake (13 January 1915) caused about 33.000 victims, strongly striking several municipalities in Abruzzi and Lazio Regions.

In answer to these devastating events, technical codes were enacted, regulating the construction and the retrofit of buildings in municipalities affected by the earthquake. Thus, at the beginning of the last century, the seismic classification of the Italian municipalities started, making compulsory several prescriptions related to the definition of seismic loads, to the design of structural details and retrofit interventions on existing buildings.

Over the last century, both the seismic classification and the contents of technical codes have changed several times. Basically, the earthquake has been

used as an occasion to test the goodness of the current classification and the enacted prescriptions. In fact, the main changes in the seismic classification have been occurred after the major seismic events of the last century, going from the 1908 Messina earthquake (Royal Decree, R.D. n.193 of 18 April 1909) to the 2002 Molise earthquake (Ordinance of the President of the Council of Ministers, OPCM n. 3274 of 20 March 2003). A similar argument is for the normative contents.

In this Chapter, the focus is on the evolution of the seismic classification of the Italian municipalities, following the occurrence of the strongest earthquakes and analysing the corresponding normative contents. Thus, a timeline of the major Italian earthquakes of the last century is firstly provided. Then, the seismic classification of the entire national territory adopted after these events is described, detecting the most relevant normative contents about the definition of seismic loads, structural details and retrofit interventions on masonry buildings.

3.2 ITALIAN EARTHQUAKES IN THE LAST CENTURY

According to the Italian Catalogue of strong earthquakes (Guidoboni et al., 2018) and to the Italian macroseismic database (Rovida et al., 2021), in the twentieth century, 24 earthquakes with an intensity equal or greater than IX in the Mercalli–Cancani–Sieberg (MCS) scale have struck the Italian territory, often causing dramatic effects. In Figure 1, the timeline of these severe seismic events is provided, distinguishing in three timespans (i.e., 1900-1940; 1940-1980; 1980-2020), that have been deeply analysed in the following sub-sections. The first timespan starts with catastrophic seismic events (i.e., 1905 Calabria and 1909 Messina earthquakes) and ended with the enactment of a nationwide technical code (R.D. n.640, 25th March 1935). In the second time span, few strong earthquakes occurred, thus no great modifications in the normative contents and seismic classification were done. Nevertheless, at the end of this time interval (23rd of November 1980), a destructive event struck the Irpinia region in the Southern Italy. Thus, the third time span is characterized by an intensive normative production to prevent the recurrence of similar catastrophic event.

This analysis is an indispensable support to deeply understand the following seismic classification and, of course, the evolution of the normative contents about the constructions and the retrofit interventions. In fact, as deeply analysed in the following sub-sections, the main normative prescriptions enacted over the years are a direct consequence of lesson-learnt after earthquake occurrence.

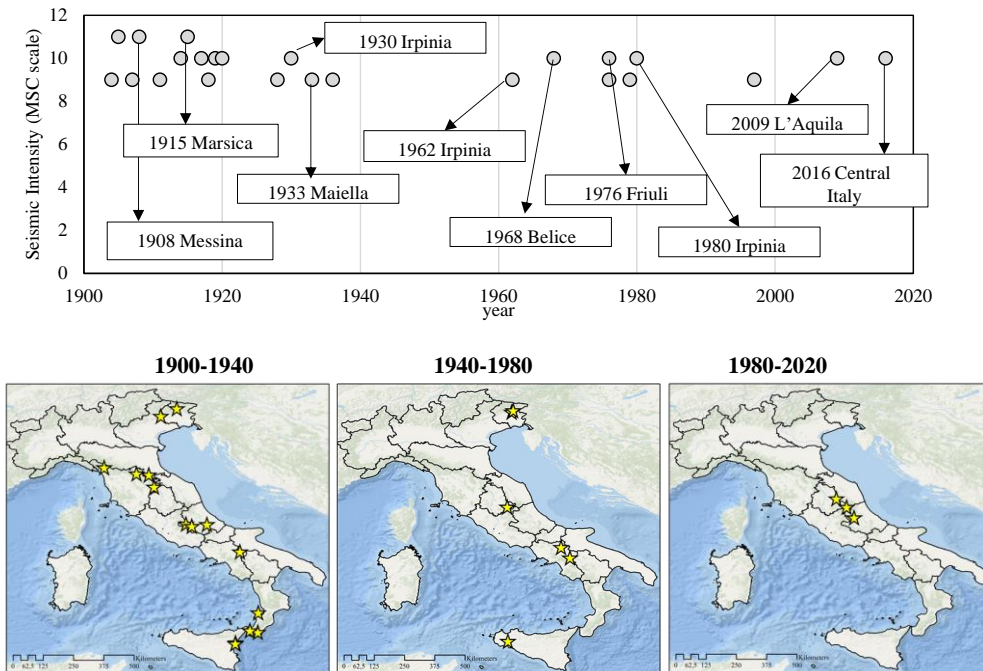


Figure 1. Main strong earthquakes ($I_{MCS} \geq IV$) occurred in Italy in the twentieth century (Rovida et al., 2021).

3.2.1 Strong earthquakes occurred between 1900 and 1940

At the beginning of the twentieth century, several areas of Calabria and Sicily regions (in southern Italy) were severely affected by seismic events, which caused widespread damage in urban centers and numerous victims. The 8th of September 1905, an earthquake with intensity XI in the MCS scale hit the current district of Vibo Valentia, razing to the ground several entire localities and affecting about 330 municipalities. The widespread damage state observed after the earthquake was the result of a highly vulnerable building's stock,

characterized by poor construction techniques and materials. An example was the so-called “breste” masonry (Baratta, 1906), namely a type of masonry, largely widespread in Calabria and in the southern Italy, composed of sun-dried bricks made of mud and straw in a crumbly mortar. Barely three years later (28th of December 1908), another catastrophic event hit the southern Italy in Messina (Sicily region) and Reggio Calabria (Calabria region) districts. This earthquake was one of the most severe ever occurred on the national territory (XI intensity in the MCS scale, I_{MCS}), with an estimated moment magnitude higher than 7.



Figure 2. *Messina Earthquake, 28 December 1908*. Description: Street in Messina, Sicily, showing damage caused by the earthquake. Photographed in January 1909. Collection of Lieutenant Commander Richard Wainwright, 1928. U.S. Naval History and Heritage Command Photograph. (Catalog #: NH 1447)

Thus, the high seismic intensity (with the consequent violent tsunami) together with the great vulnerability of constructions led to a catastrophic post-earthquake situation. In fact, in 78 localities near to Reggio Calabria and 14 ones

near to Messina, the amount of collapses was extremely high, reaching the 70-100% of the entire municipality (Guidoboni et al., 2018). Also, the high number of victims (estimated in about 120.000) contributed to make the event one of the most catastrophic of the whole Italian seismic history. In answer to this devastating event, the Royal Decree (R.D.) n.193 of 18 April 1909 was enacted to regulate the repair and reconstruction interventions and new constructions in all municipalities affected by the earthquake.

In the immediately following years, the eastern side of Sicily region was affected by two earthquakes (15th of October 1911; 8th of May 1914) with IMCS equal to X. For both the events, the great use of dry masonry (i.e., without any mortar), namely the so-called “muratura a secco”, was one of the main factors that caused the building’s collapses.



Figure 3. Avezzano 1915, Palazzo Torlonia after the earthquake. Photo retrieved from <http://marsica1915.rm.ingv.it/it/79/il-terremoto-del-1915>.

The 13th of January 1915 a large area in the central Italy was hit by a violent (with an estimated magnitude of 7) earthquake, with destructive effects on Marsica (Abruzzi) localities. It is estimated that more than 30.000 people lost

their lives (Cavasino, 1935). After the seismic event, several vulnerability factors were identified: namely, walls made of poor-quality sand, poor lime and smooth stones, insufficient foundations, cantilevered stairs, heavy vaults, heavy roofs pushing on the load-bearing walls, excessive height of buildings (Oddone, 1915). The awareness of these vulnerabilities in the building stock led to the enactment of the R.D. n.573 of 29 April 1915, to regulate the constructions in the municipalities hit by the earthquake.

Almost the entire Monterchi municipality (in Tuscany region) was razed to the ground by an earthquake of magnitude equal to 5.9 on 26th of April 1917. The post-earthquake inspection highlighted that the undamaged buildings were just the ones characterized by good quality masonry walls and low building's height (Oddone, 1918). In the years between 1917 and 1919, the Tuscan-Romagnolo Apennine was affected by several seismic events (i.e., 2nd of December 1917; 10th of November 1918; 29th of June 1919). The latter (with an estimated magnitude of 6.3) hit the Mugello area, that was already being hugely damaged by the previous events. Critical issues detected in the building stock were not only the building material, but also the structural concept of the building (Martinelli, 1919): in particular, the absence of effective connections between horizontal and vertical structures and the absence of tie rods/beams.

The 7th of September 1920 the Tuscany region was again hit by a severe seismic event. The most affected areas were the Garfagnana and Lunigiana ones, whose building stock was mainly for rural uses (so, built with particularly poor material and techniques). After the earthquake, the Law n.2089 of 23rd of October 1924, containing technical standards for the building industry, was enacted.

About ten years later (23rd of July 1930), the Vulture earthquake with a magnitude of 6.7 struck the Southern Italy (mainly Campania, Basilicata and Puglia regions), causing 1404 victims. The major damages were observed in the mountain zone between Ariano Irpino and Melfi municipalities: about 70% of the total number of residential buildings in the localities of Aquilonia, Lacedonia, Villanova del Battista and Trevico collapsed. In answer to the high number of homeless (more than 100.000 only in Avellino district), more than 400 "aseismic houses" were built by the Italian government. These buildings, designed in

accordance with the in force normative contents, were characterized by a reinforced concrete frame and walls made of solid bricks.



Figure 4. Italien, Erdbeben-Katastrophe. Description: houses collapsed due to the catastrophic earthquake of Vulture, 23 July 1930. This image was provided to Wikimedia Commons by the German Federal Archive (Deutsches Bundesarchiv).

In the 1933, Abruzzi region was again affected. The earthquake (26th of September 1933) hit the Maiella zone (in the southern side of the Abruzzi region), causing several collapses and a widespread damage. Among the main affected municipalities, Sulmona was severely damaged: only a third of the entire building stock (namely the most recent buildings, built according to the in force normative) resulted undamaged.

In the space of just over 30 years, several Italian regions were affected by severe earthquakes, often with catastrophic effects. Thus, in the 1935 a nationwide normative (R.D. 25th March 1935, n.640) was enacted, providing structural-geometric prescriptions for constructions on the entire national territory (so, not only in seismic zone).

3.2.2 Strong earthquakes occurred between 1940 and 1980

According to the Italian Catalogue of strong earthquakes (Guidoboni et al., 2018) and to the Italian macroseismic database (Rovida et al., 2021), no seismic event with $IMCS \geq IV$ occurred on the Italian territory in the first half of the considered time span (i.e., 1940-1980). In fact, just in the 1962 a new strong event hit the south Italy in the Irpinia zone (21st of August 1962) with a magnitude of 6.2. In general, few total collapses were observed after the earthquake, but several buildings had to be demolished and rebuilt because of the great damage degree. The latter was caused by some significant construction defects (Cavallo and Penta, 1962): namely, thrusting structures (such as vault and arches), heavy roofs, absence of tie rods, cantilever structures, irregular distribution of openings. As direct consequence of this seismic event, the Law n.1684 was enacted the 25th of November 1962, updating the seismic classification for 72 municipalities, and introducing the supervisory role of the Italian Genio Civile.

After about 6 years, an earthquake of magnitude 6.4 hit the western Sicily in the Belice Valley, causing 370 victims and the collapse of about 3.000 rural buildings. The most affected municipalities were Gibellina, Poggioreale and Salaparuta, not yet seismically classified: thus, almost all buildings were not equipped with adequate geometry and seismic structural details. In 1976, the Friuli-Venezia Giulia region was affected by several (about 400) earthquakes. The main shocks hit the region the 6th of April and the 11th and 15th of September, destroying about 17.000 residential buildings. After these events, the Friuli-Venezia Giulia region enacted the regional Law. n.30 of 20th June 1977, that introduced for the first time in Italy the POR method (Tomazevic, 1978) for the seismic verification of masonry buildings. The same contents were included in the regional Law n.34 (1st of July 1981) by Umbria region after 1979 Valnerina earthquake. In fact, just two years later, an earthquake of magnitude 5.8 struck the Central Italy, affecting especially the Valnerina area (19th of September 1979). About 5000 buildings resulted damaged, of which about the 12% was to be demolished (Favali et al., 1980). Many of those were old buildings in a sad state of decay or inadequately retrofitted ones: not squared or rounded stones,

poor mortar, pushing roofs and inadequate foundations were the main vulnerability aspects detected after the earthquake.

The 23rd of November 1980, a destructive earthquake hit again the Irpinia region in the Southern Italy, with dramatic effects. About 3.000 people died, about 9.000 resulted injured and about 400.000 were the homeless. Castelnuovo di Conza, Conza della Campania, Laviano, Lioni, Sant’Angelo dei Lombardi and Santomenna municipalities were completely destroyed. In Campania and Basilicata regions, about the 5% of buildings (reported in the census) collapsed, the 15% was severely damaged and about the 25% resulted slightly damaged (Guidoboni et al., 2018).



Figure 5. View of the destroyed city of Conza della Campania after the earthquake of November 1980. Photographed by Giuseppe Maria Galasso.

Six months later, the Law n.219 (14th of May 1981), containing provisions for the reconstruction of territory hit by the earthquake, was enacted. Moreover, the law made compulsory, for the first time in Italy, the seismic verification of existing masonry buildings. As accurately analysed in the following sub-

sections, after the Irpinia 1980 earthquake there was an intensive normative production to prevent the recurrence of similar catastrophic event.

3.2.3 Strong earthquakes occurred between 1980 and 2020

In the last 40 years, three seismic events with $I_{MCS} \geq IV$ occurred on the Italian territory: 1997 Umbria-Marche, 2009 L'Aquila and 2016 Central Italy earthquakes. Nevertheless, many other events have deeply affected the national territory in this period, influencing mostly the built practices and the normative provisions: among the others, the 2002 Molise earthquake and the 2012 Emilia-Romagna earthquakes.

After the 1980 Irpinia earthquake, not only great innovations were introduced in the technical codes (Law n.219, 14th of May 1981), but also several municipalities (i.e., 1530 between 1980 and 1983) were added to the list of those seismically classified. Almost 20 years later, an earthquake swarm struck Umbria and Marche regions, causing 11 victims and a widespread damage, especially in the monumental constructions of the cultural heritage. The main shock occurred the 26th of September 1997 with a magnitude equal to 5.7, after other two heavy shocks (3rd of September; 26th of September 0:33:12 UTC) and followed by thousands of aftershocks. The event highlighted the key role of cumulative damage to the collapse of existing masonry constructions (Parisi and Augenti, 2013). A few years later, a dramatic event occurred in San Giuliano di Puglia, because of an earthquake that hit Molise and Puglia regions the 31st of October 2002. The event got the attention of the public opinion, especially for the death of 27 children in the Francesco Iovine school (in the district of Campobasso). At the time of the earthquake, San Giuliano di Puglia municipality and its surroundings were not seismically classified. In fact, the criteria used to judge which municipalities should be added to the seismic zone was based on the observed occurrence of strong earthquakes. In other words, the seismically classified municipalities were those previously hit by severe earthquakes. Especially after this event, the need to radically modify such criteria become quite obvious: thus, the O.P.C.M. n.3274 was enacted about five months later (the 20th of March 2003). Basically, this law defined as seismic the entire national

territory, distinguishing in four seismic zones (with decreasing seismicity). Actually, the O.P.C.M. n.3274 has the merit of having introduced several innovative concepts (such as ductility, capacity design, the building's regularity), changing completely the previous normative philosophy. A great amount of these innovations was receipted by the following codes (D.M. 14/09/2005; D.M. 14/01/2008). However, the effective application of these latter became compulsory only after the 2009 earthquake (Law n.77 of the 24th of June 2009). This event (magnitude of 6.3) hit the Abruzzi region the 6th of April, affecting especially the city of L'Aquila, and causing 308 victims. The post-earthquake surveys highlighted the presence of some vulnerable aspects, especially in the historic centre of L'Aquila, that dates back to the post-earthquake reconstruction of the 1703 event. Out-of-plane mechanisms (namely, the partial or total overturning of the facade) have been observed in masonry buildings with poor connection at the corner. In-plane mechanisms with diagonal cracks have been found in case of irregular distribution and size of the openings or in case of slabs not partially rigid in their plane (D'Ayala et al., 2011).



Figure 6. Global collapse of the L'Aquila's Prefecture.
Photo retrieved from Augenti and Parisi, 2010.

Among the symbolic images of this seismic event, there is certainly the Government Palace of L'Aquila city, hugely damaged by the earthquake. The awareness of the great vulnerability of the Italian historic cultural heritage led to the enactment of Directive of the President of the Council of Ministers of 9th of February 2011 (D.P.C.M. 09/02/2011), for the assessment and the mitigation of the seismic risk of the cultural heritage.

The 20th and 29th of May 2012, two shakes (respectively, 5.9 and 5.8 magnitude) affected the Emilia-Romagna region, causing 28 victims and several collapses of precast concrete and masonry structures. The lack of proper connection details was the main cause of damage for both these structural typologies (Parisi et al., 2012). In fact, out-of-plane mechanisms were occurred in masonry buildings not equipped with satisfactory interlocking between orthogonal walls and between vertical and horizontal structures. Similarly, any connection between vertical structures and precast beams led to the building's collapse of several R.C. precast structures, mostly designed only for gravity loads.

Between 2016 and 2017, the Central Italy has been again struck by severe seismic events. The 24th of August 2016, the first violent shake (magnitude 6) severely affected the Accumoli municipality (in Lazio region), then the 30th of October the heavier shake (magnitude 6.5) hit Norcia municipality (in Umbria region). Overall, four Italian regions (namely, Lazio, Abruzzo, Umbria and Marche) resulted struck by the seismic sequence, and 303 casualties, 388 injuries and about 41.000 homeless were suffered. The analysis of post-earthquake damage (Sisti et al., 2018) highlighted, after all, a good seismic behaviour of masonry buildings sited in the historic centre of Norcia (Umbria region), especially in comparison with the other regions. The reason for such better behaviour is related to the awareness gained after the several previous seismic events and to the consequent adopted countermeasures (namely, the regional Law n.34, 1st of July 1981).

3.3 EVOLUTION OF THE ITALIAN SEISMIC CLASSIFICATION

As highlighted in the previous Section, for much of the last century the criteria used to define the seismic zone were based on the observed occurrence of strong earthquakes. Thus, only after observing dramatic effects due to the earthquake, a given municipality was classified as seismic-prone and added to the list of seismically classified municipalities.

This approach was introduced after the devastating 1908 Sicily-Calabria earthquake by means of Royal Decree n. 193 (R.D.18/04/1909 n.193). The code was conceived to regulate the repair and reconstruction interventions and new constructions in municipalities affected by the earthquake. Precisely, 306 municipalities (namely, 267 belonging to Calabria region and 39 to Sicily one) were included in the list. Nevertheless, the complete list of Calabria municipalities hit by the earthquake was provided few months later by R.D.15/07/1909 n.542, that seismically classified the entire Calabria region. In fact, the law added to the list all municipalities (i.e., 146 ones) of Reggio Calabria, Catanzaro and Cosenza districts and further six municipalities near to Messina, initially discarded by the classification. Thus, for these 458 municipalities a number of technical requirements became compulsory both for new and existing buildings. Conversely, no compulsory provisions were in the remaining municipalities of the Italian territory, where the new constructions and/or the interventions on existing buildings continued to be based on established built practices. Just five years later, after the events (15th of October 1911; 8th of May 1914) that affect the eastern site of Sicily region, other six municipalities (Acireale, Aci Sant'Antonio, Giarre, Riposto, Viagrande, Zafferana Etnea) were added to the list of seismic-prone municipalities by means of R.D. 11/10/1914 n.1335. In this way, the technical provisions originally enacted by R.D.18/04/1909 n.193 become compulsory also for these six municipalities. According to the adopted criteria, only the most affected municipalities were defined as seismic-prone, making compulsory the seismic normative requirements. The same criteria were used one year later, when the so-called 1915 Marsica earthquake struck the Central Italy with dramatic effects, especially in Abruzzi, Lazio and Molise regions. Overall, 285 municipalities

were added to the list by R.D. 29/04/1915 n.573: in particular, in Abruzzi, Lazio and Molise regions were defined as seismic-prone respectively 124, 147 and 10 municipalities. Moreover, also three (namely, Conca della Campania, Mignano Monte Lungo, Roccamonfina) Municipalities belonging to Campania region and one (i.e., Monte Vidon Combatte) of Marche region were seismically classified. As a result, until 1915 the presence of a real seismic risk was recognized in 743 Italian municipalities (Figure 7), namely in about 9% of the entire national territory. Therefore, according to R.D. 29/04/1915 n.573, the Italian territory was composed by two zones: in the first one, namely the seismic-prone zone, the building's construction and repair were accurately regulated; in the second one (i.e., in the remaining municipalities) no provisions were compulsory.

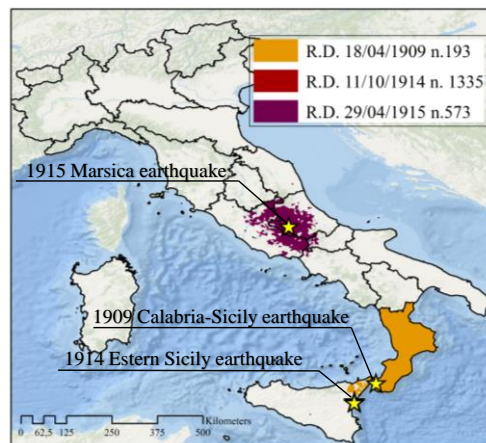


Figure 7. Seismically classified municipalities until 1915.

The concept of seismic category dates from R.D. 13/03/1927 n.431 that introduced a classification in two seismic categories (with a decreasing degree of seismicity). Therefore, the need to identify seismic-prone areas led to R.D.18/04/1909 n.193 (and following modifications), that introduced a first subdivision between seismic-prone municipalities and the remaining ones. Then, the need to consider the different degree of seismicity among the seismic-prone areas, led to the subdivision in seismic categories (R.D. 13/03/1927 n.431). This new classification (see Figure 8) included the municipalities affected by strong

earthquakes occurred between the 1915 and 1927, in addition to the ones classified by the previous laws (between the 1909 and 1915).

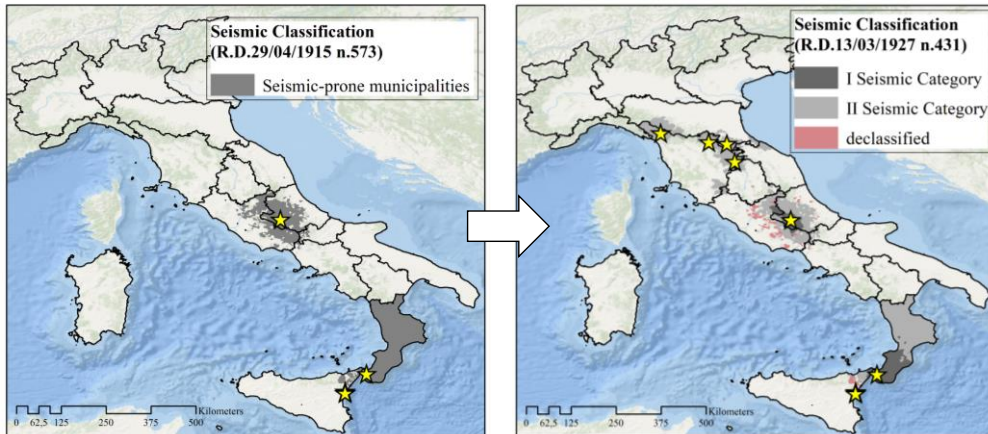


Figure 8. Evolution of the Italian seismic classification between R.D. 29/04/1915 n.573 and R.D. 13/03/1927 n.431 with the indication of the stronger earthquakes occurred until the enactment of the two Codes.

In particular, the main seismic events occurred in this time span hit the Tuscan-Romagnolo Apennines and the Tuscany region, leading a post-earthquake situation (although serious) overall less catastrophic than 1909 or 1915 earthquakes. Thus, the normative approach was to adopt less stringent provisions for the less affected areas, while acknowledging the seismic risk of the same areas. According to such approach, further 178 municipalities were classified, being included in the II seismic category. Moreover, going from the 1915 classification to the 1927 one, some municipalities (about 10%) were removed from the list of seismic-prone area. In fact, several municipalities in Sicily, Lazio and Abruzzi regions were declassified by R.D. 13/03/1927 n.431, especially under the pressure of local population. Basically, the new compulsory normative provisions were not well-received by the people that preferred to use the traditional building practices. Among the municipalities that were confirmed as seismic-prone, only a small proportion (about 13%) was classified as belonging to I seismic category, whereas the greater part belonged to the II

category. Overall, 851 municipalities were seismically classified until 1927, namely almost the 11% of the entire national territory.

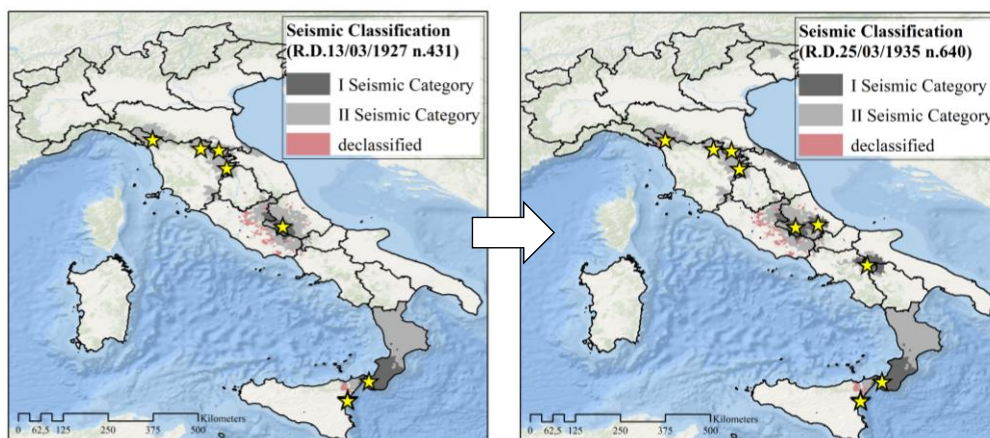


Figure 9. Evolution of the Italian seismic classification between R.D. 13/03/1927 n.431 and R.D. 25/03/1935 n.640 with the indication of the stronger earthquakes occurred until the enactment of the two Codes.

In the years immediately following the R.D. 13/03/1927 n.431, two strong events hit again the Italian territory. In particular, the so-called 1930 Vulture earthquake affected the area on the border of three regions: Campania, Basilicata, and Puglia. The 1933 Maiella event struck, especially the southern side of Abruzzi region. Actually, in these period other severe events occurred on the national territory, especially on the north side of the Marche region (30th of October 1930) and in the Friuli - Venezia Giulia region (19th of February 1932). The classification introduced by R.D. 25/03/1935 n.640 (Figure 9) reflects this situation exactly. In fact, almost the 50% of 133 new-classified municipalities belonged to Campania, Basilicata or Puglia region. The remaining part included, especially Abruzzi (20%), Marche (16%) and Friuli – Venezia Giulia (10%) municipalities. Moreover, all the classified municipalities of Friuli – Venezia Giulia region were added to the II category. Conversely, about one-third of municipalities classified in Campania, Basilicata and Puglia regions and all new-classified municipalities in Marche and Abruzzi were included in the I category. Moreover, 28 Abruzzi municipalities initially belonging to the II category (by

R.D. 13/03/1927 n.431) were moved to the I one. However, just two years later, the seismic classification (Figure 10) was again updated by means of R.D. 22/11/1937 n.2105. It should be noted that in these two years few heavy earthquakes affected the Italian territory: among the others, the Alpago-Cansiglio event that occurred on the border of Veneto and Friuli – Venezia Giulia regions the 18th of October 1936 was the most severe. Thus, the addition of municipalities in seismic zone was mainly related to these two regions: in particular, 34 municipalities (namely, 29 in Veneto and 5 in Friuli – Venezia Giulia region) were added to the II seismic category.

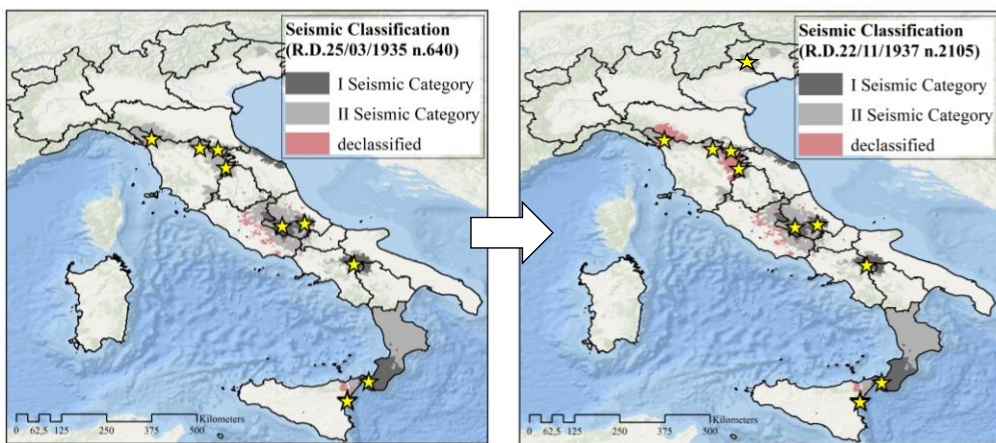


Figure 10. Evolution of the Italian seismic classification between R.D. 25/03/1935 n.640 and R.D. 22/11/1937 n.2105 with the indication of the stronger earthquakes occurred until the enactment of the two Codes.

As highlighted in Figure 10, basically R.D. 22/11/1937 n.2105 reduced the number of seismically classified municipalities rather than increased them. The “declassification” was operated especially in the Tuscany and Emilia Romagna regions (originally classified by means of R.D. 13/03/1927 n.431), where 41 municipalities were discarded from the classification, resulting non-seismically prone area. The reason of such operation could be explained by two main factors: in one hand, people were loath to change their traditional building practices; on the other hand, R.D. 25/03/1935 n.640 had been introduced compulsory prescriptions also in not seismically classified zones. Thus, some provisions

(despite less stringent) continued to be compulsory for these declassified municipalities. Unfortunately, this negative trend continued also in the following years: several municipalities (among the others, Vittorio Veneto, the district of Pesaro Urbino, the Terminillo district) requested to be exempt to the seismic classification, in order to promote the post-war reconstruction or, even, to encourage the construction of tourism structures.

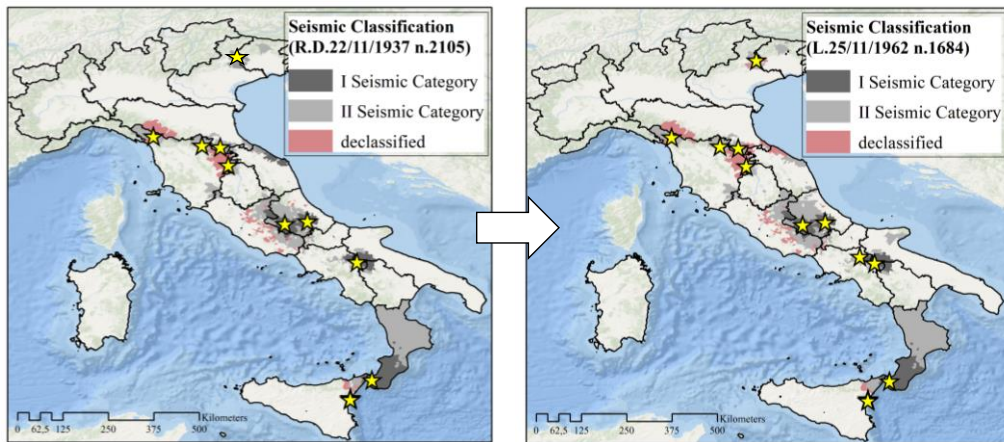


Figure 11. Evolution of the Italian seismic classification between R.D. 22/11/1937 n.2105 and L. 25/11/1962 n.1684 with the indication of the stronger earthquakes occurred until the enactment of the two Codes.

As highlighted in the previous Section (3.2.2), in the years following the enactment of R.D. 22/11/1937 n.2105, no catastrophic seismic events occurred on the national territory. This fact, together with the entry of Italy into World War II, caused a period of stagnation on seismic classification and normative provisions, up to the law L.25/11/1962 n.1684 (Figure 11). In fact, the 21st of August 1962 a magnitude 6.2 earthquake struck the Irpinia area in the southern Italy. Nevertheless, only four municipalities (namely, Moschiano, Venticano, Vallesaccarda and Scampitella) in Campania were added to the list. Similarly, only five municipalities of neighbouring regions were seismically classified: in particular, four (namely, Mattinata, Monte Sant'Angelo, San Giovanni Rotondo and San Marco in Lamis) in Puglia, one (i.e., Scampoli) in Molise and no one in Basilicata region. Conversely, the number of seismic-prone municipalities

increased in Abruzzi and Marche regions, where respectively 29 and 16 municipalities were added to the II category. Overall, at the end of 1962, 1005 Italian municipalities (namely, about the 12% of the entire national territory) had been seismically classified (among these, about 28% belonged to the I seismic category), whereas the huge part (i.e., the remaining municipalities) was considered non seismically prone area yet.

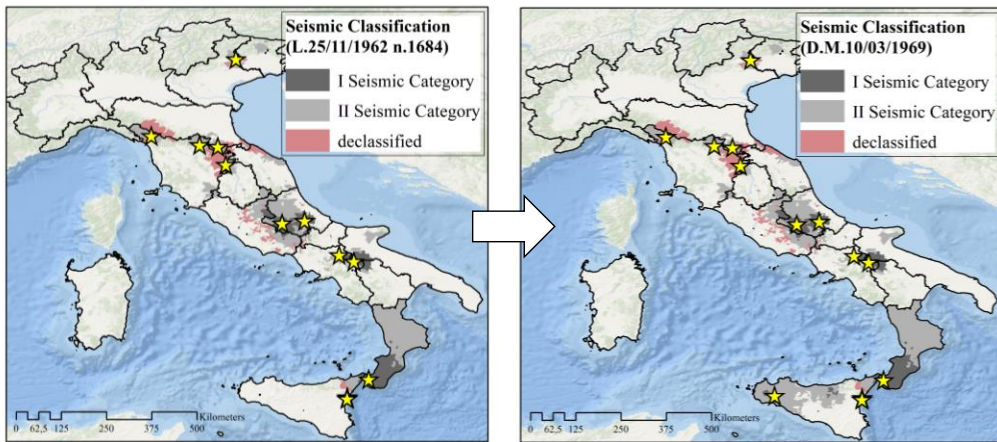


Figure 12 Evolution of the Italian seismic classification between L. 25/11/1962 n.1684 and D.M. 10/03/1969 with the indication of the stronger earthquakes occurred until the enactment of the two Codes.

The 15th of January 1968, a strong earthquake struck the western Sicily near the Belice valley. It should be noted that after the 1909 and 1914 seismic events, only 25 Sicilian municipalities were added to the list of seismic-prone areas. Thus, when the Belice earthquake occurred, just about 20% of the region had been seismically classified. Moreover, almost all classified municipalities belonged to the Messina district (eastern Sicily). The earthquake highlighted that also the western site of the region had to be considered as seismic-prone area: to this aim, two Ministerial Decrees (D.M.26/09/1968; D.M.10/03/1969) were enacted, adding 147 municipalities to the list (12 in the I seismic category).

Once again, the updating of seismic classification had followed the occurrence of catastrophic events. Similarly, in answer to the 1976 Fiuli – Venezia Giulia earthquake, the D.M.15/09/1976 was enacted, classifying 88 municipalities in

the affected region. Finally, towards the end of the following decade, the awareness of the need to change the updating approach led to the Finalizzato Geodinamica project (PFG) carried out by the Italian CNR (i.e., *Consiglio Nazionale delle Ricerche*, National Council of Research). The first result of the project was the publication in the 1979 of preliminary national maps of “shakeability” (CNR, 1979, Figure 13a), containing probabilistic processing. In particular, the exceeding probability of seismic intensity values was calculated in given time ranges.

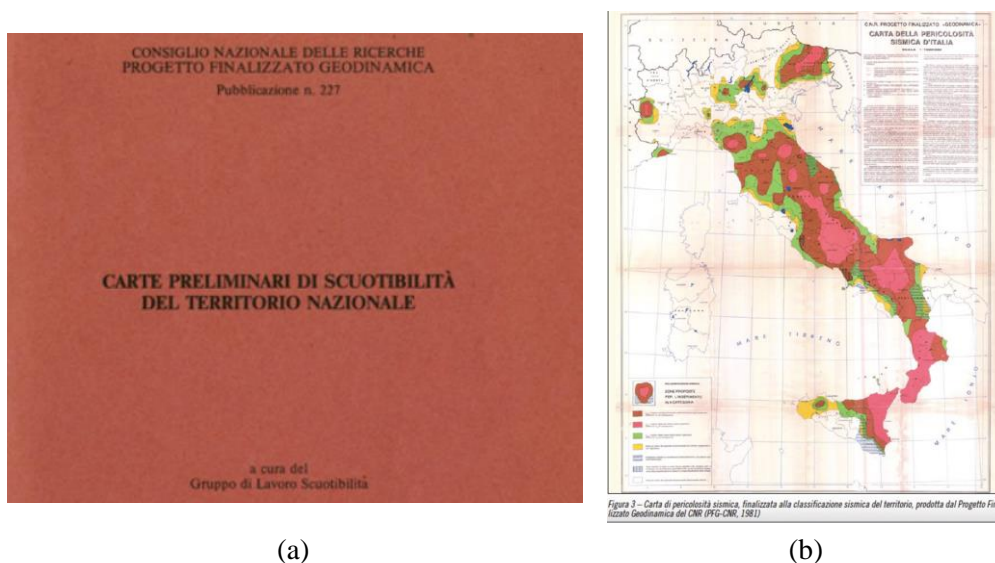


Figure 13. (a) Cover of the Publication n.277 (ESA Editor), containing the preliminary maps of shakeability (CNR, 1979). (b) Map of seismic hazard in Italy (Petrini, 1981).

The study of the Italian seismic hazard took the concrete shape of the creation of a national map of seismic hazard (Petrini, 1981) for the seismic classification of the national territory. According to this map, all municipalities with seismic hazard equal or greater than the risk in already classified zones, had to be added to the II category. Moreover, the map identified zones in which further seismotectonic studies were needed. Thus, for the first time the seismic classification was based on scientific works, rather than on a list of municipalities affected by the earthquake. Nevertheless, according to the map, a huge number

of municipalities had to move from non-seismic zone to II seismic category. With the aim of mitigating such great modification in the classification, a further category (less severe) was added to the previous two. Thus, after the dramatic 1980 Irpinia earthquake, the D.M.03/06/1981 n.515 (in addition to the earlier D.M.07/03/1981) re-defined the classification for Campania, Basilicata and Puglia regions. In the same year, several regions updated their classification: among the others, Umbria (D.M.26/06/1981), Sicilia (D.M. 23/09/1981) and Molise (D.M.09/10/1981). It should be noted that Article 3 of L.02/02/1974 n. 64 entrusted to decrees of the Minister for Public Works issued in agreement with the Minister for the Interior, after consulting the Superior Council of Public Works and the Regions, the task of updating the seismic classification. Thus, in the year between 1980 and 1984, several Ministerial Decree were enacted, updating the seismic classification at regional scale.

Table 2. Ministerial Decree for the seismic classification at regional scale enacted between 1980 and 1984.

Ministerial Decree	Region
D.M. 02/07/1980	Abruzzi
D.M. 22/09/1980	Friuli-Venezia Giulia
D.M. 07/03/1981	Basilicata, Campania and Puglia
D.M. 07/03/1981	Molise
D.M. 03/06/1981	Basilicata, Campania and Puglia
D.M. 26/06/1981	Umbria
D.M. 23/09/1981	Sicilia
D.M. 09/10/1981	Molise
D.M. 11/01/1982	Friuli-Venezia Giulia
D.M. 04/02/1982	Piemonte
D.M. 19/03/1982	Tuscany
D.M. 14/05/1982	Veneto
D.M. 27/07/1982	Sicily
D.M. 27/07/1982	Liguria
D.M. 13/09/1982	Abruzzi
D.M. 10/02/1983	Marche
D.M. 01/04/1983	Lazio
D.M. 23/07/1983	Emilia-Romagna

Ministerial Decree	Region
D.M. 29/02/1984	Tornolo municipality (Emilia-Romagna)
D.M. 29/02/1984	Fara in Sabina municipality (Lazio)
D.M. 05/03/1984	Lombardia
D.M. 14/07/1984	Roio del Sangro and Teramo municipalities (Abruzzi)

At the end of 1984, the Italian seismic classification (Figure 14) covered 2965 municipalities, of which 12% in the I category, about 85% in the II one and about 3% in the III seismic category. Overall, only slightly more than 35% of the entire land area had been recognized as seismic-prone.

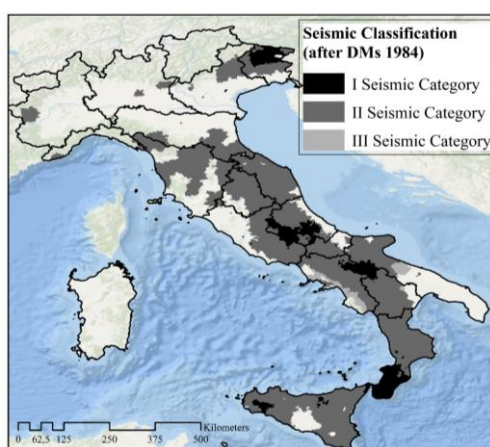


Figure 14. Italian seismic classification at the end of 1984.

Unfortunately, it was not until 2003 for the seismic classification of the entire national territory. In fact, the 31st of October 2002 Molise and Puglia regions were affected by a magnitude 6 earthquake, causing the death of 27 children in the school of San Giuliano di Puglia (in the district of Campobasso) municipality. This sad tragedy was the occasion to redesign the national classification and to update the normative contents related to the building's design and verification. To this aim, O.P.C.M. 20/03/2003 n.3274 was enacted, completely modifying the previous classification (see Figure 15). Basically, the entire national territory was recognized as seismic-prone area, by extending the seismic law to a further 65% of Italian municipalities, reaching the 100% of land territory. In particular,

the greater part (about 67%) of municipalities not already classified were added to a new seismic category. In fact, this remarkable updating was supported by the inclusion of a fourth seismic category (less stringent than the previous three). Compared with the seismic classification of 1984, the total number of municipalities in I category doubled (going from 368 to 717), the amount in II category remained about the same (going from 2499 to 2326), the municipalities in III category remarkable increased (going from 98 to 1628). Moreover, the IV category was populated by 3430 municipalities. Thus, starting from the 2003, (1) the entire Italian territory is seismic area; (2) the classification is based on four seismic categories (with decreasing degree of seismicity). It should be noted that the seismic design in IV category was at the discretion of Regions and Autonomous Provinces (O.P.C.M. 20/03/2003 n.3274).

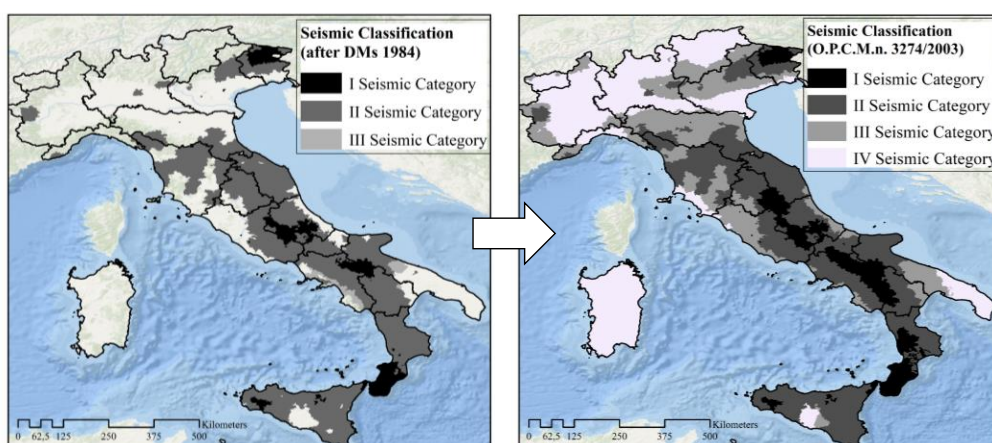


Figure 15. Evolution of the Italian seismic classification between 1984 and 2003 (according to O.P.C.M. 20/03/2003 n.3274).

According to O.P.C.M. 20/03/2003 n.3274, a value of the seismic action (in terms of maximum acceleration to the ground, a_g) is assigned to each seismic category (namely, 0.35, 0.25, 0.15 and 0.05 g, respectively, for the I, II, III and IV category). Nevertheless, the criteria defined on a transitional basis by O.P.C.M. 20/03/2003 n.3274 were soon replaced by those introduced by O.P.C.M. 28/04/2006 n.3519. This law provided to Italian Regions an innovative instrument for seismic classification, defining a range of a_g (ground acceleration

with probability of exceeding equal to 10% in 50 years) for each category according to Table 3.

Table 3. Range of ground acceleration according to O.P.C.M. 28/04/2006 n.3519.

Seismic Category	a_g
I	$>0.25\text{ g}$
II	0.15-0.25
III	0.05-0.15
IV	<0.05

It should be noted that starting from the first classification in the 1909 (R.D.18/04/1909 n.193), municipal boundaries have been considered assigning the seismic category, excluding the possibility of different seismicity in the same municipality. This approach was abandoned by means of D.M.14/01/2008, that introduced a subdivision of the whole national territory through a reference grid based on geographic coordinates. Such grid (Annex B of D.M.14/01/2008) was composed of 10.751 points with square meshes of 5 km side, independent of municipal administrative boundaries. The calculation of the seismic action was based on the use of three parameters (namely, a_g , maximum acceleration at the bedrock; F_0 , maximum amplification of the acceleration; T_c^* , period value for the definition of the spectrum shape) defined for each grid point, depending on the return period, T_R .

Thus, since 2009 (i.e., entry into force of D.M.14/01/2008) the role of previous seismic classification based on municipal administrative boundaries has been modified, resulting valid only for administrative purposes (such as request for seismic authorization).

3.4 EVOLUTION OF CODE PRESCRIPTIONS ABOUT MASONRY BUILDINGS

Together with the seismic classification, also the normative contents of the technical regulations have evolved over time, with the aim of improving the seismic behaviour of the building. Seismic events in the last century have highlighted how some structural details (such as tie rods and tie beams in masonry buildings) were needed to improve the performance of the building

under seismic loads. Similarly, the ban on the use of some structural typologies (such as thrusting structures) is the consequence of lesson-learnt after earthquake occurrence.

Thus, earthquake occurrence and its consequences allowed understanding, in one hand, where the seismic event could be occurred and, on the other hand, how the buildings should be designed with regard to the earthquake. The first lesson led to the definition (and consequent evolution) of the national seismic classification (as deeply analysed in the previous Section). The second one led to identify the design criteria based on which a satisfactory seismic behaviour could be reached. In this Section, the evolution over the years of such criteria has been analysed, focusing mostly on the normative contents about the definition of seismic loads (i.e., paragraph 3.4.1), the structural-geometric details (i.e., paragraph 3.4.2), and the retrofit interventions (i.e., paragraph 3.4.3) in masonry buildings.

3.4.1 Code prescriptions related to seismic loads

At the beginning of the twentieth century, one of the most powerful and devastating earthquakes ever occurred in Italy, struck several areas of southern Italy, causing the loss of more than 100.000 lives, and the destruction of entire villages and cities. In answer to this catastrophic event (1908 Messina earthquake), a first seismic regulation, namely R.D.18/04/1909 n.193, was introduced to regulate the building construction and reconstruction in the affected territories.

For the first time in Italy, the dynamic actions due to the earthquake had to be considered in the design, applying accelerations to the building's masses in both horizontal directions.

Therefore, the 1909 year represents a milestone for building design in seismically classified municipalities, since the definition of seismic actions became compulsory, whereas no specific requirements existed before. Nevertheless, a first quantification of seismic loads was provided only few years later (after the dramatic 1915 Avezzano earthquake).

R.D. 29/04/1915 n.573 prescribed also to consider the static forces equivalent to earthquake actions in building design, beyond those due to structural weights and live loads. The latter consisted in accelerations applied to structural masses of the building in both horizontal and vertical directions. Horizontal forces were equal to $1/8$ of the storey weight for the first floor and $1/6$ of the storey weight for the other floors of structures up to 10 m tall or $1/6$ for taller buildings. The ratio between the base shear design, V_b , and the weight of the building, W , is variable between 0.125, for a single-storey building, to 0.152, for a 3-storey building, while for buildings with a number of stories greater than 3 it is equal to 0.166, assuming an interstorey height of 3 m.

In 1927 (R.D.L. 431/1927), the national territory was classified into two seismic categories: for the buildings located in seismic category I, horizontal forces to be applied in structural analysis were equal to $1/8$ of the storey weight for structures up to 10 m tall or $1/6$ for taller buildings. Instead, for the buildings located in seismic category II, horizontal forces were equal to $1/10$ of the storey weight for structures up to 15 m tall or $1/8$ for taller buildings. In seismic category II the ratio between the base shear design and the weight of the building is equal to 0.10 for buildings defined by a number of stories between 1 and 5, whereas for taller buildings is equal to 0.125, assuming an inter-storey height of 3m.

Subsequently, the ratio between horizontal forces and storey weight was modified by several laws (R.D.L 640/1935; R.D.L. 2105/1937; L.1684/1962). In fact, the ratio between the base shear design and the weight of the building became 0.10 and 0.07 in seismic category I and II, respectively, regardless of the number of stories of the building.

In 1975 (D.M. 3/3/1975 n.40) fundamental innovations were introduced in building design: the summation of lateral force distribution applied to each storey of buildings was defined as a function of the total weight of the structural masses, the fundamental period of the structure (through R coefficient), the soil compressibility (through ε coefficient), the possible presence of structural walls (through β coefficient) and, of course, the seismic action (through C coefficient). This law, through the definition of the R coefficient, introduced for the first time the concept of response spectrum. In fact, a constant response coefficient R was

considered for fundamental periods not exceeding 0.8 seconds and a hyperbolic function thereafter. Moreover, a linear distribution of lateral seismic forces was introduced. The C seismic coefficient was equal to 0.10 and 0.07 for seismic category I and II, respectively.

After the 1980 Irpinia earthquake, a third seismic zone was introduced (D.M. 29/02/1984) and C seismic coefficients were assigned (D.M. 24/1/1986) to the three zones (0.10, 0.07 and 0.04 g respectively).

In 1996, the limit state design method was introduced (D.M.16/01/1996) for the design in seismic zone.

On the other hand, seismic classification of the Italian territory remained unchanged until 2003. In fact, only after 2002 Molise earthquake, OPCM 3274/2003 classified the entire Italian territory as seismic, introducing also a fourth seismic zone. In particular, a different horizontal acceleration value a_g (i.e., that corresponding to 0 sec period of vibration in the elastic spectrum) was assigned to each zone and the elastic response spectra were defined as a function of soil stratigraphy. Moreover, the limit states design method became mandatory for structural assessment.

Finally, a great innovation related to the definition of seismic loads was introduced by D.M. 14/01/2008. In fact, the seismic hazard parameters (i.e., input parameters of the response spectrum) were defined for a spaced grid of about 11000 points on Italian territory taking advantage of the MPS04 model (Stucchi et al. 2004, 2011).

However, it should be noted that, despite the evolution of technical codes from 1909 until now (regarding the definition of seismic forces as a function of site category and the evaluation of distribution of static forces), seismic design of a masonry building, explicitly taking into consideration seismic loads, became compulsory only after Irpinia 1980 earthquake (D.M. 9/01/1987).

In fact, all prescriptions enacted until 1980 dealing with lateral loads in design/assessment referred to only moment-resisting frame structures. In other words, for over eight decades (1909-1986) the design of ordinary masonry buildings in seismic zone has been carried out in compliance with normative prescription about:

- maximum height or maximum number of storeys of the building according to seismic category of the construction site;
- minimum thickness of the walls depending on masonry type and seismic category;
- maximum distance between load-bearing masonry walls depending on seismic category;
- the band of use of some masonry textures.

These prescriptions together with further structural detailers are briefly provided in the next section.

3.4.2 Code prescriptions related to masonry buildings

In Table 4 and Table 5, the evolution of seismic code prescriptions (1909-1975) related to ordinary masonry buildings is reported, going from R.D. 18/04/1909 n.193 to R.D. 25/03/1935 n.640 (see Table 4) and from R.D. 22/11/1937 n.2105 to D.M. 3/3/1975 n.40 (see Table 5).

It has to be noted that only bricks and natural/artificial stone in squared blocks characterized by a rough surface were allowed in masonry constructions. Rubble stones were allowed only if spaced out by horizontal courses of bricks or by continuous bands of parallelepiped-shape rectangular stones or by R.C. tie beams. Starting from 1909 (R.D. 18/04/1909 n.193), it was forbidden in seismic zone the use of pebbles; this prescription was extended also to ordinary masonry buildings in non-seismically area after 1935 (R.D. 25/03/1935 n.640).

The maximum height (or the maximum number of storeys) for masonry buildings was settled depending on seismic category of the construction site. In 1915 (R.D. 29/4/1915 n.573), up-to-two-storey masonry buildings (i.e., characterized by a maximum height H_{max} of 7 meters) were allowed in seismic area.

R.D. 13/03/1927 n.431 further modified this limitation as a function of seismic zones. In fact, construction up to two-storeys buildings (i.e., H_{max} of 8 meters) was permitted in I seismic zone, and up to three-storeys buildings (i.e., H_{max} of 12,50 meters) for II seismic zone. Subsequently (R.D. 22/11/1937 n.2105), three-storeys buildings (i.e., H_{max} of 12,50 meters) were also allowed in

I seismic zone and four-storeys buildings (i.e., H_{max} of 16,00 meters) in II seismic zone, only in case of a regular texture (natural or artificial square bricks). Starting from 1962 (Law 1684/1962), the maximum number of storeys in the first seismic category was again limited to two storeys (i.e., H_{max} of 7,50 meters) for I seismic zone and to three storeys (i.e., H_{max} of 11,00 meters) for II seismic zone.

Then, the minimum thickness of masonry walls was settled depending on two factors: seismic category of the construction site and the quality of masonry texture. The prescribed value of thickness decreased with masonry quality and increased with the site's seismicity. For example, in the II seismic zone, a minimum thickness, s_{min} , of 30 cm (for top storey) was required in case of masonry walls made of bricks or natural/artificial squared blocks; instead, in case of rubble stones masonry characterized by horizontal bricks courses, s_{min} was equal to 45 cm (R.D. 13/03/1927 n. 431). Moreover, an increment of 15 cm in thickness for each storey was required passing from the top to the ground storey. The latter prescription remained substantially unchanged until 1975.

A further prescription depending in seismic category dealt with the maximum distance between transverse load-bearing walls. Starting from 1927 (R.D. 13/03/1927 n.431), this distance in second seismic zone was limited to 7 m.

The above requirements were mainly related to geometrical prescriptions. Further prescriptions related to structural details were also enacted. For example, tie beam, characterized by a width equal to the whole depth of the wall and a height of at least 20 cm, became compulsory for all municipalities (seismically classified or not) with the enactment of R.D. 25/3/1935 n.640. Moreover, the latter also suggests for the first time for the use of RC slab in masonry buildings located in seismic zone in order to guarantee an effective connection between vertical and horizontal structures. It should be noted that the prescriptions about geometry of tie beam remained substantially unchanged in the following laws. Instead, minimum quantitative of reinforcements (introduced by R.D. 22/11/1937 n.2105) was modified several times, taking on different values as a function of the zone (seismically classified or not).

It is noteworthy that the use of masonry vaults was explicitly forbidden (except in case of vaults at the underground storeys equipped with tie rods) with

R.D.18/04/1909 n.193 and remained unchanged also for following codes until Law 1684/1962, which does not explicitly provide indication on this topic. Conversely, D.M. 3/3/1975 n.40 allows the use of masonry vaults, but only if adequately constrained by horizontal tie rods absorbing the horizontal thrust played by the former, voiding the overturning action otherwise acting on top of walls.

Then, the ban on the use of pushing structures was enacted for seismic zone for the first time with R.D. 18/4/1909 n.193, as a consequence of lesson-learned after earthquake occurrence (i.e., after the 1908 Messina earthquake). It is to be noted that this prescription became compulsory nationwide, then both for seismically classified and even not municipalities, with R.D. 25/3/1935 n.640.

Table 4. Code prescriptions related to structural-geometric details in masonry buildings between 1909 and 1935.

	R.D. 18/04/1909 n.193	R.D. 29/04/1915 n.573	R.D. 13/03/1927 n.431		R.D. 25/03/1935 n.640		
	Seismic zone	Seismic zone	1° CAT	2° CAT	1° CAT	2° CAT	NC zone
Max building's height	-	7 m	8 m	12 m	8 m	12 m	-
Max number of storeys	1	2	2	3	2	3	-
Min. wall's thickness	1/10 of the building's height	40 cm	40-60 cm	30-45 cm	40-50 cm	30-45 cm	-
Max distance between walls	every 5 m	every 5 m	every 7 m		every 6 m	every 7 m	-
Forbidden materials	pebbles and irregular stone	pebbles and irregular stone	pebbles and irregular stone		pebbles and irregular stone		pebbles
Masonry vaults	forbidden	forbidden	forbidden		forbidden		-
Cantilevered structures	forbidden	forbidden	forbidden		forbidden		-
Pushing structures	forbidden except in case of chain	forbidden except in case of chain	forbidden except in case of chain		forbidden except in case of chain		
Tie beam	-	-	-		width equal to wall's one; height min= 20cm		
RC slab	-	-	-		ribbed slab in two directions (thickness min = 5cm)		

All the above mentioned geometrical and structural requirements (wall thickness, presence of tie beams/tie rods, the removal of pushing structures, distance between walls, etc) were explicitly recalled in Section 5 of the D.M. 3/3/1975 n.40, representing the main reference masonry building design until

1987. In fact, all subsequent codes (D.M. 19/6/1984; D.M.24/01/1986) entirely confirmed these prescriptions.

Table 5. Code prescriptions related to structural-geometric details in masonry buildings between 1937 and 1975.

	R.D. 22/11/1937, n. 2105			L. 25/11/1962, n. 1684			D.M. 3/03/1975		
	1° CAT	2° CAT	NC zone	1° CAT	2° CAT	NC zone	s=6	s=9	s=12
Max building's height	12.50 m	16 m	-	7.50 m	11.0 m	-	16 m	11 m	7.5 m
Max number of storeys	3	4	-	2	3	-	-	-	-
Min. wall's thickness	40-50 cm	30-45 cm	-	40-50 cm	30-45 cm	-	30 cm	-	40 cm
Max distance between walls	every 6 m	every 7 m	-	every 6 m	every 7 m	-	every 7 m	-	-
Forbidden materials	pebbles and irregular stone		pebbles	pebbles and irregular stone		pebbles	-	-	-
Masonry vaults	forbidden		-	forbidden		-	forbidden except in case of tie rods		
Cantilevered structures	forbidden		-	forbidden		-	-		
Pushing structures	forbidden except in case of chain width equal to wall's one; min height = 20cm			forbidden width equal to wall's one; min height = 20cm			forbidden width equal to wall's one; min height = 1/2 width		
Tie beam									
RC slab	min reinforcement = 4φ14 (long); φ5/30cm (transv.)	min reinforcement = 4φ12 (long); φ5/30cm (transv.)		min reinforcement = 4φ16 (long); φ6/25cm (transv.)		min number reforc.= 4; ties every 25-30 cm; min weight reforc. = 50kg/mc	min reinforcement = 4φ16 (long); φ6/25cm (transv.)		
	ribbed slab in two directions (thickness min = 5cm)	-		Min. thickness = 4cm; min. reforc. = 1φ6/25 cm		-	linked to tie beam		

Only with D.M. 9/1/1987, the design of the masonry building must take into consideration both vertical (Section 2.4.2.2 of the Code) and horizontal (Section 2.4.2.3 of the Code) actions, similarly to what prescribed since 1909 for the moment resisting frame structures.

3.4.3 Code prescriptions related to retrofit intervention on masonry buildings

The topics of existing buildings and of retrofit intervention for structural consolidation of masonry buildings damaged by earthquake was already handled by R.D. 18/4/1909 n.193. These interventions included the repair of damaged walls through the use of good quality mortar, the construction of external framed

structure (columns connected with ties at each floor level), the removal of roof pushing structures, the insertion of circumferential or longitudinal ties and of keystones for vaulted structures and the replacement of stairs made of masonry. All these interventions were also adopted by subsequent codes, regulating the consolidation of masonry buildings only in the seismic area (R.D. 29/4/1915 n.573; R.D. 13/03/1927 n.431) and then for the whole national territory (R.D. 25/3/1935 n.640; R.D. 22/11/1937 n.2105), regardless seismic classification.

All these prescriptions were explicitly recalled in Section 9 of the D.M. 3/3/1975 n.40, with slight modifications and/or integrations: the restoration of masonry walls could also be executed with concrete conglomerates or through the insertion of metal or reinforced concrete elements; the damaged slabs had to be replaced with steel or reinforced concrete slabs effectively encased and anchored within tie beams or floor beams; tie beams, if not present, had to be made at each storey.

After the 1980 Irpinia earthquake, an intense production of technical codes focused on the restoration / consolidation of buildings affected by earthquake occurred. In particular, D.M. 2/7/1981 n.593 regulated the post-earthquake reconstruction in the regions struck by the 1980 earthquake (Basilicata, Campania and Puglia), explicitly requiring seismic assessment of existing masonry buildings to be subjected to structural interventions.

In particular, the seismic assessment was required only if, in the as-built condition, the building did not meet all the requirements of Section 5 of the D.M. 3/3/1975 n.40 and the limitations relating to the height of the buildings. Moreover, particular emphasis was given to the connections between vertical walls and between the latter and the horizontal structures, to guarantee an adequate distribution of seismic forces. It was also requested that the horizontal structures have to ensure a rigid diaphragms behaviour. Several interventions were identified by the code to guarantee these performances: localized substitutions of damaged bricks (traditional “scuci-cuci”), grouting injections, insertion of reinforced concrete plates or steel grids, insertion of columns inside the walls, both horizontal and vertical tie rods, replacement of flexible slabs with steel or reinforced concrete slabs and removal of roof pushing structures.

However, all these prescriptions, beyond seismic assessment if required, were mandatory only for municipalities affected by the Irpinia earthquake (as clarified by Law 30/7/1981 n.21745); vice versa, for the remaining municipalities seismically classified (therefore also for L'Aquila and surroundings municipalities) all the prescriptions reported in section 9 of the D.M. 3/3/1975 n.40 were remained in force.

D.M. 24/01/1986 introduced for the first time a clear distinction between seismic upgrading and seismic improvement. The former, including a series of structural measures ensuring to the building to safely withstand design seismic actions, also required the execution of seismic assessment for the building. The latter, including one or more local interventions (the same defined in the DM 2/7/1981 n.593) aimed at improving seismic behaviour of the building, did not require the execution of seismic assessment for the building. Therefore, seismic assessment for masonry building is mandatory in all municipalities, regardless their seismic classification, starting from 1986, if seismic upgrading was required.

3.5 REFERENCES

- [1] Augenti, N., & Parisi, F. (2010). Learning from construction failures due to the 2009 L'Aquila, Italy, earthquake. *Journal of Performance of Constructed Facilities*, 24(6), 536-555.
- [2] Baratta M., I terremoti di Calabria, in "Bollettino della Società Geografica Italiana", a.40, s.IV, vol.7 (1906), pp.432-459. Roma 1906 **(in Italian)**
- [3] Cavallo R., Penta F., Qualche insegnamento tratto dal terremoto irpino del 1962, in "La Ricerca Scientifica", a.34, s.II, parte II (Rendiconti), sezione A (Abiologica), vol.6, n.1 (ottobre 1964), pp.93-128. Roma. **(in Italian)**
- [4] Cavasino A., I terremoti d'Italia nel trentacinquennio 1899-1933, in "Memorie del Regio Ufficio Centrale di Meteorologia e Geofisica", s.III, appendice al vol.4. Roma, 1935. **(in Italian)**
- [5] CIRC. MIN. LL.PP. 30/07/1981, N. 21745. Legge 14 maggio 1981, n. 219 - art. 10. Istruzioni per l'applicazione della normativa tecnica per la riparazione ed il rafforzamento degli edifici in muratura danneggiati dal sisma. **(in Italian)**
- [6] D. MIN. INFRASTRUTTURE E TRASP. 14/09/2005. Norme tecniche per le costruzioni. G.U. Suppl. Ord. 23/09/2005, n. 159. **(in Italian)**

- [7] D. MIN. LL.PP. 03/06/1981. Classificazione «a bassa sismicità» S = 6 del territorio dei comuni delle regioni Basilicata, Campania e Puglia e classificazione sismica S = 9 del territorio del comune di S. Maria La Carità. G.U. 15/06/1981, n. 162. **(in Italian)**
- [8] D.MIN. LL.PP. 09/10/1981. Aggiornamento delle zone sismiche nella regione Molise. G.U. 29/12/1981, n. 355. **(in Italian)**
- [9] D.MIN. LL.PP. 23/09/1981. Aggiornamento delle zone sismiche della regione Sicilia. G.U. 14/11/1981, n. 314. **(in Italian)**
- [10] D.MIN. LL.PP. 26/06/1981. Aggiornamento delle zone sismiche della regione Umbria. G.U. 29/08/1981, n. 237. **(in Italian)**
- [11] D.P.C.M. 09/02/2011. Direttiva del Presidente del Consiglio dei Ministri, 9 febbraio 2011. Valutazione e riduzione del rischio sismico del patrimonio culturale con riferimento alle Norme tecniche per le costruzioni di cui al decreto del Ministero delle infrastrutture e dei trasporti del 14 gennaio 2008. (GU Serie Generale n.47 del 26-02-2011 - Suppl. Ordinario n. 54). **(in Italian)**
- [12] D'Ayala, D.F., Paganoni, S. Assessment and analysis of damage in L'Aquila historic city centre after 6th April 2009. Bull Earthquake Eng 9, 81–104 (2011). <https://doi.org/10.1007/s10518-010-9224-4>
- [13] Decreto Ministeriale 14 Gennaio 2008. Norme tecniche per le costruzioni. **(in Italian)**
- [14] Decreto Ministeriale 16 Gennaio 1996. Norme tecniche relative ai criteri generali di verifica di sicurezza delle costruzioni e dei carichi e sovraccarichi. **(in Italian)**
- [15] Decreto Ministeriale 17 Gennaio 2018. Norme tecniche per le costruzioni. **(in Italian)**
- [16] Decreto Ministeriale 2 Luglio 1981. Normativa per le riparazioni ed il rafforzamento degli edifici danneggiati dal sisma nelle regioni Basilicata, Campania e Puglia. **(in Italian)**
- [17] Decreto Ministeriale 20 Novembre 1987. Norme tecniche per progettazione, esecuzione e collaudo degli edifici in muratura e per il loro consolidamento. **(in Italian)**
- [18] Decreto Ministeriale 24 Gennaio 1986. Norme tecniche relative alle costruzioni antisismiche. **(in Italian)**
- [19] Decreto Ministeriale 29 Febbraio 1984. **(in Italian)**

- [20] Decreto Ministeriale 3 Marzo 1975. Approvazione delle norme tecniche per le costruzioni in zone sismiche. **(in Italian)**
- [21] Decreto Ministeriale 7 Marzo 1981. Dichiarazione in zone sismiche nelle regioni Basilicata, Campania e Puglia. **(in Italian)**
- [22] Decreto Ministeriale 9 Gennaio 1987. Norme tecniche per la progettazione, esecuzione e collaudo degli edifici in muratura e per il loro consolidamento. **(in Italian)**
- [23] Decreto Ministeriale del 10 marzo 1969. Inclusione di comuni della Sicilia nell'elenco delle località sismiche di 1 e 2 categoria. **(in Italian)**
- [24] E. Guidoboni, G. Ferrari, D. Mariotti, A. Comastri, G. Tarabusi, G. Sgattoni, G. Valensise (2018) - CFTI5Med, Catalogo dei Forti Terremoti in Italia (461 a.C.-1997) e nell'area Mediterranea (760 a.C.-1500). Istituto Nazionale di Geofisica e Vulcanologia (INGV). <http://storing.ingv.it/cfti/cfti5/> **(in Italian)**
- [25] Favali P., Giovani L., Spadea M.C., Vecchi M., Il terremoto della Valnerina del 19 Settembre 1979, in "Annali di Geofisica", vol.33, pp.67-100. (1980). **(in Italian)**
- [26] Gruppo di lavoro "Scuotibilità" (1979). Carte preliminari di scuotibilità del territorio nazionale, Pubbl. Prog. Final. Geodin. n. 227, 25 pp. **(in Italian)**
- [27] L. 02/02/1974, N. 64. Provvedimenti per le costruzioni con particolari prescrizioni per le zone sismiche. G.U. 21/03/1974, n. 76. **(in Italian)**
- [28] L. 24/06/2009, N. 77. Conversione in legge, con modificazioni, del decreto-legge 28 aprile 2009, n. 39, recante interventi urgenti in favore delle popolazioni colpite dagli eventi sismici nella regione Abruzzo nel mese di aprile 2009 e ulteriori interventi urgenti di protezione civile. G.U. 27/06/2009, n. 147. **(in Italian)**
- [29] Legge n. 1684 del 25 Novembre 1962. Provvedimenti per l'edilizia, con particolari prescrizioni per le zone sismiche. **(in Italian)**
- [30] Legge n. 219 del 14 Maggio 1981. **(in Italian)**
- [31] Legge regionale 20 giugno 1977, n. 30. Nuove procedure per il recupero statico e funzionale degli edifici colpiti dagli eventi tellurici - Ulteriori norme integrative della legge regionale 7 giugno 1976, n. 17. **(in Italian)**
- [32] Martinelli G., Macrosismi avvertiti in Italia nell'anno 1918, in "Bollettino della Società Sismologica Italiana", vol.22 (1919), pp.272-283. **(in Italian)**
- [33] O.P.C.M. 28 aprile 2006 n. 3519 Criteri generali per l'individuazione delle zone sismiche e per la formazione e l'aggiornamento degli elenchi delle medesime zone. (Gazzetta Ufficiale n. 108; 11 maggio 2006). **(in Italian)**

- [34] Oddone E., Gli elementi fisici del grande terremoto Marsicano-Fucense del 13 gennaio 1915, in "Bollettino della Società Sismologica Italiana", vol.19 (1915), pp.71-217. **(in Italian)**
- [35] Oddone E., Il terremoto dell'alta valle del Tevere del 26 aprile 1917, in "Bollettino della Società Sismologica Italiana", vol.21 (1917-1918), pp.9-27. **(in Italian)**
- [36] Ordinanza del Presidente del Consiglio dei Ministri n. 3274 del 20 marzo 2003. Primi elementi in materia di criteri generali per la classificazione sismica del territorio nazionale e di normative tecniche per le costruzioni in zona sismica. **(in Italian)**
- [37] Parisi, F., De Luca, F., Petruzzelli, F., De Risi, R., Chioccarelli, E., & Iervolino, I. (2012). Field inspection after the May 20th and 29th 2012 Emilia-Romagna earthquakes. Rep., Italian Network of Earthquake Engineering University Laboratories.
- [38] Parisi, Fulvio, and Nicola Augenti. "Earthquake damages to cultural heritage constructions and simplified assessment of artworks." *Engineering Failure Analysis* 34 (2013): 735-760.
- [39] Petrini, V. (1981). Pericolosità sismica e politica di difesa dai terremoti in Italia. Pubbl. Prog. Final. Geodin. n. 442, 17 pp. **(in Italian)**
- [40] Regio Decreto 11 ottobre 1914, n. 1335 (GU n.299 del 15-12-1914). **(in Italian)**
- [41] Regio Decreto 15/07/1909 n. 542 (Gazzetta ufficiale 09/08/1909 n. 185). **(in Italian)**
- [42] Regio Decreto 18 Aprile 1909. Provvedimenti e disposizioni in seguito al terremoto del 28 dicembre 1908. **(in Italian)**
- [43] Regio Decreto 29 Aprile 1915. Norme tecniche ed igieniche da osservarsi per i lavori edilizi nelle località colpite dal terremoto del 13/01/1915. **(in Italian)**
- [44] Regio Decreto Legge 13 Marzo 1927. Norme tecniche ed igieniche per le riparazioni, ricostruzioni e nuove costruzioni degli edifici pubblici e privati nei comuni o frazioni di comune dichiarati zone sismiche. **(in Italian)**
- [45] Regio Decreto Legge 22 Novembre 1937. Norme tecniche ed igieniche per le riparazioni, ricostruzioni e nuove costruzioni degli edifici pubblici e privati nei comuni o frazioni di comune dichiarati zone sismiche. **(in Italian)**
- [46] Regio Decreto Legge 23 Ottobre 1924, n. 2089 GU n. 303 del 30-12-1924
- [47] Regio Decreto Legge 25 Marzo 1935. Nuovo testo delle norme tecniche di edilizia con speciali prescrizioni per le località colpite dai terremoti. **(in Italian)**

- [48] Regione Umbria, 1981—Technical provisions and methodology for repair and strengthening works of buildings damaged by earthquake (art. 38 L:R. 1/7/81 n. 34) - Regione dell'Umbria, Direttive tecniche ed esemplificazione delle metodologie di interventi per la riparazione ed il consolidamento degli edifici danneggiati da eventi sismici (art. 38 L:R. 1/7/81 n. 34) **(in Italian)**
- [49] Rovida A., Locati M., Camassi R., Lolli B., Gasperini P., Antonucci A. (2021). Catalogo Parametrico dei Terremoti Italiani (CPTI15), versione 3.0. Istituto Nazionale di Geofisica e Vulcanologia (INGV). <https://doi.org/10.13127/CPTI/CPTI15.3> **(in Italian)**
- [50] Sisti, R., Di Ludovico, M., Borri, A., Prota, A., 2018. Damage assessment and the effectiveness of prevention: the response of ordinary unreinforced masonry buildings in Norcia during the Central Italy 2016–2017 seismic sequence. *Bulletin of Earthquake Engineering*, 1-21. <https://doi.org/10.1007/s10518-018-0448-z>
- [51] Stucchi, M., Akinci, A., Faccioli, E., Gasperini, P., Malagnini, L., Meletti, C., Montaldo, V., Valensise, G., 2004. Mappa di Pericolosità sismica del territorio Nazionale <http://zonesismiche.mi.ingv.it/documenti/rapportoconclusivo.pdf>. **(in Italian)**
- [52] Stucchi, M., Meletti, C., Montaldo, V., Crowley, H., Calvi, G.M., Boschi, E., 2011. Seismic hazard assessment (2003- 2009) for the Italian building code. *Bulletin of the Seismological Society of America*, 101(4), 1885-1911.
- [53] Tomazevic, M., 1978. The computer program POR, Report ZMRK, Institute for Testing and Research in Materials and Structures, Ljubljana, Slovenia, 1978.

Chapter 4.

DATABASE OF OBSERVED DAMAGE OF PAST ITALIAN EARTHQUAKES

4.1 INTRODUCTION

In the last century, the strategies (such as normative contents, seismic classification, building techniques) to avoid and/or mitigate the negative effects of the seismic event had been changed several times.

As highlighted in the previous Chapter, the earthquake's occurrence was the base on which the seismic classification has been updated over the years (namely, between 1909 and 2003), allowing to detect seismic-prone areas. Moreover, the analysis of post-earthquake damage allowed to identify those structural-geometric details able to affect the seismic behaviour negatively or positively. For example, it was possible to understand that the seismic behaviour of masonry buildings is best when those are equipped with tie rods and/or tie beams, improving the so-called box behaviour. Conversely, the presence of pushing structures (such as vault without suitable chains) has been recognized as a vulnerability factor, able to negatively affect the whole building's behaviour under seismic loads.

Therefore, the analysis of post-earthquake damage is a valuable source of information about the building's behaviour under seismic loads. With this in mind, the Italian DPC (*Dipartimento della Protezione Civile*, Department of

Civil Protection), with the support of Eucentre Foundation (European Centre for Training and Research in Earthquake Engineering), provided an online platform, called Da.D.O. (*Database del Danno Osservato*, Database of Observed Damage) (Dolce et al., 2019), which allows the access to a large database of buildings, collected during the visual inspections done right after the main earthquakes occurred in Italy in the last 50 years. Such large amount of data is particularly useful in the vulnerability and/or fragility studies of the existing built, allowing to detect, for example, a relation between the damage attitude and the building's features. The analysis of this data could be a support to identify the most vulnerable building's typologies, directing possible policies of seismic risk mitigation.

In this Chapter, the focus is on the Da.D.O. platform, emphasizing the motivations and purposes of such valuable project, and deeply describing the available data collected after each earthquake. Obviously, the data resulting from different seismic events (namely, adopting different survey forms developed over the years) are not immediately comparable with each other. Moreover, the survey campaign could be conducted following different criteria, reaching different degree of completeness, especially between the areas farthest and nearest to the epicenter. All these issues (together with other ones) could affect the use of data. Therefore, the last paragraph of the present Chapter is dedicated to the description of such issues, with particular emphasis on numerousness and completeness of the available data.

4.2 DA.D.O. PLATFORM: MOTIVATIONS, PURPOSES AND CONTENTS

Over the years, the role of the Italian DPC (*Dipartimento della Protezione Civile*, Department of Civil Protection) in the management of post-earthquake activities and in the study of seismic risk mitigation strategies has become increasingly important. The DPC carries out activities to assess, prevent and mitigate the seismic risk in Italy: among the others, two relevant tasks are the development of technical-scientific skills for predicting the impact of the earthquake on the territory and the improvement of interventions in emergency conditions and/or during the post-earthquake reconstruction. These tasks are

carried out with the scientific support of the Centres of Competence for seismic risk: among these, the INGV (*Istituto Nazionale di Geofisica e Vulcanologia*, National Institute of Geophysics and Volcanology) provides support for seismological aspects; ReLUIS (*Rete dei Laboratori Universitari di Ingegneria Sismica*, the Network of University Laboratories of Seismic Engineering) and Eucentre (*Centro Europeo per la formazione e la ricerca in ingegneria sismica*, European Centre for Training and Research in Earthquake Engineering) give support about engineering issues. Moreover, Article 19 of the new Civil Protection Code (Decree Law 2/1/2018), issued at the beginning of the 2018, strongly emphasizes the role of the scientific community as support in prevision and prevention activities of the DPC.

In this framework of suitable collaboration between DPC and Centres of Competence, the Da.D.O. (*Database del Danno Osservato*, Database of Observed Damage) platform (Dolce et al., 2019) was conceived. This web-gis platform allows the access to a large database of buildings, collected during the visual inspections done right after the main earthquakes occurred in Italy in the last 50 years. Thus, the main aims of such project are collecting, cataloguing, and comparing data related to severe earthquakes occurred in Italy from the 1976 Friuli earthquake. In particular, data related to 9 seismic events of national relevance (namely, 1976 Friuli; 1980 Irpinia; 1984 Abruzzo; 1997 Umbria-Marche; 1998 Pollino; 2002 Molise; 2003 Emilia; 2009 L'Aquila; 2012 Emilia), are provided by the Da.D.O. platform. Such huge amount of data (more than 300.000 buildings) is certainly a useful support in the forecasting and mitigation policies against earthquakes.

Generally speaking, soon after the earthquake the DPC manages and carries out, with the support of technicians from different institutions and professional organizations, an in-situ survey campaign of all the buildings sited in the affected areas, in order to define the safety level of each damaged building, considering also the possible occurrence of aftershocks. Thus, after each event, the main information about location and morphological-functional characteristics of the building, also considering information about the observed damage, are collected. Additionally, information about losses (victims, injured, homeless), Macro-

seismic intensity values at municipality level and sometimes even for specific location, about the magnitude of the event and the location of the hypocenter are reported. The quantity and the quality of the information collected after the 9 considered events result very different, essentially due to substantial changes in the different survey forms used during the inspections. Nevertheless, the DPC with the support of Eucentre has spent huge efforts in the homogenization process of all parameters collected through the years in order to make them (as much as possible) comparable. In general, the parameters collected in the platform can be grouped in different macro-sections:

- *Building identification*: information about the municipality where each building is sited and its position (i.e., building's address, geographic coordinates).
- *Building description*: building's description in term of geometry (i.e., number of storeys, inter-storey height, storey surface area), use and age (i.e., periods of construction and, eventually, retrofit).
- *Building typology*: information about the building's structural typologies (namely, vertical, horizontal, and roof structures). Such description strongly depends on the survey form used after the earthquake. Additional information (such as the presence of tie rods or tie beams, of isolated columns, on mixed type structures, structural regularity) is provided only by the most recent survey forms.
- *Damage*: damage description at building or component level. Such information strongly depends on the survey form used after each seismic event. In fact, different damage scales and/or building's components have been considered over the time. Moreover, only the most recent forms also provide the damage extent.

In Figure 16, the whole Da.D.O. database has been subdivided in nine portions, providing the percentage amount of data related to each considered seismic event. In fact, the remarkable dissimilarities among data collected after different seismic events (both in terms of amount and type) hindered the definition of a unique database merging all the available collected data.

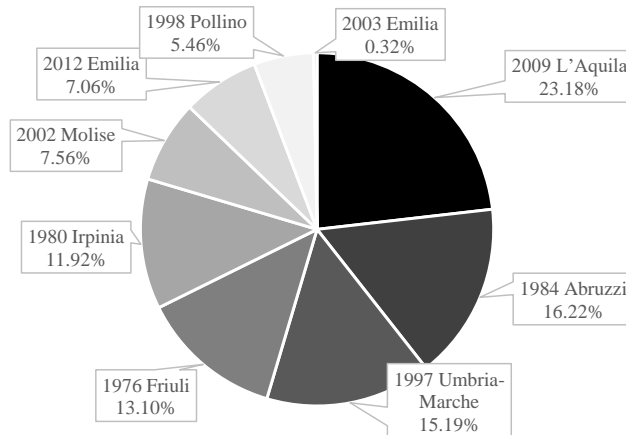


Figure 16. Percentage distribution of Da.D.O. data among the nine seismic events.

The greater part of inspected buildings (i.e., 23% of the entire database) belongs to the data collected after the 2009 L'Aquila earthquake. Other databases highly populated are those composed by data collected after 1984 Abruzzi (i.e., 16%) and 1997 Umbria-Marche (i.e., 15%) seismic events. Conversely, 2002 Molise (i.e., about 8%), 2012 Emilia (i.e., 7%), 1998 Pollino (i.e., 5%), and especially 2003 Emilia (i.e., 0.32%) amount of data does not reach the 10% of the entire Da.D.O. database.

As previously mentioned, the survey form adopted after each seismic event evolved over the time, leading to great differences especially in the definition of building's structural typology and in the damage description. For example, after the three earthquakes occurred between 1979 and 1984, three different survey forms have been used. Conversely, starting from 1997 seismic event, the so-called AeDES (*Agibilità e danno nell'emergenza sismica*, Usability and damage in seismic emergency) form has been adopted to carry on the post-earthquake inspections. Nevertheless, the same AeDES form (Baggio et al., 2007) has been modified several times, updating the required building's parameters. In Table 6, the survey form adopted after each considered seismic event has been detected. Thus, it can be derived that about the 60% of available data has been collected in

accordance with the requirements of the AeDES form (and its modifications), conversely the remaining part derives from other three survey-formats.

Table 6. Survey form adopted after each considered seismic event.

Seismic event	Adopted survey form
1976 Friuli	Friuli 1976
1980 Irpinia	Irpinia 1980
1984 Abruzzi	Abruzzo 1984
1997 Umbria-Marche	AeDES 09/1997
1998 Pollino	AeDES 06/1998
2002 Molise	AeDES 05/2000
2003 Emilia	AeDES 05/2000
2009 L'Aquila	AeDES 06/2008
2012 Emilia	AeDES 06/2008

Clearly, the use of different survey forms directly affected the amount and the quality of the collected building information. Therefore, a preliminary crucial step in the data review is the analysis of the different survey forms. So, in the following Section, a detailed review of the Italian survey forms for post-earthquake inspections is shown, given their direct influence on the available building's information.

4.3 POST-EARTHQUAKE SURVEYS: EVOLUTION OF THE SURVEY FORM

In the last 50 years (namely, from 1979 Friuli earthquake to 2012 Emilia one), the scientific knowledge on the building behaviour under seismic loads has been improved certainly. The widespread awareness that some building's features (such as the tie rods/beams in masonry buildings) could directly affect the seismic damage attitude of the building allowed to the definition of ever more detailed post-earthquake survey forms. Moreover, also the final scope of the survey slightly changed over the time (Dolce et al., 2019), going from the vulnerability analysis (for the first types of form) to the usability one (for the AeDES form).

A first subdivision among the forms adopted after the nine considered seismic events is between the AeDES form and the previous ones. In fact, the filling of the AeDES form is based on a different survey philosophy, assigning to the surveyor more responsibilities. In fact, the approach used until the 1997 is

basically a descriptive approach: thus, the main task of the surveyor was to detect the building's material among those of a given list, without any evaluation on structural behaviour of the building. Conversely, in the AeDES form the descriptive approach has been replaced with behavioural one, being the surveyor an evaluator rather than an observer (Baggio et al., 2007).

In more practical terms, such evolution in the adopted survey philosophy and in the role of surveyor led to radical differences in the building's description. Whilst the pre-AeDES forms provide, for example, a materic description of the (vertical and horizontal) structures, in the AeDES form a classification based on the expected seismic performance is used. For example, the masonry walls are classified based on the masonry quality (rather than on the basis of the used materials). Similarly, the horizontal structures are classified as a function of the slab stiffness.

Among the pre-AeDES forms, 1976 Friuli, 1980 Irpinia, and 1984 Abruzzo are the ones used to collect a part (about 40%) of the Da.D.O. data. The building's description provided by these three forms are based on different parameters and/or different parameter's classification (see Figure 17). For example, whilst the number of storeys is required by every survey form, the inter-storey height and the floor surface is available only for one or some of them. In addition, despite the construction age is always provided, different timespans are considered (namely, *<1850*, *1850-1920*, *1920-1950*, *>1980* for 1976 Friuli form; *<1900*, *1900-1943*, *1943-1962*, *1962-1971*, *>1971* for 1980 Irpinia form). Moreover, no information about the presence of retrofit intervention is in these three types of survey form. As anticipated, the building's typology in such forms is based on a descriptive approach, providing a materic description of the structural features (see Figure 17). For example, the vertical structure of masonry buildings is described by 2 (3 in the 1980 Irpinia form) possible attributes: namely, rubble masonry and bricks (plus tuff in the 1980 Irpinia form). The description of horizontal structures (available only for 1980 Irpinia and 1984 Abruzzi forms) is based on 4 typologies (i.e., masonry vaults, wooden-, iron-, and reinforced concrete- slabs).

(a)

(b)

(c)

Dati metrici		Età	
Superficie media di piano	N° Piani	Costruzione e ristrutturazione	
A $\leq 50 \text{ m}^2$	H $800 \div 1000$	$\bigcirc 1$ $\bigcirc 6$	1 $\bigcirc \leq 1919$
B $50 \div 100$	I > 1000	$\bigcirc 2$ $\bigcirc 7$	2 $\bigcirc 19 - 45$
C $100 \div 200$		$\bigcirc 3$ $\bigcirc 8$	3 $\bigcirc 46 - 60$
D $200 \div 300$		$\bigcirc 4$ $\bigcirc 9$	4 $\bigcirc 61 - 71$
E $300 \div 400$		$\bigcirc 5$ $\bigcirc \geq 10$	5 $\bigcirc 72 - 81$
F $400 \div 600$	Piani interrati	A \bigcirc Sì	6 $\bigcirc 82 - 91$
G $600 \div 800$		B \bigcirc No	7 $\bigcirc > 91$

Uso - Esposizione			
Uso	N° unità d'uso	Utilizzazione	Occupanti
A \bigcirc Abitativo	1 $\bigcirc 1 - 2$	A $\bigcirc > 75\%$	1 $\bigcirc \leq 10$
B \bigcirc Produttiva	2 $\bigcirc 3 - 4$	B $\bigcirc 10 \div 75\%$	2 $\bigcirc 11 - 50$
C \bigcirc Commercio	3 $\bigcirc 5 - 8$	C $\bigcirc < 10\%$	3 $\bigcirc 51 - 100$
D \bigcirc Uffici	4 $\bigcirc 9 - 15$	D \bigcirc In costruzione	4 $\bigcirc \geq 100$
E \bigcirc Serv. Pubb.	5 $\bigcirc 16 - 30$	E \bigcirc Non finito	Proprietà
F \bigcirc Deposito	6 $\bigcirc > 30$	F \bigcirc Abbandonato	
G \bigcirc Strategico			A \bigcirc Pubblica
			B \bigcirc Privata

	Muratura				Cemento armato			
	Tessitura irregol. e cattiva qualità		Tessitura regol. e buona qualità		Pilastri isolati	Strut. intelaiata con piano non tamponato	Strut. intelaiata con piani tutti tamponati	Acciaio
	Pietrame, ciottoli, senza catene o cordoli	Pietrame, ciottoli, con catene o cordoli	Blocchi, mattoni, pietra squadrata, senza catene o cordoli	Blocchi, mattoni, pietra squadrata, con catene o cordoli				
	A	B	C	D	E	F	G	H
1 Volte in muratura	<input type="radio"/>	<input type="radio"/>	<input type="radio"/>	<input checked="" type="radio"/>	Sì			<input type="radio"/>
2 In legno	<input type="radio"/>	<input type="radio"/>	<input type="radio"/>	<input checked="" type="radio"/>	<input type="radio"/>			<input type="radio"/>
3 Acciaio voltine	<input type="radio"/>	<input type="radio"/>	<input type="radio"/>	<input checked="" type="radio"/>				<input type="radio"/>
4 Acciaio tavelloni	<input type="radio"/>	<input type="radio"/>	<input type="radio"/>	<input checked="" type="radio"/>				<input type="radio"/>
5 In c.a.	<input type="radio"/>	<input type="radio"/>	<input type="radio"/>	<input type="radio"/>	NO	<input type="radio"/>	<input type="radio"/>	<input type="radio"/>
6 Non identificate	<input type="radio"/>	<input type="radio"/>	<input type="radio"/>	<input type="radio"/>	<input type="radio"/>	<input type="radio"/>	<input type="radio"/>	<input type="radio"/>

(1-multiscelta: sono ammesse più scelte. Le caselle più evidenziate indicano situazioni peggiori)

Figure 18. Building's description according to AeDES 09/1997 form.

A first version (AeDES 09/1997) of the AeDES form was adopted by Marche Region after the seismic event, that struck the Umbria and Marche regions the 26th of September 1997. All previously listed building's parameters (number of storeys, floor surface, construction age) were re-proposed (despite the different data range), together with new ones. For the first time, also the presence of retrofit interventions is reported, specifying the time period when the retrofit was carried on. The materic description of the vertical structures was replaced by a behavioural description, going from *rubble-bricks* attributes to *bad-good quality* ones. Conversely, the horizontal structures were again described by materic attributes (basically the same of the previous forms), adding a further subdivision between vaults with and without chains. Additional information (such as the presence of ring-beams or tie roads, the presence of isolated columns, the building's regularity) was provided.

The same form was adopted, with minor revisions, in the following earthquakes: 1998 Pollino event (AeDES 06/1998), 2002 Molise and 2003 Emilia ones (AeDES 05/2000), 2009 L'Aquila and 2013 Emilia seismic events (AeDES 06/2008). Moreover, the use of such survey form was regulated with the DPCM 5th May 2011 (i.e., *Approval of the model for the detection of damage, prompt intervention and usability for ordinary buildings in the post-seismic emergency and its compilation manual*), and subsequently transposed by the DPCM 8th of July 2014 (G.U. No. 243 of 18/10/2014).

SEZIONE 2 Descrizione edificio									
Dati metrici			Età		Uso - esposizione				
N° Piani totali con interrati	Altezza media di piano [m]	Superficie media di piano [m ²]	Costruzione e ristrutturaz. [max 2]	Uso	N° unità d'uso	Utilizzazione	Occupanti		
<input type="radio"/> 1 <input type="radio"/> 9	1 <input type="radio"/> ≤ 2.50	A <input type="radio"/> ≤ 50 I <input type="radio"/> 400 ÷ 500	1 <input type="checkbox"/> ≤ 1919	A <input type="checkbox"/> Abitativo	<input type="checkbox"/> <input type="checkbox"/> <input type="checkbox"/>	A <input type="radio"/> > 65%	<input type="checkbox"/> 100	<input type="checkbox"/> 10	<input type="checkbox"/> 1
<input type="radio"/> 2 <input type="radio"/> 10	2 <input type="radio"/> 2.50 ÷ 3.50	B <input type="radio"/> 50 ÷ 70 L <input type="radio"/> 500 ÷ 650	2 <input type="checkbox"/> 19 ÷ 45	B <input type="checkbox"/> Produttivo	<input type="checkbox"/> <input type="checkbox"/> <input type="checkbox"/>	B <input type="radio"/> 30-65%	<input type="checkbox"/> 1	<input type="checkbox"/> 1	<input type="checkbox"/> 1
<input type="radio"/> 3 <input type="radio"/> 11	3 <input type="radio"/> 3.50 ÷ 5.0	C <input type="radio"/> 70 ÷ 100 M <input type="radio"/> 650 ÷ 900	3 <input type="checkbox"/> 46 ÷ 61	C <input type="checkbox"/> Commercio	<input type="checkbox"/> <input type="checkbox"/> <input type="checkbox"/>	C <input type="radio"/> < 30%	<input type="checkbox"/> 2	<input type="checkbox"/> 2	<input type="checkbox"/> 2
<input type="radio"/> 4 <input type="radio"/> 12	4 <input type="radio"/> > 5.0	D <input type="radio"/> 100 ÷ 130 N <input type="radio"/> 900 ÷ 1200	4 <input type="checkbox"/> 62 ÷ 71	D <input type="checkbox"/> Uffici	<input type="checkbox"/> <input type="checkbox"/> <input type="checkbox"/>	D <input type="radio"/> Non utilizz.	<input type="checkbox"/> 3	<input type="checkbox"/> 3	<input type="checkbox"/> 3
<input type="radio"/> 5 <input type="radio"/> > 12		E <input type="radio"/> 130 ÷ 170 O <input type="radio"/> 1200 ÷ 1600	5 <input type="checkbox"/> 72 ÷ 81	E <input type="checkbox"/> Serv. Pub.	<input type="checkbox"/> <input type="checkbox"/> <input type="checkbox"/>	E <input type="radio"/> In costruz.	<input type="checkbox"/> 4	<input type="checkbox"/> 4	<input type="checkbox"/> 4
<input type="radio"/> 6	Piani interrati	F <input type="radio"/> 170 ÷ 230 P <input type="radio"/> 1600 ÷ 2200	6 <input type="checkbox"/> 82 ÷ 91	F <input type="checkbox"/> Deposito	<input type="checkbox"/> <input type="checkbox"/> <input type="checkbox"/>	F <input type="radio"/> Non finito	<input type="checkbox"/> 5	<input type="checkbox"/> 5	<input type="checkbox"/> 5
<input type="radio"/> 7		G <input type="radio"/> 230 ÷ 300 Q <input type="radio"/> 2200 ÷ 3000	7 <input type="checkbox"/> 92 ÷ 01	G <input type="checkbox"/> Strategico	<input type="checkbox"/> <input type="checkbox"/> <input type="checkbox"/>	G <input type="radio"/> Abbandon.	<input type="checkbox"/> 6	<input type="checkbox"/> 6	<input type="checkbox"/> 6
<input type="radio"/> 8		H <input type="radio"/> 300 ÷ 400 R <input type="radio"/> > 3000	8 <input type="checkbox"/> ≥ 2002	H <input type="checkbox"/> Turis-ricet.	<input type="checkbox"/> <input type="checkbox"/> <input type="checkbox"/>		<input type="checkbox"/> 7	<input type="checkbox"/> 7	<input type="checkbox"/> 7
				Proprietà		A <input type="radio"/> Pubblica B <input type="radio"/> Privata			

SEZIONE 3 Tipologia (multiscelta; per gli edifici in muratura indicare al massimo 2 tipi di combinazioni strutture verticali-solai)												
Strutture verticali / Strutture orizzontali		Non identificate	Strutture in muratura						Altre strutture			
			A tessitura irregolare e di cattiva qualità (Pietrame non squadrato, ciottoli...)		A tessitura regolare e di buona qualità (Blocchi; mattoni; pietra squadrata...)		Pietra isolata	Mista	Rinforzata	Telai in c.a.		
			Senza catene o cordoli	Con catene o cordoli	Senza catene o cordoli	Con catene o cordoli				Telai in c. a.	Telai in acciaio	
		A	B	C	D	E	F	G	H	REGOLARITA'		
										Non regolare A	Regolare B	
1	Non identificate	<input type="checkbox"/>	<input type="checkbox"/>	<input type="checkbox"/>	<input type="checkbox"/>	<input type="checkbox"/>	SI	<input type="checkbox"/>	<input type="checkbox"/>	1	Forma pianta ed elevazione	<input type="checkbox"/>
2	Volte senza catene	<input type="checkbox"/>	<input type="checkbox"/>	<input type="checkbox"/>	<input type="checkbox"/>	<input type="checkbox"/>	<input type="checkbox"/>	G1	H1	2	Disposizione tamponature	<input type="checkbox"/>
3	Volte con catene	<input type="checkbox"/>	<input type="checkbox"/>	<input type="checkbox"/>	<input type="checkbox"/>	<input type="checkbox"/>	<input type="checkbox"/>		<input type="checkbox"/>			
4	Travi con soletta deformabile (travi in legno con semplice tavolato, travi e volte...)	<input type="checkbox"/>	<input type="checkbox"/>	<input type="checkbox"/>	<input type="checkbox"/>	<input type="checkbox"/>	NO	G2	H2	Copertura		
5	Travi con soletta semirigida (travi in legno con doppio tavolato, travi e tavoloni...)	<input type="checkbox"/>	<input type="checkbox"/>	<input type="checkbox"/>	<input type="checkbox"/>	<input type="checkbox"/>	<input type="checkbox"/>	<input type="checkbox"/>	<input type="checkbox"/>	1 <input type="radio"/> Spingente pesante		
6	Travi con soletta rigida (solai di c.a., travi ben collegate a solette di c.a...)	<input type="checkbox"/>	<input type="checkbox"/>	<input type="checkbox"/>	<input type="checkbox"/>	<input type="checkbox"/>	<input type="checkbox"/>	G3	H3	2 <input type="radio"/> Non spingente pesante		
										3 <input type="radio"/> Spingente leggera		
										4 <input type="radio"/> Non spingente leggera		

Figure 19. Building's description according to AeDES 06/2008 form.

In Figure 19, the building's description according to the AeDES 06/2008 version of the form has been provided. The *Section 2* of the form (namely, building's description in terms of geometry, use and age) has not changed a lot from the previous versions of the form. For example, the number of underground

storeys is provided, whereas in the AeDES 09/1997 version only the presence of underground storeys was required. The inter-storey height (not provided by AeDES 09/1997) is required by the newer version form. *Section 3* of the form (namely, the building's typology) remained the same as in AeDES 09/1997, except for minor differences. For example, the materic description of the horizontal structures has been replaced with a behavioural description, classifying the horizontal structures based on the slab's stiffness. Moreover, additional structural details are provided by AeDES 06/2008 form: namely, the presence of mixed structures and of localized reinforcements.

In Table 7 and Table 8, a brief review of the parameters for the building's description (geometry, use and age) and the structural typology definition respectively is provided. Despite the minor differences between the several versions of the AeDES forms, greater uniformity (both in terms of quantity and quality of the needed parameters) is shown by the forms adopted starting from 1997. Conversely, the lack of some remarkable parameters (such as the presence of retrofit interventions) is proper to the previous forms (especially Friuli 1979 one).

Table 7. Brief review of parameters needed to the building's description according to the different survey forms.

Adopted survey form	Number of storeys	Inter-storey height	Floor Surface	Building's use	Construction age	Retrofit age
Friuli 1976	•			•	•	
Irpinia 1980	•		•	•	•	
Abruzzo 1984	•		•	•	•	
AeDES 09/1997	•		•	•	•	•
AeDES 06/1998	•	•	•	•	•	•
AeDES 05/2000	•	•	•	•	•	•
AeDES 06/2008	•	•	•	•	•	•

Table 8. Brief review of parameters needed to the structural typology definition according to the different survey forms.

Adopted survey form	Vertical structures	Horizontal structures	Roof structures	Tie rods/beams and isolated columns	Building regularity	Mixed structures
Friuli 1976	4 types; description approach					
Irpinia 1980	5 types; description approach	4 types; description approach	4 types; description approach			
Abruzzo 1984	4 types; description approach	4 types; description approach				
AeDES 09/1997	4 types; behavioural approach	5 types; description approach		•	•	
AeDES 06/1998	7 types; behavioural approach	5 types; behavioural approach	4 types; behavioural approach	•	•	•
AeDES 05/2000	7 types; behavioural approach	5 types; behavioural approach	4 types; behavioural approach	•	•	•
AeDES 06/2008	7 types; behavioural approach	5 types; behavioural approach	4 types; behavioural approach	•	•	•

Also, the data on damage strongly depends on the survey form used after each seismic event. Such description has been modified several times in the forms adopted after the considered seismic events. For example, (5+1) damage levels (including the null damage) have been used to describe the building's damage after 1976 Friuli earthquake. Conversely, for Irpinia 1980 the damage database contains (7+1) damage levels, while for Abruzzo 1984 the damage levels are (5+1), coherently with the European Macroseismic Scale EMS-98 (Grunthal, 1998). Starting from the Umbria-Marche 1997 event, the first level AeDES survey form for post-earthquake damage and usability assessment was used (Baggio et al., 2007), considering (3+1) damage levels.

Moreover, not only the number of damage levels changes between the several forms, but also the object of the damage description. In fact, Friuli 1976 form (see Figure 20(a)) provides the building's damage by means a reparability

judgment (i.e., *restorable without structural intervention*; *restorable with structural intervention*; *partially reparable*; *not reparable*; *destroyed*), whereas the following forms describe the damage at component level.

GIUDIZIO SINTETICO SULL'EDIFICIO

8 Distrutto ☐

9 Non ripristinabile ☐

10. Ripristinabile: totalmente ☐ parzialmente ☐ Necessitano riparazioni strutturali? sì ☐ no ☐

11. Riparazioni già eseguite: in tutto ☐ in parte ☐

12 Non necessitano interventi ☐

ENTITA' DEL DANNO

NESSUN DANNO
 IRRELEVANTE - RIPARAZIONE NON URGENTE
 LIEVE - DA RIPARARE
 NOTEVOLE - DA SGOMBRARE PARZIALMENTE - RIPARABILE
 GRAVE - DA SGOMBRARE - RIPARABILE
 GRAVISSIMO - DA SGOMBRARE E DEMOLIRE
 CROLLATO PARZIALMENTE - DA DEMOLIRE
 DISTRUTTO

STRUTTURA PORTANTE
 SOLAI
 TETTI
 PARETI INTERNE
 PARETI ESTERNE
 SCALE

SOURCE OF INFORMATION ON DESTROYED BUILDINGS
 1 INFORMATION DIRECT
 2 PHOTO
 3 PREVIOUS STUDIES

SIGNATURE AND QUALIFICATION

CARATTERISTICA DEL DANNO ALLE STRUTTURE

	Struttura verticale	Struttura orizzontale				Tetto	Tamponamenti esterni	Pareti interne	Scale	Sorgenti	Emergenze
		1*	2*	3*	4*						
1 Lieve											
2 Rilevante											
3 Grave											
4 Gravissimo											
5 Distruzione											

Figure 20. Damage description according to (a) 1976 Friuli, (b) 1980 Irpinia, and (c) 1984 Abruzzi form.

In particular, among the pre-AeDES forms, Irpinia 1980 form provides the damage of vertical, horizontal, and roof structures, of internal and external infills, and of stairs (Figure 20(b)). Almost the same components are in the Abruzzi 1984 form, that provides the damage of slabs separately for each floor (Figure 20(c)). Conversely, in the first version (AeDES 09/1997) of the AeDES form (Figure 21(a)), the damage is described only for three structural components

(namely, the vertical and horizontal structures, and the stairs), whereas all following versions (i.e., AeDES 06/1998 to AeDES 06/2008; see Figure 21(b)) consider five components (i.e., vertical, horizontal, and roof structures, stairs and infills).

Livello Tipo struttura	DANNO								
	D4-D5 Graviss o crollo			D2-D3 Medio grave			D0-D1 Nullo o leggero		
	$\geq 2/3$	$1/3 - 2/3$	$< 1/3$	$\geq 2/3$	$1/3 - 2/3$	$< 1/3$	$\geq 2/3$	$1/3 - 2/3$	$< 1/3$
	A	B	C	D	E	F	G	H	I
1 Strutture verticali	<input type="radio"/>	<input type="radio"/>	<input type="radio"/>	<input type="radio"/>	<input type="radio"/>	<input checked="" type="radio"/>	<input type="radio"/>	<input type="radio"/>	<input type="radio"/>
2 Strutture orizzont.	<input type="radio"/>	<input type="radio"/>	<input type="radio"/>	<input type="radio"/>	<input type="radio"/>	<input checked="" type="radio"/>	<input type="radio"/>	<input type="radio"/>	<input type="radio"/>
3 Scale	<input type="radio"/>	<input type="radio"/>	<input type="radio"/>	<input type="radio"/>	<input type="radio"/>	<input checked="" type="radio"/>	<input type="radio"/>	<input type="radio"/>	<input type="radio"/>
4 Danno preesist.	<input type="radio"/>	<input type="radio"/>	<input type="radio"/>	<input type="radio"/>	<input type="radio"/>	<input checked="" type="radio"/>	<input type="radio"/>	<input type="radio"/>	<input type="radio"/>

(a)

Livello - estensione Componente strutturale - Danno preesistente	DANNO ⁽¹⁾								
	D4-D5 Gravissimo			D2-D3 Medio grave			D1 Leggero		
	$\geq 2/3$	$1/3 - 2/3$	$< 1/3$	$\geq 2/3$	$1/3 - 2/3$	$< 1/3$	$\geq 2/3$	$1/3 - 2/3$	$< 1/3$
	A	B	C	D	E	F	G	H	I
1 Strutture verticali	<input type="checkbox"/>	<input type="checkbox"/>	<input type="checkbox"/>	<input type="checkbox"/>	<input type="checkbox"/>	<input type="checkbox"/>	<input type="checkbox"/>	<input type="checkbox"/>	<input type="checkbox"/>
2 Solai	<input type="checkbox"/>	<input type="checkbox"/>	<input type="checkbox"/>	<input type="checkbox"/>	<input type="checkbox"/>	<input type="checkbox"/>	<input type="checkbox"/>	<input type="checkbox"/>	<input type="checkbox"/>
3 Scale	<input type="checkbox"/>	<input type="checkbox"/>	<input type="checkbox"/>	<input type="checkbox"/>	<input type="checkbox"/>	<input type="checkbox"/>	<input type="checkbox"/>	<input type="checkbox"/>	<input type="checkbox"/>
4 Copertura	<input type="checkbox"/>	<input type="checkbox"/>	<input type="checkbox"/>	<input type="checkbox"/>	<input type="checkbox"/>	<input type="checkbox"/>	<input type="checkbox"/>	<input type="checkbox"/>	<input type="checkbox"/>
5 Tamponature-tramezzi	<input type="checkbox"/>	<input type="checkbox"/>	<input type="checkbox"/>	<input type="checkbox"/>	<input type="checkbox"/>	<input type="checkbox"/>	<input type="checkbox"/>	<input type="checkbox"/>	<input type="checkbox"/>
6 Danno preesistente	<input type="checkbox"/>	<input type="checkbox"/>	<input type="checkbox"/>	<input type="checkbox"/>	<input type="checkbox"/>	<input type="checkbox"/>	<input type="checkbox"/>	<input type="checkbox"/>	<input type="checkbox"/>

(b)

Figure 21. Damage description according to (a) AeDES 09/1997, and (b) AeDES 06/2008 form.

Moreover, unlike the previous forms, the AeDES ones also provides the damage extension, assigning to the damage level of a given structural component a further value (namely, $<1/3$; $1/3-2/3$; $>2/3$).

Lastly, a brief review of the damage description of eight considered survey forms is reported in Table 9, providing the number of damage levels (including the null damage), the scale of the damage description (i.e., building or component scale), the number and the type of structural components (i.e., vertical structures, VS; horizontal structures, HS; roof, R; infill partitions, IP; stairs, S) and the presence of damage extension.

Table 9. Brief review of parameters needed to the damage description according to the different survey forms.

Adopted survey form	Number of Damage Levels	Object of the description	Components	Damage extension
Friuli 1976	5+1	building		
Irpinia 1980	7+1	component	VS HS R IP S	
Abruzzo 1984	5+1	component	VS HS R IP S	
AeDES 09/1997	3	component	VS HS S	•
AeDES 06/1998	3+1	component	VS HS R IP S	•
AeDES 05/2000	3+1	component	VS HS R IP S	•
AeDES 06/2008	3+1	component	VS HS R IP S	•

Clearly, also for the damage description a greater uniformity of data is guaranteed starting from 1997, by means of the use of the AeDES form. Conversely, remarkable differences and/or potential shortcomings (the number of damage levels, the object of the damage description, the absence of damage extensions) are in the previous forms.

4.4 CRITICAL REVIEW OF DA.D.O. POST-EARTHQUAKE DATA

In this Section, each database related to a specific seismic event, belonging to Da.D.O. platform, is analysed focusing on the amount of data and on quality of the available building's features.

Table 10. Structural typologies of buildings reported in Da.D.O. platform for each available database.

Seismic Event	Number of buildings (Da.D.O. platform)			
	Masonry	RC	Others	TOT
1976 Friuli	29641	469	11742	41852
1980 Irpinia	30033	3868	4178	38079
1984 Abruzzo	46763	2092	2962	51817
1997 Umbria-Marche	41852	50	6623	48525
1998 Pollino	14515	1285	1642	17442
2002 Molise	19086	2206	2849	24141
2003 Emilia	899	0	112	1011
2009 L'Aquila	49365	12019	12665	74049
2012 Emilia	17881	1795	2878	22554

As highlighted in previous paragraphs, after the nine events reported in the Da.D.O. platform, seven different survey form have been used (see Table 6) for post-earthquake inspections. Basically, the same form has been used both after 2002 Molise and 2003 Emilia earthquakes (AeDES 05/2000), and both after 2009

L'Aquila and 2012 Emilia ones (AeDES 06/2008). Despite the significant differences among the building's features collected by different forms, for all database a first classification based on structural typology can be performed, dividing between masonry and reinforced concrete (R.C.) buildings, and other typologies. Thus, Table 10 shows the number of buildings available for each database, subdivided as a function of structural types. About 80% of the population is constituted by masonry buildings, while only 8% by RC buildings and the remaining 12% by other types (steel, mixed, ...). About masonry buildings, 40% of the total is represented by Abruzzo 1984 and L'Aquila 2009 databases. On the other hand, about 70% of the RC buildings is represented by Irpinia 1980 and L'Aquila 2009 databases. Note that Emilia 2003 database is constituted by very few buildings (only 0.4% of masonry buildings and no R.C. buildings, respectively). Moreover, Umbria-Marche 1997 database reports a significant number of masonry buildings (similar to Abruzzo 1984 and L'Aquila 2009 databases), and a limited number of RC buildings (just 0.2% of the total).

In this thesis work, the focus is on residential masonry buildings. So, starting from the total number of inspected buildings, an additional requirement about the residential use has been applied, detecting the only residential buildings.

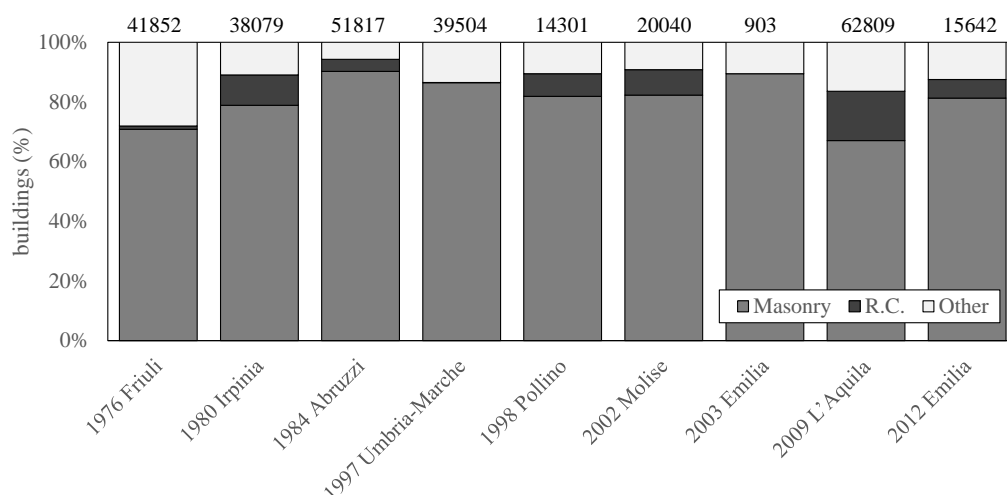


Figure 22. Structural typology distribution for residential buildings of Da.D.O. platform.

In Figure 22, the percentage distribution of structural typology is provided for each dataset of Da.D.O. platform, considering only residential buildings. Thus, the number over each bar is the number of residential buildings inspected after the seismic event (reported in abscissa): basically, this amount has been obtained as difference between the total number reported in Table 10 and the number of non-residential (productive, commercial, industrial,...) buildings, and is about the 90% of the whole database.

Also considering the only residential use, the greater proportion (almost the 80%) of data in each dataset is about masonry buildings. Such result is consistent with the ISTAT 2011 census, according to which about 57% of the current Italian building's stock is composed by masonry buildings. Obviously, the proportion of masonry buildings has been changed over the time, decreasing progressively for the increasing widespread of reinforced concrete buildings. Undoubtedly, nowadays masonry buildings are a significant part of the Italian building's stock, resulting in a worthy of study topic.

The study of damage data provided by the Da.D.O. platform cannot prescind from careful analysis of the data's completeness. Such issue, well-known in the literature, is a direct result of the survey campaign, often more focused on the areas most affected by the earthquake. For example, after 2009 L'Aquila earthquake, the major part of the inspections were done in municipalities near to the epicenter, because a building-by-building survey was planned only where the felt macroseismic intensity was at least equal to VI (Dolce and Goretti, 2015; Zucconi et al., 2018; Rosti et al., 2018; Del Gaudio et al., 2019). Conversely, in the municipalities farthest from the epicenter, where shaking was light, the inspection was performed only under request of the building's owner, thus likely only in case of damaged building. This rule, on one side allowed a faster survey campaign, on the other hand, may have introduced a systematic overestimation of the damage at low seismic intensities (Rossetto et al., 2013). To prevent this bias, in several studies (Colombi et al., 2008; Zucconi et al., 2018; D'Amato et al., 2020) the underestimation of the total number of buildings has been overcome, integrating the original database by means of census data. In other works (Sabetta et al., 1998; Goretti and Di Pasquale, 2004; Rota et al., 2008; Del

Gaudio et al., 2019), the fragility assessment has been performed discarding from the original database all buildings located in the less inspected municipalities. Lastly, a two-step mixed approach is adopted in still other studies (Del Gaudio et al., 2021; Scala et al., 2022), combining the first two solutions. All these approaches are based on the evaluation of a completeness ratio, C.R., for each municipality belonging to a given database.

$$C.R. = \frac{N_{b,DaDO}}{N_{b,ISTAT}} \quad (1)$$

Basically, C.R. is defined as the ratio between the number of inspected residential buildings contained in the Da.D.O. platform ($N_{b,DaDO}$), and the number of residential buildings contained in census data ($N_{b,ISTAT}$). Obviously, the lower the C.R. the higher the number of not inspected buildings, conversely when C.R. approaches to 1 (or overcomes 1) it means that all the buildings sited in the considered municipality have been inspected. Clearly, a partial or incomplete subset of buildings (i.e., C.R. $\ll 1$), if not statistically representative of the damage suffered by buildings of that area, could strongly biases fragility estimation (Rossetto et al., 2013).

The evaluation of C.R. was carried out considering the data provided by ISTAT 2001 census. It is to be noted that the census data is, in some cases, not coeval with the period when the inspection took place, for example for 1984 Abruzzo (17 year before), for 2009 L'Aquila (8 years later) and for 2012 Emilia (11 years later). The use of ISTAT 2001 census is motivated by (i) the fact that is about in the middle of the range defined by the occurrence of considered earthquake (from 1976 to 2012), (ii) the buildings constructed in the decade 2001-2011 for the considered area are substantially negligible (evaluated using the updated version of census data, ISTAT 2011) and (iii) the earlier version of census (ISTAT 1991) deals with a structural unit that is not consistent with that of the survey (dwelling), introducing further uncertainties for their conversion (Colombi et al., 2008). Obviously, the use of ISTAT 2001 suits good for 1997 Umbria-Marche, 1998 Pollino, 2002 Molise, and 2003 Emilia databases. Then,

for Friuli 1976 and Abruzzo 1984 the following approach has been used to obtain a reliable comparison between the considered sources (Da.D.O. and ISTAT 2001). Firstly, only buildings from ISTAT 2001 constructed before 1981 have been considered. Then, the number of collapsed buildings (from Da.D.O.) has been added to this sample to account for those demolished between the earthquake year and 2001 (Colombi et al., 2008). Note that this analysis has not been done for Irpinia 1980 database, since all 41 municipalities reported in Da.D.O. have been chosen by the DPC among the over 600 affected by the 1980 earthquake to be subjected to complete investigations (Braga et al., 1982) as representative of the isoseismals to which they belong.

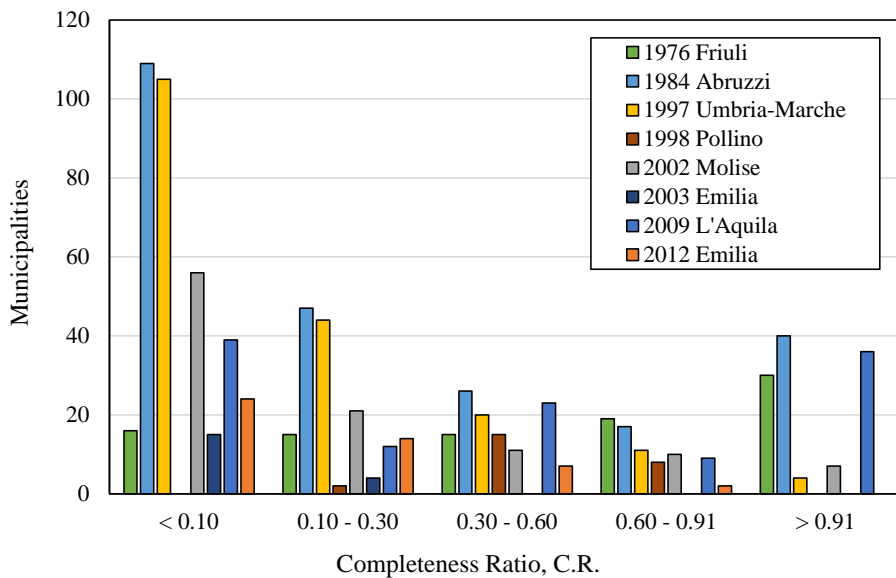


Figure 23. Completeness Ratio, C.R., for all municipalities of each considered database.

Figure 23 shows the distribution of the C.R. for the eight considered databases (namely, all reported in the Da.D.O. platform, except 1980 Irpinia one). To detect the *completely* inspected municipalities, values of completeness threshold used in previous studies are of the order of 0.75 (Sabetta et al., 1998), 0.80 (Goretti and Di Pasquale, 2004), 0.60 (Rota et al., 2008), 0.91 (Del Gaudio et al., 2020; Rosti et al, 2020a, Rosti et al, 2020b). This latter value has been considered as

completeness threshold in the present thesis work. Therefore, 1976 Friuli, 1984 Abruzzo, 1997 Umbria-Marche, 2002 Molise and 2009 L'Aquila databases present at least some municipalities with CR higher than 0.91, whereas Pollino 1998 and Emilia 2012 does not present any municipalities with C.R. higher than 0.91. Moreover, the greater part of completely inspected (according to the definition herein considered) municipalities derives from 1976 Friuli, 1984 Abruzzi and 2009 L'Aquila, to which correspond 30, 40 and 36 completely surveyed municipalities respectively. In addition, 41 municipalities where a building-by-building survey has been carried on derive from 1980 Irpinia database.

Table 11. Number of masonry buildings sited in the *completely* surveyed municipalities for each database of Da.D.O. platform.

Seismic Event	Number of masonry buildings in completely inspected municipalities
1976 Friuli	13.489
1980 Irpinia	30.033
1984 Abruzzo	22.147
1997 Umbria-Marche	1.617
1998 Pollino	0
2002 Molise	8.134
2003 Emilia	0
2009 L'Aquila	28.966
2012 Emilia	0

In Table 11 the number of residential masonry buildings sited in completely surveyed municipalities is reported for each database. Clearly zero buildings correspond to 1998 Pollino, 2003 Emilia and 2012 Emilia databases, since no buildings-by-buildings survey was carried out in the inspected municipalities. Conversely, the most populated databases are 1980 Irpinia, 1984 Abruzzi and 2009 L'Aquila ones, that represent, respectively, the 29%, 28%, and 21% of the entire complete data.

The present thesis work is about the seismic vulnerability and fragility analysis of residential masonry buildings, focusing on 2009 L'Aquila database. The choice of considering a unique database is aimed to avoid any merging assumption, preventing bias both in the building's taxonomy and in the damage

analysis. As highlighted in Section 4.3, remarkable differences in collected data are caused by the use of different survey forms over the years. Such differences may be related to the building geometry (Table 7), the structural typology (Table 8), and the observed damage (Table 9). The major differences are between AeDES form and the previous ones, deriving from a different survey philosophy. Therefore, the merge of all available databases into one is not feasible, except by specific assumptions (Dolce et al., 2019). Moreover, the choice of 2009 L'Aquila database as study data is motivated by the following issues:

1. The use of an AeDES survey form allows to investigate relevant building's features (not provided by previous forms). Among the others, the presence of retrofit interventions is a remarkable feature, provided only by AeDES forms.
2. Great amount of complete data (namely, residential masonry buildings sited in *completely* inspected municipalities) characterizes the 2009 L'Aquila database. Among the datasets deriving from AeDES forms, this latter is the most populated one.

It is worth pointing out that reconnaissance field trips performed after the earthquake were carried out by teams of highly trained technicians, coordinated by the Italian Department of Civil Protection. Several institutions (such as Municipal Technical Offices, Universities, National Research Council, Fire Brigades, European Centre for Training and Research in Earthquake Engineering, ...) had provided their support in carrying out surveys. Moreover, on-site short courses were planned to guarantee high levels of preparation of all surveyors (Dolce and Goretti, 2015). Of course, expertise degree of surveyors is a quite relevant issue in empirical studies since it is related to the reliability of collected data. In fact, it is expected that measurement errors (Rossetto et al., 2013) are less recurrent when the post-earthquake survey is carried out by expert technicians.

Therefore, in the following Chapters such database has been deeply analysed, focusing the attention on several building's feature (among the others, quality of

masonry walls, type of horizontal structures, presence of retrofit interventions, construction age, ...) able to affect the behaviour under seismic loads. Such critical review of available data led to the definition of a complex building's taxonomy, adopted both in vulnerability and fragility assessment.

4.5 REFERENCES

- [1] Baggio, C., Bernardini, A., Colozza, R., Corazza, L., Della Bella, M., Di Pasquale, G., Papa, F., 2007. Field manual for post-earthquake damage and safety assessment and short term countermeasures (AeDES). European Commission—Joint Research Centre—Institute for the Protection and Security of the Citizen, EUR, 22868.
- [2] Braga F., Dolce M., Liberatore D., 1982. A statistical study on damaged buildings and an ensuing review of the MSK-76 scale. Proceedings of the seventh European conference on earthquake engineering, Athens, Greece, 431-450.
- [3] Colombi, M., Borzi, B., Crowley, H. et al., 2008. Deriving vulnerability curves using Italian earthquake damage data. *Bull Earthquake Eng* 6, 485–504. <https://doi.org/10.1007/s10518-008-9073-6>
- [4] D'Amato M, Laguardia R, Di Trocchio G, Coltellacci M, Gigliotti R. Seismic Risk Assessment for Masonry Buildings Typologies from L'Aquila 2009 Earthquake Damage Data. *Journal of Earthquake Engineering* 2020; 00(00): 1-35. DOI: 0.1080/13632469.2020.1835750.
- [5] Decreto del Presidente del Consiglio dei Ministri, D.P.C.M., 05/05/2011 n° 109, G.U. 15/07/2011. **(in Italian)**
- [6] Decreto del Presidente del Consiglio dei Ministri, D.P.C.M., 8 luglio 2014 Istituzione del Nucleo Tecnico Nazionale (NTN) per il rilievo del danno e la valutazione di agibilita' nell'emergenza post-sismica e approvazione dell'aggiornamento del modello per il rilevamento dei danni, pronto intervento e agibilita' per edifici ordinari nell'emergenza post-sismica e del relativo manuale di compilazione. (14A07921) (GU Serie Generale n.243 del 18-10-2014) **(in Italian)**
- [7] Decreto Legislativo del 2 gennaio 2018, n. 1. Codice della protezione civile. (GU Serie Generale n.17 del 22-01-2018) **(in Italian)**
- [8] Del Gaudio C., De Martino G., Di Ludovico M., Manfredi G., Prota A., Ricci P., Verderame G.M., 2019. Empirical fragility curves for masonry buildings after the 2009 L'Aquila, Italy, earthquake. *Bulletin of Earthquake Engineering*. <https://doi.org/10.1007/s10518-019-00683-4>.

- [9] Del Gaudio, C., Di Ludovico, M., Polese, M. et al. Seismic fragility for Italian RC buildings based on damage data of the last 50 years. *Bull Earthquake Eng* 18, 2023–2059 (2020). <https://doi.org/10.1007/s10518-019-00762-6>
- [10] Del Gaudio, C., Scala, S.A., Ricci, P., Verderame G.M., 2021. Evolution of the seismic vulnerability of masonry buildings based on the damage data from L'Aquila 2009 event. *Bull Earthquake Eng* (2021). <https://doi.org/10.1007/s10518-021-01132-x>
- [11] Dolce M., Goretti A., 2015. Building damage assessment after the 2009 Abruzzi earthquake. *Bulletin of Earthquake Engineering* 13, 2241–2264 (2015). <https://doi.org/10.1007/s10518-015-9723-4>.
- [12] Dolce, M., Speranza, E., Giordano, F., Borzi, B., Bocchi, F., Conte, C., Pascale, V., 2019. Observed damage database of past Italian earthquakes: the Da. DO WebGIS. *Bollettino di Geofisica Teorica ed Applicata*, 60(2).
- [13] Goretti, A., & Di Pasquale, G. (2004). Building inspection and damage data for the 2002 Molise, Italy, earthquake. *Earthquake Spectra*, 20(1_suppl), 167-190.
- [14] Grünthal M., 1998. European Macro-seismic Scale. *Cahiers du Centre Européen de Géodynamique et de Séismologie*, Vol. 15. European Macro-seismic Scale 1998. European Center for Geodynamics and Seismology. **(in French)**
- [15] ISTAT 1991. Istituto Nazionale di Statistica (National Institute of Statistics). 13° Censimento generale della popolazione e delle abitazioni. **(in Italian)**
- [16] ISTAT 2001. Istituto Nazionale di Statistica (National Institute of Statistics). 14° Censimento generale della popolazione e delle abitazioni. **(in Italian)**
- [17] ISTAT 2011. Istituto Nazionale di Statistica (National Institute of Statistics). 15° Censimento generale della popolazione e delle abitazioni. Dati sulle caratteristiche strutturali della popolazione, delle abitazioni e variabili. **(in Italian)** <http://www.istat.it/it/archivio/104317>
- [18] Rossetto T., Ioannou I., Grant D.N., 2013. Existing empirical fragility and vulnerability functions: Compendium and guide for selection, GEM Technical Report 2013-X, GEM Foundation, Pavia, Italy.
- [19] Rosti A., Del Gaudio C., Di Ludovico M., Magenes G., Penna A., Polese M., Verderame G.M., 2020a. Empirical vulnerability curves for Italian residential buildings. *Bollettino di Geofisica Teorica ed Applicata*, 61(3).
- [20] Rosti A., Del Gaudio C., Rota M., Ricci P., Di Ludovico M., Penna A., Verderame G.M., 2020b. Empirical fragility curves for Italian residential RC

- buildings. Bull Earthquake Eng (2020). <https://doi.org/10.1007/s10518-020-00971-4>.
- [21] Rosti A., Rota M., Penna A., 2018. Damage classification and derivation of damage probability matrices from L'Aquila (2009) post-earthquake survey data. Bulletin of Earthquake Engineering 16.9 (2018): 3687-3720.
- [22] Rota M., Penna A., Strobbia C.L., 2008. Processing italian damage data to derive typological fragility curves. Soil Dynamics and Earthquake Engineering, 933-947.
- [23] Sabetta F., Goretti A., Lucantoni A., 1998. Empirical Fragility Curves from Damage Surveys and Estimated. 11th European Conference on Earthquake Engineering © 1998 Balkema, Rotterdam, ISBN 90 5410 982 3.
- [24] Scala S.A., Del Gaudio C., Verderame G.M., 2022. Influence of construction age on seismic vulnerability of masonry buildings damaged after 2009 L'Aquila Earthquake (**under review**)
- [25] Zucconi M., Ferlito R., Sorrentino L., 2018. Simplified survey form of unreinforced masonry buildings calibrated on data from the 2009 L'Aquila earthquake. Bulletin of Earthquake Engineering, 16(7), 2877-2911.

Chapter 5.

CRITICAL REVIEW OF DATA COLLECTED AFTER L'AQUILA 2009 EARTHQUAKE

5.1 INTRODUCTION

In this Chapter, starting from the raw data collected after 2009 L'Aquila event and provided by the Da.D.O. platform (Dolce et al., 2019), the database (DB) adopted in this study has been defined based on two main requirements, namely the building taxonomy's detail and the data's completeness.

As deeply investigated in literature (Zuccaro et al., 2015), the seismic behaviour of masonry buildings is affected by several building's features (such as the masonry layout, the type of horizontal structure, the presence of tie rods or/and tie beams, the presence of retrofit intervention, ...). Therefore, a taxonomy able to consider several features allows most accurate evaluations. Nevertheless, the greater the number of classes, the less the number of buildings for each class. Thus, the building taxonomy should be the better compromise between accuracy of building's description and the numerosity of the classes.

The second issue, well-known in literature, is about the data completeness and is a direct result of the survey campaign, often more focused on the areas most affected by the earthquake. As shown in Section 4.4, also after L'Aquila earthquake, such survey type has been done, planning a building-by-building survey only where the felt macroseismic intensity was at least equal to VI (Dolce

and Goretti, 2015; Zucconi et al., 2018; Rosti et al., 2018; Del Gaudio et al., 2019). Such procedure could introduce a systematic overestimation of the damage (i.e., underestimation of the number of undamaged buildings), leading biases in vulnerability and fragility analysis (Rossetto et al., 2013).

To overcome such issue, as in many other literature's works (Rosti et al., 2018; Del Gaudio et al., 2019; Del Gaudio et al., 2021; Scala et al., 2022), a completeness ratio (C.R.) has been evaluated for each inspected municipalities, using the census data. Thus, damage data has been differently processed, based on the corresponding completeness value, dividing in three degrees of detail (namely, $C.R. < 0.1$; $0.1 < C.R. < 0.91$; $C.R. > 0.91$) of survey. Basically, data related to municipalities with $C.R. > 0.91$ has been considered as "positive evidence" of the damage. Conversely, the few data in municipalities slightly surveyed ($C.R. < 0.10$) represent the "negative evidence" of the damage, because such data has been replaced with not damaged buildings. The number of these latter has been derived from census data, whereas the building's features from the related distributions of complete data. Lastly, data related to buildings sited in municipalities with completeness between 0.10 and 0.91 has been discarded.

5.2 POST-EARTHQUAKE SURVEY AND COLLECTED DATA

After a seismic event, certainly, several activities have to be organized and several institutions are required to manage the post-earthquake state. Among these activities, the post-earthquake survey's campaign managed by the Italian Department of Civil Protection (DPC) results very relevant in this study. In fact, data collected after the earthquake is particularly useful in the vulnerability and/or fragility studies of the existing built, allowing to detect, for example, a relation between the damage attitude and the building's features.

The 6th of April 2009, at 3:32 a.m., an earthquake of magnitude 5.9 on the Richter scale (M_w 6.3) hit the city of L'Aquila and some tens of surrounding municipalities. To evaluate the immediate occupancy and the structural and non-structural damage of the affected built, just after the event a reconnaissance field trip was performed. At the end of August 2009, the survey was carried out on

over than 70.000 buildings (Dolce et al. 2009), some of which inspected more than once because of aftershocks.

The reconnaissance field trips were performed by groups of expert technicians, under the supervision of the Italian Department of Civil Protection and with the support of several institutions (Municipal Technical Officers, Universities, National Research Council, Fire Brigades, ...).

The outcome of the survey campaign was an extensive building's database, composed by 74.049 inspected buildings. As highlighted in the previous Chapter, to assess the post-earthquake damage and short-term countermeasures, the first-level survey AeDES (Baggio et al. 2007) form was filled for each inspected building. For the surveyor, the first step after identifying (*Section 1* of the form) the building, was to provide an extensive building's description (*Section 2* of the form), specifying the geometry (i.e., the number of storeys, the inter-storey height, the storey surface area, ...), the use (residential, commercial, productive, ...) and the construction age of the inspected building. The *Section 3* of the form was about the building's typology, seen as structural typology: the data collected in this section (vertical and horizontal structures, presence of tie rods and/or tie beams, structural regularity, type of roof) allows to describe the building in terms of seismic performance, compatibly with the limits of a visual inspection.

The damage description of the structural components (*Section 4* of the form) was based on (3+1) levels scale, going from null damage (D0) to very high damage (D4-D5), and on 3 damage extents. To assign a damage level, the focus of the surveyor was on the presence of cracks, changes in the geometry, and in general on phenomena that could cause a loss of seismic performance. Also, information about damage to non-structural elements (*Section 5*) and the presence of dangers external to the inspected building (*Section 6*) was collected in the form. The site morphology and the possible presence of landslides were provided by *Section 7*. Lastly, the surveyor was required to assess the building's usability (*Section 8*) for an immediate occupancy.

A building-by-building survey was done in the municipalities where the felt macroseismic intensity in the Mercalli-Cancani-Sieberg (MCS) scale was at least equal to VI (Dolce and Goretti, 2015; Zucconi et al., 2018; Rosti et al., 2018; Del

Gaudio et al., 2019). Conversely, the inspections were carried out only under request in the remaining affected areas. This rule, one side allowed a faster survey campaign, on the other hand, may have introduced a systematic overestimation of the damage at low seismic intensities (Rossetto et al., 2013). To prevent this bias, in several studies (Colombi et al., 2008; Zucconi et al, 2018; D'Amato et al, 2020) the underestimation of the total number of buildings is overcome, integrating the original database by means census data. In other works (Sabetta et al., 1998; Goretti and Di Pasquale, 2004; Rota et al., 2008; Del Gaudio et al., 2019), the fragility assessment is performed discarding from the original database all buildings located in the less inspected municipalities. Lastly, a two-step mixed approach is adopted in still other studies (Del Gaudio et al., 2021; Scala et al., 2022), combining the first two solutions. The latter approach is based on the evaluation of a completeness ratio, C.R., (namely the ratio between the number of inspected buildings and the total one) for each municipality, distinguishing in three levels of detail (namely, *slightly*, *partially* and *completely surveyed* municipalities) as a function of the survey's completeness. In particular, the completely surveyed municipalities are characterized by C.R. greater than 0.91 (Del Gaudio et al., 2019; Rosti et al., 2020b; Rosti et al., 2020c), whereas the slightly surveyed ones by a C.R. less than 0.1. Lastly, the partially surveyed municipalities are characterized by C.R. ranging between 0.1 and 0.91.

According to such approach, the 129 municipalities inspected after the 2009 seismic event have been classified in three data classes, that have been differently processed.

Table 12. Number of Abruzzi municipalities as a function of the Completeness Ratio (C.R.).

Not inspected Abruzzi municipalities (C.R.=0)	Slightly surveyed municipalities (C.R.<0.10)	Partially surveyed municipalities (0.1<C.R.<0.91)	Completely surveyed municipalities (C.R>0.91)
176	49	44	36

In Table 12, the number of municipalities belonging to each of these classes has been reported. Thus, about the 28% of the inspected municipalities has been

subjected to a complete survey (according to selected threshold of 0.91). Conversely, the remaining part is characterized by incomplete surveys with degree of completeness between 0.1 and 0.91 (34%) or less than 0.1 (38%). Moreover, also the number of not inspected Abruzzi municipalities has been reported in Table 12.

The same information is provided by Figure 24, in which all Abruzzi municipalities have been classified according to the three levels of detail of the post-earthquake survey. Note that the not inspected municipalities have been grouped with the slightly surveyed ones.

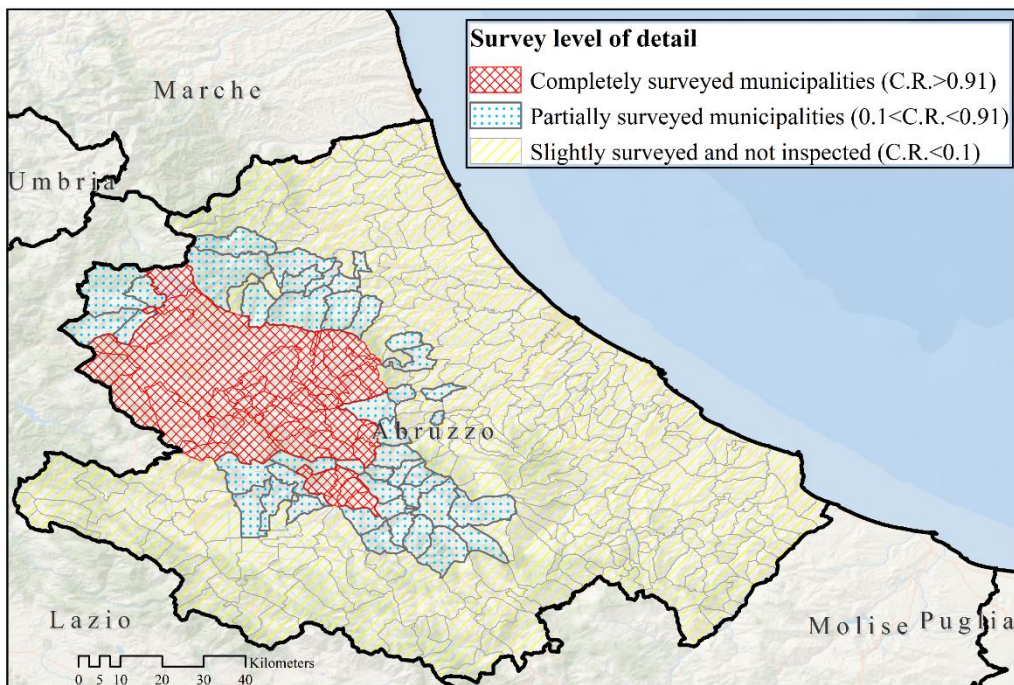


Figure 24. Survey level of detail (as a function of the completeness ratio, CR) for all Abruzzi municipalities.

As anticipated, data with different degree of completeness has been differently processed. Thus, in the following paragraph, the procedure adopted for each degree of completeness has been explained, dividing in *slightly*, *partially* and *completely surveyed* municipalities.

5.2.1 Completely inspected municipalities

The data collected in the 36 completely surveyed municipalities (out of 129 inspected ones) form the so-called “*damaged database*”, namely the positive evidence of the damage (Del Gaudio et al., 2021; Scala et al., 2022), coming from the post-earthquake inspections.

Basically, 28.967 residential masonry buildings (out of the 49.365 ones surveyed after the earthquake) are located in these municipalities. Nevertheless, only for 27.778 buildings, among these 28.967, the survey form is completely filled; whereas, for the remaining buildings, some building’s information (such as the construction age, the structural typology or the presence of retrofit intervention) is not reported. Thus, these latter are discarded from the considered database.

Therefore, in the following, 27.778 buildings characterized by a *complete survey form* has been considered (*damaged database*).

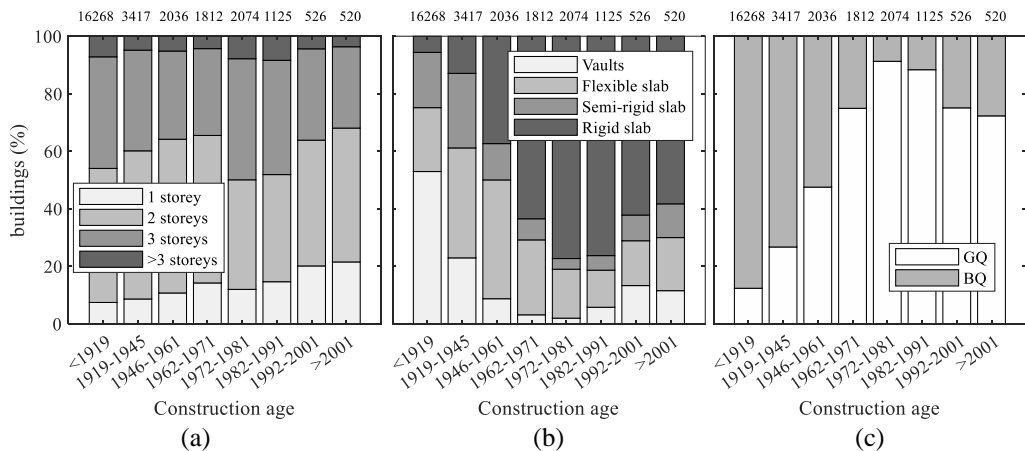


Figure 25. Period of construction versus (a) number of storeys, (b) horizontal structures and (c) masonry layout distributions for residential masonry buildings.

In Figure 25, some relevant building’s features (i.e., number of stories, horizontal structures, masonry quality) about geometry and structure have been investigated, providing the evolution of such features over the time (namely, increasing the construction age of buildings). In the plots, the number over each bar is the number of buildings built in the period reported by x-axis. The figure

shows that a significant percentage (about 58%) of buildings were built prior to 1919. This testifies their ancient origin, that can be traced back to 1259 when the City of L'Aquila were founded after a first destruction by *Manfredi di Sicilia*. The ancient settlement was divided into 4 portions (called *Quarters*), arose in an area originally unbuilt, albeit surrounded by numerous villages and castles that promoted its foundation. The subdivision into the four Quarters went strongly beyond the limit to the intra moenia city, influencing the building development of a large area of the surrounding countryside, which first urban fabric date back between the 13th and 15th centuries. The original settlement has been subjected to deep urban transformations due to renewed residential needs, as well as to the consolidation/reconstruction interventions after past seismic events (for example the 1703 earthquake) or due to contingent events (i.e. the destruction of an entire area of San Pietro Quarter by the Spaniards for the construction of the Fort in the 16th century). The information that can be deduced from the post-earthquake data, although allowing to localization of each single building (through its geographical coordinates), not allow to exactly characterize its construction age before 1919, thus merging all the buildings constructed starting from about 1250 until 1919. A close examination on the exact construction age of the buildings constructed before 1919 and/or of the possible interventions they have been subjected over the years, would require in-depth studies that go beyond the scope of this work and will be avoided in what follows.

Buildings characterized by a number of storeys between two and three amounts to about 84% of the sample, with a slight predominance of 2-storey buildings. This result is not particularly affected by the period of construction; in fact, only a slight increase in 1-storey buildings against 2- and 3-storey buildings is observed over time (see Figure 25a). Figure 25b shows that a substantial percentage (53%) of the most ancient buildings, i.e. built before 1919, is characterized by vault, a great part by flexible slabs and semi-rigid slabs (respectively 19% and 22%), and only 6% by rigid slabs.

A progressive reduction of percentage of buildings with vaults is observed through the years against an increase of stiffer horizontal types. In fact, after 1962 the majority (about 70%) of masonry buildings is characterized by rigid slabs.

In Figure 25c, the distribution of buildings as a function of masonry layout and period of construction is shown. It has to be noted that according to AeDES form only bad or good quality outcomes are allowed to characterize masonry layout. Nonetheless, a detailed description on how to assign these outcomes for the most widespread masonry typologies characterizing the Italian buildings stock, supported also by graphic and photographic documentations, is reported in the AeDES form's Manual.

Specifically, the AeDES form distinguishes the vertical structure of masonry building in two classes, based on the material used, on the layout of the wythes, on the mortar quality and the constructive procedures: good quality/regular (GQ) layout and bad quality/irregular (BQ) layout. A classification based on two masonry types (*type I* and *II*) is provided, based firstly on the analysis of external parameters (*first knowledge level*), see Figure 26 and Table 13. Clearly, at this level a visual inspection of external or internal masonry layer, thus without the presence of plaster, is required to the surveyor. Nevertheless, an in-depth analysis is sometime required for a reliable assignment regarding *type I* (bad quality masonry) or *II* (good quality), especially in case of masonry made of rough-worked element (i.e. *code type B* in Table 13).

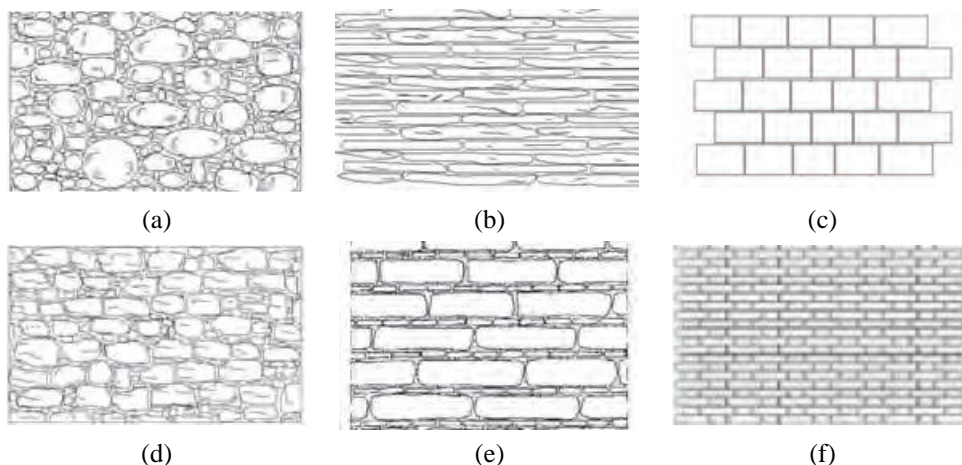


Figure 26. Abaci of masonry layouts (first level of knowledge according to AeDES manual). (a) Rounded stones or pebbles; (b) raw stones or rubble; (c) plate-shaped elements; (d) pseudo-regular elements; (e) natural hewn stones; (f) artificial stones.

Table 13. Classification of masonry structures based on material features

Masonry	Type code	Type of elements	Code type	Presence of courses	Masonry type (AeDES)	Masonry type (this study)
Irregular masonry	A	Rounded stones or pebbles	A1	N	I	BQ
				Y	I	BQ
		Raw stones or rubble	A2	N	I	BQ
				Y	I/II	BQ/GQ
Rough masonry	B	Plate-shaped elements	B1	N	I/II	BQ/GQ
				Y	I/II	BQ/GQ
		Pseudo-regular elements	B2	N	I/II	BQ/GQ
				Y	I/II	BQ/GQ
Regular masonry	C	Natural hewn stones	C1	N	I/II	BQ/GQ
		Artificial stones (bricks)	C2	Y	II	GQ
					II	GQ

For example, in case of natural hewn stone, the AeDES manual suggests doing an in-depth analysis, beyond the examination of the exterior wythes, collecting more information on the mortar quality (attesting if it is very friable and easy to crumble or more resistant) and on the wall section (verifying if it has well connected wythes or not) to properly typify the vertical structures. Thus, additional information is required to reduce these uncertainties: the mortar quality (*second knowledge level*) or the kind of masonry section (*third knowledge level*). However, despite that, uncertain cases characterized by a double classification (*type I/II*) are still provided in Table 13.

In general, the bad quality (BQ) masonry buildings are typically characterized by an irregular layout, constituted by rounded stones (or pebbles) and/or raw stones (or rubble) with or without courses. The good quality (GQ) masonry buildings are characterized by a regular layout, constituted by natural or/and artificial stones (bricks). Obviously, this macro-differentiation has already in view its effect on seismic behaviour, as buildings with bad quality/irregular layout show significant vulnerability with respect to both the in-plane actions, due to the low resistance of their constituents (brick and mortar) and to the poor friction which may develop among the stone elements, due to the irregular configuration of the wall and the out-of-plane actions, with possible disgregation of the wall. Conversely, buildings with good quality/regular layout show a strong resistance to both the in-plane and the out-of-plane actions.

It has to be noted that the majority of considered buildings (about 70%) is characterized by an irregular layout and/or bad masonry quality, defined in AeDES form as masonry *type I*, (i.e. “bad quality masonry”, “BQ” in the following); the remaining 30% of buildings are characterized by a regular layout and/or good quality, defined in AeDES form as masonry *type II*, (i.e. “good quality masonry”, “GQ” in the following). In particular, only after 1962 the percentage of buildings with regular layout overtakes those of irregular layout. However, buildings dated back after 1962 amount, overall, only to 21% of the total sample. Clearly, also the horizontal structure (i.e., vaults, flexible-, semi-rigid- and rigid-slab) is detected by inspectors during the survey and defined according to the field manual of AeDES form (see Figure 27).

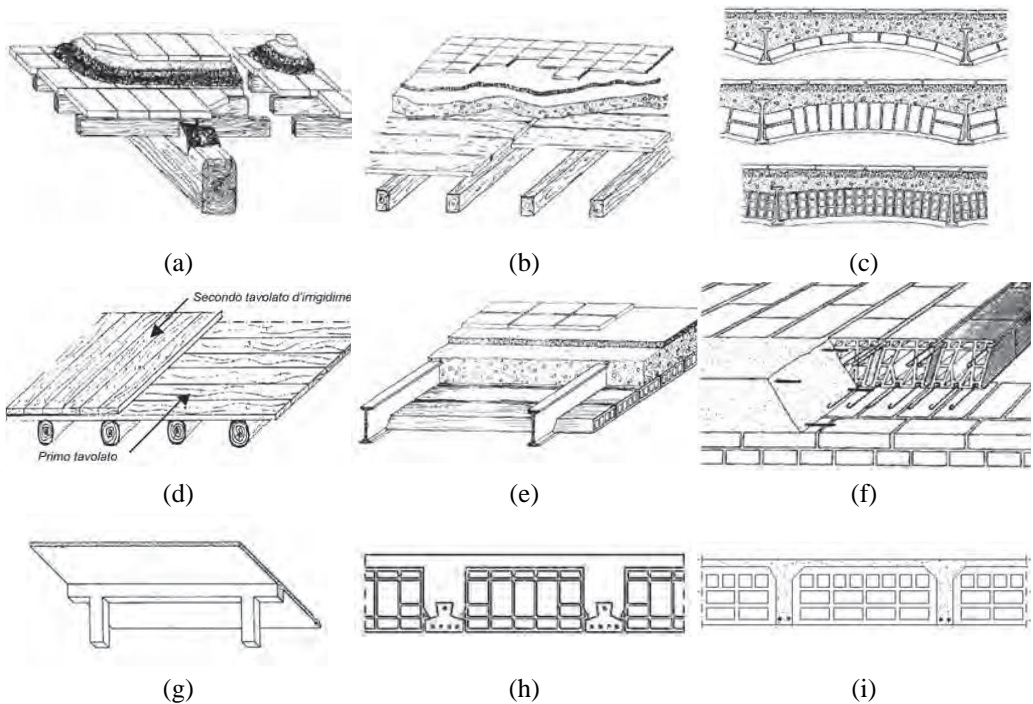


Figure 27. Abaci of flat horizontal structures (retrieved from AeDES Manual). Wooden slab with (a) brick elements (“mezzane”); (b) single layer of wood planks; (d) double layers of wood planks; iron beams with (c) shallow arch vaults; (e) hollow flat blocks; (f) prefabricated slab (SAP type); (g) R.C. slab; R.C. joists with hollow clay brick, either (i) cast-in-place or (h) prefabricated

The latter firstly distinguishes between flat and vaulted horizontal structures, and further differentiated the former in flexible, semi-rigid and rigid slabs as a function of the structures they are made. Flexible slabs are made of wooden beams with a single layer of wood planks/brick elements or made of iron beams with shallow arch vaults. Semi-rigid slabs are made of iron beams with hollow flat blocks or made of wooden beams with two perpendicular layers of wood planks or prefabricated shell made of hollow clay bricks with longitudinal reinforcement without upper slabs. Rigid slabs are made of reinforced concrete joists with hollow clay brick, either cast-in-place or prefabricated, with an upper reinforced concrete slab or solid reinforced concrete floors or any kind of floor with an upper concrete slab suitably reinforced and connected to all the walls.

These typologies of horizontal structures play a different role in distributing the seismic force between the walls and in restraining them in the horizontal plane they have defined. Flexible horizontal structures do not allow any rigid distribution of seismic forces among walls based on their stiffness and are unable to play any restrains between the walls parallel to the seismic force and the orthogonal ones. Semi-rigid horizontal structures formally allow the distribution of seismic force among the walls, especially when effective ring-beams and/or dovetails and widespread seams are present, although not guaranteeing a rigid floor redistribution. The restrain actions between parallel and orthogonal (to the seismic actions' direction) walls firmly increase but not granting a full box behavior. Lastly, rigid horizontal structures exert a rigid floor redistribution of seismic actions among the walls, playing also an effective restrain between them ensuring a proper global box behaviour and guaranteeing a proper transferring of the out-of-plane seismic forces from the parallel to the transversal walls.

The distribution of number of storeys and the type of horizontal structure varying the period of construction are then shown in Figure 28 for only BQ masonry buildings. The comparison between Figure 25b and Figure 28b shows a clear difference for distribution of horizontal structural type of BQ buildings, due to the removal of post 1962 GQ buildings from the original sample. In fact, after 1962 it can be observed a significant decrease (from about 68% to 32%) in the use of rigid slab for BQ buildings respect to the original database, containing

also GQ buildings. An increase of buildings with vault after 1980 is observed for BQ masonry (from about 10% to 35%), probably influenced by indications provided by D.M. 3/3/1975.

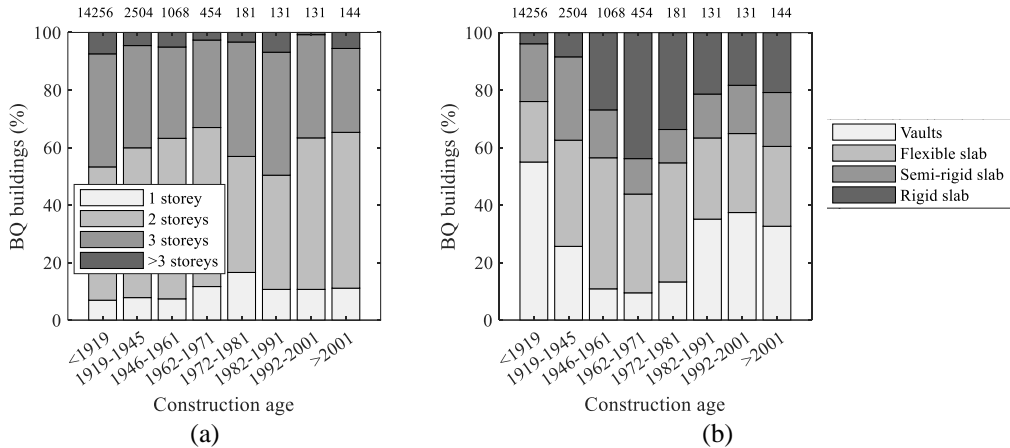


Figure 28. Period of construction versus (a) number of storeys and (b) horizontal structures percentage distributions for BQ residential masonry building.

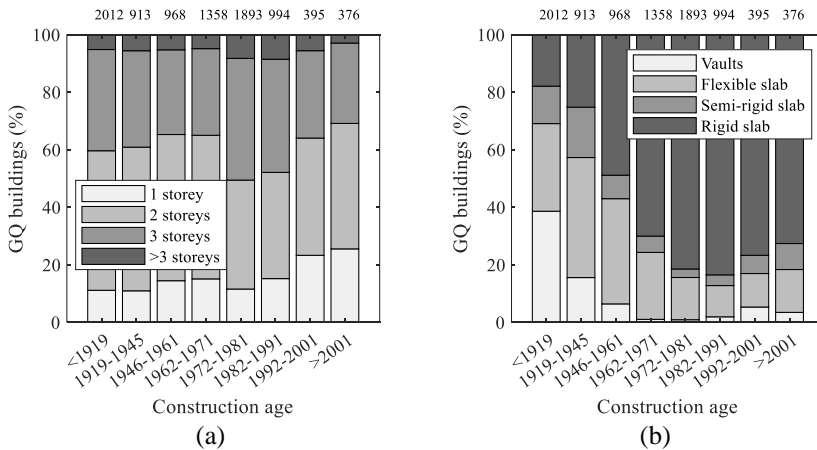


Figure 29. Period of construction versus (a) number of storeys and (b) horizontal structures percentage distributions for GQ residential masonry.

Figure 29 show the same distributions (namely, number of storey and horizontal structures versus the construction age) for masonry buildings with good quality and/or regular layout, GQ. The distribution of the number of storeys

again is substantially constant over the time, with great percentage of 2- and 3-storeys buildings (see Figure 29a). Figure 29b shows that about 40% of buildings constructed before 1919 presents, as horizontal structure, the masonry vaults. However, this percentage quickly decreases in the following ages. On the contrary, buildings with rigid slabs significantly increases, going from about 20% (before 1919) to about 80% (after 1971). Semi-rigid slabs are quite widespread before 1972, whereas flexible slabs are not very common regardless the construction age (the maximum observed percentage is about 20% in 1919-1945 period).

In several previous studies (among the others, Rota et al., 2008; Dolce and Goretti, 2015; Del Gaudio et al., 2019; Rosti et al., 2020c), such parameters (related to horizontal and vertical structures) have been considered to define the building's taxonomy, dividing the whole database in several building's classes. Nevertheless, this primary classification, which is considered true on average, could undergo variations based on several relevant factors (such as the type of roof, the number of floors and the time of construction) (Dolce and Goretti, 2015). In fact, classifying buildings based purely on structural-geometric features could lead to group together buildings with very different seismic performances (Karababa and Pomonis, 2010), due for example to changes in the in force normative contents or to different degree of building's decay.

In this view, a crucial building's feature is of course the construction age. It should be noted that the greater part of building's features (structural typology, material characteristics, structural details) could be related to the building location and to the period of construction. In fact, a general improvement in construction practices and the enhancement of building materials over the years, also related to the subsequent enactment of seismic prescriptions, is already observed in previous study (Del Gaudio et al, 2021).

Moreover, also the type of design (based on building's location and period of construction) is one of the key parameters. Basically, buildings with the same construction age and sited in different locations could show great differences in terms of seismic performances, because designed following different code prescriptions. Similarly, buildings sited in the same municipality and built in

different periods of time could behave differently under seismic loads, because of different seismic prescriptions.

To consider such issue, the subdivision between building constructed in seismic areas or not has been done by comparing the period of construction of each building with the year of first seismic classification of the municipality where it is sited. More precisely, since the available information on period of construction is given by the AeDES form as periods of fixed length (i.e., <1919; 1919-1945; 1946-1961; 1962-1971; 1972-1981; 1982-1991; 1992-2001; >2001), their centroid is used for the comparison with the year of first seismic classification.

To this aim, the software package ECS-it, *Evolution of the Italian Seismic Classification* (Del Gaudio et al., 2015) has been used, allowing the definition of the seismic classification of each municipality of Italian territory considering all (over 37) the classification codes enforced since 1909 to 2015. Clearly, if the period of construction follows the year of the first seismic classification, the masonry building was designed according to seismic prescriptions (Seismic Designed - SD), vice versa the design class is GD (only Gravity load Designed), i.e. the masonry building was built without any normative prescription (before R.D. 640/1935) or was designed according to prescriptions compulsory nationwide (after 1935).

Figure 30 summarizes the evolution of the seismic classification laws (with different colors), together with C.R. values (with different line texture) for each Municipality of Abruzzi region. Note that the majority (33 out of 36) of the completely inspected municipalities have been seismically classified for the first time in 1915 (R.D. 29/04/1915 n.573), whereas *Campotosto*, *Calascio*, and *San Benedetto in Perillis* municipalities have been classified thereafter: the former in 1927 (R.D. 13/03/1927 n. 431) and the latter two in 1962 (Law 1684/1962). Masonry buildings therein located amount overall to 1.065 units (647, 300 and 118, respectively) out of the total ones (27.778). Thus, a clear relationship exists between period of construction and design type for the building stock investigated in this study, namely all masonry buildings dated back to before

1919 have been designed without any seismic prescriptions (GD), conversely the majority of those constructed thereafter meet seismic requirements (SD).

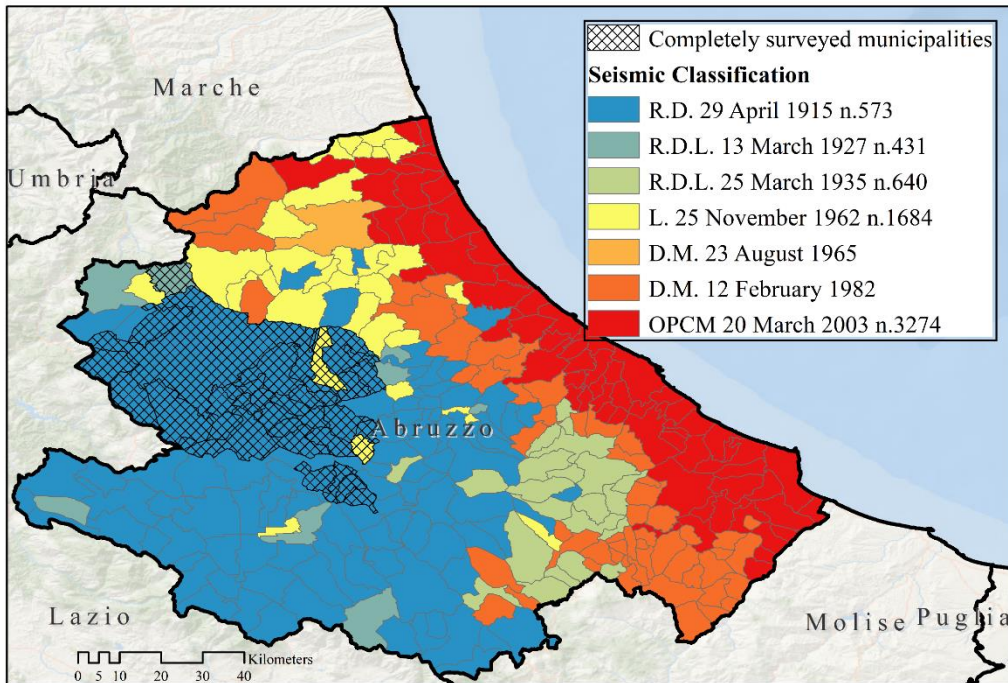


Figure 30. Seismic classification of Abruzzi municipalities, detecting the completely surveyed municipalities.

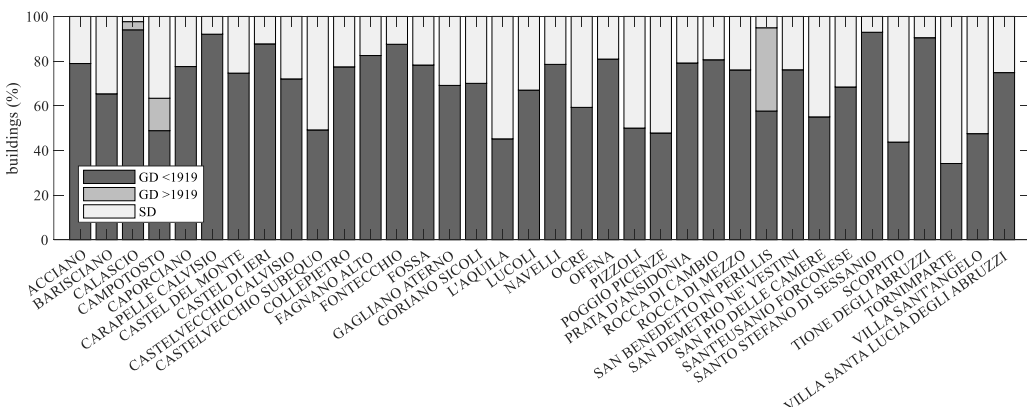


Figure 31. Percentage of buildings belonging to the two considered design classes for all 36 completely inspected municipalities

Figure 31 precisely reports the strong relationship between period of construction and design types and resultant percentages for all the 36 Municipalities under study. Obviously, the simple relationship that buildings constructed after 1919 can be considered seismically designed does not firmly apply to buildings sited in *Campotosto*, *Calascio*, and *San Benedetto in Perillis* municipalities, being seismically classified after 1915. In fact, a small sample (149) out of 1.065, although constructed after 1919 result gravity-loads designed, and has been discarded hereinafter for sake of simplicity. In quantitative terms, about 59% (16.174 buildings) of residential masonry buildings was constructed before 1919, without any seismic prescriptions, whereas the remaining 49% (11.455 buildings) constructed thereafter follow seismic prescriptions thoroughly reported previously.

Moreover, the survey form allows gaining information also on the period when structural interventions are executed, beyond the original period of construction. Thus, the survey form for buildings subjected to structural interventions contains a double filled field regarding period, the oldest referring to its construction and the most recent referring to its retrofit. Obviously, this information is typically obtained by inspectors through a direct interview reliably granted by the owner. Additionally, the information on type of interventions, among injections or unreinforced coating, (H1), reinforced masonry or masonry with reinforced coating (H2), other or unidentified strengthening (H3), is also reported. Nonetheless, in almost all cases (about 98%) this information was not filled by surveyor. Probably the rapidity required by emergency condition together with the way the inspections were conducted (only visual) did not allow to precisely determine the kind of structural intervention, although they were aware that there had been. Thus, buildings, which survey form reports double filled field regarding period, referring to construction and retrofit, are considered herein as been subjected to structural interventions over the years.

Finally, the original *damaged DB* made up of 27.629 residential masonry buildings shows that a remarkable percentage of buildings belonging to the *damaged DB* has been subject to retrofit intervention, especially those built before 1919 (see Figure 32a).

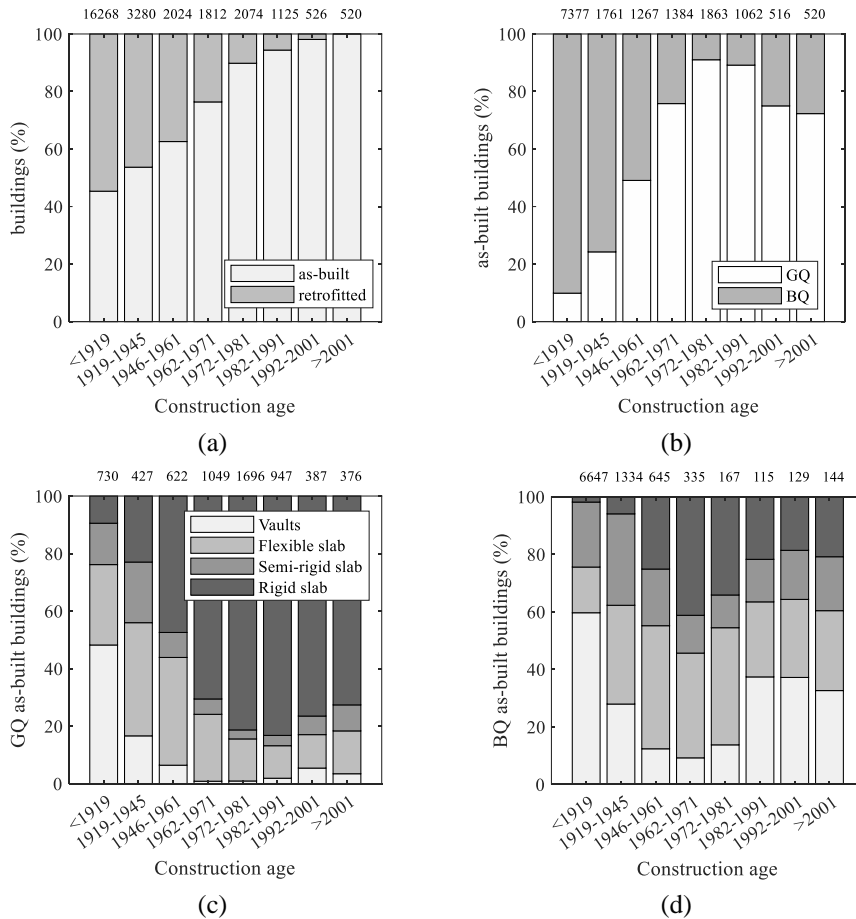


Figure 32. Presence/absence of retrofit intervention (a); masonry quality for not-retrofitted buildings (b); horizontal structure for as-built GQ (c) and BQ (d) buildings, given the construction age.

Conversely, for more recent construction ages, the percentage of retrofitted buildings decreases, going from about 45% before 1919 to 0% after 2001. Moreover, the most ancient not-retrofitted buildings are mostly denoted by bad quality masonry and/or irregular layout, whereas the use of good quality masonry and/or regular layout is typical for the most recent buildings (see Figure 32b). About the horizontal structure, a progressive use of rigid slabs (such as R.C. ones) and the consequent abandonment of the less rigid ones are observed for both the not-retrofitted GQ (Figure 32c) and BQ (Figure 32d) typologies. It

worthy to note that for BQ typologies, the use of vaults and flexible slabs (such as wooden ones) is predominant, since these typologies are mainly composed by ancient buildings. Conversely, for GQ typologies the most widespread horizontal structures are rigid slabs. The greater part (about 94%) of retrofit interventions has been performed over building originally built until the 1961 (Figure 32a): in fact, the numbers of retrofitted masonry buildings, built in the first three construction's periods (i.e., <1919; 1919-1945 and 1946-1961), are 8.891 (75%), 1.519 (13%), and 757 (6%), respectively.

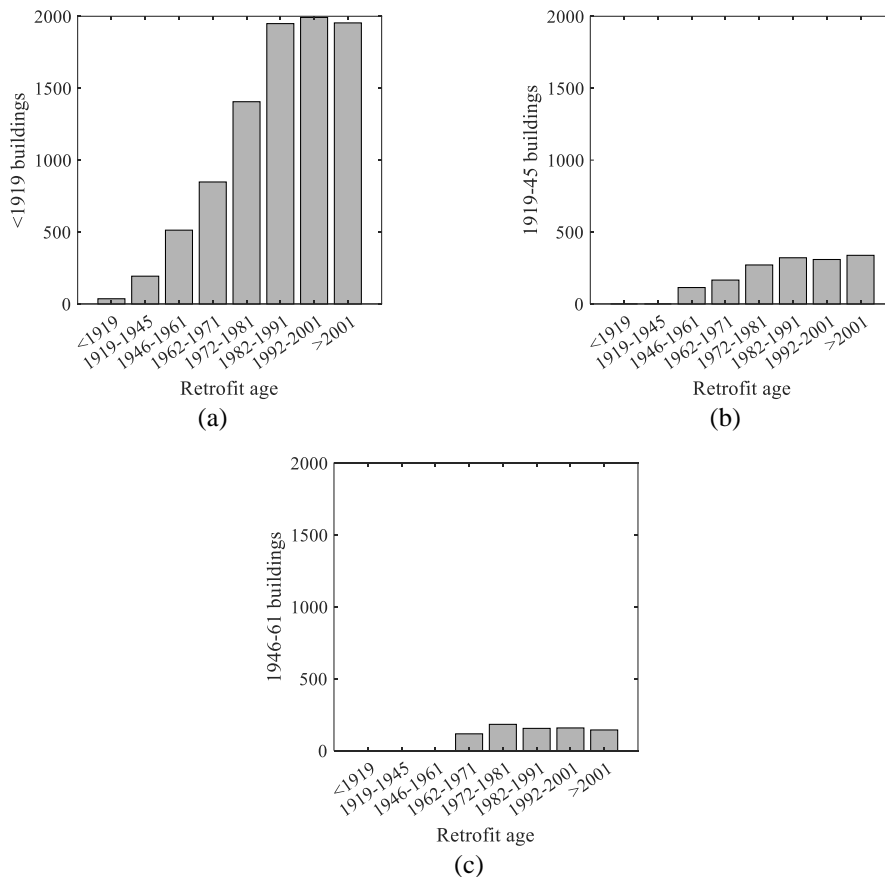


Figure 33. Period of retrofit intervention for buildings built before 1919 (a), between 1919 and 1945 (b), and between 1946 and 1961 (c).

Thus, in Figure 33 the distribution of the retrofit age is provided for buildings built in <1919 (Figure 33a), 1919-1945 (Figure 33b), and 1946-1961 (Figure 33c) timespans. It is worth noting that for at least 80% of buildings these structural interventions were executed after 1971, regardless the original period of construction. In particular, the considerable efforts addressed to retrofit interventions after 1980 are probably due to the awareness that effective countermeasures were required against earthquakes, especially after the lesson learnt of Irpinia 1980 and Abruzzi 1984 events.

A clear attention on topic can be also highlighted in the context of legislative drafting, through the enacting of a specific regulation on strengthening, design, execution, and acceptance criteria of masonry buildings (D.M. 9/01/1987).

In Figure 34, the percentage distributions about vertical and horizontal structures are shown for all retrofitted buildings originally constructed before 1919 (first row of plots, Figure 34a-d-g), between 1919 and 1945 (second row, Figure 34b-e-h), and between 1946 and 1961 (third row, Figure 34c-f-i). In general, the greater part of retrofit interventions has been performed on buildings denoted by bad quality and/or irregular layout of masonry walls (see Figure 34a-b-c). It depends on the fact that the major part (75%) of interventions has been done on the most ancient buildings (namely, built before 1919), mainly denoted by bad quality masonries.

Moreover, such proportion between bad and good quality buildings (substantially independent of retrofit age) changes over the time, just like it happens for as-built buildings. In fact, the percentage of BQ masonry buildings decreases, increasing the construction age, both for retrofitted and not-retrofitted buildings (going from about 85% to about 55%).

For what concern the horizontal structures, again similarities between retrofitted and not-retrofitted buildings can be observed. In fact, also for retrofitted buildings an increasing use of most rigid structures, and a progressive abandonment of masonry vaults are observed over the time (namely increasing the construction age). Such trends are not influenced by the masonry quality, but the masonry quality affects the proportion among the four horizontal types.

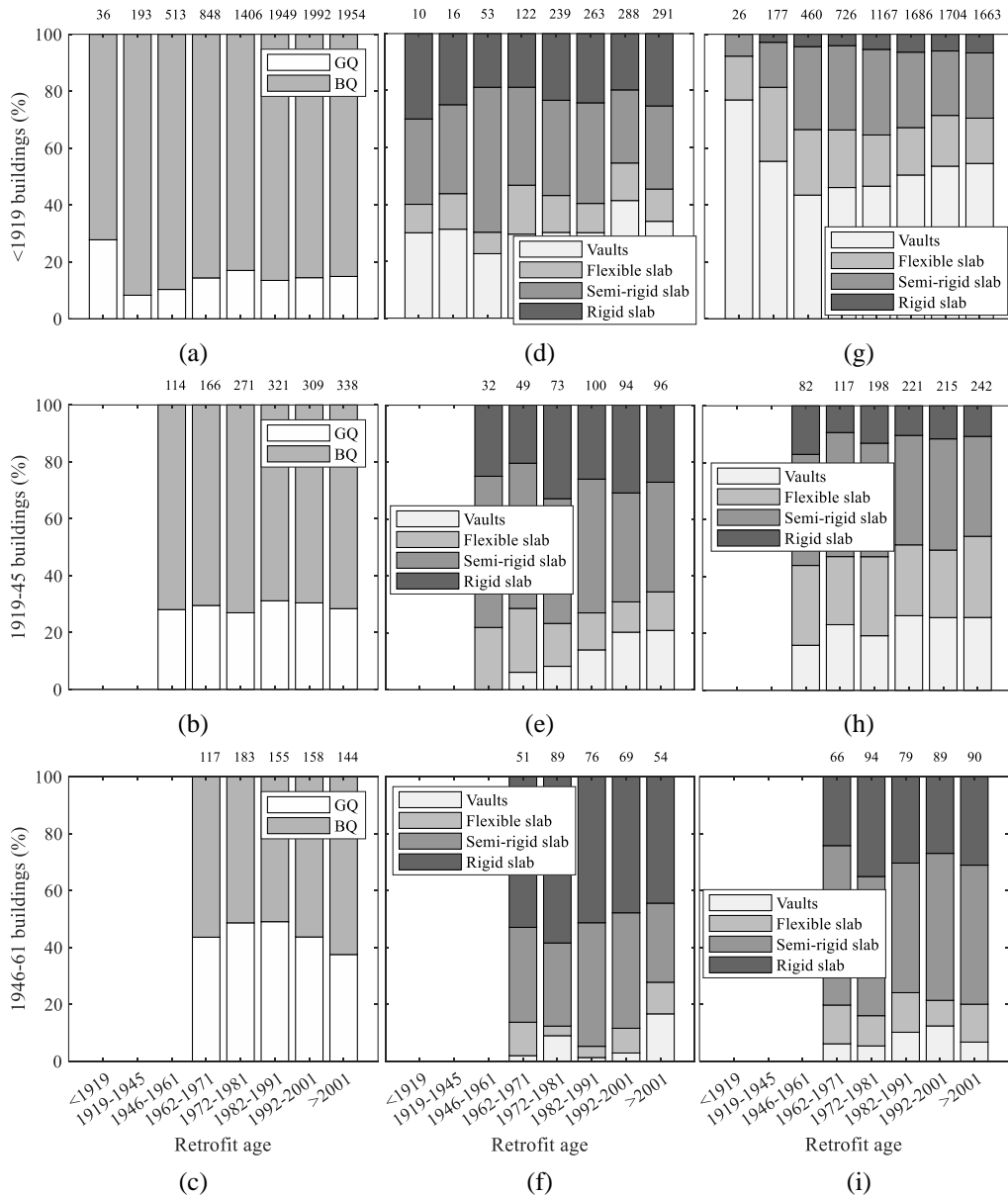


Figure 34. Masonry quality for retrofitted buildings constructed before 1919 (a), between 1919 and 1946 (b) and before 1946 and 1961 (c); horizontal structures for GQ and BQ retrofitted buildings built in <1919 (d-g), 1919-1946 (e-h) and 1946-1961 (f-i) time periods.

In fact, for both GQ and BQ buildings, the trend is an increasing use of most rigid solutions (able to guarantee a suitable box-behavior) over the time, but for GQ buildings (differently from BQ ones) also before 1919 the use of rigid slabs is quite widespread (Figure 34d).

Conversely, for BQ buildings originally built before 1919 (Figure 34g), rigid slabs are very uncommon: the use of such typology slightly increases with the retrofit age, going from 0% for interventions done before 1919 to about 7% for those performed after 2001. Generally speaking, a slight decrease (of approximately 10%) in the percentages of vaults and flexible slabs is observed compared to those observed for not retrofitted buildings constructed before 1919, compensated by an increase in semi-rigid and rigid slabs. A further slight decrease (about 5%) in the percentages of vaults and flexible slabs respect to previous case (retrofitted buildings constructed before 1919), counterbalanced by the corresponding increase in percentage of rigid slabs, is observed for BQ buildings originally built between 1919 and 1945 (Figure 34h). Lastly, the same decreasing trend is observed for BQ buildings originally built between 1946 and 1961 (Figure 34i).

Finally, the *damaged* database, representing the positive evidence of the damage and derived from post-earthquake survey (i.e., from Da.D.O. platform), consists of 27.629 masonry buildings sited in municipalities with C.R.>0.91 and denoted by survey form completely filled.

5.2.2 Partially inspected municipalities

In these municipalities, the percentage of inspected buildings varies from 10% to 90% of the actual number of buildings (provided by the census ISTAT data). Thus, building-by-buildings survey has not been performed, being the macroseismic intensity less than VI. The data collected in these municipality has been discarded from the following elaborations, because the completeness does not reach the considered threshold equal to 0.91 (Del Gaudio et al., 2019; Rosti et al., 2020b; Rosti et al., 2020c).

As explained in the Chapter 2, other methodologies available in the literature are based on the following approach: basically, the number of buildings in

municipalities with a completeness ratio less than the adopted threshold is increased to the number reported in the Census data. However, such approach leads to uncertainties in the damage association to the not surveyed buildings.

Thus, in the present work, all data with completeness between 10% and 91% are discarded, despite it means that an important number of buildings are excluded from the study database.

5.2.3 Slightly inspected municipalities

As mentioned above, in the slightly surveyed municipality less than the 10% of the actual number of buildings has been inspected after the earthquake. These municipality are typically the furthest from the earthquake's epicenter, where building-by-building surveys were not done (see Figure 35).

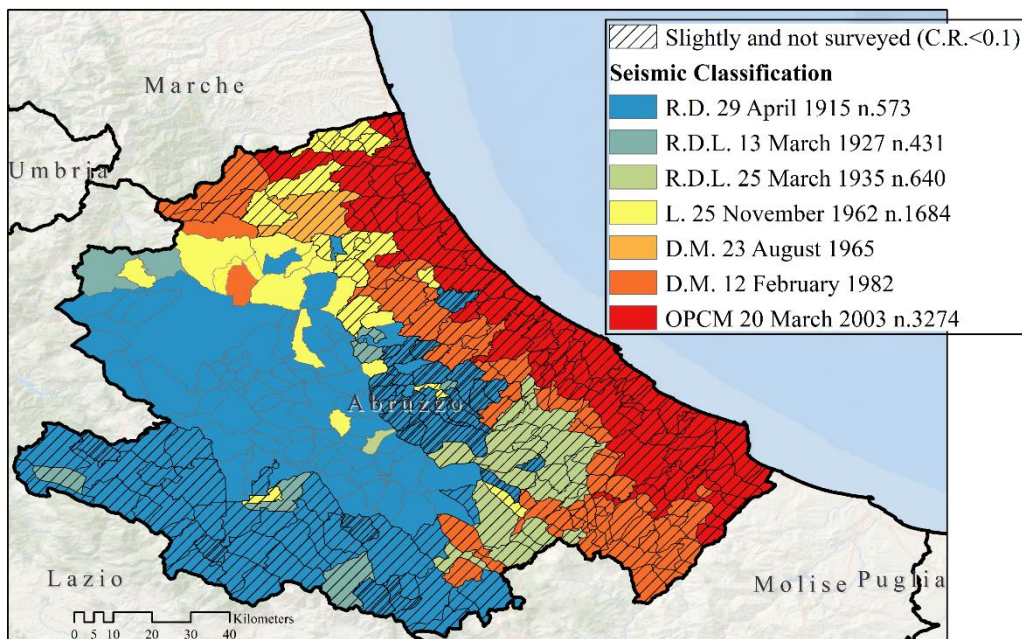


Figure 35. Seismic classification of Abruzzi municipalities, detecting the slightly surveyed and the not inspected municipalities.

Thus, the few data collected in these 49 municipalities is discarded from the further fragility assessment, being not very reliable. It should be noted that the remaining percentage of building (at least 90%) located in these municipalities

likely has not been inspected, because not damaged. A similar argument is about the 176 not inspected municipalities of Abruzzi region. Thus, in order to investigate the building's fragility also for lower PGA values (namely, in the zones farthest from the epicenter), a null damage has been assigned to each building located in the slightly surveyed and not inspected municipalities. Therefore, *damaged* database has integrated with an additional source of data, standing for the negative evidence of damage, constituted by *undamaged* masonry buildings, located in the Abruzzi municipalities subjected to a very small number of inspection (C.R. <0.1) or not surveyed after L'Aquila 2009 earthquake (see Figure 35), amounting to 167.034 units according to ISTAT 2011 data. Among such undamaged buildings, 37.576 units are sited in municipalities where a slight survey (C.R.<0.10) was done, whereas the remaining 129.458 ones are sited in Abruzzi municipalities not inspected after the earthquake. Note that this integration allows to reduce potential biases in vulnerability estimation (Del Gaudio et al., 2020; Rosti et al., 2020), due to the un-representativeness of the sample (a small number of inspections) respect to the whole population, for the systematic neglecting of undamaged buildings.

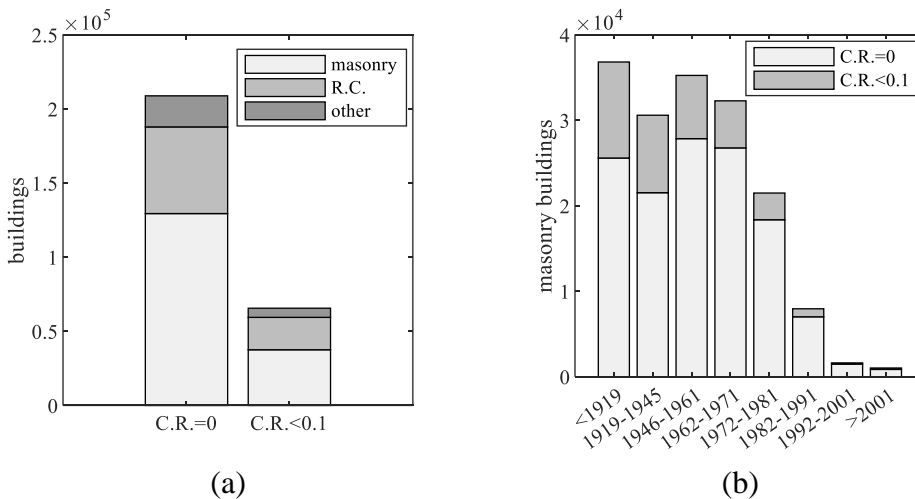


Figure 36. (a) Number of buildings (i.e., masonry, R.C. and other material) and (b) distribution of construction age for masonry ones, provided by ISTAT 2011 for all slightly surveyed and not inspected Abruzzi municipalities.

Moreover, whilst the *damaged DB* directly derives from the Da.D.O. platform, the *undamaged DB* is the result of a complex elaboration: in fact, the number of buildings for each construction age is provided by the census data, whereas the building's features (such as the masonry quality, the horizontal structure, or the presence of retrofit intervention, the retrofit age) derives from the distribution observed on the *damaged DB*, given the construction age. In fact, the required level of knowledge is not available for census data, since their quantification arises from ISTAT 2011 census data allowing only to achieve information on structural (masonry, R.C., and others) types (Figure 36(a)), period of construction (Figure 36(b)) and number of storeys. Further information about the vertical (good/regular or bad/irregular layout) and horizontal (i.e., vaults, flexible, semi-rigid or rigid slab) structural type and the presence of retrofit interventions is not obtainable. So, the percentage of these characteristics are retrieved from Da.D.O. data, taking advantage of their correlation with period of construction. Thus, the available information on period of construction has been used as key to subdivide the original sample of 167.034 *undamaged* buildings as a function of the quality for vertical masonry structures, of the horizontal structural types and of the presence of structural interventions. In other words, it is assumed that the same percentage of above-mentioned parameters for the *damaged* data given the period of construction can be extended also to *undamaged* data.

Basically, the distributions shown in Figure 32 and Figure 34 are applied to the number of buildings deriving from census data, given the construction age (Figure 36(b)). So, applying the distribution of Figure 32(a), for each construction age, it is possible distinguish between as-built and retrofitted buildings. Then, Figure 32(c) and Figure 32(d) allow to assign to each not-retrofitted building a structural (vertical + horizontal) typology, given the construction age. Lastly, the distributions shown in Figure 34 allow to assign structural typology and retrofit age. Clearly, such procedure could be applied for each building's feature provided by the survey form (i.e., surface area, inter-storey height, presence of tie rods and/or tie beams, ...).

Nevertheless, to guarantee a strong consistency in terms of seismic classification between the *damaged* and the *undamaged* DBs, the latter have been restrained to those municipalities of Abruzzi Region which have been seismically classified for the first time in 1915. Thus, the *undamaged* DB is composed by all buildings located in the 61 slightly or not surveyed municipalities classified in 1915, depicted in Figure 35 (i.e., light blue background field). In particular, only 37.761 (Figure 37(b)) out of 167.034 *undamaged* buildings coming from ISTAT census have been considered to characterize the negative evidence of damage.

Overall, the database considered in this thesis work is composed by:

- 27.629 masonry buildings (Figure 37(a)) belonging to *damaged* DB (i.e., positive evidence of damage), derived from Da.D.O. platform;
- 37.761 masonry buildings (Figure 37(b)) belonging to *undamaged* DB (i.e., negative evidence of damage), derived from census data.

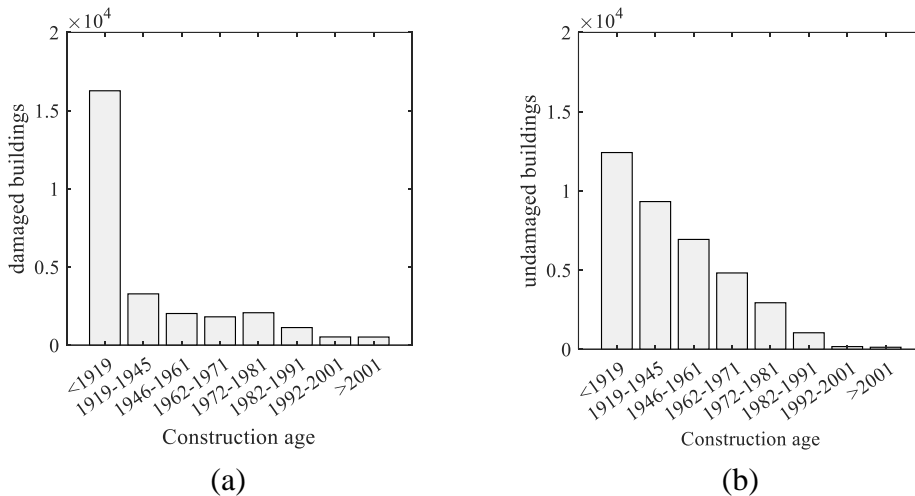


Figure 37. (a) Damaged and (b) undamaged DBs, varying the construction age.

In the following section, starting from such database (i.e., *damaged* + *undamaged* DBs), a building's taxonomy has been introduced, dividing the entire database in several homogeneous building's classes.

5.3 BUILDING'S TAXONOMY

In this section, the building taxonomy is introduced and used to subdivide in building's classes the database constituted by residential masonry buildings belonging to *damaged* and *undamaged* databases.

As deeply described in Chapter 2, several previous studies have dealt with the introduction of taxonomies, providing their building classification systems (e.g., Brzev et al., 2012; Jaiswal et al., 2010; Kircher et al., 2006). These latter typically require a very detailed knowledge of buildings, taking into consideration a great number of factors. Thus, most empirical studies (especially those based on post-earthquake data) do not adopt such taxonomies, preferring bespoke building classes (namely, defined on the basis of the available data).

As above explained, the present work exploits information collected by means of AeDES form, reaching a level of knowledge less informative than those required by GEM or Hazus taxonomies, for example. In fact, although the information on masonry layer (*level 1*), the analysis of the mortar's quality (*level 2*) and also of the section of the masonry's wall (*level 3*) are required to the technician in order to typify the masonry layout, the final outcome reported in the AeDES form is synthesized in only two possible attribute's values (i.e., good and bad quality).

In general, to obtain a robust building taxonomy, a fair compromise between the need to consider all the available parameters and the necessity to obtain reliable and homogeneous sample is generally desired. Of course, several building features play a role in the seismic response of a buildings. Nevertheless, also the combination of these factors could increase or reduce the vulnerability. Thus, a building's taxonomy able to consider all together several building features (such as structural typology, building's material, the presence of retrofit intervention, the construction age, the number of stories, ...) leads to the most accurate vulnerability's analysis, avoiding any cross-correlation between the building features.

However, such high level of detail could result in small sample sizes. For this reason, the adopted taxonomy should be the better compromise between the level

of detail in the building description and the sample size of each defined class (Rossetto et al., 2013).

5.3.1 Building's features according to AeDES form

As already pointed out in the previous Section, the AeDES form allows to gather several information for each surveyed building. In particular, those reported of *Section 2* (i.e., construction age, the retrofit age and the number of storeys among others), and *Section 3* of the form (i.e., vertical and horizontal structural typology, presence of tie rods/beams) could generally affect the seismic behaviour of the masonry buildings (Zuccaro and Cacace, 2015; Zucconi et al., 2018; Del Gaudio et al., 2021).

Thus, all these parameters and their influence on seismic vulnerability of investigated building stock have been thoroughly analysed in sight of a taxonomy as broadest and most exhaustive as possible. Firstly, the type of vertical (i.e., bad and good quality) and horizontal (i.e., vaults, flexible-, semi-rigid- and rigid-slab) structures and the presence/absence of retrofit have been already analysed together with the construction age, in the previous Section. It is worth pointing out that in the present work the presence of retrofit interventions has been assigned using a simplified criterion, based on information of *Section 2* of the AeDES form. Basically, it has been assumed that buildings subjected to structural interventions are those with a double filled field regarding period (the oldest referring to its construction and the most recent referring to its retrofit). As previously mentioned, such criterion does not allow taking into consideration the type of intervention, but only separating buildings subjected to whatever structural intervention from those in their original state (i.e., "as-built" ones). Thus, although very different types of interventions may have been carried out on considered buildings, all those have been grouped together as "retrofitted" buildings.

Secondly, as far as the *damaged* DB is defined, also the seismic classification has been considered, discarding the buildings sited in municipalities classified before the 1915 and built between the 1915 and the year of seismic classification.

Therefore, in Table 14, the number of buildings belonging to the *damaged* DB is reported as a function of 64 ($= 2$ vertical structures \times 4 horizontal structures \times 8 construction ages) not retrofitted building typologies. Some classes are most populated than others, due to changes in the use of some materials and/or techniques. As mentioned above, a progressive abandonment of irregular layout (BQ) for regular one (GQ) is observed over the time.

Moreover, increasing the construction age, the use of vaults (V) and flexible (F) slabs decreases. Conversely, the most rigid horizontal structures (i.e., S and R) become ever more popular in the time.

Thus, a general improvement in the building's concept is observed over the time, increasing the quality of the vertical structures and the stiffness of the horizontal ones. On the contrary, the less populated classes are, likely, the less representative ones.

At this stage, a minimum sample's size is introduced to guarantee the reliability and homogeneity of considered sample (Rossetto et al., 2013). In this study, such threshold is set equal to 100 buildings (Del Gaudio et al., 2021; Scala et al., 2022). Thus, all typologies with a smaller consistency (reported with grey color in Table 14) have been discarded from the database. Consequently, only 27 (i.e., the black marked in Table 14) out of 64 as-built classes are well populated according to the adopted threshold.

Table 14. Number of as-built masonry buildings belonging to *damaged* DB for each structural type given the construction age.

Construction age	Vaults (V)		Flexible slab (F)		Semi-rigid slab (S)		Rigid slab (R)	
	GQ	BQ	GQ	BQ	GQ	BQ	GQ	BQ
<1919	352	3968	105	1501	204	1056	67	122
1919-45	71	373	90	424	168	458	100	79
1946-61	40	80	54	127	233	276	295	162
1962-71	9	31	56	44	244	122	740	138
1972-81	16	23	53	19	248	68	1379	57
1982-91	18	43	34	17	107	30	788	25
1992-01	21	48	25	22	45	35	296	24
>2001	13	47	34	27	56	40	273	30

Table 15. Number of retrofitted buildings belonging to *damaged* DB for each construction and retrofit age.

Retrofit age	Construction age							
	<1919	1919-45	1946-61	1962-71	1972-81	1982-91	1992-01	>2001
<1919	36	-	-	-	-	-	-	-
1919-45	193	0	-	-	-	-	-	-
1946-61	513	114	0	-	-	-	-	-
1962-71	848	166	117	0	-	-	-	-
1972-81	1406	271	183	116	0	-	-	-
1982-91	1949	321	155	119	79	0	-	-
1992-01	1992	309	158	105	68	25	0	-
>2001	1954	338	144	88	64	38	10	0

In Table 15, the number of retrofitted buildings is provided as a function of the construction and the retrofit age. As highlighted in Figure 32a, the percentage of retrofitted buildings decreases increasing the construction age, becoming 0% after 2001. So, the greater part of the retrofit interventions has been performed on the most ancient buildings (namely, on those built before 1919). Moreover, these interventions have been done mostly after the 1980 (Figure 33).

As well as as-built buildings, also for retrofitted ones, 64 (= 2 vertical structures \times 4 horizontal structures \times 8 construction ages) typologies have been considered. Clearly, such 64 typologies have been combined with the 8 retrofit ages, resulting 512 retrofitted typologies.

Nevertheless, only for the first three construction ages (i.e., <1919; 1919-1945; 1946-1961) the number of buildings is quite high. Thus, in Table 16, Table 17, and Table 18, the number of buildings as a function of (vertical + horizontal) structural typology and retrofit age, is provided only for those built up to 1961. According to the adopted minimum simple size of 100 buildings, only 22 (out of 512) retrofitted classes could be considered (i.e., the black marked in Table 16). All these classes are populated by buildings built before 1919; whereas, for the following ages (Table 17 and Table 18), the number of buildings in each structural class is always less than 100.

Table 16. Number of retrofitted buildings built before 1919 belonging to *damaged* database.

Retrofit age	Vaults (V)		Flexible slab (F)		Semi-rigid slab (S)		Rigid slab (R)	
	GQ	BQ	GQ	BQ	GQ	BQ	GQ	BQ
<1919	3	20	1	4	3	2	3	0
1919-45	5	98	2	46	5	28	4	5
1946-61	12	200	4	106	27	134	10	20
1962-71	36	335	21	147	42	215	23	29
1972-81	72	544	31	210	80	351	56	62
1982-91	79	852	27	281	93	447	64	106
1992-01	119	914	38	304	74	386	57	100
>2001	99	908	33	265	85	381	74	109

Table 17. Number of retrofitted buildings built between 1919 and 1945 belonging to *damaged* database.

Retrofit age	Vaults (V)		Flexible slab (F)		Semi-rigid slab (S)		Rigid slab (R)	
	GQ	BQ	GQ	BQ	GQ	BQ	GQ	BQ
1946-61	0	13	7	23	17	32	8	14
1962-71	3	27	11	28	25	51	10	11
1972-81	6	38	11	55	32	79	24	26
1982-91	14	58	13	55	47	85	26	23
1992-01	19	55	10	51	36	84	29	25
>2001	20	62	13	69	37	85	26	26

Table 18. Number of retrofitted buildings built between 1946 and 1961 belonging to *damaged* database.

Retrofit age	Vaults (V)		Flexible slab (F)		Semi-rigid slab (S)		Rigid slab (R)	
	GQ	BQ	GQ	BQ	GQ	BQ	GQ	BQ
1962-71	1	4	6	9	17	37	27	16
1972-81	8	5	3	10	26	46	52	33
1982-91	1	8	3	11	33	36	39	24
1992-01	2	11	6	8	28	46	33	24
>2001	9	6	6	12	15	44	24	28

Moreover, among such 22 classes, only one is composed by masonry buildings with good quality and/or regular layout. In fact, about 86% of buildings built before 1919 and subject to retrofit interventions are denoted by bad quality masonry (Figure 34(a)).

For sake of simplicity, only BQ retrofitted (built before 1919) classes have been considered in the following fragility assessment. Conversely, the considerably lower amount of retrofitted buildings built between 1919 and 1961 has been used only for vulnerability evaluations in terms of mean damage, grouping together several retrofit ages. Overall, in the following sections, 27 as-built classes and 21 retrofitted ones will be considered to perform the fragility assessment.

In Figure 38 and Figure 39, the distributions of the number of storeys have been reported for the considered 27 as-built typologies. It can be noted that 2- and 3-storeys buildings are the most common typologies (even if with slight differences in some cases). For GQ masonry (Figure 38), at least 68% of buildings with rigid and semi-rigid slabs is characterized by 2 and 3 storeys. On the other hand, higher percentage (85% and 78%) of 2- and 3-storeys buildings are observed for those with vaults and flexible slabs (constructed before 1919).

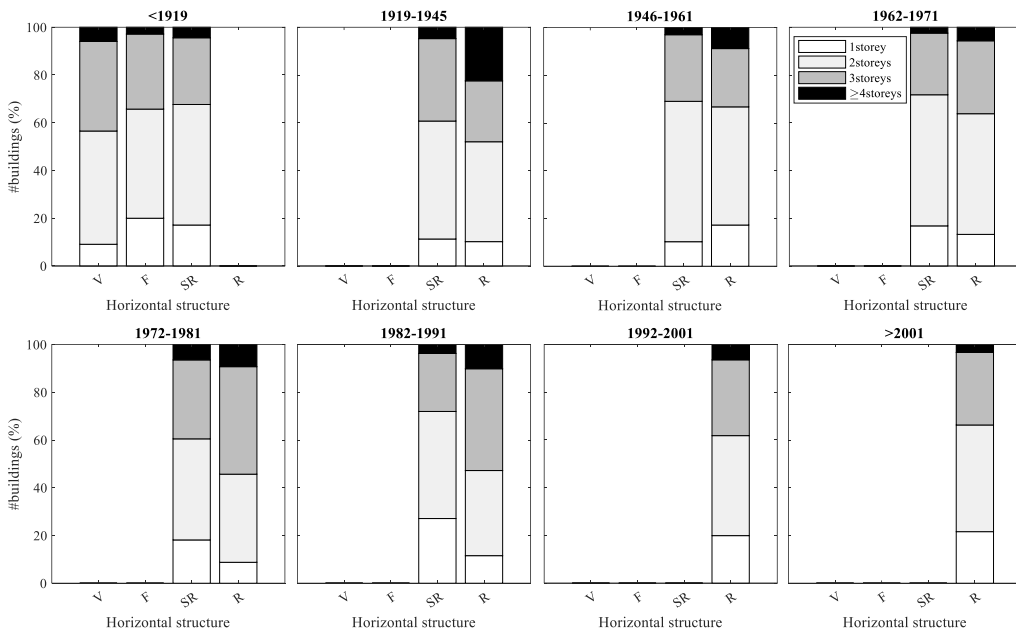


Figure 38. Distributions of number of storeys, given the horizontal structural type and the construction age (*damaged* database) for considered as-built GQ typologies.

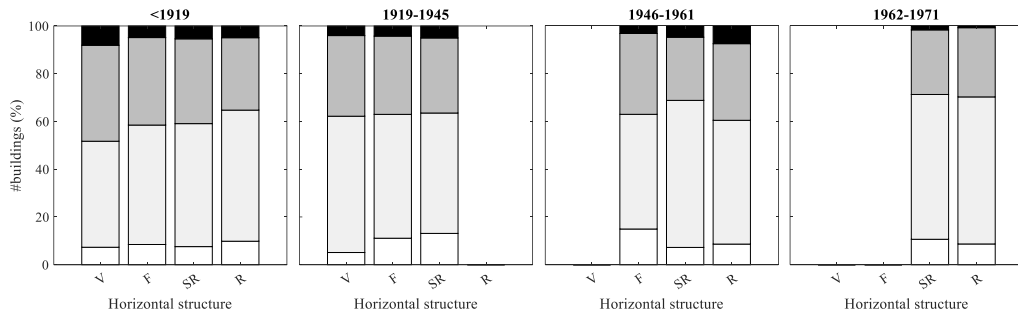


Figure 39. Distributions of number of storeys, given the horizontal structural type and the construction age (*damaged* database) for considered as-built BQ typologies.

These slight scatters could be ascribed to the different normative prescriptions enacted throughout the years. In fact, before 1915, no limitations exist on the maximum number of storeys. Conversely, starting from the Royal Decree 19/04/1915 n.573, limitations about the building's height or the number of storeys were enacted, allowing 1-4 storeys buildings (Royal Decree 22/11/1937, n. 2105). Such consideration could explain the greater percentage of 4-storeys buildings with good quality and rigid slabs built in the 1919-1945 period. About BQ buildings (Figure 39), almost the same percentage distribution is observed regardless to the construction age and the horizontal structures. In fact, the greater difference is observed only for buildings built after the 1962, presenting a very small percentage of 4-storeys buildings.

Retrofitted BQ buildings originally built before 1919 overall show distributions similar to those of not retrofitted buildings. The slight differences are about the percentage of 4-storeys buildings that increases, decreasing the amount of 1-story ones. As for as-built typologies, again 2- and 3-storeys buildings are the most common configurations. However, the slight differences in the distribution of the number of storeys get to not further subdivide the sample, safeguarding its reliability and homogeneity.

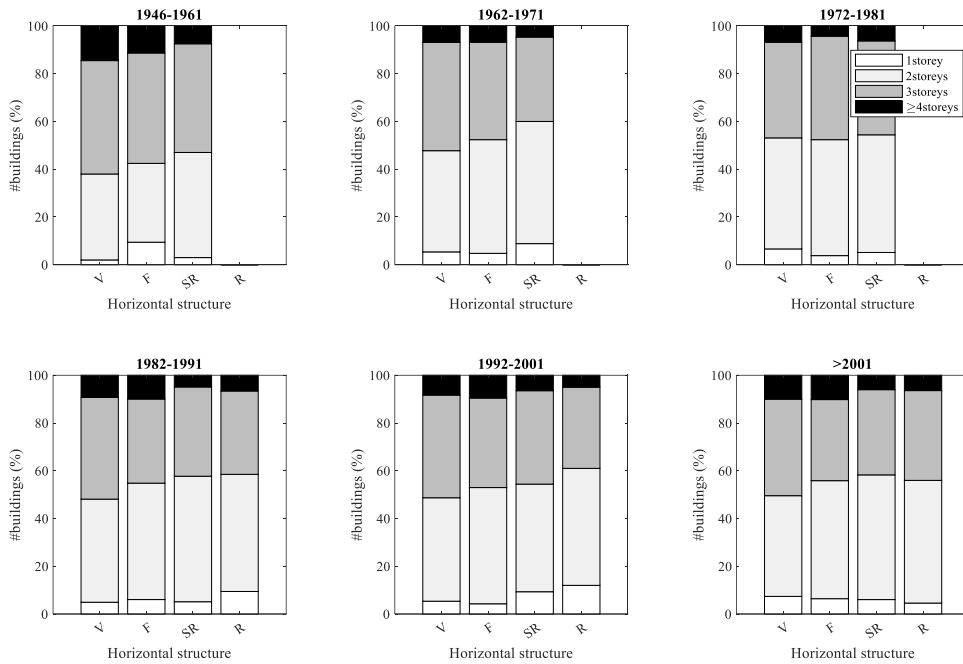


Figure 40. Distributions of number of storeys, given the horizontal structural type and the retrofit age (*damaged* database) for considered retrofitted BQ typologies.

Lastly, the presence/absence of tie rods and/or tie beams is a critical parameter, able to modify the building's behaviour under seismic actions (Sorrentino et al., 2017). In Figure 41, the distribution of GQ buildings with/without tie beams and/or tie rods are shown, given the construction age and the structural horizontal type. Before 1919-1945, the presence of these structural details is quite uncommon: in fact, about 20% of the buildings is equipped with tie rods/beams. This result can be explained by the fact that the construction of tie rods in masonry buildings started to be regulated only in 1935 (Royal Degree 22/03/1935 n.640) in seismic zone and through the Royal Degree 22/11/1937 n.2105 also in non-seismic zone.

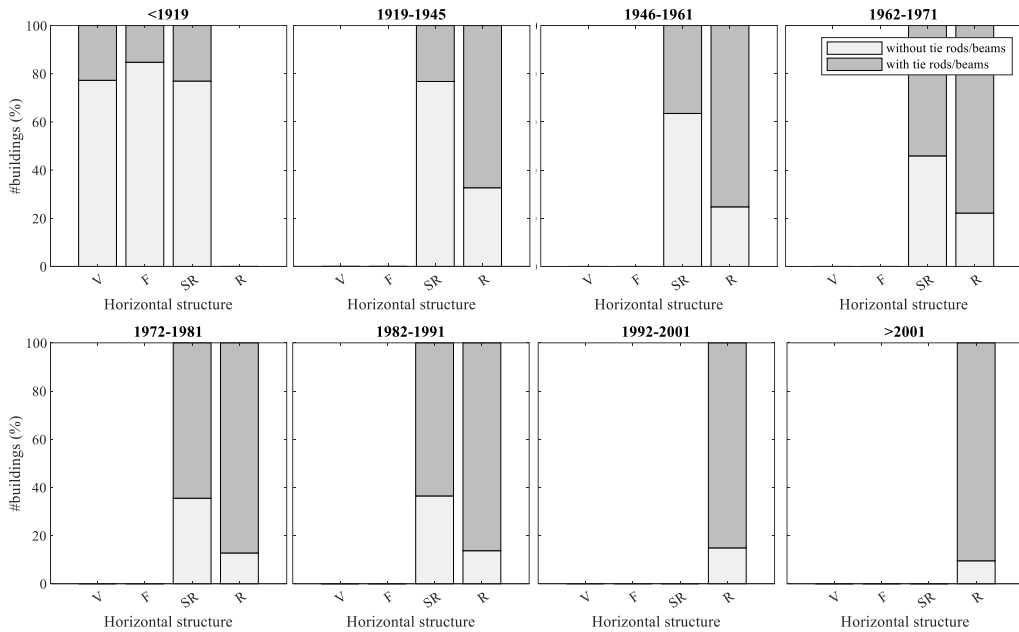


Figure 41. Distributions of presence/absence of tie rods/beams, given the horizontal structural type and the construction age (*damaged* database) for as-built GQ buildings.

Subsequently, a slow increase of buildings with tie rods/beams is observed for buildings with semi-rigid slabs between 1946 and 1971, going from about 35% to about 55%. Then, a percentage equal to 60% is observed between 1972-1991. Conversely, about 65% of buildings with rigid slabs are equipped with tie rods/beams already from 1919-1945. This percentage increases up to about 80% in 1946-1961 age, remaining constant up to 2001. Lastly, for buildings with rigid slabs built after 2001, the percentage of buildings with tie rods/beams reaches 90%. The not-negligible percentage of buildings without tie rods/beams after 1935, could be related to the recurrent construction practices in those years (between 1919 and 1960), i.e. precast and Hourdis hollow-tile slabs, as highlighted in (Donà et al., 2020).

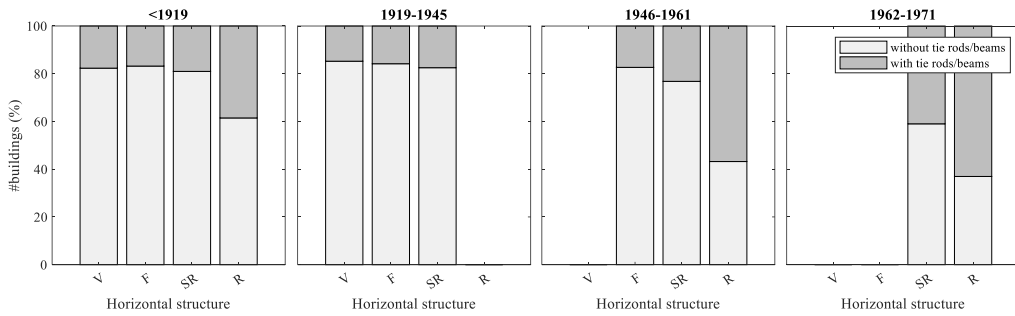


Figure 42. Distributions of presence/absence of tie rods/beams, given the horizontal structural type and the construction age (*damaged* database) for as-built BQ buildings.

The same statistics are provided by Figure 42 and Figure 43 respectively for as-built and retrofitted BQ masonry buildings, given the horizontal structure and the construction/retrofit age. It should be noted that in previous study, the presence of tie beams/tie rods resulted not to have a significant influence on damage distribution of buildings with poor quality masonry (D'Ayala and Paganoni, 2011; Sisti et al., 2018; D'Amato et al., 2020). Additionally, post-earthquake damage data shows that neither as-built nor retrofitted BQ buildings are characterized by high percentage of tie beams/tie rods. In fact, although the use of such a device became compulsory starting from 1935 (R.D. 640/1935) for all masonry buildings regardless the design type, percentages from 20% (for vaults or flexible slabs) up to 60% (for rigid slabs) of buildings equipped with tie beams/tie rods and constructed after 1946 can be observed in Figure 42.

This inconsistency with requirements enforced by technical codes can be justified by the fact that inspections were performed by means of rapid visual inspection (Zucconi et al., 2018; Del Gaudio et al., 2021), which not always guarantee a complete awareness of all structural details, requiring sometimes more refined and invasive investigation (such as plaster scarifying for the detection of tie beams), which are in poor agreement with the urgency required by the emergency phases. Therefore, even if effective, this parameter has not been considered in the present taxonomy, being its reliability strongly influenced by the way the inspections were performed.

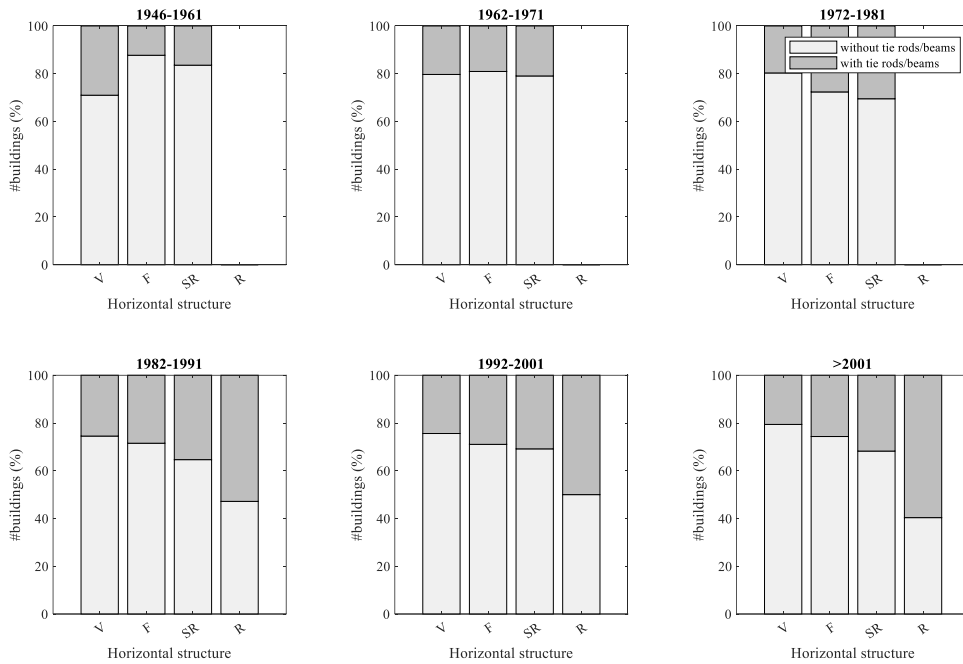


Figure 43. Distributions of presence/absence of tie rods/beams, given the horizontal structural type and the retrofit age (*damaged* database) for retrofitted BQ typologies.

On the other hand, the reduced increase in the percentage of buildings equipped with tie beams/tie rods between retrofitted and non-retrofitted buildings seems to reveal that these devices represented a limited choice for structural interventions. In fact, the percentages of buildings with tie rods/beams increase from 17 to 23%, from 17 to 25%, from 19 to 30% and from 38% to 52%, respectively in case of vaults, flexible-, semi-rigid- and rigid slabs (Figure 43).

5.3.2 Proposed building's taxonomy

In Figure 44, the proposed taxonomy, based on 5 parameters has been summarized: the structural typology (masonry buildings), the presence/absence of retrofit interventions, the quality of the vertical structures, the construction age (together with the seismic classification) and on the horizontal structure.

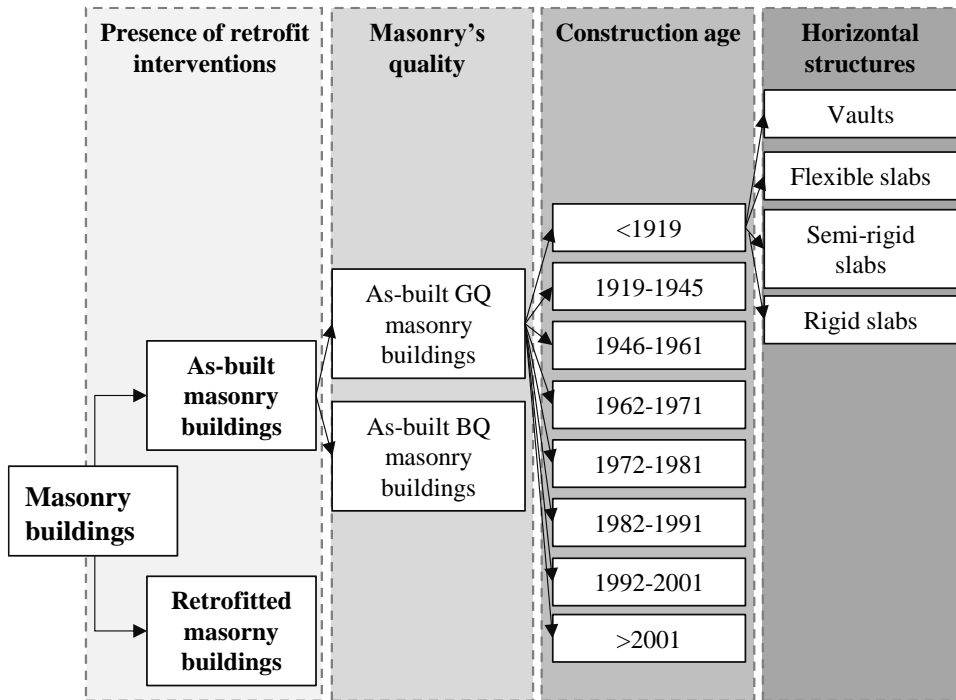


Figure 44. Proposed building's taxonomy based on presence of retrofit interventions, masonry's quality, construction age and horizontal structural type.

Basically, the first implicit subdivision of the entire database is based on structural typology: masonry, reinforced concrete, and other types of structures. Among masonry buildings (object of the present thesis work), those subjected to retrofit interventions should be separated to as-built ones according to the proposed taxonomy. As matter of fact, such criterion allows to avoid potential bias due to an inhomogeneous sample, because a lower damage attitude could characterize retrofitted buildings. Among non-retrofitted masonry buildings, it is crucial to detect how and when the building has been constructed. In other words, the structure's features (i.e., the quality of wall and the horizontal type) and the construction age should be considered to define the building's taxonomy. Such further subdivision is due to the fact that (1) buildings with the same structural features built in different period could be present a different vulnerability because of different normative prescriptions and/or working practices. In the

other hand, also (2) buildings of the same period denoted by different structural characteristics could show a highly different behaviour under seismic loads.

Thus, combining the available attributes related to the masonry quality (i.e., 2), horizontal structures (i.e., 4) and construction age (i.e., 8), overall, 64 as-built classes are considered by the present taxonomy.

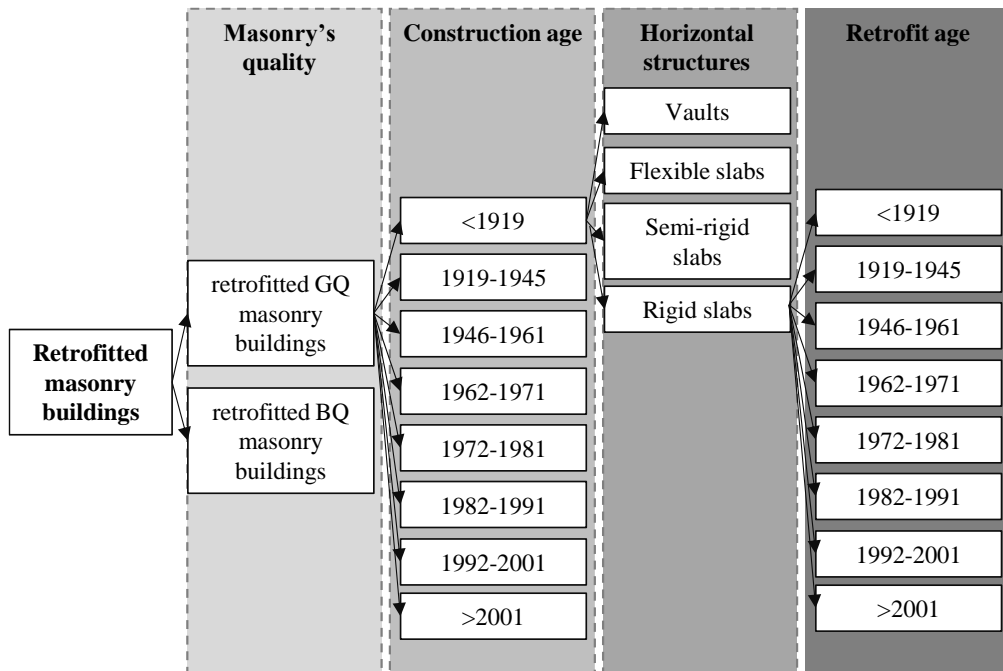


Figure 45. Proposed building's taxonomy for retrofitted buildings.

For what concerns the retrofitted ones, a further feature should be took into account, i.e., the retrofit age. In fact, as highlighted in the Section 3.4.3 the normative prescriptions about the retrofit of masonry buildings have been improved over the time. Namely, starting from the year of first seismic classification (mainly 1915) up to nowadays, several normative contents (together with constructive practices) have been changed, leading to a potential different damage attitude of retrofitted building. Thus, whilst the classification of as-built buildings follows the taxonomy of Figure 44 based on 3 features (i.e., vertical and horizontal structure, and construction age), the classification of

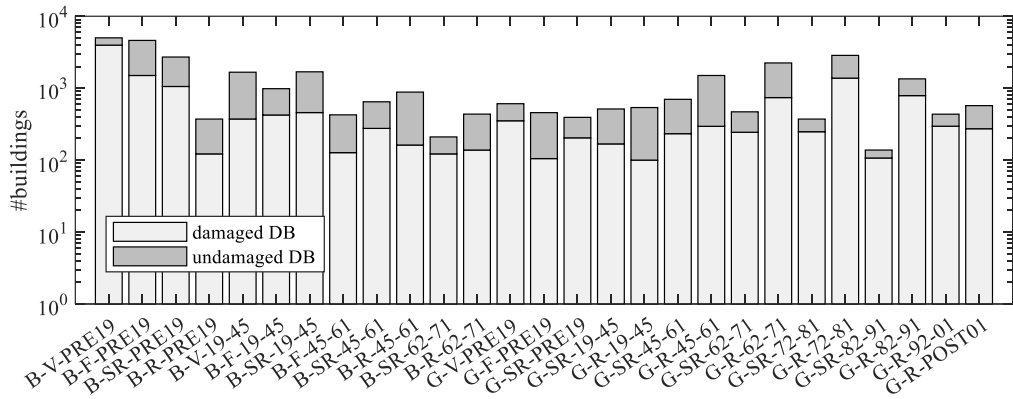
retrofitted ones requires a taxonomy based on 4 features (i.e., vertical and horizontal structure, and construction and retrofit age). It should be noted that in the taxonomy of Figure 44 the branch related to retrofitted buildings is missing because it is reported in Figure 45. Therefore, whilst for as-built buildings 64 building's classes can be defined according to the present taxonomy, for retrofitted ones 64 x 8 classes are obtained, considering the 8 retrofit ages.

As highlighted in the previous paragraph, the reliability of a sample data is affected by its numerosness. For this reason, a minimum number of buildings equal to 100 has been introduced, discarding all classes less populated. Such procedure leads to consider:

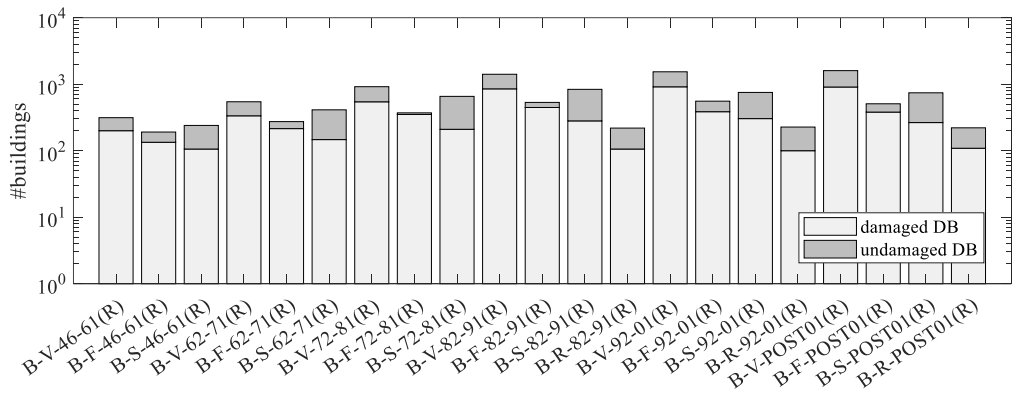
- 27 as-built classes
- 21 retrofitted classes

The taxonomy shown in Figure 44 and Figure 45 has been adopted also for the *undamaged database* (Figure 37(b)), using the de-aggregation approach shown in Sect. 5.2.3, extending the relationship between parameters achieved from the *damaged* to the *undamaged* database. So, the presence/absence of retrofit interventions has been assigned to the number of undamaged buildings given the construction age of Figure 37(b) by means of percentage distribution of Figure 32(a). Then, the (vertical + horizontal) structure has been assigned to resulting undamaged as-built buildings using Figure 32(c-d) and to retrofitted ones using distribution of Figure 34.

Finally, data reported in Figure 46 provides the total number of *damaged* and *undamaged* buildings, employed in the following chapters for vulnerability and fragility evaluations. Thus, each building's class is composed not only by damaged buildings (reported in Table 14 and Table 16, respectively for as-built and retrofitted buildings), but also by undamaged ones. So, the total number of buildings for each considered class (i.e., 27 as-built + 21 retrofitted) is reported in Figure 46, distinguishing between buildings belonging to *damaged* and *undamaged* DBs. Note that the y-axis is in the logarithmic scale to show the numerosity of each class, despite the high variability.



(a)



(b)

Figure 46. Number of buildings for each considered class, deriving from damaged and undamaged DBs, for (a) as-built and (b) retrofitted typologies.

5.4 REFERENCES

- [1] Baggio, C., Bernardini, A., Colozza, R., Corazza, L., Della Bella, M., Di Pasquale, G., Papa, F., 2007. Field manual for post-earthquake damage and safety assessment and short term countermeasures (AeDES). European Commission—Joint Research Centre—Institute for the Protection and Security of the Citizen, EUR, 22868.
- [2] Braga F., Dolce M., Liberatore D., 1982. A statistical study on damaged buildings and an ensuing review of the MSK-76 scale. Proceedings of the seventh European conference on earthquake engineering, Athens, Greece, 431-450.

- [3] Brzev S., Scawthorn C., Charleson A.W., Allen L., Greene M., Jaiswal K.S., et al., GEM Building Taxonomy, Version 2.0, GEM Technical Report, GEM Foundation, Pavia, Italy, 2013-02, p. 188, <https://doi.org/10.13117/GEM.EXP-MOD>.
- [4] Colombi, M., Borzi, B., Crowley, H. et al., 2008. Deriving vulnerability curves using Italian earthquake damage data. *Bull Earthquake Eng* 6, 485–504. <https://doi.org/10.1007/s10518-008-9073-6>
- [5] D’Ayala D.F., Paganoni S., 2011. Assessment and analysis of damage in L’Aquila historic city centre after 6th April 2009. *Bulletin of Earthquake Engineering*, 9(1), 81-104.
- [6] D’Amato M, Laguardia R, Di Trocchio G, Coltellacci M, Gigliotti R. Seismic Risk Assessment for Masonry Buildings Typologies from L’Aquila 2009 Earthquake Damage Data. *Journal of Earthquake Engineering* 2020; 00(00): 1-35. DOI: 0.1080/13632469.2020.1835750.
- [7] Decreto Ministeriale 3 Marzo 1975. Approvazione delle norme tecniche per le costruzioni in zone sismiche. **(in Italian)**
- [8] Decreto Ministeriale 9 Gennaio 1987. Norme tecniche per la progettazione, esecuzione e collaudo degli edifici in muratura e per il loro consolidamento. **(in Italian)**
- [9] Del Gaudio C., De Martino G., Di Ludovico M., Manfredi G., Prota A., Ricci P., Verderame G.M., 2019. Empirical fragility curves for masonry buildings after the 2009 L’Aquila, Italy, earthquake. *Bulletin of Earthquake Engineering*. <https://doi.org/10.1007/s10518-019-00683-4>.
- [10] Del Gaudio, C., Di Ludovico, M., Polese, M. et al. Seismic fragility for Italian RC buildings based on damage data of the last 50 years. *Bull Earthquake Eng* 18, 2023–2059 (2020). <https://doi.org/10.1007/s10518-019-00762-6>
- [11] Del Gaudio, C., Scala, S.A., Ricci, P., Verderame G.M., 2021. Evolution of the seismic vulnerability of masonry buildings based on the damage data from L’Aquila 2009 event. *Bull Earthquake Eng* (2021). <https://doi.org/10.1007/s10518-021-01132-x>
- [12] Dolce M., Goretti A., 2015. Building damage assessment after the 2009 Abruzzi earthquake. *Bulletin of Earthquake Engineering* 13, 2241–2264 (2015). <https://doi.org/10.1007/s10518-015-9723-4>.
- [13] Dolce, M., Giovinazzi, S., Iervolino, I., Nigro, E., & Tang, A. (2009). Emergency management for lifelines and rapid response after L’Aquila earthquake.

- [14] Dolce, M., Kappos, A., Masi, A., Penelis, G., & Vona, M. (2006). Vulnerability assessment and earthquake damage scenarios of the building stock of Potenza (Southern Italy) using Italian and Greek methodologies. *Engineering Structures*, 28(3), 357-371.
- [15] Dolce, M., Speranza, E., Giordano, F., Borzi, B., Bocchi, F., Conte, C., Pascale, V., 2019. Observed damage database of past Italian earthquakes: the Da. DO WebGIS. *Bollettino di Geofisica Teorica ed Applicata*, 60(2).
- [16] Donà M, Carpanese P, Follador V, Sbrogiò L, da Porto F (2020) Mechanics-based fragility curves for Italian residential URM buildings. *Bull Earthq Eng* 19(7):256. <https://doi.org/10.1007/s10518-020-00928-7>
- [17] Goretti, A., & Di Pasquale, G. (2004). Building inspection and damage data for the 2002 Molise, Italy, earthquake. *Earthquake Spectra*, 20(1_suppl), 167-190.
- [18] ISTAT 2011. Istituto Nazionale di Statistica (National Institute of Statistics). 15° Censimento generale della popolazione e delle abitazioni. Dati sulle caratteristiche strutturali della popolazione, delle abitazioni e variabili. **(in Italian)** <http://www.istat.it/it/archivio/104317>
- [19] Jaiswal K., Wald D., Porter K., A global building inventory for earthquake loss estimation and risk management, *Earthq. Spectra* 26 (2010) 731–748, <https://doi.org/10.1193/1.3450316>.
- [20] Karababa, F.S., Pomonis, A., 2011. Damage data analysis and vulnerability estimation following the August 14, 2003 Lefkada Island, Greece, Earthquake. *Bull Earthquake Eng* 9, 1015–1046. <https://doi.org/10.1007/s10518-010-9231-5>
- [21] Kircher C.A., Whitman R.V., Holmes W.T., HAZUS earthquake loss estimation methods, *Nat. Hazards* 7 (2006) 45–59, [https://doi.org/10.1061/\(ASCE\)1527-6988\(2006\)7:2\(45\)](https://doi.org/10.1061/(ASCE)1527-6988(2006)7:2(45)).
- [22] Legge n. 1684 del 25 Novembre 1962. Provvedimenti per l'edilizia, con particolari prescrizioni per le zone sismiche. **(in Italian)**
- [23] Regio Decreto 18 Aprile 1909. Provvedimenti e disposizioni in seguito al terremoto del 28 dicembre 1908. **(in Italian)**
- [24] Regio Decreto 29 Aprile 1915. Norme tecniche ed igieniche da osservarsi per i lavori edilizi nelle località colpite dal terremoto del 13/01/1915. **(in Italian)**
- [25] Regio Decreto Legge 13 Marzo 1927. Norme tecniche ed igieniche per le riparazioni, ricostruzioni e nuove costruzioni degli edifici pubblici e privati nei comuni o frazioni di comune dichiarati zone sismiche. **(in Italian)**

- [26] Regio Decreto Legge 22 Marzo 1935. Nuovo testo delle norme tecniche di edilizia con speciali prescrizioni per le località colpite dai terremoti. **(in Italian)**
- [27] Regio Decreto Legge 22 Novembre 1937. Norme tecniche ed igieniche per le riparazioni, ricostruzioni e nuove costruzioni degli edifici pubblici e privati nei comuni o frazioni di comune dichiarati zone sismiche. **(in Italian)**
- [28] Rossetto T., Ioannou I., Grant D.N., 2013. Existing empirical fragility and vulnerability functions: Compendium and guide for selection, GEM Technical Report 2013-X, GEM Foundation, Pavia, Italy.
- [29] Rosti A., Del Gaudio C., Di Ludovico M., Magenes G., Penna A., Polese M., Verderame G.M., 2020a. Empirical vulnerability curves for Italian residential buildings. *Bollettino di Geofisica Teorica ed Applicata*, 61(3).
- [30] Rosti A., Del Gaudio C., Rota M., Ricci P., Di Ludovico M., Penna A., Verderame G.M., 2020b. Empirical fragility curves for Italian residential RC buildings. *Bull Earthquake Eng* (2020). <https://doi.org/10.1007/s10518-020-00971-4>.
- [31] Rosti A., Rota M., Penna A., 2018. Damage classification and derivation of damage probability matrices from L'Aquila (2009) post-earthquake survey data. *Bulletin of Earthquake Engineering* 16.9 (2018): 3687-3720.
- [32] Rosti A., Rota M., Penna A., 2020c. Empirical fragility curves for Italian URM buildings. *Bulletin of Earthquake Engineering*.
- [33] Rota M., Penna A., Strobbia C.L., 2008. Processing italian damage data to derive typological fragility curves. *Soil Dynamics and Earthquake Engineering*, 933-947.
- [34] Sabetta F., Goretti A., Lucantoni A., 1998. Empirical Fragility Curves from Damage Surveys and Estimated. 11th European Conference on Earthquake Engineering © 1998 Balkema, Rotterdam, ISBN 90 5410 982 3.
- [35] Scala S.A., Del Gaudio C., Verderame G.M., 2022. Influence of construction age on seismic vulnerability of masonry buildings damaged after 2009 L'Aquila Earthquake **(under review)**
- [36] Sisti R., Di Ludovico M., Borri A., Prota A., 2018. Damage assessment and the effectiveness of prevention: the response of ordinary unreinforced masonry buildings in Norcia during the Central Italy 2016–2017 seismic sequence. *Bulletin of Earthquake Engineering*, 1-21. <https://doi.org/10.1007/s10518-018-0448-z>.

- [37] Sorrentino L., D'Ayala D., de Felice G. et al., 2017. Review of out-of-plane seismic assessment techniques applied to existing masonry buildings. *Int J Archit Herit* 11:2–21. <https://doi.org/10.1080/15583058.2016.1237586>.
- [38] Zuccaro G., Cacace F., 2015. Seismic vulnerability assessment based on typological characteristics. The first level procedure “SAVE”. *Soil Dynamics and Earthquake Engineering* 69 (2015) 262–269.
- [39] Zucconi M., Ferlito R., Sorrentino L., 2018. Simplified survey form of unreinforced masonry buildings calibrated on data from the 2009 L'Aquila earthquake. *Bulletin of Earthquake Engineering*, 16(7), 2877-2911.

Chapter 6.

DAMAGE ANALYSIS AND VULNERABILITY CURVES

6.1 INTRODUCTION

In this Chapter, starting from the building's classes above defined, the damage analysis was performed. To this aim, damage data collected in the post-earthquake survey and provided by the AeDES form (Baggio et al., 2007), has been converted in damage states consistent with the European Macroseismic Scale, *EMS98* (Grunthal, 1998). Such conversion is based on damage metric of Rota et al., 2008, considering the damage observed on vertical structures, typically the most severe one (Del Gaudio et al., 2019; D'Amato et al., 2020; Scala et al., 2022).

The seismic vulnerability of each building class has been investigated first by means of mean damage (mean of damage distribution), deriving vulnerability trends. The analysis of mean damage values reveals the general trends as a function of the main influential parameters, i.e. construction age, horizontal structural types, presence of retrofit interventions, and quality layout. Then, the same trends have been analysed in terms of vulnerability curves, introducing as intensity measure the *peak ground acceleration*, PGA, derived from the ShakeMap by Italian National Institute of Geophysics and Volcanology (INGV) (Michellini et al., 2020). Vulnerability curves were derived assuming a lognormal

statistical model, through a minimization procedure of the distance between predicted and observed mean damage.

Lastly, a comparison between building's classes in terms of median PGA values has been shown, assuming a common logarithmic standard deviation. Basically, the vulnerability trends obtained by means of mean damage, vulnerability curves, and median PGAs, are substantially the same, highlighting a clear hierarchy in terms of construction age, (vertical + horizontal) structural typology, and presence of retrofit.

6.2 ANALYSIS OF DAMAGE DATA PROVIDED BY AeDES FORM

In the previous Chapter, the database considered in this Thesis work has been defined, taking into account several remarkable issues. Among the others, the data completeness has been guaranteed by means of a mixed approach (Del Gaudio et al., 2021), defining two samples of data: namely, the so-called *damaged* and *undamaged* databases. The first one is obtained considering the residential buildings sited in the only municipalities completely inspected after the earthquake (i.e., at least the 91% of the actual number of buildings has been subjected to the post-earthquake survey). The second one derives from the census data and contains all buildings located in municipalities slightly or not surveyed after the earthquake. Thus, the *damaged* DB represents the positive evidence of the damage (occurrence of damage) deriving from the inspections, whereas the *undamaged* one is the negative evidence of the damage (not occurrence of damage). Such approach assumes that the not inspected buildings are basically not damaged ones. For this reason, null damage is assigned to each *undamaged* building. Conversely, the damage of *damaged* buildings derives from the post-earthquake survey. In particular, *Section 4* of the AeDES form (see Figure 47) provides the damage description of the structural components (such as vertical, horizontal and roof structures) based on (3+1) damage levels (i.e., D1, D2-D3, D4-D5) and on 3 damage extents (i.e., $<1/3$, $1/3-2/3$, $>2/3$).

Moreover, in the previous Chapter, the buildings classes considered in this work have been detected, after introducing a building's taxonomy and a minimum sample size of 100 *damaged* buildings for each class (Del Gaudio et

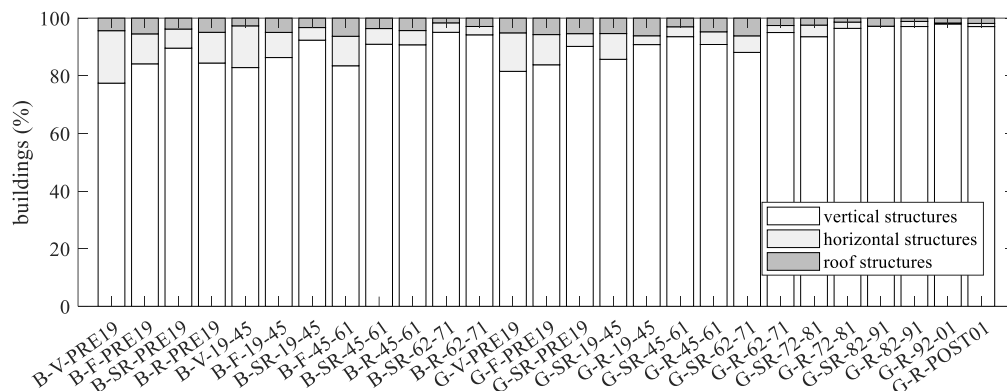
al., 2021; Scala et al., 2021). In particular, the study is based on 27 as-built and 21 retrofitted classes, each of them characterized by a different (vertical + horizontal) structural typologies and construction/retrofit age.

Livello - estensione Componente strutturale - Danno preesistente		DANNO ⁽¹⁾									
		D4-D5 Gravissimo			D2-D3 Medio grave			D1 Leggero			Nullo
		> 2/3	1/3 - 2/3	< 1/3	> 2/3	1/3 - 2/3	< 1/3	> 2/3	1/3 - 2/3	< 1/3	
		A	B	C	D	E	F	G	H	I	
1	Strutture verticali	<input type="checkbox"/>	<input type="checkbox"/>	<input type="checkbox"/>	<input type="checkbox"/>	<input type="checkbox"/>	<input type="checkbox"/>	<input type="checkbox"/>	<input type="checkbox"/>	<input type="checkbox"/>	<input type="radio"/>
2	Solai	<input type="checkbox"/>	<input type="checkbox"/>	<input type="checkbox"/>	<input type="checkbox"/>	<input type="checkbox"/>	<input type="checkbox"/>	<input type="checkbox"/>	<input type="checkbox"/>	<input type="checkbox"/>	<input type="radio"/>
3	Scale	<input type="checkbox"/>	<input type="checkbox"/>	<input type="checkbox"/>	<input type="checkbox"/>	<input type="checkbox"/>	<input type="checkbox"/>	<input type="checkbox"/>	<input type="checkbox"/>	<input type="checkbox"/>	<input type="radio"/>
4	Copertura	<input type="checkbox"/>	<input type="checkbox"/>	<input type="checkbox"/>	<input type="checkbox"/>	<input type="checkbox"/>	<input type="checkbox"/>	<input type="checkbox"/>	<input type="checkbox"/>	<input type="checkbox"/>	<input type="radio"/>
5	Tamponature-tramezzi	<input type="checkbox"/>	<input type="checkbox"/>	<input type="checkbox"/>	<input type="checkbox"/>	<input type="checkbox"/>	<input type="checkbox"/>	<input type="checkbox"/>	<input type="checkbox"/>	<input type="checkbox"/>	<input type="radio"/>
6	Danno preesistente	<input type="checkbox"/>	<input type="checkbox"/>	<input type="checkbox"/>	<input type="checkbox"/>	<input type="checkbox"/>	<input type="checkbox"/>	<input type="checkbox"/>	<input type="checkbox"/>	<input type="checkbox"/>	<input type="radio"/>

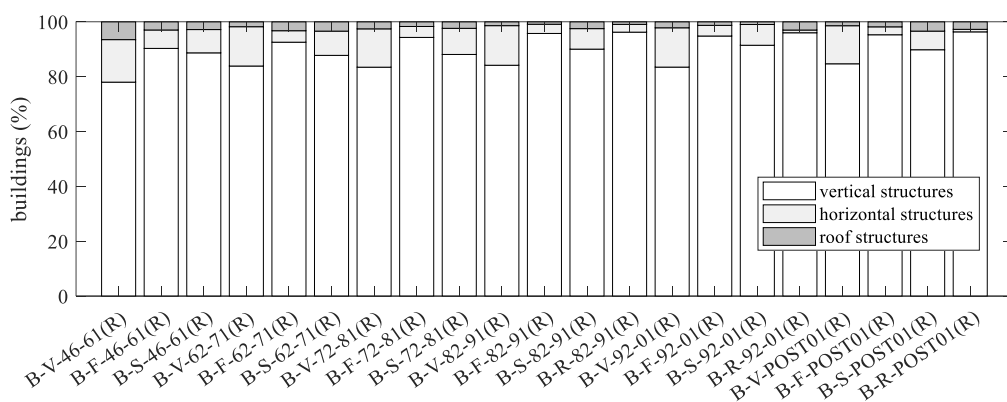
Figure 47. Section 4 (damage description) of AeDES 06/2008 form.

Thus, Figure 48 reports, for each quite populated building's class, the percentage of the cases in which the maximum damage is experienced respectively in vertical, horizontal and roof structures. The damage comparison is done considering, first, the three damage levels (i.e., D1, D2-D3, D4-D5), plus the null damage D0, provided by the survey form and then, also the damage extent (i.e., <1/3, 1/3-2/3, >2/3). Moreover, in case of equal damage between vertical structure and another component, it is assumed that the maximum damage is reached by the vertical structures. Similarly, if both horizontal and roof structures show the maximum damage, it is assumed that the horizontal structures exhibit the greater damage. Thus, not simultaneously attainment of maximum damage by different components is considered. It should be noted that in the greater part (about 89%) of the considered as-built buildings, the most severe damage regards the vertical structures (Figure 48(a)). It occurs especially for buildings with rigid and semi-rigid slabs. In the remaining cases, it is attained in the horizontal (about 8%) and roof (about 3%) structures. Similar results are shown also for the retrofitted classes (Figure 48(b)): overall, the maximum

damage is attained by vertical structures in about 90% of the cases, by horizontal structures in about 8% and, lastly, by roof structures in 2%.



(a)

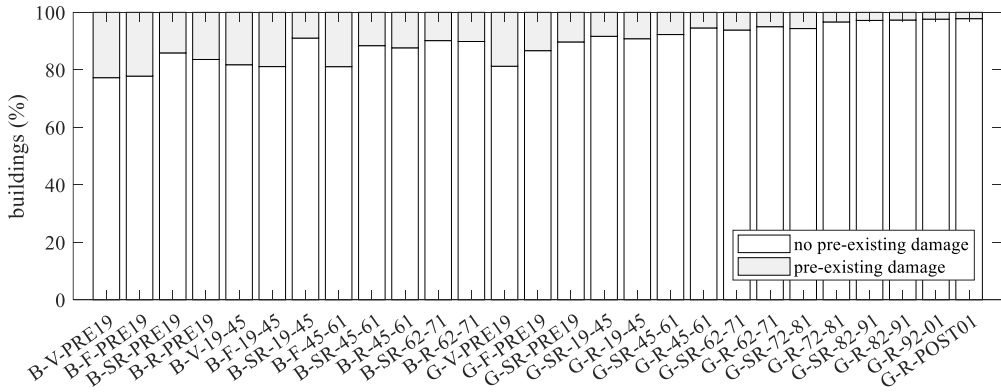


(b)

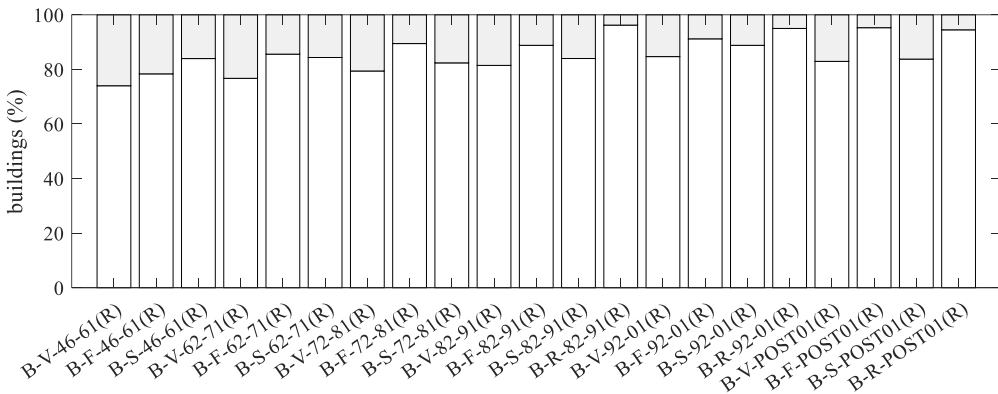
Figure 48. Maximum damage observed among vertical, horizontal and roof structures, given the building's class for (a) as-built and (b) retrofitted typologies.

Moreover, *Section 4* of the AeDES form provides a further information about the presence of pre-existing damage, describing the building condition before the seismic event. It means that, if any, also the damage not caused by the earthquake is syntactically described by the survey form (in particular in the sixth row of the damage matrix) by means of 3+1 damage levels and 3 damage extents. Such damage description is not provided for a specific structural component, being

related to the entire building. Thus, in Figure 49 the percentage of case in which pre-existing damage is equal or greater than the maximum damage over all structural components is shown, given the building class for both as-built (Figure 49(a)) and retrofitted (Figure 49(b)) typologies.



(a)



(b)

Figure 49. Presence of pre-existing damage equal or greater than the maximum damage among all structural components, given the building's class for (a) as-built and (b) retrofitted typologies.

We can note that the cases in which pre-existing damage is at least equal to the maximum damage attained by all structural components are more frequent in the most ancient typologies, likely lacking constant maintenance (Dolce and

Goretti, 2015). In fact, such percentage decreases increasing the construction age for as-built classes in Figure 49(a) and is almost constant in retrofitted typologies built before 1919 (in Figure 49(b)). However, it is quite difficult for the surveyor distinguish between pre-existing damage and damage caused by the earthquake, in particular for lower levels of damage (Rosti et al., 2018). Thus, such information provided by the survey form is not very reliable and often discarded by the damage evaluation (among the others, D'Amato et al., 2020; Rosti et al., 2020; Del Gaudio et al., 2021; Scala et al., 2022).

6.3 DAMAGE DISTRIBUTION AND MEAN DAMAGE

The damage analysis adopted in this work takes advantage of damage data collected in *Section 4* of AeDES form, which provides information on severity and extension of damage detected on several structural components based on classification inspired by the European Macroseismic Scale *EMS98* (Grunthal et al., 1998). Damage severity is based on 3+1 levels (D0, *no damage*; D1, *slight damage*; D2-D3, *medium-severe damage*; D4-D5, *very heavy damage*), with 3 range of extension (lower than 1/3, between 1/3 and 2/3, and greater than 2/3 of elements/area). In several recent studies (Del Gaudio et al., 2019; Dolce et al., 2019; D'Amato et al., 2020; Del Gaudio et al., 2021; Scala et al., 2022), vulnerability and/or fragility assessment has been done considering as damage level the damage states defined in the European Macroseismic scale. This latter is articulated in five damage states (plus the case of no damage, DS0) related to the entire building: negligible to slight damage DS1, moderate damage DS2, substantial to heavy damage DS3, very heavy damage DS4 and destruction DS5. Thus, conversion rules are needed to passage from damage observed on structural elements during the post-earthquake survey to a global damage consistent with *EMS98* scale.

Within the literature, one of the most used conversion schemes has been proposed by Rota et al, 2008, according to the rules reported in Table 19. Such scheme has been recently updated by Dolce et al., 2019, adding the conversion rules also for buildings with two or three damage values for the same structural component.

Table 19. Conversion's rule of the damage levels in Damage State consistent with the EMS-98.

AeDES		EMS 98	
Damage Level (extension)	Description	Damage State	Description
D0	<i>No damage</i>	DS0	<i>No Damage</i>
D1 (<1/3)	<i>Slight</i>	DS1	<i>Negligible to Slight damage</i>
D1 (1/3 – 2/3)			
D1 (>2/3)			
D2-D3 (<1/3)	<i>Medium - severe</i>	DS2	<i>Moderate damage</i>
D2-D3 (1/3 – 2/3)		DS3	<i>Substantial to</i>
D2-D3 (>2/3)			<i>Heavy damage</i>
D4-D5 (<1/3)	<i>Very heavy</i>	DS4	<i>Very heavy damage</i>
D4-D5 (1/3 – 2/3)			
D4-D5 (>2/3)		DS5	<i>Destruction</i>

Clearly, several methods available in literature allow to estimate the global damage starting from the observed component's damage. Such methods can be grouped in two main categories (e.g., Rosti et al., 2018; D'Amato et al., 2020): methods belonging to the first one category (Angeletti, 2002; Di Pasquale and Goretti, 2001; Lagomarsino et al., 2015) estimate the global damage through a weighted sum of damages of all (or almost all) structural components, combining damage level and extent by means of different weights for each component. Conversely, methods of the second category (e.g., Rota et al, 2008; Di Pasquale and Goretti 2001; Dolce and Goretti 2015; Del Gaudio et al. 2017) define the global damage as the maximum among all (or almost all) structural components. Moreover, different number of structural components is considered by the mentioned works to define the global damage.

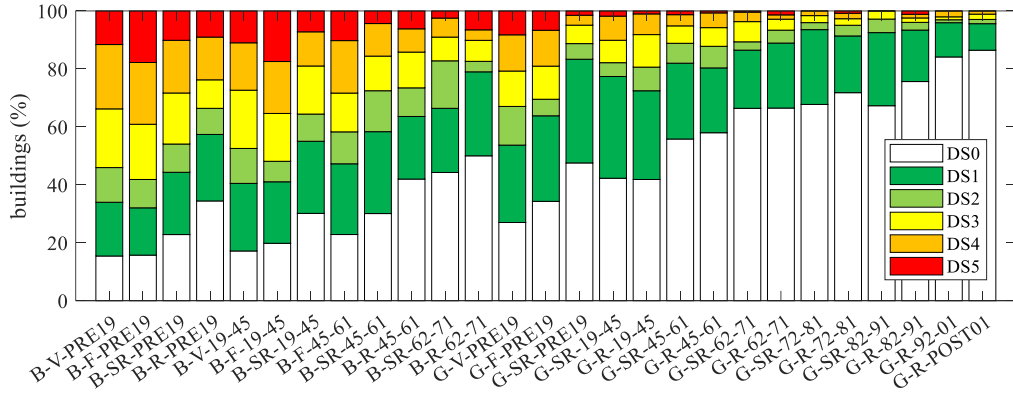
For example, Rota et al, 2008 considered the damage observed among the vertical, the horizontal and the roof structures. Conversely, damage of the only vertical bearing structures has been considered by Dolce and Goretti 2015. However, comparing the various methods, most conservative results are typically obtained, using the maximum damage approach (D'Amato et al., 2020) because of the general overestimation with respect to the weighted sum based approaches.

Moreover, the maximum damage is usually the main factor affecting the building usability and the related repair cost (Rota et al, 2008).

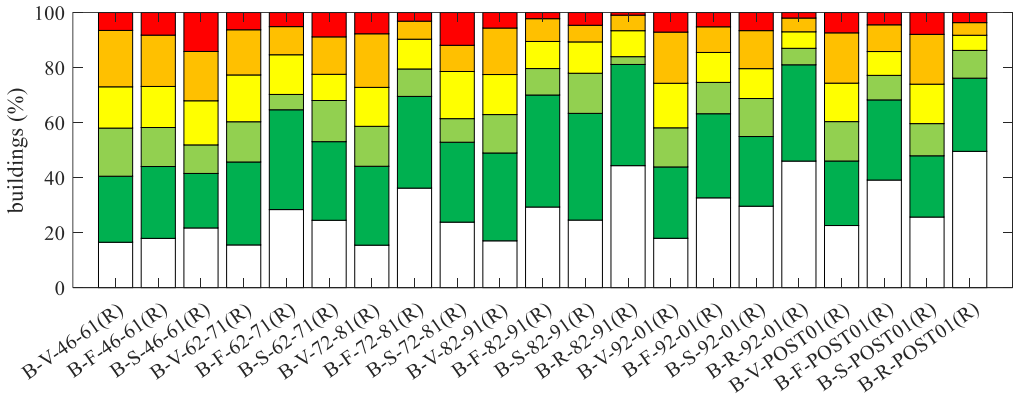
In this work, the conversion between damage levels detected on vertical structures (masonry walls) and the 5+1 *EMS98* damage grades for the whole building was carried out based on the scheme of Rota et al. 2008. The adoption of damage conversion scheme based on only vertical structures is pursued also in other studies (among the others, Braga et al. 1982; Dolce and Goretti 2015; Del Gaudio et al., 2019). In fact, although other studies consider the maximum damage detected among vertical, horizontal and roof structures (Rota et al., 2008) or a weighted average of damage suffered by several components (Zucconi et al., 2017; De Martino et al., 2017; Lagomarsino et al., 2021), it can be stated that damage to vertical structures in the vast majority of cases is the most severe among all considered components (see Paragraph 6.2, or also previous studies such as Del Gaudio et al., 2019; D’Amato et al., 2020; Scala et al., 2022).

Once the damage to vertical structures has been converted into global damage consistent with *EMS98* scale, the damage distributions (Figure 50) for all considered building’s classes have been derived.

Figure 50(a) shows the damage distribution for all the 27 as-built considered classes. It should be noted that the first 12 classes are all denoted by bad quality masonry and/or irregular layout, whereas the remaining 15 classes are characterized by good quality. Among the classes with the same masonry quality, firstly the most ancient are represented. Moreover, among the classes with the same masonry quality and the same construction age, damage distribution is provided first for classes equipped with vaults and then with flexible, semi-rigid and rigid slabs. Thus, moving from left to right, masonry quality, construction age and slab’s stiffness increase. We can note that the percentage of null damage increases with the slab’s stiffness (namely, going from vaults to rigid slabs), with the construction age and with the masonry quality. Conversely, the amount of buildings in DS5 decreases, increasing the same parameters.



(a)



(b)

Figure 50. Damage distributions, given the building's class for (a) as-built and (b) retrofitted typologies.

Almost the same representation is provided by Figure 50(b) for retrofitted buildings. It is worthy of note that all these buildings are denoted by bad quality masonry and/or irregular layout (BQ) and have been built before 1919. Moreover, as previously explained, different types of structural interventions may have been done on such buildings (the lack of data regarding the kind of intervention does not allow further classifications). In Figure 50(b), moving from left to right, first the slab's stiffness and then the retrofit age increase. We can note that the percentage distribution mainly varies with the horizontal structure

respect to the retrofit age. In other words, the retrofit age seems to affect the damage distribution less than the horizontal structure.

In order to better investigate such damage trends, a synthetic parameter has been introduced, according to the following equation:

$$\mu_D = \frac{\sum_{i=0}^5 N_B(DS=ds_i) i}{N_B} \quad (2)$$

where, $N_B(DS=ds_i)$ is the number of buildings, belonging to a given class, suffering a damage level equal to ds_i and N_B the total number of buildings belonging to that class. Thus, such parameter, called *mean damage* in the following sections, is a weighted average of damage distribution for a given building class. In the following sub-sections, the mean damage has been evaluated according to Equation (2) for all as-built and retrofitted classes, varying the construction and retrofit age respectively.

6.3.1 Mean damage for as-built classes

In the Chapter 5, the building's classes considered in the present Thesis work have been defined, after defining the building taxonomy and the minimum sample size. Figure 51 shows the number of *damaged* buildings for each of the 64 (8 construction ages \times 4 horizontal structures \times 2 layout types) classes covering the whole as-built taxonomy. Moreover, the minimum simple size of 100 buildings is represented with a horizontal red line, highlighting those classes where the minimum sample size is exceeded.

It should be noted that a significant diffusion of masonry buildings with an irregular layout/bad quality (BQ) is observed up to 1950, especially in the most ancient ages (before 1919); whereas masonry buildings with regular layout/good quality (GQ) became most widespread after the 1950s. In parallel, a gradual abandonment of the vaults and flexible slabs and a progressive diffusion in the use of semi-rigid and rigid slabs are observed throughout the years. Therefore, a reliable comparison can be performed between GQ and BQ classes, only

considering 15 classes for GQ masonry buildings and 12 classes for BQ masonry buildings.

The latter are composed by 2 classes characterized by vaults (<1919 and 1919-1945), 3 classes for flexible slabs (<1919; 1919-1945; 1946-1961), 4 classes for semi-rigid slabs (<1919; 1919-1945; 1946-1961; 1962-1971), and 3 with rigid slabs (<1919; 1946-1961; 1962-1971). About GQ masonry buildings, in the cases of vaults and flexible slabs the mean damage value can be determined only for <1919 construction age. Lastly, 6 construction ages for semi-rigid slabs (<1919; 1919-1945; 1946-1961; 1962-1971; 1972-1981; 1982-1991), and 7 ages for rigid slabs (i.e., all ages except <1919) can be considered.

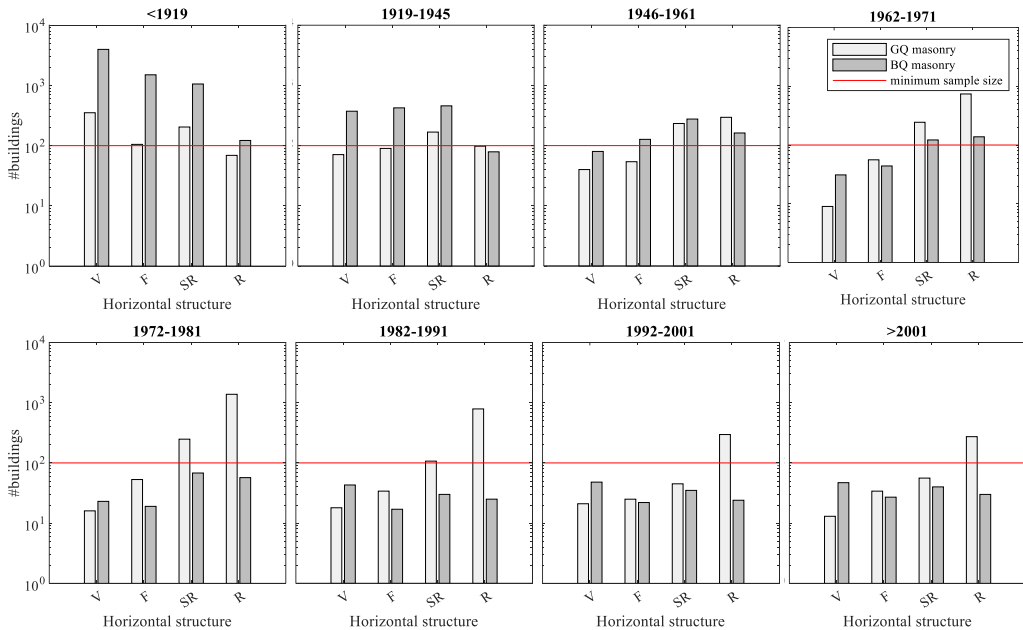


Figure 51. Number of as-built buildings with GQ and BQ, given the horizontal structural type and the construction age (*damaged* database).

Therefore, Figure 52 reports the trend of mean damage for all these 27 as-built classes: namely, the mean damage is provided for each construction age as a function of horizontal structural types (marked in a different color) and quality layouts of masonry (identified through a different symbol).

Generally speaking vulnerability (*i*) decreases, increasing the construction age (highlighting the improvement in construction material, normative prescriptions and building's techniques), whatever the horizontal structural types are considered, (*ii*) decreases, increasing the slab's stiffness, i.e. going from vaults to rigid slab (except for masonry buildings with semi-rigid slabs built before 1919, where a dubious value is reported) and then (*iii*) a very similar trend is observed between buildings with vaults and flexible slabs and between buildings with semi-rigid and rigid slabs.

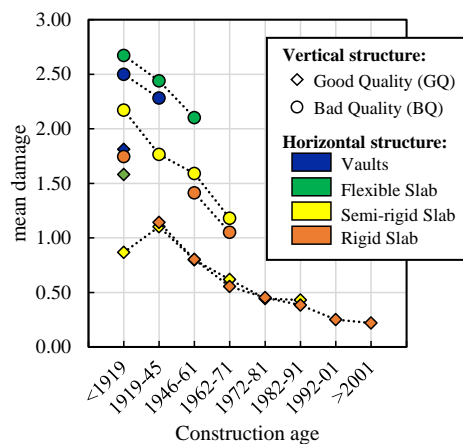


Figure 52. Mean damage for as-built classes

In addition, it can be noted that (*iv*) mean damage values of BQ masonry buildings result systematically higher than the corresponding values of GQ buildings given the horizontal structural type and the construction age.

It should be noted that a mean damage going from 1.05 to 2.7 is observed for bad quality masonry buildings; as matter of fact, construction age and horizontal structure (albeit with different weights) could cause a variation of mean damage up to 60% in BQ masonry buildings. For GQ masonry buildings the mean damage varies between 0.2 and 1.8, resulting in a maximum variation of about 90%. Actually, if the construction age is limited up to 1971 (i.e., where also BQ typologies are available), mean damage of GQ masonry buildings belongs to 0.55-1.8 range and, thus, the maximum variation is about 70%.

6.3.2 Mean damage for retrofitted classes

In Chapter 5, after introducing the building's taxonomy based on structural typology, construction age and presence of retrofit, only BQ buildings built before 1919 have been considered as retrofitted classes, being the sample size consistent with the chosen threshold (100 buildings).

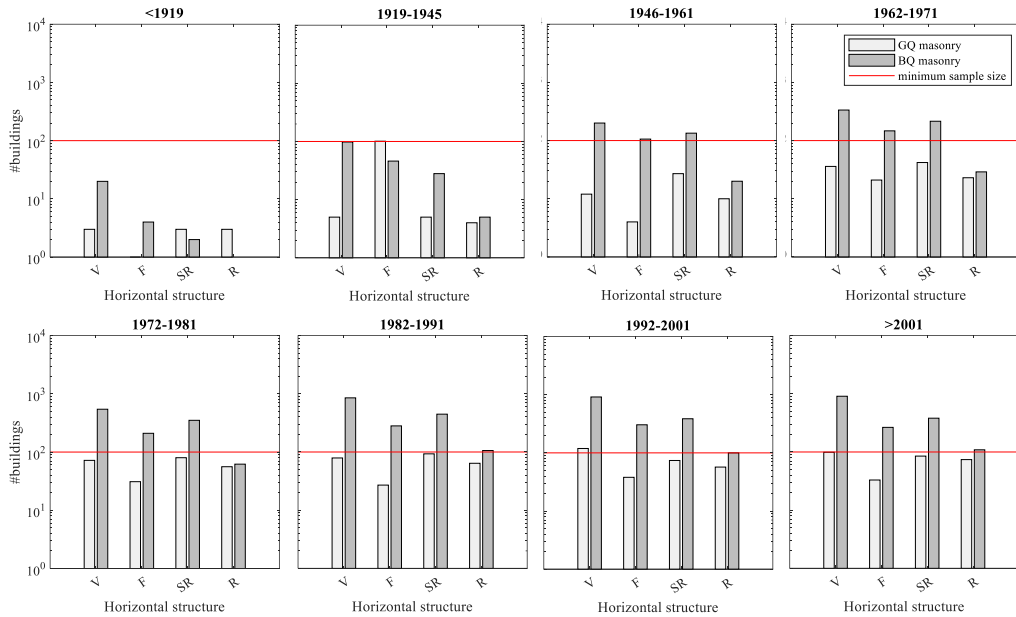


Figure 53. Number of retrofitted buildings with GQ and BQ built before 1919, given the horizontal structural type and the retrofit age (*damaged* database).

In Figure 53 the number of *damaged* buildings built before 1919 and then retrofitted (the period of retrofit is reported above each plot) is reported as a function of the horizontal structural typology and the retrofit age. In the first two retrofit age, no class is quite populated. Conversely, starting from 1946-1961 time span up to the last one, the mean damage of BQ buildings with vaults, flexible and semi-rigid slabs can be investigated (resulting in 18 classes = 3 structural typologies x 6 retrofit ages). Lastly, also the behaviour of BQ buildings with rigid slabs can be analysed, considering the last three retrofit ages (from 1982-1991 to >2001).

Thus, the influence of structural interventions for masonry buildings is analysed, starting from such 21 retrofitted classes constructed before 1919, as shown in Figure 54, which reports the mean damage, given the horizontal structural type, as a function of the period of retrofit. Furthermore, mean damage values for non-retrofitted masonry buildings constructed before 1919 are also reported in figure, assumed as reference for comparison.

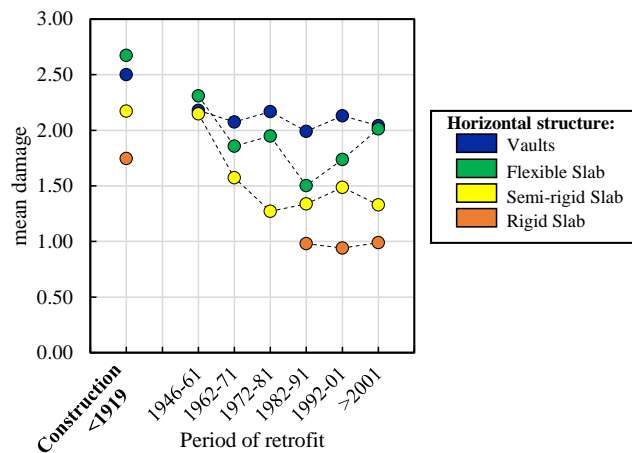


Figure 54. Mean damage: influence of structural interventions for masonry buildings constructed before 1919, given the period of retrofit, for each horizontal structural type.

The reduction of mean damage due to the presence of structural interventions agrees with previous studies for the same area (Indirli et al. 2013; Rossetto et al., 2011; Azzaro et al., 2011; D'Ayala and Paganoni 2011; Zucconi et al., 2018; D'Amato et al., 2020). It can be noted an overall reduction of mean damage for retrofitted buildings, due to the structural interventions, compared to the values of those non-retrofitted and constructed in the same years (<1919), for each horizontal structural type. This reduction increases increasing the slab's stiffness (i.e., going to vaults to rigid slabs). A constant decrease in μ_D of about 17% is observed in case of retrofitted masonry buildings with vaults, regardless the period of retrofit; similarly, a constant decrease in μ_D of about 40% is observed in case of buildings with rigid slabs. Lastly, in the case of flexible and semi-rigid

slabs, a decreasing trend is observed until 1971, after which an irregular trend is observed; the overall reduction is, on average, 31% and 34%, respectively.

Moreover, also for retrofitted masonry buildings the same hierarchy, already noted for those as-built, in terms of mean damage with the horizontal structural type is observed, except for vaults and flexible slabs, whose trends exactly present an inverted hierarchy.

It has to worth noting that some irregular trends are expected in Figure 54, since each subset could contain different kinds of interventions, which influence cannot be precisely isolated due to the achieved level of knowledge.

As shown in Chapter 5 (Table 17 and Table 18), retrofitted masonry buildings constructed between 1919-1945 and between 1946-1961 provide poorly populated classes, when the taxonomy based on structural type and retrofit age is applied. Therefore, such evaluation cannot be done for all the subsets of period of retrofit, since none of them overcome the assumed sample threshold of 100 buildings. Nonetheless, at least to appreciate the influence of retrofit intervention, mean damage trends can be derived as averaged as a function of wider time intervals (namely, regardless of retrofit age).

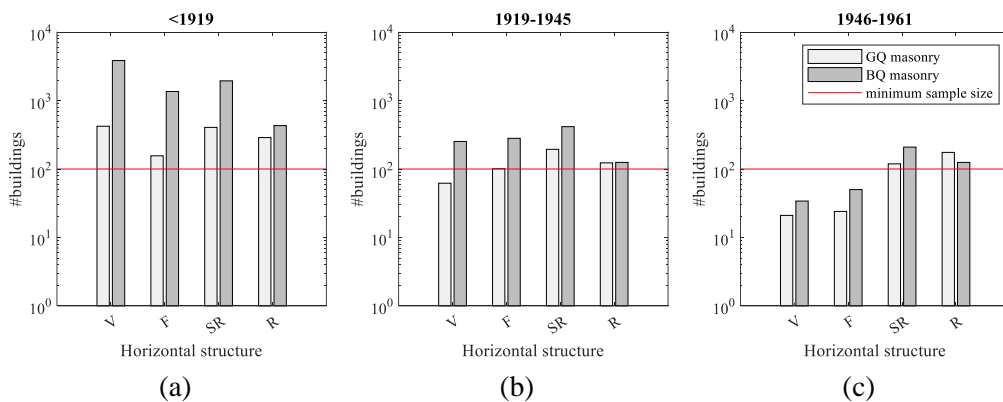


Figure 55. Number of retrofitted buildings with GQ and BQ built before 1919 (a), between 1919 and 1945 (b), between 1946 and 1961 (c), given the horizontal structural type (*damaged database*).

In Figure 55 the number of retrofitted buildings constructed before 1919 (Figure 55a), between 1919 and 1945 (Figure 55b), and between 1946 and 1961

(Figure 55c) is provided regardless of the retrofit age, given the (vertical + horizontal) structural typology. Clearly, all BQ classes built before 1919 are populated by at least 100 buildings. Moreover, the same result is for GQ buildings (Figure 55a). Among retrofitted buildings constructed between 1919 and 1945, all BQ classes and GQ ones with semi-rigid and rigid slabs are quite populated (Figure 55b). Lastly, only classes with semi-rigid and rigid slabs can be considered among retrofitted buildings constructed between 1946 and 1961 (Figure 55c). Thus, mean damage regardless of the retrofit age could be derived for 18 retrofitted classes (i.e., 8 constructed before 1919; 6 between 1919 and 1945; 4 between 1946 and 1961).

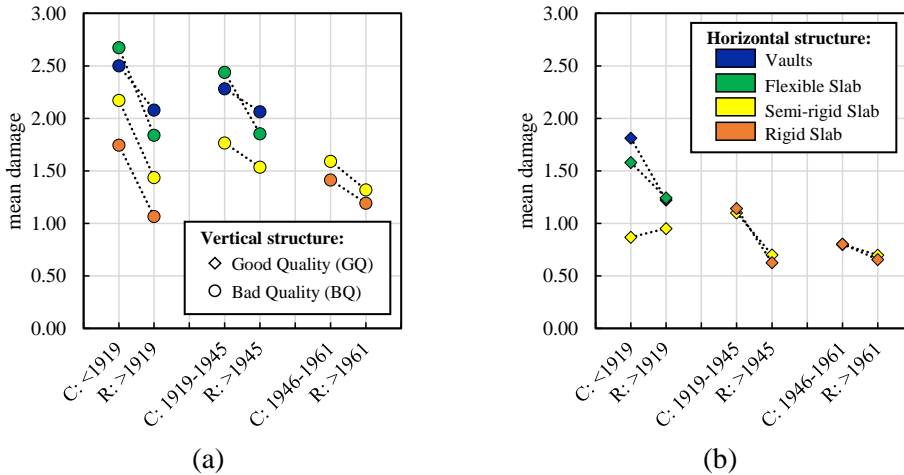


Figure 56. Mean damage: influence of structural interventions for masonry buildings constructed in (<1919), (1919-1945), (1946-1961) periods, given the horizontal structural type for BQ (a) and GQ (b) typologies.

Figure 56 reports mean damage trends for non-retrofitted classes constructed <1919, between 1919 and 1945, between 1946 and 1961, besides those of constructed in the same years and retrofitted thereafter. Thus, for a given structural type, firstly the mean damage of non-retrofitted buildings is provided and then also the corresponding value of retrofitted buildings. In such way, influence of retrofit on damage attitude of a given class is analysed. It should be noted that the comparison between presence and absence of retrofit interventions

has been done considering 16 classes (i.e., 7 constructed before 1919; 5 between 1919 and 1945; 4 between 1946 and 1961), despite 18 retrofitted classes could be analysed according from Figure 55. As matter of fact, mean damage of non-retrofitted classes GQ-R-PRE19 and BQ-R-1919-1945 is not available, being such classes poorly populated (i.e., sample with less than 100 buildings). The influence of structural intervention on BQ masonry buildings is provided by Figure 56(a): a clear effectiveness is evident in any cases. An overall reduction of mean damage in case of retrofit ranging between 10-17% as a function of period of construction is observed for buildings with vaults and between 24-31% for flexible slabs. Contrarily, for buildings with semi-rigid and rigid slabs a substantial reduction of the effectiveness of retrofit intervention can be observed increasing the construction age (from 34-39% for those built before 1919 to 16-17% for those constructed between 1946 and 1961). Also, for GQ buildings, structural interventions affect the mean damage, leading to a general decrease of damage attitude, except for GQ-SR-PRE19 class (as highlighted in Figure 52 for such class, the obtained value is quite dubious). Discarding such latter result, one can observe that structural interventions allow a reduction of 33% and 21% respectively for buildings with vaults and flexible slabs built before 1919. Moreover, a very similar behaviour is for retrofitted buildings with rigid and semi-rigid slabs, when built in 1919-1945 and 1946-1961 periods.

Obviously, the trends reported in Figure 54, Figure 55 and Figure 56 do not explicitly consider the influence of intensity measure to which the building was subject. To this aim, vulnerability curves, considering the above defined minimum sample size of 100 masonry buildings to ensure their reliability, are introduced in the following Section.

6.4 VULNERABILITY CURVES

In the previous Section, mean damage has been evaluated for each considered building class, deriving vulnerability trends as a function of several building's features such as presence of retrofit interventions, masonry quality, horizontal structure, construction age, seismic classification and, if any, retrofit age.

As above highlighted, mean damage does not take into account the seismic intensity measure (IM) value to which the building has been subjected. Thus, the obtained trends could be affected by IM distributions. To investigate the damage attitude varying the IM value, in the present Section vulnerability curves have been derived, providing vulnerability trends by means of mean damage given IM values. So, vulnerability curve for a given building class is the relationship between IM values (to which buildings belonging to the considered class have been subjected) and the corresponding damage measure values (in terms of mean damage given IM value). To perform such analysis, the entire domain of PGA has been categorized in several PGA bins. Hence, for each considered building's class, a set of values of mean damage (i.e., one per each PGA bin) can be evaluated, calculating the weighted average of the damage distribution in a given range of the chosen intensity measure, similarly to existing studies (e.g., Dolce et al., 2003; Lagomarsino and Giovinazzi, 2006; Rota and Rosti., 2017; Del Gaudio et al., 2021; Scala et al., 2022) and according to following equation:

$$\mu_{D,j} = \frac{\sum_{i=0}^5 N_{B,j}(DS=ds_i) i}{N_{B,j}} \quad (3)$$

Note that $N_{B,j}(DS=ds_i)$ is the number of buildings, belonging to a given class, within j^{th} IM value and with a damage level equal to ds_i ; whereas, $N_{B,j}$ is the total number of buildings, within j^{th} IM value, belonging to the same class. In such way, several data pairs $(IM_j; \mu_{D,j})$ are obtained for each building class, resulting in a vulnerability curve thanks to a weighted fitting procedure (Del Gaudio et al., 2021; Scala et al., 2022), assuming the lognormal distribution with a free logarithmic standard deviation as functional form.

Therefore, in the following paragraphs, first the adopted intensity measure has been defined introducing the ShakeMap in terms of PGA provided by Italian National Institute of Geophysics and Volcanology (*Istituto Nazionale di Geofisica e Vulcanologia*, INGV), and the adopted regression procedure (including the fitting method and the chosen function form) has been explained.

Then, vulnerability curves have been derived for both as-built and retrofitted classes belonging to defined building's taxonomy. Lastly, so-obtained vulnerability trends in terms of mean damage and vulnerability curves have been compared with those in terms of median PGA, assuming a constant logarithmic standard deviation.

6.4.1 Intensity measure

The 6th of April 2009, at 3:32 a.m., an earthquake of magnitude 5.9 on the Richter scale (Mw 6.3) hit the city of L'Aquila and some tens of surrounding municipalities. The seismic event was recorded by the digital strong-motion stations operated by the Italian Strong Motion Network managed by the Italian Department of Civil Protection (DPC) and by the broadband stations of the Italian National Institute of Geophysics and Volcanology (*Istituto Nazionale di Geofisica e Vulcanologia*, INGV).

These records allowed to derive maps of the seismic shaking in terms of peak ground motion parameters (such as peak ground acceleration or spectral pseudo-acceleration for different periods of vibration). Thus, just after the earthquake, the INGV published the ShakeMaps of the event, derived by means the procedure of Michelini et al., 2008. Lately, a new version of the ShakeMaps was obtained using the procedure of Michelini et al., 2020.

In Figure 57, the ShakeMap of the April 6th 2009 event are provided in terms of peak ground acceleration (PGA), according to the newer procedure. This have been generated through the software package ShakeMap, originally developed by the U.S. Geological Survey Earthquake Hazards Program (Worden et al., 2017).

Basically, the map is the result of an interpolation performed between real measurements and values predict by means Ground Motion Prediction Equations (GMPEs). Clearly, the real measurements are provided in the station locations by the Italian Strong Motion Network (namely, the RAN) and by the station network of the INGV. On the other hand, the GMPEs are used to derive the acceleration value for "phantom stations", chosen as a function of the magnitude of the event and the region of interest. The map obtained by means of the

mentioned interpolation represents the ground shaking at the bedrock. To account for site effects, the obtained map is scaled up, using a geological map. This latter is typically calibrated as a function of the average velocity of shear wave in the top 30 mt of the subsurface profile (VS₃₀).

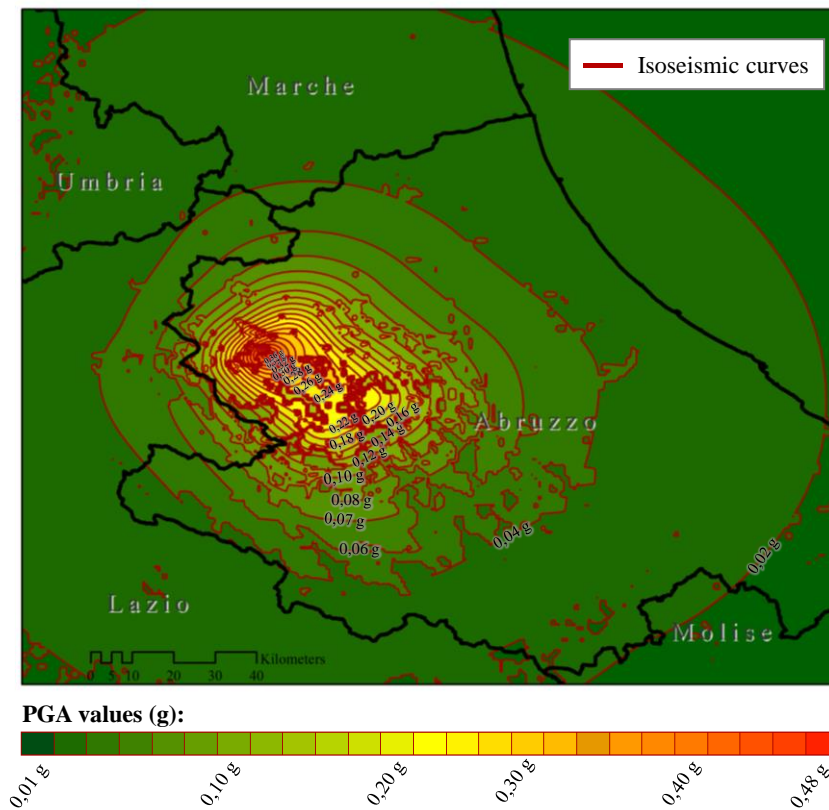


Figure 57. ShakeMap in terms of Peak Ground Acceleration (PGA) derived by means of procedure proposed by in Michelini et al. 2020.

As matter of fact, the most recent version of ShakeMaps is the natural evolution of the older procedure. In fact, the main differences between the two versions are about the GMPEs and VS₃₀ map.

In the procedure of Michelini et al., 2020, recently developed ground-motion models and an updated map of VS₃₀ for the local site effects have been used. In this work, the ShakeMap in terms of PGA (Figure 57) has been adopted as

intensity measure (IM), deriving the vulnerability and fragility curves. Note that the isoseismic curves, ranging from 0.01 to 0.48g, define isoseismic areas. So, each area corresponds to a PGA bin with width equal to 0.02 g, except the first and fifth ones with width equal to 0.01 g.

Moreover, it should be noted that survey form used after the 2009 earthquake provide the coordinates (longitude and latitude) of each inspected building. Thus, a PGA value has been assigned to each building belonging to *damaged* database. Conversely, *undamaged* buildings are not geo-referenced (deriving from the Census data) and, so their position (i.e., longitude and latitude) is not known. In this case, PGA value is evaluated in the municipality's centroid, applying them to all buildings therein located, according to several previous studies (Rosti et al., 2020b; Rosti et al., 2020c; Del Gaudio et al, 2021).

6.4.2 Functional form and fitting procedure

To obtain the relation between damage and seismic intensity measure, several different approaches have been adopted in literature. Basically, starting from the obtained data pairs (IM_j ; $\mu_{D,j}$) for a given building class, two main issues have to be addressed: namely, the functional form of the curve and the type of regression model.

According to Rossetto et al., 2013, the most common and widely used functional forms in fragility evaluations are the cumulative lognormal, normal and the exponential distributions, in that order. One of the reasons why cumulative lognormal distribution (e.g., D'Amato et al., 2020; Rosti et al., 2020; Del Gaudio et al., 2021; Scala et al., 2022) is the most used is about its x-axis, defined in $(0, +\infty)$ range, as well as almost all the ground motion intensity measures. In fact, the normal cumulative distribution (e.g., Spence et al, 1992; Orsini, 1999; Karababa and Pomonis, 2010) is mostly preferred when the adopted intensity measure ranges between $(-\infty, +\infty)$, being defined in the same range. Conversely, exponential function (e.g., Rossetto and Elnshai, 2003; Amiri et al., 2007; Rosti et al., 2020) is unconstrained both in x- and y-axes.

In the present Thesis, the cumulative lognormal distribution has been selected as functional form for fitting the observed damage data points, because the

adopted intensity measure (i.e., PGA) is defined only in the set of positive reals number. Moreover, as highlighted in Rosti et al., 2020 where both lognormal and exponential distributions have been used to derive vulnerability curves, higher efficiency (Nash and Sutcliffe, 1970) in reproducing the observed data is provided by the first one function.

The lognormal parameters that better fit the observed data typically are estimated by minimising the objective function, or also by its maximisation (Rossetto et al., 2013). The merit function in the minimisation approach is the sum of least squares errors, calculated as difference between observed and predicted values.

$$\operatorname{argmin} \left[\sum_j \varepsilon_j^2 \right] = \operatorname{argmin} \left[\sum_j w_j \left(y_j - f(\operatorname{IM}_j, x) \right)^2 \right] \quad (4)$$

In Equation (4), y_j and $f(\operatorname{IM}_j, x)$ are respectively the observed and the predicted values, given the j^{th} IM value. Thus, the difference between such values is the error ε_j . In this approach, the sum of all squared errors (ε_j) has to be minimized to find the x parameter of the selected functional form, f .

Moreover, w_j is the weight of each data point when the adopted procedure is a weighted regression model. Such approach is widely used in the literature (Rota et al., 2008; Rosti et al., 2020; Del Gaudio et al., 2021; Scala et al., 2022). Alternatively, the maximization approach is used (e.g., Ioannou et al., 2012; Del Gaudio et al., 2019; Charvet et al. 2014; Del Gaudio et al., 2020), maximizing the likelihood objective function.

In this work, to derive vulnerability curves, the LSE (*Least Square Estimation*) technique has been used, assuming a lognormal cumulative function as curve's shape. The LSE technique allows to minimize the sum of the squares of the distance between the observed mean damages and the predicted ones, according to Equation (4). This latter become the following equation, considering the involved variables:

$$\operatorname{argmin}_{\mu, \beta} \left[\sum_j N_{B,j} \left(\frac{\mu_{D,j}}{5} - p(\text{PGA}_j, \mu, \beta) \right)^2 \right] \quad (5)$$

In Equation (5), the functional form p is the cumulative log-normal distribution, completely described by means two parameters: the logarithmic mean μ (or, similarly, the median $\theta = e^\mu$) and logarithmic standard deviation β . Lastly, $N_{B,j}$ is the weight of the fitting procedure, to mitigate the potential inhomogeneity in the amount of buildings among the different PGA's bins. In this way, the fitting procedure is greater affected by $\mu_{D,j}$ values related to the most populated PGA bins, assumed as the most reliable.

Surely, the reliability of a given IM bin can be guaranteed by means other weights or/and approaches. In Rota et al., 2008, the inverse of standard deviation estimated through a bootstrap technique has been considered as weight of the fitting procedure. In some works (Karababa and Pomonis, 2010; Spence et al., 1992), a minimum number of buildings belonging to each IM bin has been defined, discarding all values related to less populated bins.

In other studies (Del Gaudio et al., 2019), IM bins with variable width has been considered (instead of fixed width), in order to obtain a similar number of buildings in each bin.

6.4.3 Vulnerability curves for as-built classes

In Figure 58 and Figure 59, vulnerability curves for all available as-built building classes of considered taxonomy have been provided.

In particular, Figure 58 show vulnerability trends for buildings constructed in the first four time periods (i.e., <1919; 1919-1945; 1945-1961; 1962-1971), whereas Figure 59 is related to the remaining ones (i.e., 1972-1981; 1982-1991; 1992-2001; >2001).

Each row of plots is referred to a different construction period, whereas each column is about a different horizontal structure (i.e., vaults, flexible, semi-rigid, and rigid slabs). Lastly, the vertical structure is marked by different line color (i.e., black for GQ and grey for BQ).

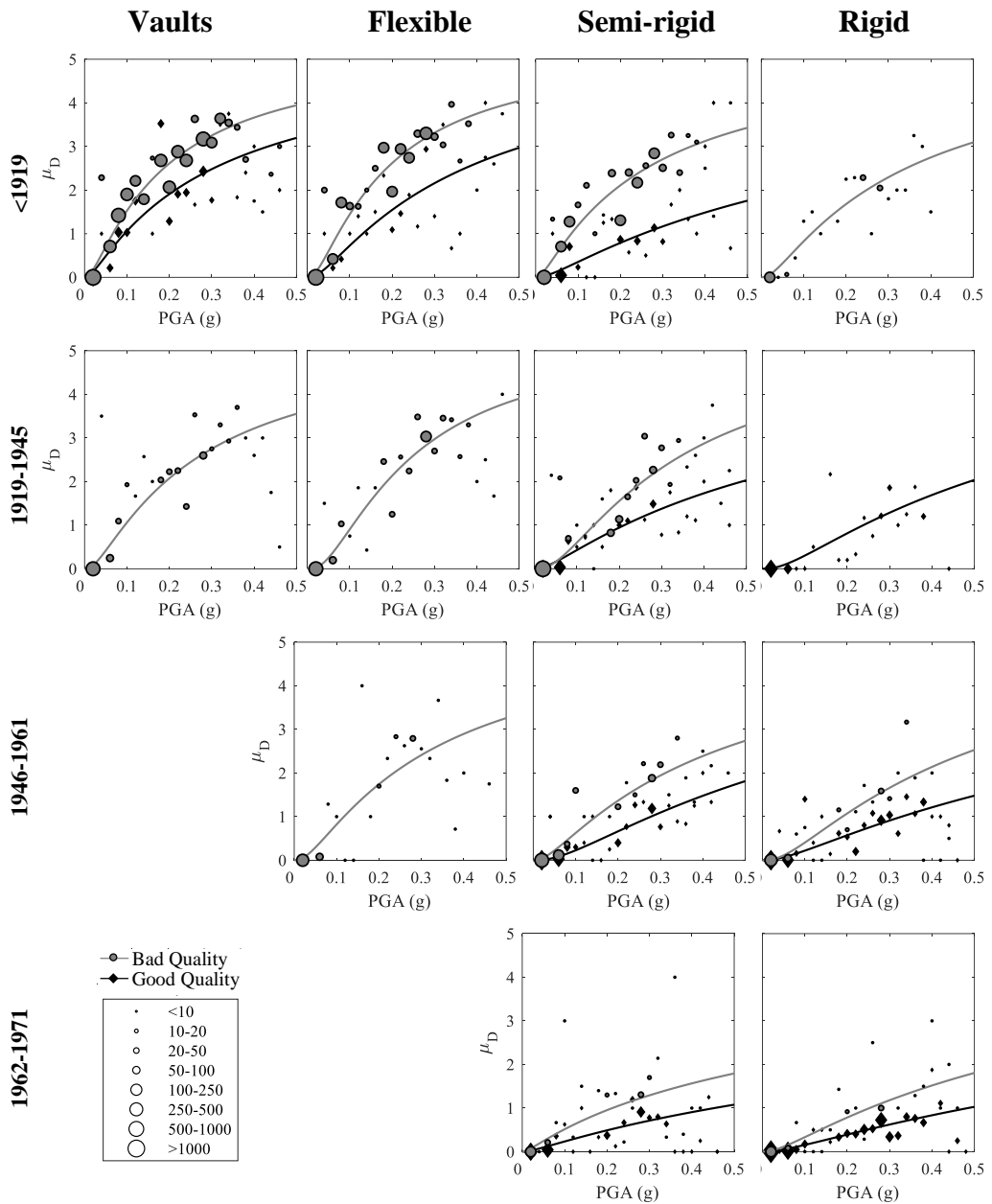


Figure 58. Vulnerability curves for as-built masonry buildings built up to 1962-1971 timespan, as a function of construction age and structural types.

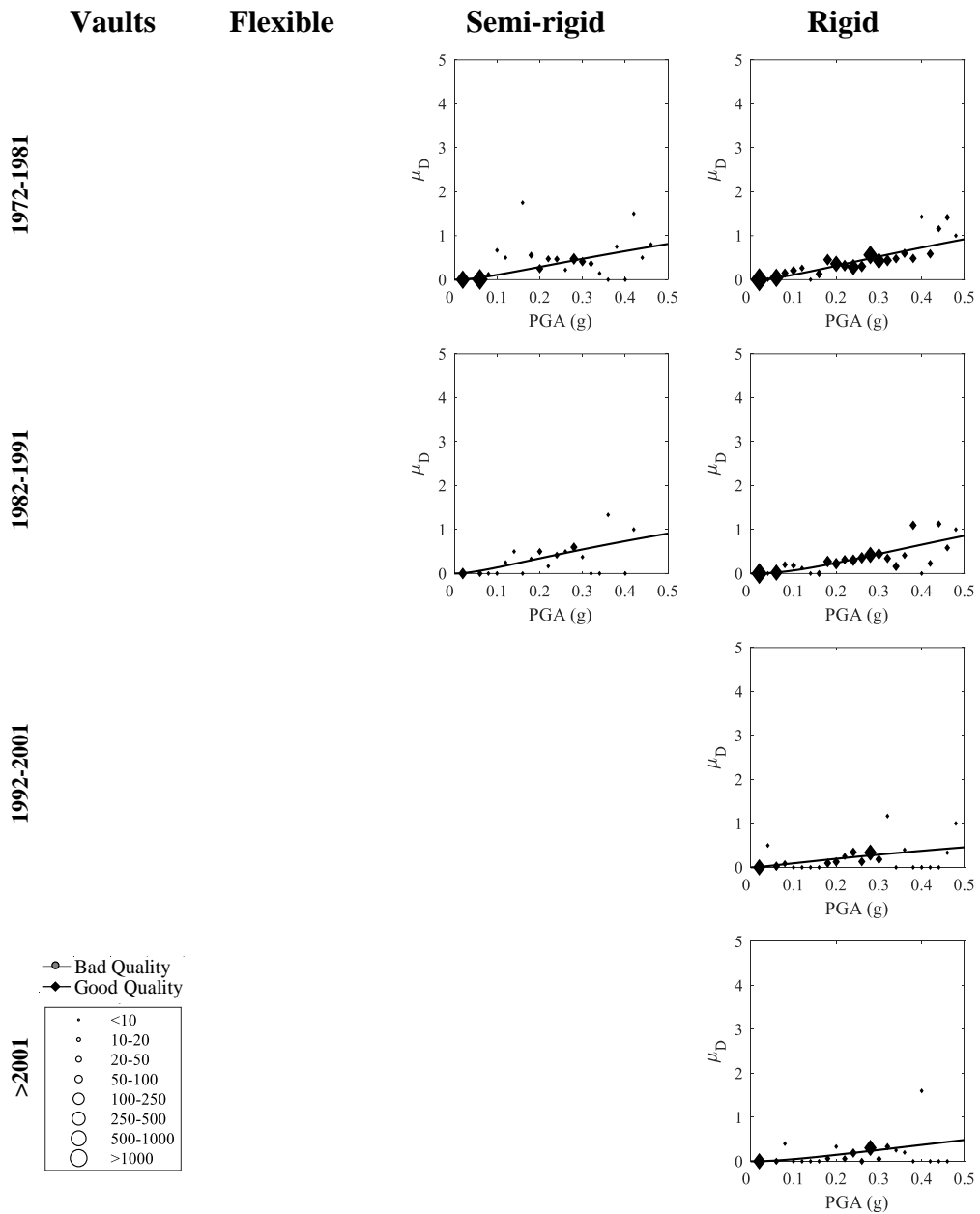


Figure 59. Vulnerability curves for as-built masonry buildings built starting from 1972-1981 timespan, as a function of construction age and structural types.

It has to be noted that observed mean damage data ($\mu_{D,j}$) for each class, employed for the minimization procedure of Eq.5, are reported in figure with grey rhombus (GQ) and black circles (BQ), which area represent the number of buildings in that PGA bin ($N_{B,j}$).

So-represented vulnerability curves allow identifying several damage trends as a function of considered building's features. In particular, it can be stated that:

- BQ masonry buildings result systematically less vulnerable of GQ buildings given the horizontal structural type and the construction age (Figure 58). The vulnerability decreases with the quality layout of masonry, i.e. going from BQ to GQ buildings, given the construction age and the horizontal structure. In fact, several studies (Carocci and Lagomarsino 2009; Augenti and Parisi 2010; D'Ayala and Paganoni 2011; Rossetto et al. 2011; Zucconi et al., 2018; Rosti et al., 2018) emphasized the fact that the buildings with poor quality masonry and/or lacking construction details (lack of connection between masonry leaves) undergo to the most severe damage.
- The vulnerability decreases with the slab's stiffness, i.e. going from vaults to rigid slabs, given the construction age, indistinctly for BQ and GQ masonry buildings. In particular, as shown in Figure 52 in terms of mean damage, also in terms of vulnerability curves a very similar vulnerability can be observed between buildings equipped with vaults and flexible slabs and between buildings equipped with semi-rigid and rigid slabs, regardless the quality layout and the construction age. Such result can be better analysed in Figure 60 and Figure 61, where vulnerability curves with different horizontal structures have been compared, given the construction age for GQ (Figure 60) and BQ (Figure 61) buildings.

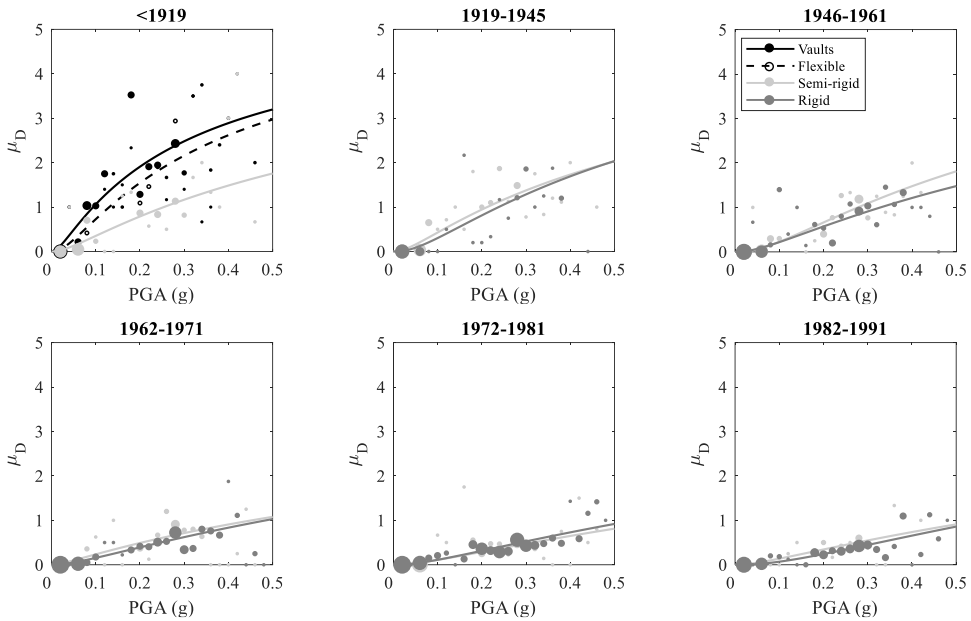


Figure 60. Vulnerability curves for GQ as-built typologies. Comparison in terms of horizontal structure, given the construction age.

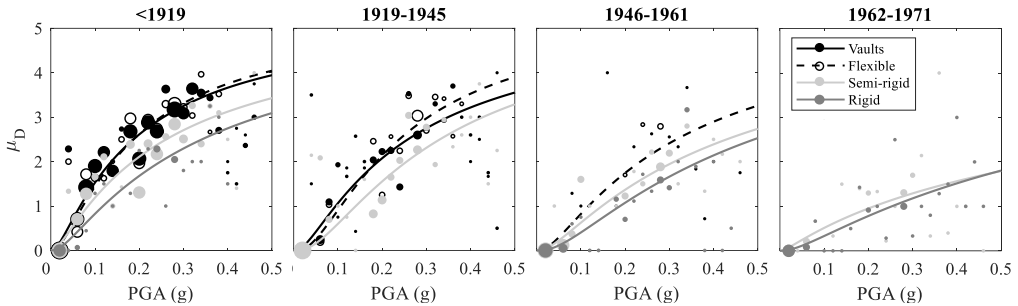


Figure 61. Vulnerability curves for BQ as-built typologies. Comparison in terms of horizontal structure, given the construction age.

- The vulnerability decreases increasing the construction age, given the (vertical and horizontal) structural typology. This effect has been already highlighted only in few studies (namely, in Dolce and Goretti, 2015; Del Gaudio et al., 2021) and can be ascribed to the improvements in the building construction and enhancement in the quality of materials, together with the continuous enactment of increasingly stringent code prescriptions. Such

result can be better analysed in Figure 62, where vulnerability curves with different construction ages have been compared, given the (vertical + horizontal) structural typology.

A clear hierarchy in terms of construction age is shown by each structural type, except by GQ-SR (i.e., masonry buildings with regular layout and/or good quality masonry and semi-rigid slabs). This latter typology, as seen also in terms of mean damage (see Figure 52), seems to be more vulnerable if built before 1919, respect to the following age (1919-1945). Note that for GQ-R class, curves related to 1992-2001 and >2001 periods are overlapped, meaning a common seismic behaviour starting from 1992.

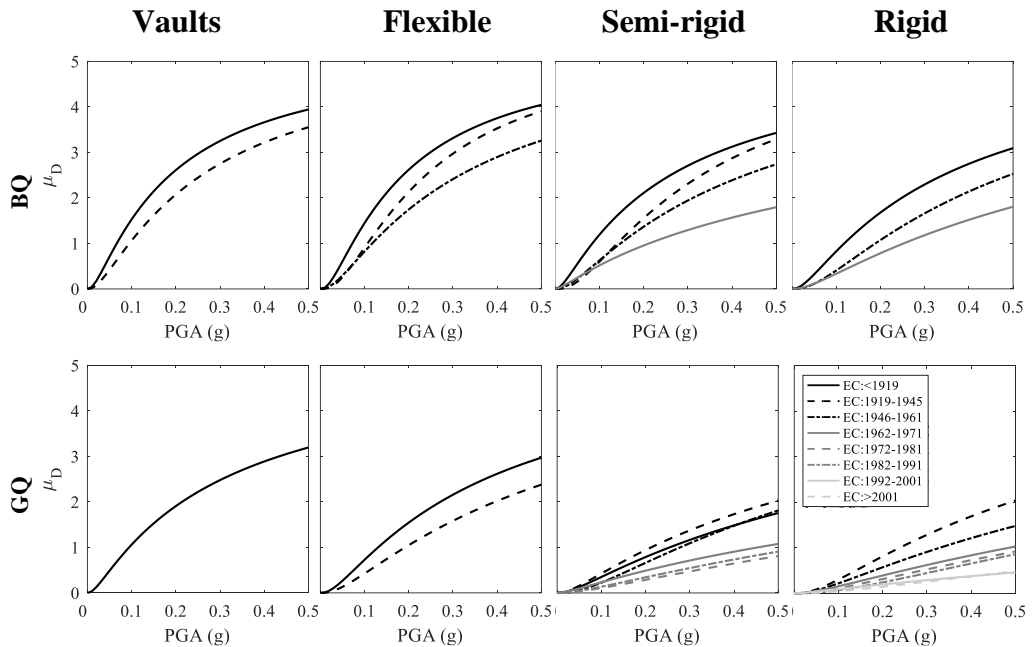


Figure 62. Vulnerability curves for as-built typologies. Comparison in terms of construction age (*EC*), given the structural type.

Moreover, Table 20 and Table 21 provide the corresponding lognormal parameters, namely the median θ and the logarithmic standard deviation β , distinguishing between BQ (Table 20) and GQ (Table 21) masonry types.

Table 20. Log-normal parameters for as-built buildings with bad quality (BQ) texture as a function of horizontal structural typology and construction age.

Construction age	Vaults		Flexible slab		Semi-rigid slab		Rigid slab	
	θ	β	θ	β	θ	β	θ	β
<1919	0.19	1.23	0.19	1.13	0.26	1.34	0.34	1.26
1919-1945	0.26	1.19	0.24	0.95	0.33	1.02	-	-
1946-1961	-	-	0.32	1.18	0.43	1.27	0.49	1.14
1962-1971	-	-	-	-	0.95	1.78	0.82	1.40

Table 21. Log-normal parameters for as-built buildings with good quality (GQ) texture as a function of horizontal structural typology and construction age.

Construction age	Vaults		Flexible slab		Semi-rigid slab		Rigid slab	
	θ	β	θ	β	θ	β	θ	β
<1919	0.30	1.39	0.37	1.24	0.88	1.47		
1919-1945	-	-	-	-	0.70	1.42	0.67	1.22
1946-1961	-	-	-	-	0.76	1.20	1.04	1.37
1962-1971	-	-	-	-	2.08	1.81	1.77	1.54
1972-1981	-	-	-	-	2.32	1.56	1.85	1.45
1982-1991	-	-	-	-	2.12	1.59	1.68	1.28
1992-2001	-	-	-	-	-	-	8.46	2.13
>2001	-	-	-	-	-	-	3.71	1.54

It should be noted that no constraint on β values has been imposed (such as a common value for several classes). Thus, the reported values are directly the result of minimization technique of Eq.5, namely the logarithmic standard deviation that, together with the corresponding median value, better fits the observed damage data.

However, at the end of the present Chapter, also the assumption of constant β has been analysed in order to compare the median PGAs of available building classes.

6.4.4 Vulnerability curves for retrofitted classes

The influence of structural interventions on vulnerability curves of masonry buildings with bad quality layout constructed before 1919 is shown in Figure 63. Vulnerability curves are reported, for each horizontal structural type, as a function of the corresponding period of retrofit (mostly, 1945-1961; 1962-1971, 1972-1981; 1982-1991; 1992-2001; >2001).

Note that for buildings with rigid slab, vulnerability curves have been derived only with the reference to the last three periods of retrofit (i.e., 1982-1991; 1992-2001; >2001), because of the poor number of BQ-R buildings retrofitted in the previous ages. Furthermore, vulnerability curves for non-retrofitted masonry buildings constructed before 1919 are also reported in figure, assumed as reference for comparison.

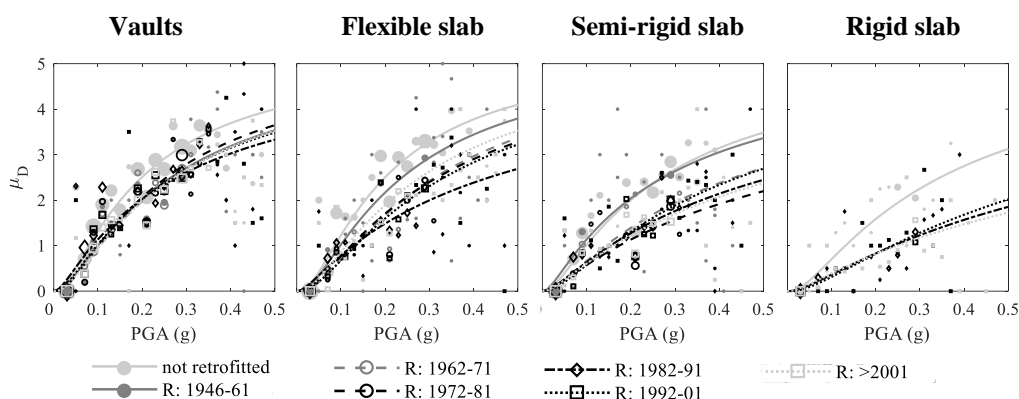


Figure 63. Vulnerability curves for BQ typologies built before 1919. Comparison in terms of presence/absence of retrofit interventions, given the structural type.

A clear effectiveness of structural interventions is shown, demonstrated by the lower vulnerability of retrofitted masonry buildings compared to those as-built, regardless of the period of retrofit.

In particular, with reference to the results of Figure 63, it should be noted that:

- masonry buildings with vaults show a similar vulnerability behaviour for all periods of retrofit;
- masonry buildings with flexible slabs show a decreasing vulnerability with the period of retrofit until 1991. Surprisingly the vulnerability of buildings retrofitted thereafter (in 1991-2001 period and especially after 2001) results quite similar to those retrofitted during the previous periods;
- the masonry buildings with semi-rigid slabs retrofitted in 1946-1961 period show almost the same vulnerability of not retrofitted ones, being the corresponding curves overlapped. Quite similar vulnerability is shown by buildings retrofitted thereafter, regardless to the retrofit age.

- the masonry buildings with rigid slabs show a similar vulnerability behaviour for the three considered periods of retrofit.

The decreasing vulnerability of retrofitted masonry buildings with the period of retrofit is probably due to the improvement in construction practice and to an increasing attention to anchorage details, which make the difference between a more effective intervention or not (Indirli et al. 2013; Rossetto et al., 2011; Azzaro et al., 2011). However, such decreasing trend is not common to all considered structural typologies: in fact, for some of these (i.e., BQ buildings with vaults or rigid slabs), retrofit age seems to have no great influence on damage attitude.

It should be noted that based on the available data, it is not possible to know how type of retrofit intervention has been carried out on. It is quite likely that considered retrofitted classes include buildings subjected to different structural interventions, leading to uncertainties in the present analysis. To overcome such issue, vulnerability curve (or equivalently mean damage) should be derived considering buildings subjected to the same type of intervention. In this way, the comparison between retrofitted classes could allow evaluating the influence of a given retrofit type on damage attitude of a given structural typology, and its evolution over the time.

As explained in Chapter 5, although Section 3 of AeDES form should provide information on type of interventions (among injections, reinforced coating, or other/unidentified strengthening), in almost all cases this information was not filled by surveyor after L'Aquila earthquake (probably because of the emergency condition). However, Figure 63 shows how retrofit interventions performed over the years have improved the seismic response of a given the structural typology, regardless to the type of intervention.

In Table 22, the lognormal parameters (namely, the median PGA, θ , and the logarithmic standard deviation, β) related to curves of Figure 63 have been reported.

Table 22. Lognormal parameters of vulnerability curves for BQ retrofitted masonry buildings built before 1919 as a function of horizontal structural typology and period of retrofit.

Period of retrofit	Vaults		Flexible slab		Semi-rigid slab		Rigid slab	
	θ	β	θ	β	θ	β	θ	β
1946-1961	0.27	1.16	0.24	1.05	0.27	1.35	-	-
1962-1971	0.27	1.13	0.31	1.04	0.43	1.32	-	-
1972-1981	0.26	1.10	0.32	1.13	0.63	1.53	-	-
1982-1991	0.28	1.37	0.44	1.46	0.52	1.45	0.80	1.43
1992-2001	0.27	1.20	0.33	1.09	0.44	1.24	0.68	1.25
>2001	0.27	1.13	0.28	1.08	0.55	1.45	0.94	1.57

Moreover, the influence of structural interventions on seismic behaviour of BQ masonry buildings constructed between 1919-1945 and between 1946-1961, representing the most reliable subset as highlighted in Chapter 5.3, is herein evaluated given the horizontal structural type. Nonetheless, such an evaluation cannot be done for all the subsets of period of retrofit, since none of them overcome the assumed sample threshold of 100 buildings.

Thus, as for mean damage (Figure 56(a)), vulnerability curves are presented as averaged as a function of wider time intervals. Basically, the comparison in terms of vulnerability curves for retrofitted and not retrofitted buildings constructed before 1919 (first row), between 1919 and 1945 (second row), between 1946 and 1961 (third row) is reported in Figure 64, given the horizontal structural type. So, vulnerability curves for retrofitted buildings is herein evaluated merging together damage outcomes for all retrofit periods.

As already shown, the effectiveness of retrofit intervention on buildings constructed before 1919 increases with slab's stiffness, going from a slightly influence in case of vaults to a substantial influence in case of rigid slabs.

For the following construction ages, a general decrease in the retrofit effectiveness can be observed, given the structural type.

Such result is shown also in terms of mean damage in Figure 56(a), where the difference between as-built and retrofitted buildings decreases increasing the construction age.

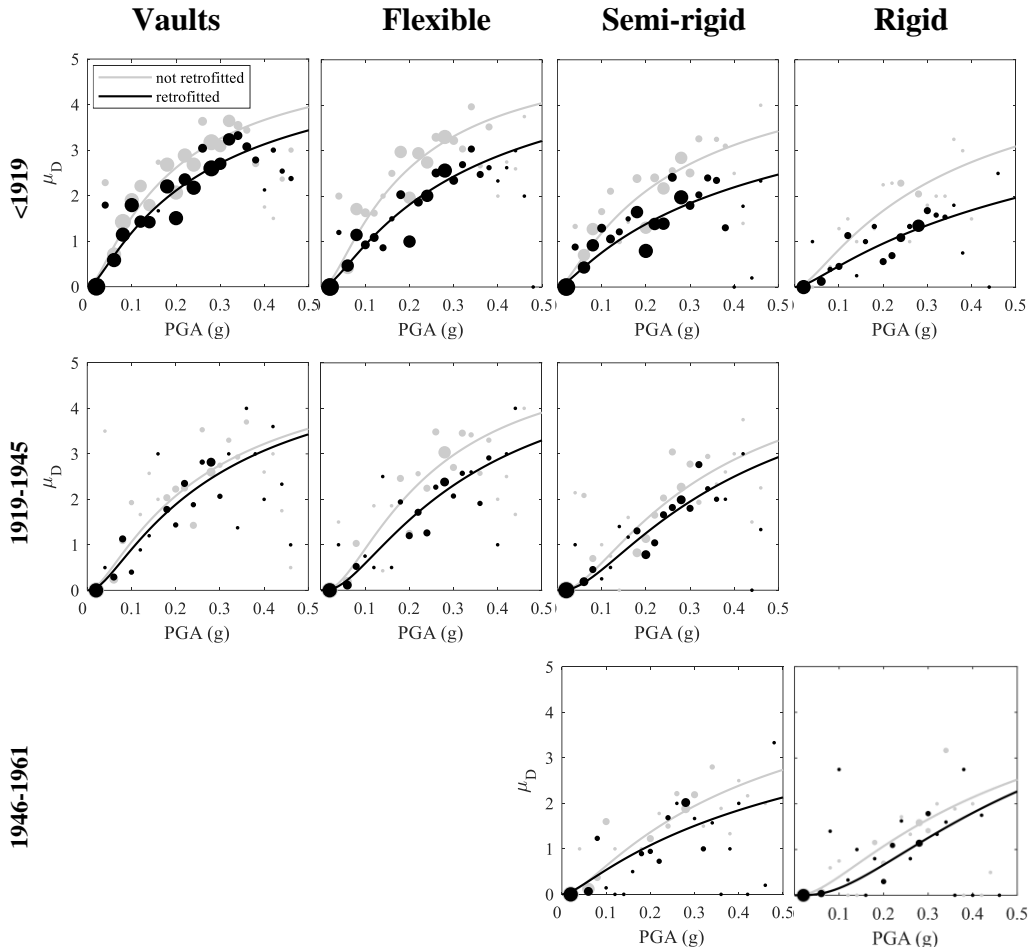


Figure 64. Vulnerability curves for BQ typologies. Comparison in terms of presence/absence of retrofit interventions, given the structural type.

Similar results are obtained also for GQ retrofitted buildings, both in terms of mean damage (Figure 56(b)) and vulnerability curves (Figure 65). Actually, such evaluation has been performed regardless of the kind of structural intervention and of the period of retrofit. Thus, some irregular trends are expected, given the presence of different interventions performed in different time-periods. Definitely, we can observe that the presence of retrofit interventions allows to reduce the damage attitude, especially for the most ancient buildings (i.e., built before 1919).

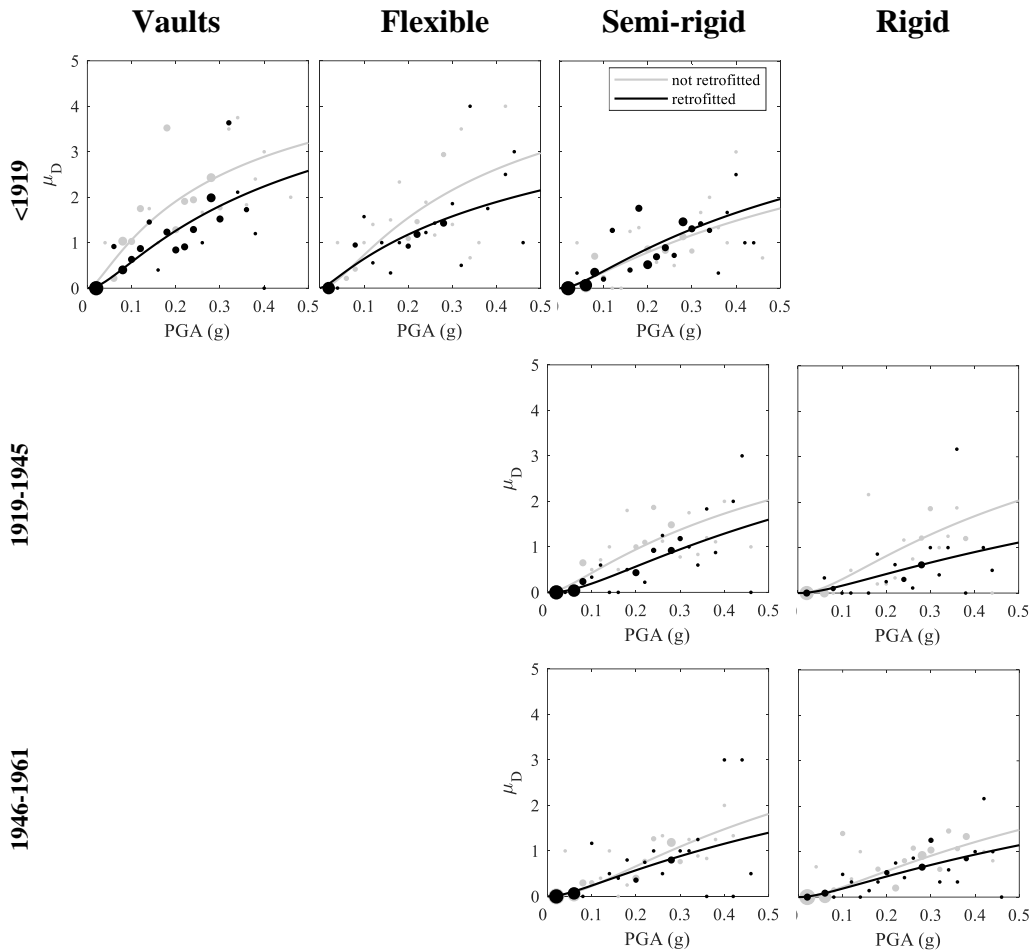


Figure 65. Vulnerability curves for GQ typologies. Comparison in terms of presence/absence of retrofit interventions, given the structural type.

Note that for GQ-S class built before 1919, no differences seem to be between as-built and retrofitted conditions. Actually, such class as highlighted in Figure 52 and Figure 62, shows a damage attitude less than expected one. The similarity between as-built and retrofitted curves could mean that some retrofitted buildings have been defined as not-retrofitted ones during the post-earthquake survey, leading to such underestimation of damage.

Lastly, in Table 23 and Table 24 the lognormal parameters of obtained curves, i.e. the median θ and the logarithmic standard deviation β , are reported

respectively for the curves of Figure 64 and Figure 65 as a function of structural typology and construction period.

Table 23. Lognormal parameters of vulnerability curves for retrofitted BQ masonry buildings as a function of horizontal structural typology and period of construction.

Construction age	Vaults		Flexible slab		Semi-rigid slab		Rigid slab	
	θ	β	θ	β	θ	β	θ	β
<1919	0.26	1.34	0.31	1.28	0.51	1.58	0.76	1.53
1919-1945	0.29	1.15	0.33	1.01	0.40	1.03	-	-
1946-1961	-	-	-	-	0.66	1.53	0.56	0.92

Table 24. Lognormal parameters of vulnerability curves for retrofitted GQ masonry buildings as a function of horizontal structural typology and period of construction.

Construction age	Vaults		Flexible slab		Semi-rigid slab		Rigid slab	
	θ	β	θ	β	θ	β	θ	β
<1919	0.47	1.30	0.67	1.68	0.73	1.38	-	-
1919-1945	-	-	-	-	0.89	1.24	1.56	1.49
1946-1961	-	-	-	-	1.19	1.48	1.59	1.55

6.4.5 Vulnerability trends in terms of median PGA: common β case

In paragraph 6.4.2, the fitting procedure to derive lognormal vulnerability curves from damage data has been explained, applying Equation 5 to each building class separately. As result, the vulnerability curve of single class is described by means of the two lognormal parameters (i.e., the median θ and the logarithmic standard deviation β) that better fit the observed data, without any further constraint. It means that so-obtained median PGA values are not directly comparable, being the β values different for all considered building's classes.

In order to make a direct comparison among the median values obtained for the different classes results necessary to fix the remaining parameters, i.e. the logarithmic standard deviation β . To this aim, the optimization procedure of Equation 5 is performed simultaneously for all classes, regardless of the construction ages, the horizontal structural types and the quality layout of masonry, assuming a common value of β for all classes. In such assumption, if

the number of building classes is N_{class} , the minimization of the scatter between predicted and observed mean values expressed by Equation 5 become:

$$\operatorname{argmin}_{\mu, \beta} \left[\sum_s^{N_{class}} \sum_j N_{B,j,s} \left(\frac{\mu_{D,j,s}}{5} - p(\text{PGA}_j, \mu_s, \beta) \right)^2 \right] \quad (6)$$

where $N_{B,j,s}$ is the number of buildings belonging to s^{th} building class within j^{th} IM value (PGA_j), whereas $\mu_{D,j,s}$ is the corresponding mean damage. As result of such fitting procedure, $N_{class} + 1$ lognormal parameters (namely, N_{class} values of median PGA + 1 value of β , common to all classes) are obtained.

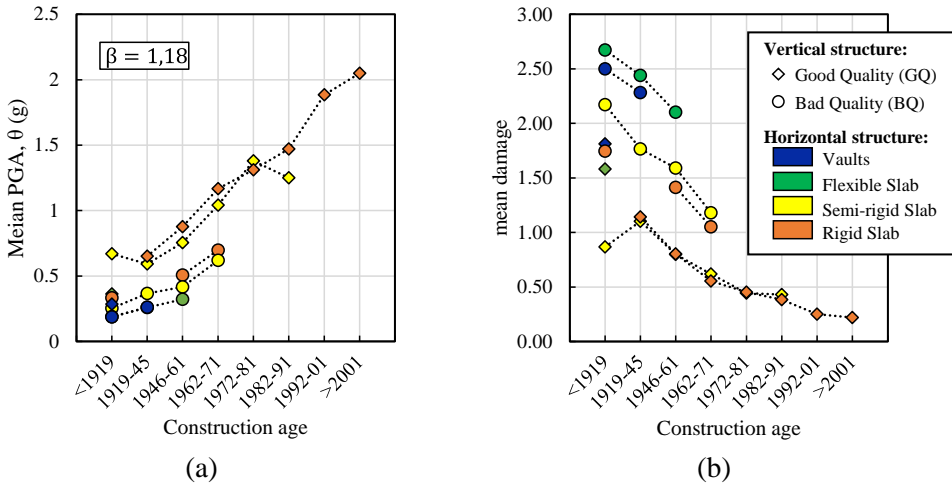


Figure 66. Median PGA (a) and mean damage (b) values for as-built classes as a function of construction age and (horizontal + vertical) structural typologies.

Figure 66(a) reports the median values, θ , for all classes obtained according to the above approach, whereas common β value resulting from optimization procedure is equal to 1.18. It can be noted a systematic increasing trend for θ with the quality layout of masonry and with the construction age, whatever the horizontal types are considered.

Similar considerations done in terms of mean damage (reproposed in Figure 66(b)) can be also moved to θ values, considered the opposite trend (the lower the quality layout the lower the θ values and vice versa).

Secondly, it can be noted clear couplings of data as a function of the horizontal structural types: both mean damage data and θ values result very similar between buildings equipped with vaults and flexible slabs and between buildings equipped with semi-rigid and rigid slabs, regardless of the quality layout and the construction age. This would suggest a similar behaviour for the abovementioned classes.

θ values range between 0.19-0.70 g for BQ and 0.28-2.05 g for GQ masonry buildings, given a β equal to 1.18. Therefore, the maximum variation of median PGA is 73% for BQ and 86% (76%, limiting the construction age up to 1971) for GQ buildings.

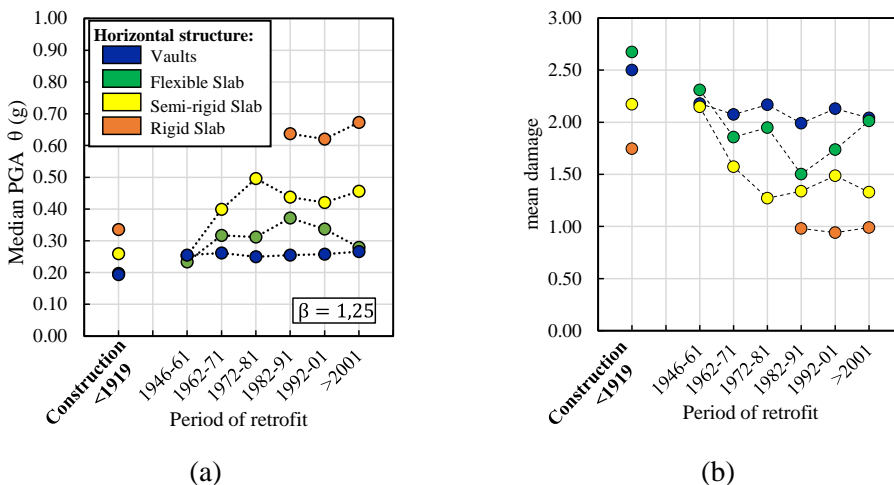


Figure 67. Median PGA (a) and mean damage (b) values for retrofitted BQ classes built before 1919 as a function of retrofit age and horizontal type.

In Figure 67(a), also the influence of retrofit intervention has been derived according to the procedure of Equation (6), namely under the assumption of a common logarithmic standard deviation β between as-built and all retrofitted BQ typologies constructed before 1919.

Thus, median values are shown in Figure 67(a), whereas common β value resulting from optimization procedure is equal to 1.25. Again, comparing the so-obtained trends with those in terms of mean damage (reproposed in Figure 67(b)), the same hierarchy among considered classes can be observed. θ values of retrofitted classes range between 0.25-0.27 g for BQ buildings with vaults, between 0.23-0.37 g in case of flexible slabs, between 0.25-0.51 g in case of semi-rigid slabs, and between 0.65-0.69 g in case of rigid slabs, allowing a maximum increase of median PGA equal to 40%, 96%, 96% and 103% respectively.

Such results confirm that the effectiveness of retrofit intervention on buildings constructed before 1919 increases with slab's stiffness. Probably, the effectiveness of structural interventions is limited in case of vaults or flexible slabs due to the absence of effective horizontal elements or devices acting to improve the box-like behaviour, without any specific intervention in this regard (introduction of stainless-steel tie rods, substitution of original flexible slabs).

6.4.6 Influence of seismic input: ShakeMap of Michellini et al., 2008

All results derived in the present Chapter (namely, vulnerability curves and median PGA values) are based on the use of PGA (*peak ground acceleration*) as intensity measure.

As explained in paragraph 6.4.1, such seismic intensity has been derived from the ShakeMap provided by the INGV according to the procedure of Michellini et al., 2020. Basically, this latter is the natural evolution of the older procedure (Michellini et al., 2008), since it is obtained using recently developed ground-motion prediction models and an updated map of VS_{30} for the local site effects.

In order to analyse the influence of the seismic input, in the present paragraph the main results up to now described have been derived based on a ShakeMap consistent with Michellini et al., 2008.

This latter is shown in Figure 68, together with the considered Abruzzi municipalities (i.e., completely surveyed ones, and not inspected and slightly surveyed ones seismically classified in 1915).

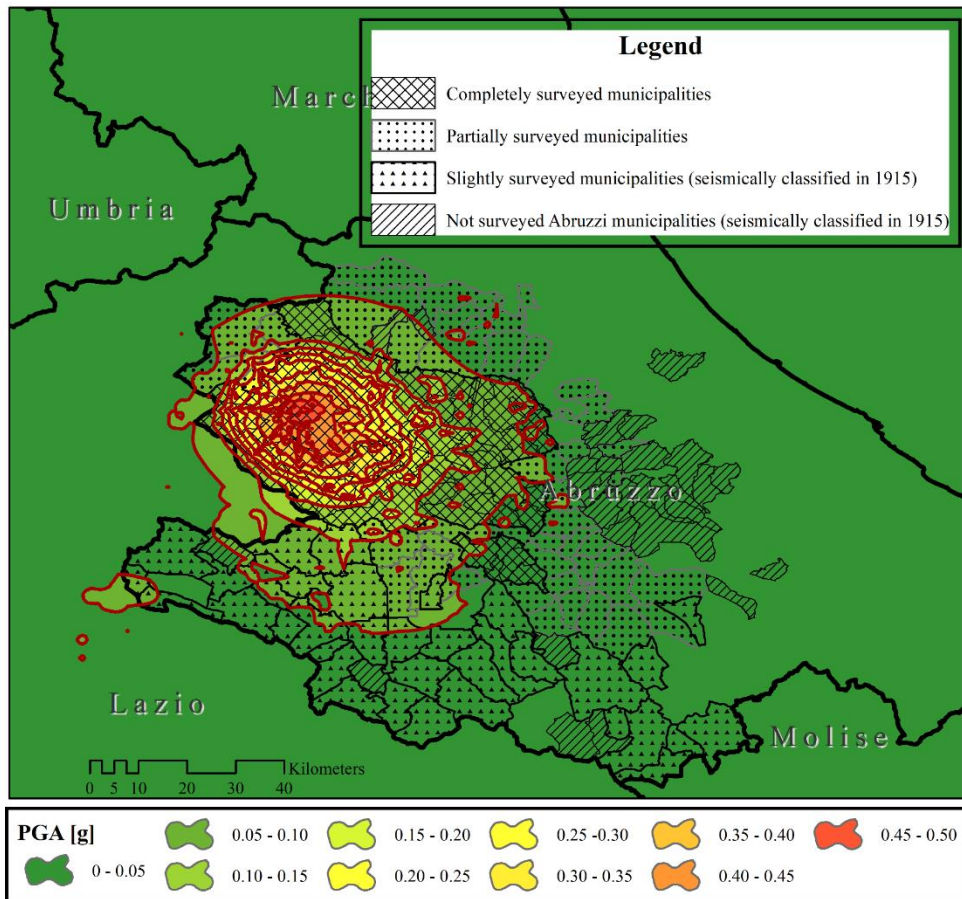


Figure 68. ShakeMap in terms of peak ground acceleration according to the procedure of Michelini et al., 2008.

In Figure 69 and Figure 70, vulnerability curves of as-built classes have been provided given the construction age and the structural typology. Note that such curves are substantially the same shown in Figure 58 and Figure 59, because the only difference is in the seismic input.

Conversely, the considered taxonomy, the metric of damage (and consequently also the mean damage given the PGA bin) and the fitting procedure (Equation 5) are exactly the same.

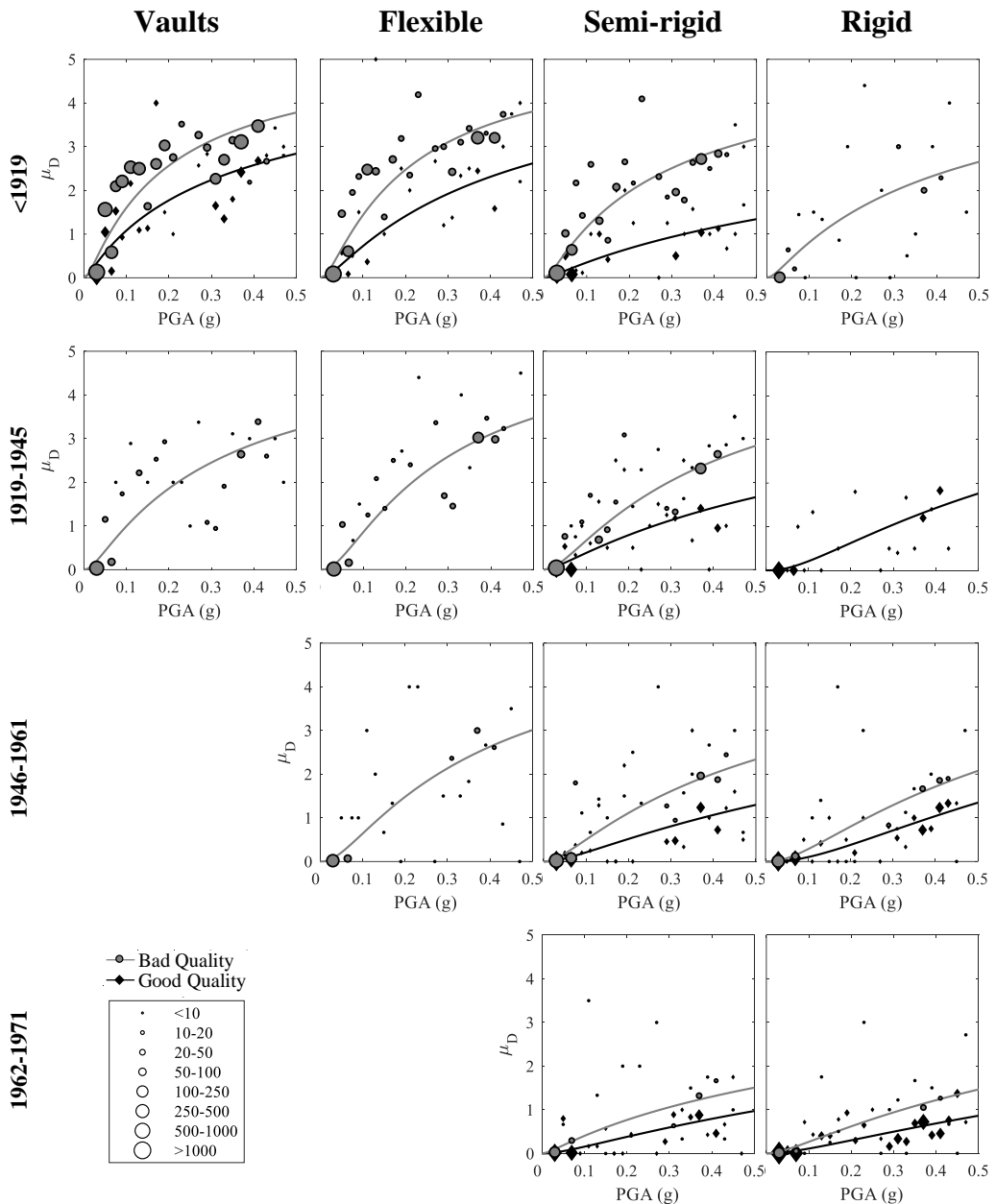


Figure 69. Vulnerability curves for as-built masonry buildings built up to 1962-1971 timespan, as a function of construction age and structural types. ShakeMap of Michelini et al., 2008.

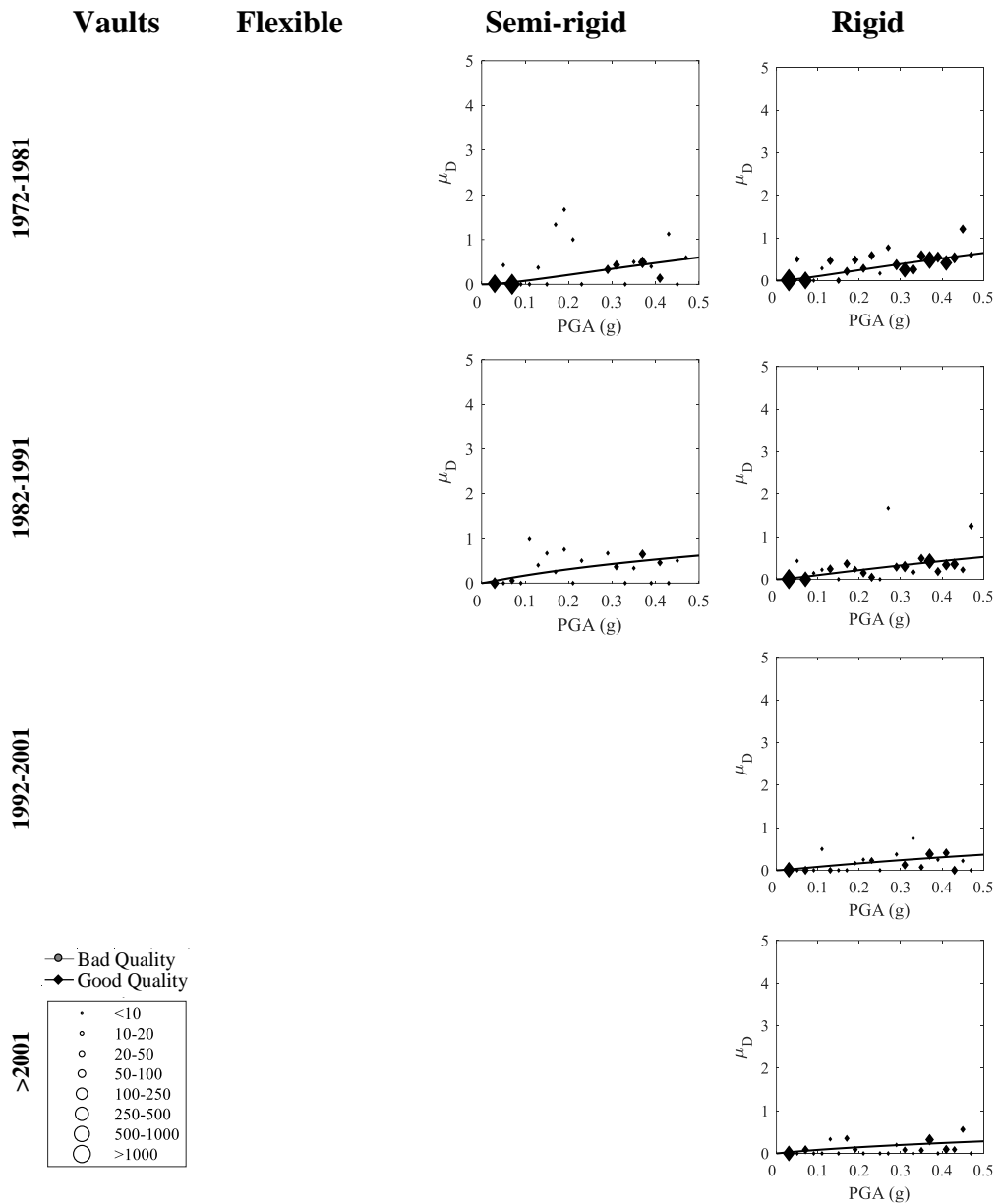


Figure 70. Vulnerability curves for as-built masonry buildings built starting from 1972-1981 timespan, as a function of construction age and structural types. ShakeMap of Michelini et al., 2008.

It should be noted that the above obtained vulnerability trends are confirmed: as matter of fact, seismic vulnerability decreases (1) increasing the construction age, (2) increasing the masonry quality (i.e., going from bad to good quality), (3) increasing the slab's stiffness (i.e., going from vaults to rigid slabs).

Table 25. Log-normal parameters for as-built BQ buildings as a function of horizontal structural typology and construction age. ShakeMap of Michelini et al., 2008.

Construction age	Vaults		Flexible slab		Semi-rigid slab		Rigid slab	
	θ	β	θ	β	θ	β	θ	β
<1919	0.19	1.39	0.20	1.26	0.30	1.48	0.45	1.51
1919-1945	0.31	1.33	0.29	1.11	0.40	1.25	-	-
1946-1961	-	-	0.37	1.13	0.56	1.32	0.64	1.17
1962-1971	-	-	-	-	1.30	1.83	1.13	1.50

Table 26. Log-normal parameters for as-built GQ buildings with as a function of horizontal structural typology and construction age. ShakeMap of Michelini et al., 2008.

Construction age	Vaults		Flexible slab		Semi-rigid slab		Rigid slab	
	θ	β	θ	β	θ	β	θ	β
<1919	0.38	1.69	0.46	1.43	1.49	1.78	-	-
1919-1945	-	-	-	-	1.00	1.59	0.77	1.17
1946-1961	-	-	-	-	1.27	1.45	0.99	1.12
1962-1971	-	-	-	-	2.00	1.61	2.06	1.50
1972-1981	-	-	-	-	3.48	1.66	3.59	1.74
1982-1991	-	-	-	-	8.30	2.42	6.07	1.99
1992-2001	-	-	-	-	-	-	14.88	2.34
>2001	-	-	-	-	-	-	52.90	2.95

Nevertheless, comparing the lognormal parameters (Table 25 and Table 26) with those above analysed (Table 20 and Table 21), a general increase in the median PGA values is observed, regardless of the building class. The same outcome is obtained if a common logarithmic standard deviation β is assumed (Figure 71(a)).

In fact, θ values range between 0.19-1.00 g for BQ and 0.33-3.58 g for GQ masonry buildings, given a β equal to 1.34 (Figure 71(a)). Conversely, using the updated version of the ShakeMap, the maximum θ values are 0.70 g and 2.05 g

for BQ and GQ masonry buildings respectively (Figure 66(a)), given a β equal to 1.18.

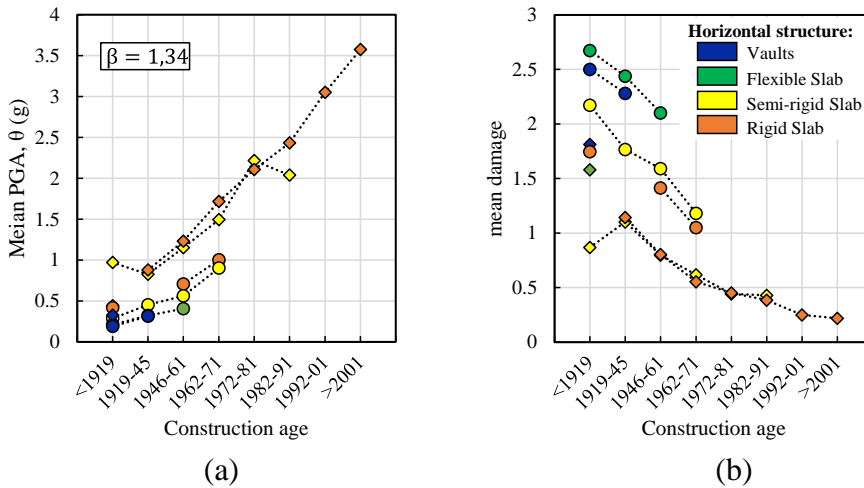


Figure 71. Median PGA (a) and mean damage (b) distributions for each horizontal structural type given the construction age, for both GQ and BQ non-retrofitted masonry buildings. ShakeMap of Michelini et al., 2008.

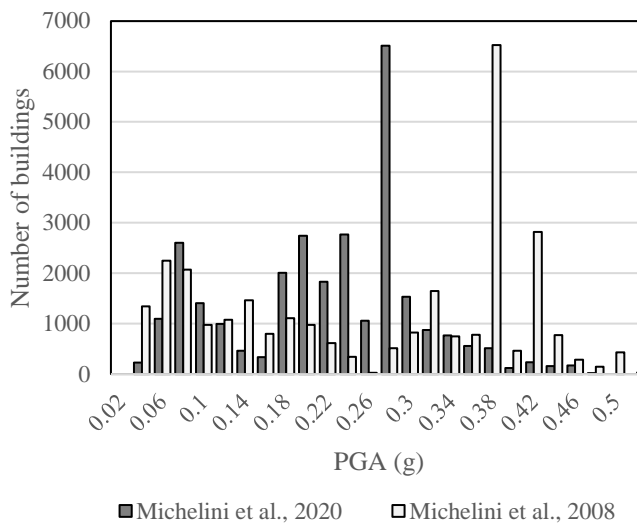


Figure 72. PGA distribution according the two considered procedures (Michelini et al., 2008 and Michelini et al., 2020).

Clearly, the mean damage distribution (Figure 66(a)) does not change if ShakeMap changes, because it is independent from the seismic input. Thus, such increase in terms of median PGA is due only to the different seismic intensity measure.

In Figure 72 the number of damaged buildings within each PGA bin (in abscissa) are shown considering both the procedures (Michellini et al., 2008 and Michellini et al., 2020) and categorizing the entire domain of PGA in bins of width equal to the isoseismic areas considered by Michellini et al., 2020

Compared with PGA values deriving from Michellini et al., 2020, the older version (1) slightly overestimates the number of buildings subjected to the lower values of PGA (less than 0.07 g), and (2) widely overestimates those subjected to the higher ones (greater than 0.35 g). Conversely, using the updated version of ShakeMap, a significant concentration of buildings subjected to 0.28 g is obtained. Thus, going from the older version to the updated one, a relevant proportion of buildings results subjected to less severe seismic intensities, basically moving data pairs ($PGA_j; \mu_{D,j}$) toward lower PGA values. It leads on average to a most severe damage for lower PGA values, causing more vulnerable curves when the fitting procedure is applied, regardless of building class.

Table 27. Lognormal parameters for BQ retrofitted masonry buildings built before 1919. ShakeMap of Michellini et al., 2008.

Period of retrofit	Vaults		Flexible slab		Semi-rigid slab		Rigid slab	
	θ	β	θ	β	θ	β	θ	β
1946-1961	0.30	1.61	0.25	1.30	0.33	1.76	-	-
1962-1971	0.29	1.53	0.38	1.46	0.52	1.60	-	-
1972-1981	0.27	1.52	0.39	1.52	0.78	1.80	-	-
1982-1991	0.30	1.76	0.61	1.92	0.69	1.80	1.46	1.93
1992-2001	0.29	1.57	0.40	1.50	0.64	1.75	1.16	1.71
>2001	0.30	1.53	0.31	1.42	0.73	1.86	1.41	1.96

For sake of completeness, also vulnerability curves (see Figure 73 and Table 27) and median PGA trends (see Figure 74) (in the assumption of a common

logarithmic standard deviation) for retrofitted BQ buildings constructed before 1919 have been derived, using the ShakeMaps of Michellini et al., 2008.

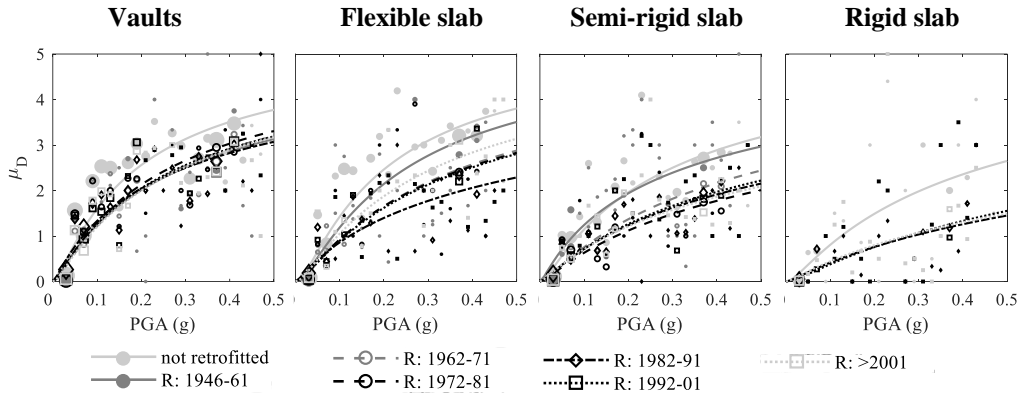


Figure 73. Vulnerability curves for BQ typologies built before 1919. Comparison in terms of presence/absence of retrofit interventions, given the structural type. ShakeMap of Michellini et al., 2008.

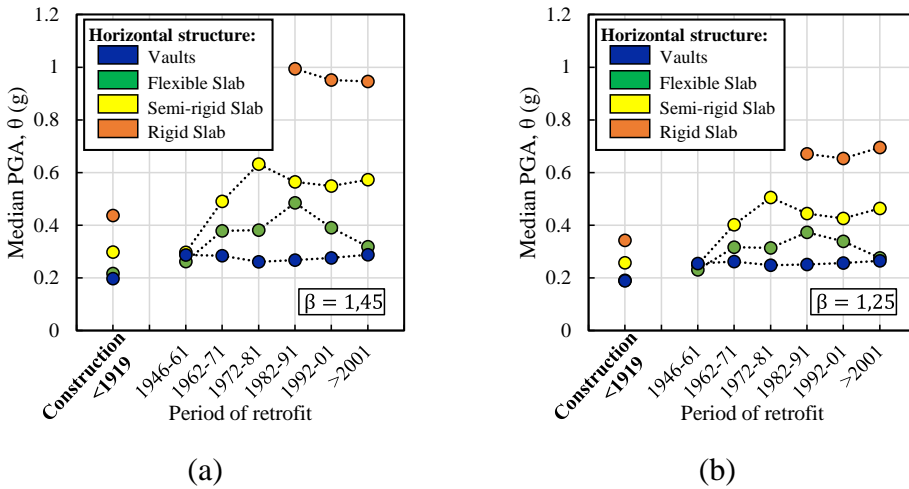


Figure 74. Median PGA values for retrofitted BQ buildings constructed before 1919, according to Michellini et al., 2008 (a) and Michellini et al. 2020 (b) ShakeMap.

As highlighted, the so-obtained minor vulnerability (or similarly the major median value of PGA) is not related to a specific class but on average to all classes. As matter of fact, also for retrofitted buildings, one can observe that

hierarchy between curves (Figure 73) are the same derived with the updated ShakeMap (see Figure 63), despite different lognormal parameters (Table 27) are obtained by means of regression procedure.

In Figure 74, the trends in terms of median PGA given the structural typology and the retrofit age have been derived, using the two considered ShakeMaps and assuming a common logarithmic standard deviation. Also in this case, the hierarchy between all considered classes does not change, but the values of PGA change, increasing for Michelini et al., 2008.

Therefore, the following outcomes have been derived, using the older version of the ShakeMap:

- hierarchies between curves do not change compared with those derived by means of the updated version, confirming the above obtained vulnerability trends;
- on average reduction of vulnerability (or similarly, increase of median PGA values) due to a general translation of mean damages toward higher seismic intensities, is observed regardless of the building class.

6.5 REFERENCES

- [1] Amiri G.G., Jalalian M., Amrei S.A.R. (2007). Derivation of vulnerability functions based on observational data for Iran. Proceedings of International Symposium on Innovation & Sustainability of Structures in Civil Engineering.
- [2] Angeletti P, Baratta A, Bernardini A, Cecotti C, Cherubini A, Colozza R, Decanini L, Diotallevi P, Di Pasquale G, Dolce M, Goretti A, Lucantoni A, Martinelli A, Molin D, Orsini G, Papa F, Petrini V, Riuscetti M, Zuccaro G (2002). Valutazione e riduzione della vulnerabilità sismica degli edifici, con particolare riferimento a quelli strategici per la protezione civile. Rapporto finale della commissione tecnico-scientifica per l'aggiornamento dell'inventario e della vulnerabilità degli edifici residenziali e pubblici per la stesura di un glossario (**in Italian**)
- [3] Augenti N, Parisi F (2010) Learning from Construction Failures due to the 2009 L'Aquila, Italy, earthquake. J Perform Constr Facil 24(6):536–555
- [4] Azzaro R., Barbano M. S., D'Amico S., Tuvè T., Scarfi L., Mostaccio A., 2011. The L'Aquila 2009 earthquake: an application of the European Macroseismic Scale to

- the damage survey in the epicentral area. *Bollettino di Geofisica Teorica ed Applicata*, 52(3), 561-581.
- [5] Baggio, C., Bernardini, A., Colozza, R., Corazza, L., Della Bella, M., Di Pasquale, G., Papa, F., 2007. Field manual for post-earthquake damage and safety assessment and short term countermeasures (AeDES). European Commission—Joint Research Centre—Institute for the Protection and Security of the Citizen, EUR, 22868.
 - [6] Braga F., Dolce M., Liberatore D., 1982. A statistical study on damaged buildings and an ensuing review of the MSK-76 scale. *Proceedings of the seventh European conference on earthquake engineering*, Athens, Greece, 431-450.
 - [7] Carocci C.F., Lagomarsino S., 2009. Gli edifici in muratura nei centri storici dell'Aquilano, *Progettazione Sismica*, vol 3. IUSS Press, Pavia, pp 117–131 **(in Italian)**
 - [8] Charvet I, Ioannou I, Rossetto T, Suppasri A, Imamura F (2014) Empirical fragility assessment of buildings affected by the 2011 Great East Japan tsunami using improved statistical models. *Nat Hazards* 73:951–973.
 - [9] D'Ayala D.F., Paganoni S., 2011. Assessment and analysis of damage in L'Aquila historic city centre after 6th April 2009. *Bulletin of Earthquake Engineering*, 9(1), 81-104.
 - [10] D'Amato M, Laguardia R, Di Trocchio G, Coltellacci M, Gigliotti R. Seismic Risk Assessment for Masonry Buildings Typologies from L'Aquila 2009 Earthquake Damage Data. *Journal of Earthquake Engineering* 2020; 00(00): 1-35. DOI: 0.1080/13632469.2020.1835750.
 - [11] De Martino, G., Di Ludovico, M., Prota, A. et al. Estimation of repair costs for RC and masonry residential buildings based on damage data collected by post-earthquake visual inspection. *Bull Earthquake Eng* 15, 1681–1706 (2017). <https://doi.org/10.1007/s10518-016-0039-9>
 - [12] Decreto Ministeriale 9 Gennaio 1987. Norme tecniche per la progettazione, esecuzione e collaudo degli edifici in muratura e per il loro consolidamento. **(in Italian)**
 - [13] Del Gaudio C., De Martino G., Di Ludovico M., Manfredi G., Prota A., Ricci P. and Verderame G.M.; 2017: Empirical fragility curves from damage data on RC buildings after the 2009 L'Aquila earthquake. *Bull. Earthquake Eng.*, 15, 1425-1450.
 - [14] Del Gaudio C., De Martino G., Di Ludovico M., Manfredi G., Prota A., Ricci P., Verderame G.M., 2019. Empirical fragility curves for masonry buildings after

- the 2009 L'Aquila, Italy, earthquake. *Bulletin of Earthquake Engineering*. <https://doi.org/10.1007/s10518-019-00683-4>.
- [15] Del Gaudio, C., Di Ludovico, M., Polese, M. et al. Seismic fragility for Italian RC buildings based on damage data of the last 50 years. *Bull Earthquake Eng* 18, 2023–2059 (2020). <https://doi.org/10.1007/s10518-019-00762-6>
- [16] Del Gaudio, C., Scala, S.A., Ricci, P., Verderame G.M., 2021. Evolution of the seismic vulnerability of masonry buildings based on the damage data from L'Aquila 2009 event. *Bull Earthquake Eng* (2021). <https://doi.org/10.1007/s10518-021-01132-x>
- [17] Di Pasquale G, Goretti A (2001) Functional and economic vulnerability of residential buildings affected by recent Italian earthquakes. In: *Proceedings of the 10th national conference of seismic engineering in Italy, Potenza-Matera, Italy (in Italian)*
- [18] Dolce M., Goretti A., 2015. Building damage assessment after the 2009 Abruzzi earthquake. *Bulletin of Earthquake Engineering* 13, 2241–2264 (2015). <https://doi.org/10.1007/s10518-015-9723-4>.
- [19] Dolce M., Masi A., Marino M. and Vona M.; 2003: Earthquake damage scenarios of the building stock of Potenza (southern Italy) including site effects. *Bull. Earthquake Eng.*, 1, 115-140.
- [20] Dolce M., Speranza E., Giordano F., Borzi B., Bocchi F., Conte C., Di Meo A., Faravelli M. and Pascale V.; 2019: Observed damage database of past Italian earthquakes: the Da.D.O. Webgis. *Boll. Geof. Teor. Appl.*, 60, 141-164.
- [21] Grünthal M., 1998. European Macro-seismic Scale. *Cahiers du Centre Européen de Géodynamique et de Séismologie*, Vol. 15. European Macro-seismic Scale 1998. European Center for Geodynamics and Seismology. **(in French)**
- [22] Indirli M., S. Kouris L.A., Formisano A., Borg R.P., Mazzolani F.M., 2013. Seismic damage assessment of unreinforced masonry structures after the Abruzzo 2009 earthquake: The case study of the historical centers of L'Aquila and Castelvechio Subequo. *International Journal of Architectural Heritage*, 7(5), 536-578.
- [23] Ioannou, I., Rossetto, T., & Grant, D. N. (2012, September). Use of regression analysis for the construction of empirical fragility curves. In *Proceedings of the 15th world conference on earthquake engineering*, September.

- [24] Karababa, F.S., Pomonis, A., 2011. Damage data analysis and vulnerability estimation following the August 14, 2003 Lefkada Island, Greece, Earthquake. *Bull Earthquake Eng* 9, 1015–1046. <https://doi.org/10.1007/s10518-010-9231-5>
- [25] Lagomarsino G. and Giovinazzi S.; 2006: Macroseismic and mechanical models for the vulnerability and damage assessment of current buildings. *Bull. Earthquake Eng.*, 4, 415-443.
- [26] Lagomarsino S, Cattari S, Ottonelli D (2015) Derivazione di curve di fragilità empiriche per classi tipologiche rappresentative del costruito Aquilano sulla base dei dati del danno dell'evento sismico del 2009. Research Project DPC-ReLUIS 2015 **(in Italian)**
- [27] Lagomarsino, S., Cattari, S. & Ottonelli, D. The heuristic vulnerability model: fragility curves for masonry buildings. *Bull Earthquake Eng* 19, 3129–3163 (2021). <https://doi.org/10.1007/s10518-021-01063-7>
- [28] Michelini A., Faenza L., Lauciani V., Malagnini L., 2008. ShakeMap implementation in Italy. *Seismological research letters*, 79(5); 2008, 688–697.
- [29] Michelini, A., Faenza, L., Lanzano, G., Lauciani, V., Jozinović, D., Puglia, R., & Luzi, L. (2020). The new ShakeMap in Italy: Progress and advances in the last 10 yr. *Seismological Research Letters*, 91(1), 317-333.
- [30] Nash J.E. and Sutcliffe J.V.; 1970: River flow forecasting through conceptual models: Part I, a discussion of principles. *J. Hydrol.*, 10, 282-290.
- [31] Orsini G., 1999. A model for buildings' vulnerability assessment using the Parameterless Scale of Seismic Intensity (PSI). *Earthquake Spectra*, 15(3), 463-483.
- [32] Rossetto T., Ioannou I., Grant D.N., 2013. Existing empirical fragility and vulnerability functions: Compendium and guide for selection, GEM Technical Report 2013-X, GEM Foundation, Pavia, Italy.
- [33] Rossetto T., Peiris N., Alarcon J.E. et al., 2011. Field observations from the Aquila, Italy earthquake of April 6, 2009. *Bull Earthquake Eng* 9, 11–37 (2011). <https://doi.org/10.1007/s10518-010-9221-7>.
- [34] Rossetto, T. and Elnashai, A. (2003) Derivation of Vulnerability Functions for European-Type RC Structures Based on Observational Data. *Engineering Structures*, 25, 1241-1263. [http://dx.doi.org/10.1016/S0141-0296\(03\)00060-9](http://dx.doi.org/10.1016/S0141-0296(03)00060-9)
- [35] Rosti A., Del Gaudio C., Di Ludovico M., Magenes G., Penna A., Polese M., Verderame G.M., 2020a. Empirical vulnerability curves for Italian residential buildings. *Bollettino di Geofisica Teorica ed Applicata*, 61(3).

- [36] Rosti A., Del Gaudio C., Rota M., Ricci P., Di Ludovico M., Penna A., Verderame G.M., 2020b. Empirical fragility curves for Italian residential RC buildings. *Bull Earthquake Eng* (2020). <https://doi.org/10.1007/s10518-020-00971-4>.
- [37] Rosti A., Rota M., Penna A., 2020c. Empirical fragility curves for Italian URM buildings. *Bulletin of Earthquake Engineering*.
- [38] Rosti, A., Rota, M., & Penna, A. (2018). Damage classification and derivation of damage probability matrices from L'Aquila (2009) post-earthquake survey data. *Bulletin of Earthquake Engineering*, 16(9), 3687-3720.
- [39] Rota M. and Rosti A.; 2017: Comparison of PSH results with historical macroseismic observations at different scales - Part 1: methodology. *Bull. Earthquake Eng.*, 15, 4585-4607.
- [40] Rota M., Penna A., Strobbia C.L., 2008. Processing italian damage data to derive typological fragility curves. *Soil Dynamics and Earthquake Engineering*, 933-947.
- [41] Scala S.A., Del Gaudio C., Verderame G.M., 2022. Influence of construction age on seismic vulnerability of masonry buildings damaged after 2009 L'Aquila Earthquake (**under review**)
- [42] Spence R.J.S., Coburn A.W., Pomonis A. 1992. "Correlation of ground motion with building damage: The definition of a new damage-based seismic intensity scale", *Proceedings of 10th World Conference on Earthquake Engineering*, Balkema, Rotterdam.
- [43] Worden C. B., Thompson E. M., Hearne M., and Wald D. J. 2017. ShakeMap V4 manual: Technical manual, user's guide, and software guide, U.S. Geological Survey.
- [44] Zucconi M., Ferlito R., Sorrentino L., 2018. Simplified survey form of unreinforced masonry buildings calibrated on data from the 2009 L'Aquila earthquake. *Bulletin of Earthquake Engineering*, 16(7), 2877-2911.
- [45] Zucconi M., Sorrentino L., Ferlito R., 2017. Principal component analysis for a seismic usability model of unreinforced masonry buildings. *Soil Dynamics and Earthquake Engineering* 96 (2017): 64-75.

Chapter 7.

FRAGILITY CURVES

7.1 INTRODUCTION

Fragility curves describe, for a given building or class of buildings, the probability of experiencing or exceeding a particular level of damage, given the seismic intensity measure value. The aim of this Chapter is to derive fragility curves according to the considered very detailed taxonomy, in order to identify fragility trends of a given structural typology as a function of construction and, if any, retrofit ages. Thus, the main aim is to understand how the seismic fragility of a specific structural class (defined in terms of vertical and horizontal structures) changes varying the construction age and how the fragility of a given retrofitted class (defined in terms of structural typology and construction age) changes, varying the retrofit age.

Two regression models have been adopted deriving lognormal fragility curves, in order to quantify possible differences and to understand if the obtained fragility trends are influenced by the regression's procedure. So, lognormal parameters are obtained, in the first case (*LSE*) minimizing the distance between observed and predicted cumulative damage distributions, and in the second case (*MLE*), maximizing a multinomial likelihood function.

Thus, fragility curves have been firstly derived according to the two approaches, quantifying the difference between the corresponding DPMs by means of the error $err_{i,j}$ for a given (j^{th}) PGA value and a given (i^{th}) DS.

Secondly, starting from such fitting approaches (in the following, called “*unconditioned*” model), further two regression models have been considered, first constraining the median PGA values (“*conditioned*” model) and then, also the logarithmic standard deviation (“*conditioned(β)*” model).

Basically, the constraint of median PGA values allows to derive the optimum solution of the fitting procedure that also complies the trends derived in terms of mean damage (Section 6.3) and vulnerability curves (Section 6.4). In particular, the constraints have been applied on the median parameters, ensuring the same hierarchy in terms of structural typology and construction age derived by means of vulnerability curves. Then, a third approach (so-called *Conditioned(β)* model) is introduced to overcome the presence of crossing curves. Basically, starting from the *Conditioned* model, a further constraint is introduced in the fitting procedure, assuming a constant logarithmic standard deviation (Kircher et al., 2006; FEMA 2012; Karababa and Pomonis 2011; Coburn and Spence 2003; Del Gaudio et al., 2019) for all classes with the same masonry quality.

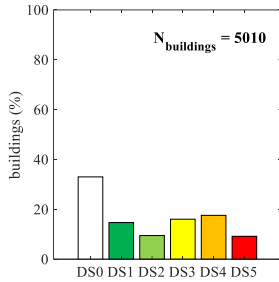
Lastly, in order to quantify the difference between the three considered (*unconditioned*, *conditioned*, *conditioned(β)*) models and then the influence of each assumption (i.e., constraint on median PGA and constant β value), again the comparison between the corresponding DPMs have been done, using the error $err_{i,j}$. In the last Section, the three regression models have been applied also to retrofitted classes, providing fragility curves according to assumptions of each of them.

7.2 FRAGILITY CURVES ACCORDING OBSERVED DPM

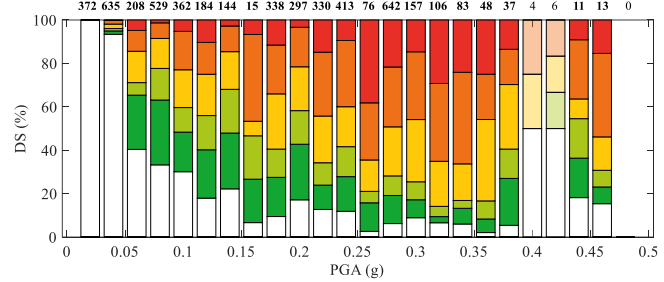
As above mentioned, the Section 4 of the AeDES form (Baggio et al. 2007) provides the damage description for the structural components (namely, vertical and horizontal structures, stairs, roof). For each of them, the surveyor is required to assign a damage level and a relating extent. Three damage levels (i.e., *slight*, *medium-severe*, *very heavy*), in addition to null damage (DS0), and three damage

extents (i.e., $<1/3$, $1/3-2/3$, $>2/3$) are considered. The conversion rule defined by Rota et al., 2008 has been used to convert the damage classification related to the only vertical structures in damage description of the entire building, consistent with the European Macroseismic Scale, EMS 98 (Grünthal et al. 1998).

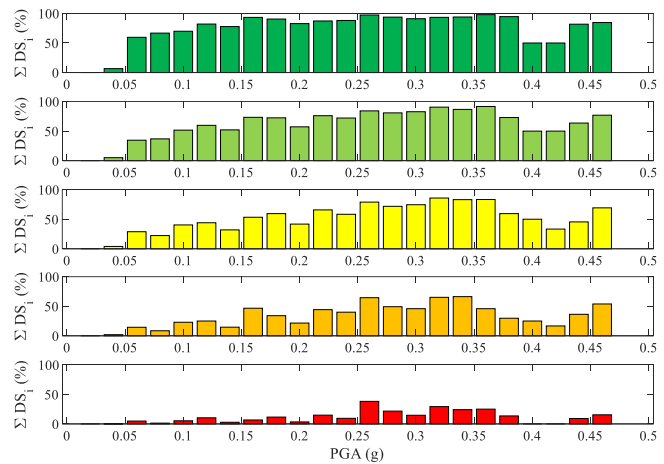
Step 1: damage distribution



Step 2: DPM



Step 3: cumulative DPM



Step 4: probability of exceeding

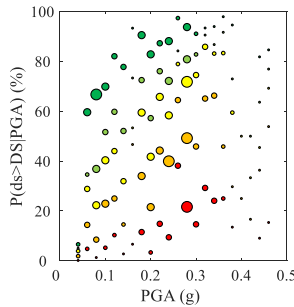


Figure 75. From observed damage distribution to probability of exceeding of a given DS for each PGA value (BQ-V-PRE1919 class).

For each building class defined in Chapter 5 damage distribution can be derived, considering the occurrence of each DS (*Step 1* in Figure 75). This representation allows to see the amount of buildings of a given class in each damage state. For example, about the 33% of buildings belonging to the BQ-V-PRE19 class exhibit a DS0. Nevertheless, this distribution is not conditioned by

any seismic intensity measure. Thus, this representation basically does not allow to understand how many buildings belonging in DS0 have been subject to low or high intensities. Most informative is the damage probability matrix, DPM, (*Step 2* in Figure 75), that provides the damage distribution for each PGA value. So, it is possible to note that major part of buildings in DS0 has been subject to lower PGA. Conversely, increasing the PGA, a greater occurrence of higher DS is observed. Obviously, the greater the number of PGA values, the less the number of buildings for each damage distribution given the intensity measure. For this reason, in Figure 75 (*Step 2*) above each bar (i.e., damage distribution given the PGA value) the number of buildings subject to the j^{th} PGA value, $N_{b,PGAj}$, is reported. It should be noted that unexpected distributions could be due to very small $N_{b,PGAj}$ values (e.g., less than 10). This issue has been addressed, deriving the fragility curves by means a weighted regression procedure.

Clearly, the percentage damage distribution for a given PGA value represents, in the frequentist view, the probability of occurrence of each DS for the same PGA value. Thus, the corresponding cumulative distribution (*Step 3* in Figure 75) is the probability of exceeding each DS for the same PGA value. Of course, the cumulative DPMs are discrete distributions, that provide the probability of exceeding each DS only for the available PGA values. So, these probabilities can be represented as points in the space $PGA - P(ds \geq DS|PGA)$. It should be noted that in Figure 75 (*Step 4*), the dimension of the obtained data points is proportional to the number of buildings in the i^{th} DS subjected to the j^{th} value of PGA, $N_{b,PGAj,DSi}$.

The fragility curve of a given DS is a continuous relation between an intensity measure (such as the PGA) and the probability of exceeding the considered DS, given the intensity measure. Therefore, to derive fragility curves starting from the obtained data point, it is necessary to apply a regression procedure in the entire PGA range, after assuming a certain functional form.

In literature, the most used functional form is the lognormal cumulative distribution function (Rossetto et al. 2013), whose parameters are the logarithmic mean μ (or, equivalently, the median $\theta = e^\mu$) and the logarithmic standard deviation β (see Equation 6). This function, in fact, is particularly suitable for

fitting data clustered at low ground motion intensities. Moreover, both x- and y-axes are constrained in eligible ranges. As matter of fact, the abscissa is defined only for positive values (like almost all the seismic intensity measures); whereas the ordinate returns values between 0 and 1 (like the probability of exceeding).

$$P(ds \geq DS|PGA) = \Phi\left(\frac{\ln(PGA) - \mu}{\beta}\right) \quad (6)$$

In this study, cumulative lognormal fragility curves have been derived by means of two fitting techniques, namely LSE and MLE ones. In this way, also the influence of the fitting procedure in the fragility assessment has been analysed.

7.2.1 LSE regression procedure

The first approach adopted in this work to derive fragility curves is based on the nonlinear LSE fitting procedure, also used in several fragility studies (among the others, Rossetto and Elnashai, 2003; Amiri et al, 2007; Rota et al, 2008; Del Gaudio et al., 2017). This method searches for the lognormal parameters (namely, μ and β) that provide the most accurate description of the data, minimizing the sum (over all PGA values) of the squared difference between the observed values (i.e., data points in Figure 75 (*Step 4*)) and those predicted by a certain function (cumulative lognormal distribution in this work). Thus, the lognormal parameters at a certain DS (namely, μ_{DS} and β_{DS}) are evaluated as follow:

$$[\mu_{DS}, \beta_{DS}] = \operatorname{argmin} \left[\sum_j \left(\Phi\left(\frac{\ln(PGA_j) - \mu_{DS}}{\beta_{DS}}\right) - \frac{\sum_{i=ds}^5 N_{b,PGA_j,DSi}}{N_{b,PGA_j}} \right)^2 \right] \quad (7)$$

Applying the LSE technique separately to each DS, ordinal hierarchy among the DSs could be not ensured. Conversely, a direct comparison between the curves (or equivalently, between the median values θ_{DS}) is possible only assuming a common β for all DSs (e.g., Lallemand et al., 2015; Del Gaudio et

al., 2020; Rosti et al., 2020; Karababa and Pomonis 2011; Coburn and Spence 2003), namely a common dispersion for each set of fragility curves. Moreover, as highlighted in Figure 75, some observed data points derive from a very small number of buildings (subjected to a given PGA value and belonging to a given DS). Clearly, the sample size could affect the reliability of the single data point. To overcome such issue, a weighted fitting procedure is typically adopted. In Rota et al., 2008, the inverse of the standard deviation estimated, in each PGA bin, by means bootstrap technique is used as fitting weight. Whereas the number of buildings in each PGA value is used in other studies (Sabetta 1998; Del Gaudio et al., 2017). Therefore, the LSE technique in the present work is based on two assumptions:

- a common β for all DSs is considered to avoid unexpected hierarchy between DSs;
- the number of buildings in each PGA bin is used as weight in the fitting procedure to mitigate the influence of the less-populated data points.

Under these two assumptions, Equation 7 can be re-written as follow:

$$[\theta_{DS}, \beta] = \operatorname{argmin} \left[\sum_{ds} \sum_j \left(\Phi \left(\frac{\ln(PGA_j / \theta_{ds})}{\beta} \right) - \frac{\sum_{i=ds}^5 N_{b,PGAj,DSi}}{N_{b,PGAj}} \right)^2 N_{b,PGAj} \right] \quad (8)$$

7.2.2 MLE regression procedure

In the second approach, the fitting procedure is performed maximizing the likelihood function.

Therefore, the obtained lognormal parameters represent the ones that most likely have produced the observed data. In previous studies, the likelihood function is binomial (e.g., Ioannou et al., 2012; Del Gaudio et al., 2019) or multinomial (e.g., Charvet et al. 2014; Del Gaudio et al., 2020; Rosti et al., 2020). In this work, the repartition of buildings in the different DSs, is described by a multinomial distribution, for each PGA value.

Thus, the likelihood function can be written as:

$$\prod_j \prod_i \frac{N_{b,PGA_j}!}{N_{b,PGA_j,DS_i}!} P(ds = DS_i | PGA_j)^{N_{b,PGA_j,DS_i}} \quad (9)$$

In Equation 9, $P(ds = DS_i | PGA_j)$ is the probability of occurrence of DS_i , given the j^{th} value of PGA. Clearly, this probability can be written as a function of the corresponding probability of exceeding (see Equation 10), herein assumed as a lognormal cumulative function.

$$\begin{aligned} & P(ds = DS_i | PGA_j) \\ &= \begin{cases} 1 - P(ds \geq DS_1 | PGA_j) & i = 0 \\ P(ds \geq DS_i | PGA_j) - P(ds \geq DS_{i+1} | PGA_j) & i \in [1; 4] \\ P(ds \geq DS_5 | PGA_j) & i = 5 \end{cases} \quad (10) \end{aligned}$$

Moreover, also in this approach, a common β for all DSs is assumed. Thus, for each building's class, 6 lognormal parameters, namely the medians θ_{DS_i} (going from DS1 to DS5) and a single value of β , are provided by the optimization technique (see Equation 11).

$$\begin{aligned} [\theta_{DS}, \beta] &= \operatorname{argmax} \left[\log \left(\prod_j \prod_i \frac{N_{b,PGA_j}!}{N_{b,PGA_j,DS_i}!} P(ds = \right. \right. \\ & \quad \left. \left. DS_i | PGA_j)^{N_{b,PGA_j,DS_i}} \right) \right] = \\ & \operatorname{argmax} \left[\sum_j \sum_i \log \left(\frac{N_{b,PGA_j}!}{N_{b,PGA_j,DS_i}!} P(ds = DS_i | PGA_j)^{N_{b,PGA_j,DS_i}} \right) \right] \quad (11) \end{aligned}$$

Note that in Equation 11 the logarithm of the likelihood function is maximized. In this way, the results of the maximization are the same obtained maximizing directly the likelihood function. Nevertheless, the introduction of the logarithm allows to simplify the calculation, because the logarithm of the product is the sum of the logarithm (as shown in Equation 11).

7.3 FRAGILITY CURVES FOR AS-BUILT CLASSES

In this section, fragility curves of the 27 available as-built building's classes are provided. Each class is univocally defined in terms of structural typology (i.e., masonry's quality and/or texture and type of horizontal structure), construction age (i.e., <1919; 1919-1945; 1946-1961; 1962-1971; 1972-1981; 1982-1991; 1992-2001; >2001) and absence of retrofit interventions.

In particular, the 27 as-built classes have been defined, combining the two masonry's quality (i.e., bad quality, BQ, and good quality, GQ) with the four horizontal structures (i.e., vaults, flexible-, semi-rigid- and rigid-slabs) and the eight construction ages and considering a minimum sample size of 100 buildings. The resulting 12 BQ as-built classes cover a timespan until 1971; whereas the 15 GQ ones reach the >2001 time period.

In this section, fragility curves are obtained by means of two approaches described in the previous paragraph (namely, LSE and MLE techniques). In Figure 76, the fragility assessment performed on masonry buildings with bad quality and/or irregular layout (i.e., BQ) is reported, distinguishing as a function of the construction age (rows of the matrix) and of the horizontal structure (columns of the matrix). Thus, each plot provides the fragility curves of a given building's class (univocally defined in terms of vertical and horizontal structure, construction age and absence of retrofit interventions).

As mentioned above, the dimension of data points is proportional to the number of buildings subjected to the j^{th} PGA value and belonging to the i^{th} DS, $N_{b,PGAj,DSi}$. Moreover, to avoid affecting the regression procedure, any subdivision in PGA bin has been considered. In fact, each data point corresponds to an observed PGA value, leading a huge difference in terms of number of buildings for each of them. Thus, a weighted regression procedure is adopted to overcome such issue, giving greater weight to the most populated points.

The curves derived according to nonlinear weighted LSE approach are drowned with solid lines, whereas dashed lines are used for curves of MLE procedure.

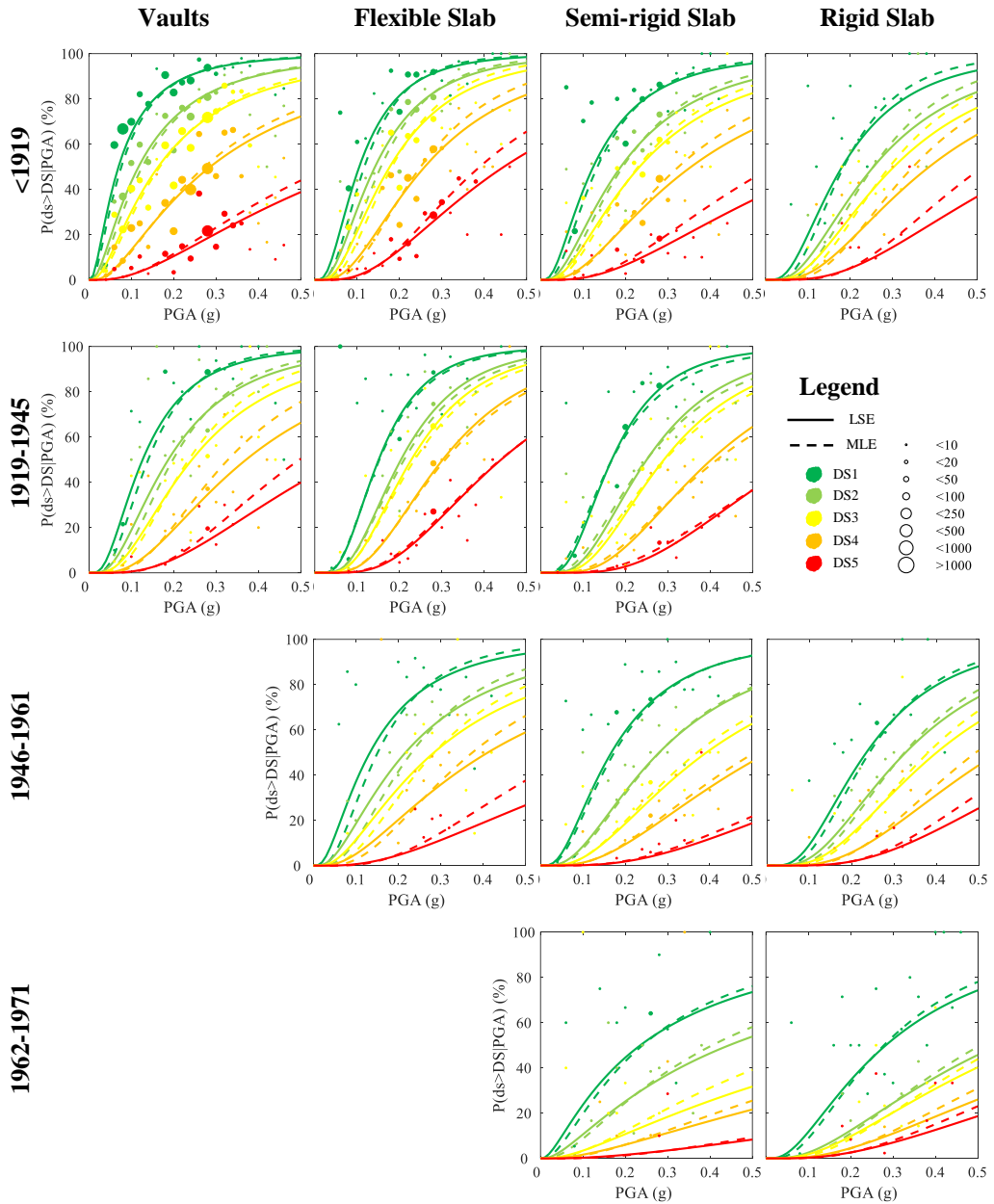


Figure 76. Fragility curves for all BQ classes given the construction age and the horizontal structures. Comparison between LSE (solid line) and MLE (dashed line) technique.

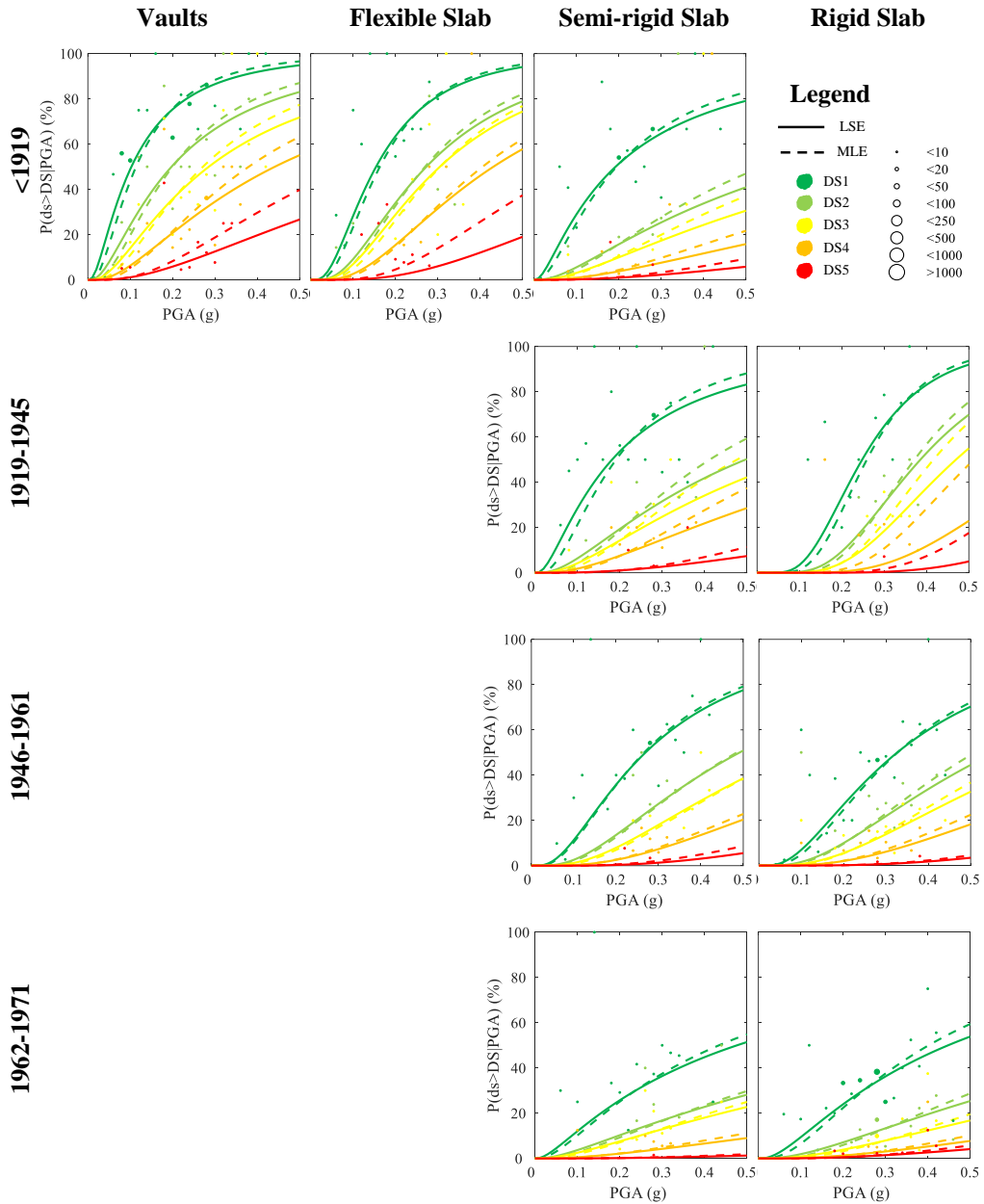


Figure 77. Fragility curves for GQ classes (built until 1971) given the construction age and the horizontal structures. Comparison between LSE (solid line) and MLE (dashed line) technique.

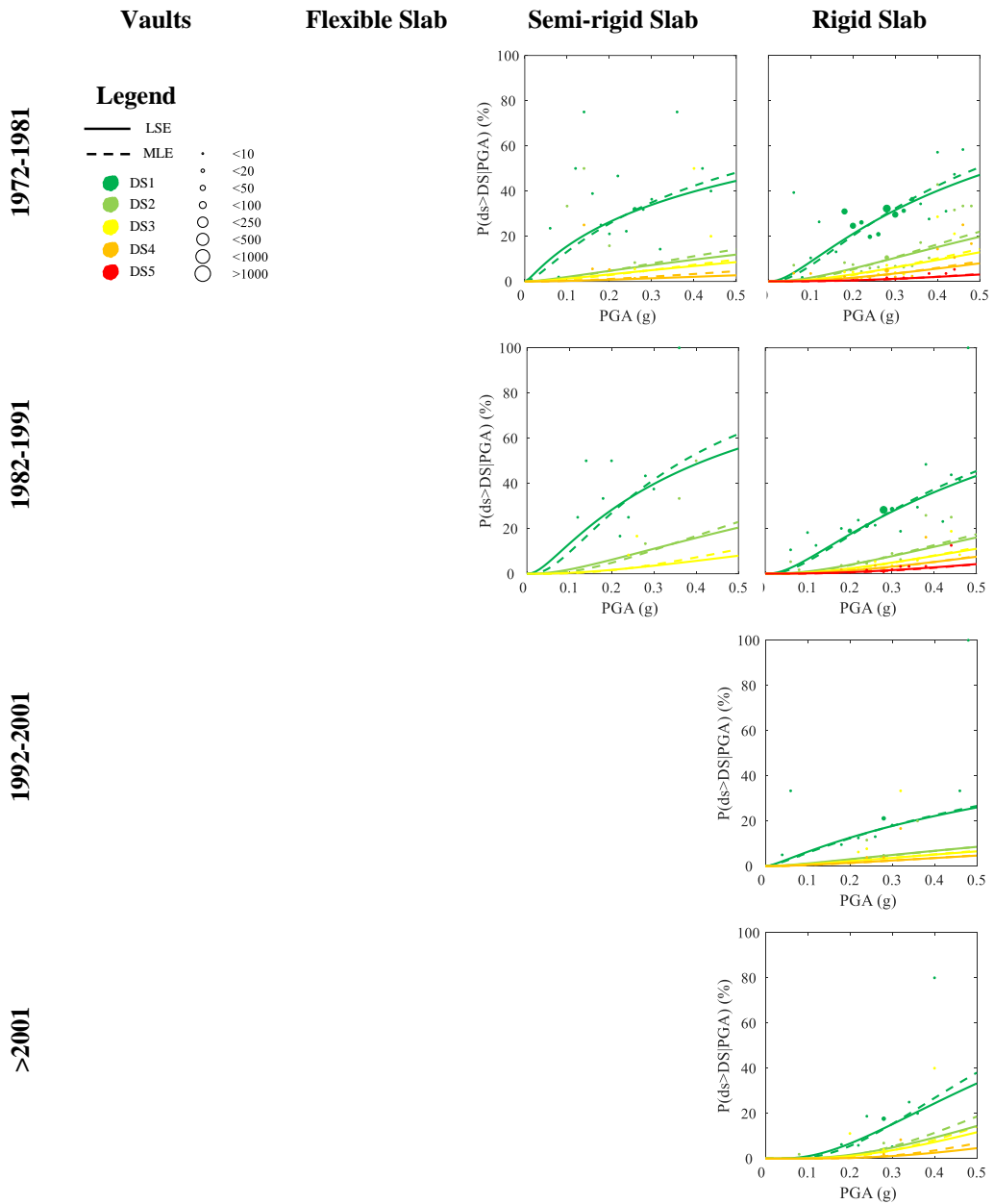


Figure 78. Fragility curves for GQ classes (built after 1971) given the construction age and the horizontal structures. Comparison between LSE (solid line) and MLE (dashed line) technique.

Clearly, there are no intersections between curves of the same class, due to the constant logarithmic standard deviation for all DSs. No significant difference in the obtained curves is observed if the LSE or MLE approaches are used. The main differences seem to be clustered in the higher PGA values, especially for the higher DSs. In all these cases, the MLE approach provides the most conservative results, namely higher probabilities of exceeding than LSE approach.

Both the approaches describe the same trends: the building's fragility mainly (1) increases with the DS, given the structural typology (namely, the BQ masonry's quality and the type of horizontal structure) and the construction age; (2) decreases with the construction age, given the DS and the structural typology; (3) decreases with the slab's stiffness, given the DS, the construction age and the masonry's quality (i.e. BQ).

Similar results are shown in Figure 77 and Figure 78 for masonry buildings with good quality and/or regular layout (i.e., GQ). Thus, also for GQ buildings, the major differences between MLE and LSE curves are about the higher DS (especially DS5 for the classes built before 1919).

Nevertheless, the same fragility trends are described by the two approaches: the seismic fragility of GQ buildings mainly increases with the DS and decreases with the construction age and the stiffness slabs, given all the others features. Moreover, as deeply investigated in the literature (Scala et al., 2021; Del Gaudio et al., 2019; D'Amato et al., 2020; amongst others), the GQ classes seem to be less fragile than the BQ ones, given the DS, the period of construction and the type of slab.

In Table 28 and Table 29, lognormal parameters, namely the median at each DS (from DS1 to DS5), θ_{DSi} , and the common logarithmic standard deviation β , are provided for each considered as-built class, according to the two considered regression models (LSE and MLE respectively).

It should be noted that any minimum sample size (in terms of $N_{b,DSi}$) has been considered to derive the curves. Nevertheless, the fragility of some classes (namely, GQ-S built in 1972-1981 and 1982-1991 timespans; GQ-R built in 1991-2001 and >2001 timespans) has been evaluated only with reference to the

lower DSs, discarding the DS4 and (especially) the DS5 curves. In fact, for such classes the corresponding $N_{b,DSi}$ at higher DSs is really limited.

Table 28. Lognormal parameters (median and logarithmic standard deviation) for each as-built building class, according to LSE technique.

Building Class		LSE technique					β	
		θ_{DS1} (g)	θ_{DS2} (g)	θ_{DS3} (g)	θ_{DS4} (g)	θ_{DS5} (g)		
BQ	<1919	V	0.07	0.12	0.16	0.29	0.65	0.94
		F	0.11	0.14	0.18	0.26	0.45	0.72
		S	0.12	0.19	0.23	0.35	0.68	0.81
		R	0.18	0.25	0.30	0.39	0.63	0.70
	1919-45	V	0.13	0.19	0.24	0.37	0.60	0.71
		F	0.15	0.20	0.23	0.30	0.44	0.56
		S	0.17	0.25	0.29	0.40	0.61	0.58
	1946-61	F	0.13	0.22	0.28	0.41	0.86	0.87
		S	0.17	0.28	0.39	0.54	0.97	0.75
	1962-71	R	0.24	0.33	0.40	0.55	0.77	0.64
		S	0.24	0.45	0.88	1.28	2.62	1.20
		R	0.28	0.55	0.62	0.88	1.09	0.87
GQ	<1919	V	0.10	0.20	0.29	0.44	0.91	0.97
		F	0.15	0.27	0.30	0.43	0.97	0.75
		S	0.19	0.66	0.91	1.63	3.20	1.18
	1919-45	S	0.18	0.50	0.62	0.91	2.29	1.05
		R	0.25	0.39	0.47	0.72	1.14	0.50
		1946-61	S	0.27	0.49	0.63	0.98	1.84
	R		0.33	0.56	0.72	1.03	2.14	0.80
	1962-71	S	0.48	1.08	1.35	2.98	9.80	1.33
		R	0.45	1.06	1.50	2.53	3.61	1.14
	1972-81	S	0.64	4.41	6.22	17.30	-	1.84
		R	0.55	1.45	2.06	2.90	5.22	1.25
	1982-91	S	0.53	1.69	3.05	-	-	1.29
		R	0.66	1.9	2.15	2.77	3.89	1.19
	1992-2001	R	0.9	2.08	7.86	10.65	-	1.82
	>2001	R	0.95	2.08	1.39	2.12	-	0.86

Table 29. Lognormal parameters (median and logarithmic standard deviation) for each as-built building class, according to MLE technique.

Building Class		MLE technique						
		θ_{DS1} (g)	θ_{DS2} (g)	θ_{DS3} (g)	θ_{DS4} (g)	θ_{DS5} (g)	β	
BQ	<1919	V	0.08	0.13	0.17	0.27	0.57	0.88
		F	0.12	0.16	0.18	0.25	0.39	0.62
		S	0.13	0.19	0.23	0.33	0.55	0.72
		R	0.18	0.25	0.29	0.35	0.51	0.58
	1919-45	V	0.14	0.20	0.24	0.33	0.50	0.61
		F	0.15	0.21	0.24	0.31	0.44	0.58
		S	0.17	0.25	0.29	0.42	0.63	0.65
	1946-61	F	0.15	0.23	0.29	0.38	0.62	0.69
		S	0.17	0.28	0.37	0.51	0.88	0.72
	1962-71	R	0.24	0.33	0.38	0.49	0.65	0.56
		S	0.24	0.41	0.66	0.98	1.94	1.03
		R	0.28	0.51	0.56	0.73	0.87	0.76
GQ	<1919	V	0.11	0.20	0.27	0.38	0.62	0.81
		F	0.16	0.27	0.31	0.41	0.62	0.67
		S	0.19	0.54	0.69	1.09	1.85	0.99
	1919-45	S	0.19	0.41	0.48	0.65	1.33	0.81
		R	0.26	0.37	0.42	0.51	0.75	0.43
	1946-61	S	0.27	0.48	0.63	0.89	1.44	0.78
		R	0.33	0.51	0.64	0.86	1.69	0.72
	1962-71	S	0.43	0.92	1.09	2.04	5.52	1.16
		R	0.40	0.84	1.10	1.60	2.13	0.92
	1972-81	S	0.54	2.49	3.52	6.31	-	1.50
		R	0.49	1.15	1.58	2.15	3.68	1.08
	1982-91	S	0.53	1.69	1.71	-	-	1.00
		R	0.66	1.9	1.82	2.32	3.26	1.08
	1992-2001	R	0.9	2.08	6.43	8.65	-	1.71
	>2001	R	0.95	2.08	1.07	1.44	-	0.71

7.3.1 Comparison between observed and predicted DPMs

To evaluate the reliability of the obtained fragility trends, the observed DPMs (e.g., *Step 2* in Figure 75) are compared with those derived from the fragility curves (e.g., *Step 6* in Figure 79) of both regression's approaches.

These latter are the probabilities of occurrence of each DS for a given PGA value and can be obtained from the corresponding probabilities of exceeding, applying Equation 10. Clearly, for each PGA value, the corresponding probabilities of exceedance of DS_i (with $i = 1, \dots, 5$) are obtained by means the fragility curves (as shown in *Step 5* of Figure 79). The obtained DPMs (i.e., the probability of occurrence of each DS, given a certain PGA value) are the “expected” ones, predicted by the adopted regression models. Thus, comparing the observed and the expected DPMs, an evaluation about the predictive capacity of the two considered approaches can be obtained.

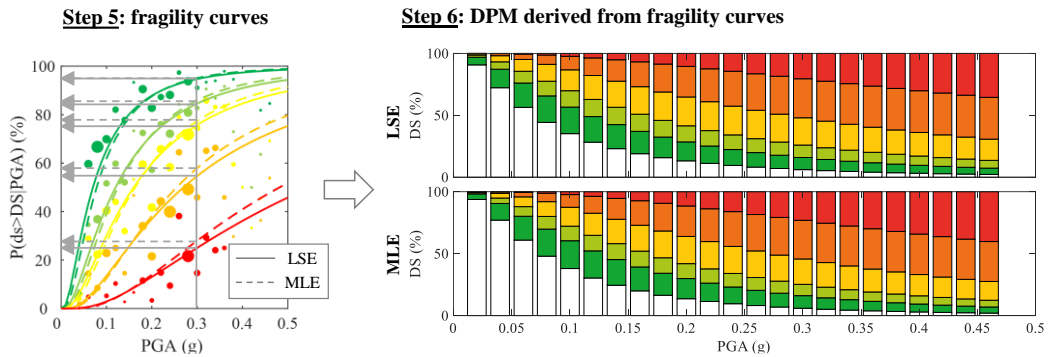


Figure 79. From fragility curves to corresponding DPMs (BQ-V-PRE1919 class).

A parameter used in the literature (Lallemant et al., 2015) to synthetically describe the comparison between DPMs is the Pearson's cumulative chi-squared statistics χ^2 (Ang and Tang, 2007). Basically, this parameter is evaluated, for each given PGA value, as the sum over all DSs of the squared difference between expected and observed DPMs (divided by the expected value). Thus, the lower the χ^2 value, the smaller the distance between the observed and the expected DPMs.

In this work, in order to obtain a percentage measure of the error, a similar parameter has been adopted, evaluating the error ($err_{i,j}$) for a given (j^{th}) PGA value and a given (i^{th}) DS.

$$err_{i,j} = \frac{|E_{i,j} - O_{i,j}|}{\sum_{i=1}^{N_{DS}} O_{i,j}} = \frac{\left| \left(\logncdf(PGA_j, \mu_{DS_i}, \beta_{DS_i}) - \logncdf(PGA_j, \mu_{DS_{i+1}}, \beta_{DS_{i+1}}) \right) \cdot N_{PGA_j}^{OBS} - N_{DS_i, PGA_j}^{OBS} \right|}{N_{PGA_j}^{OBS}} \quad (11)$$

In particular, $err_{i,j}$ is the difference in absolute terms between predicted ($E_{i,j}$) and observed ($O_{i,j}$) numbers of buildings subjected to j^{th} PGA value and belonging to DS_i , divided by the observed number of buildings subjected to the same PGA value ($N_{PGA_j}^{OBS}$). Thus, for each building class $N_{DS} \times N_{PGA}$ values of $err_{i,j}$ have been evaluated for both LSE and MLE regression models.

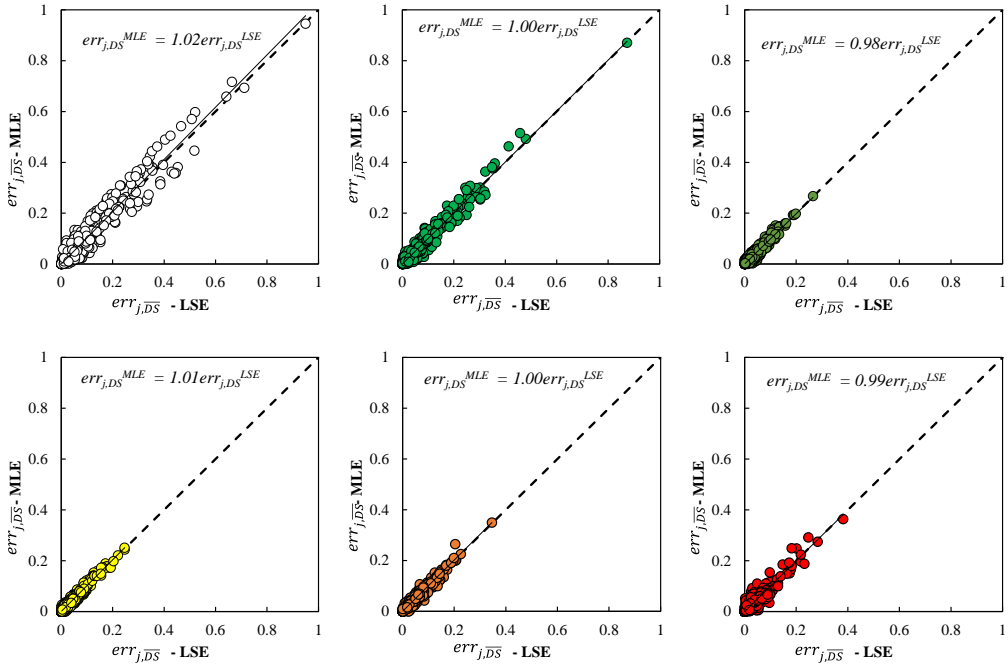


Figure 80. Comparison between LSE and MLE regression models in terms of error given the DS.

Such errors are reported in Figure 80, distinguishing in the 5+1 DSs (so, each plot is related to a given DS). Thus, for a given DS the direct comparison between error provided by the two regression approaches has been shown, being the coordinates of each point just the errors deriving from LSE (abscissa) and MLE (ordinate) procedure. In the picture, also the bisector is reported: thus, if data point belongs to this line, the same error is provided by the two considered approaches. Conversely, if data point is over or under the line, a greater error is for, respectively, MLE or LSE approach.

It should be noted that the obtained values do not differ much from the bisector, highlighting a very similar behaviour between the two regression approaches. Regardless of the used approach, the major errors are for lower DSs (namely, DS0 and DS1), conversely lower errors are obtained for the remaining DS (namely, 0-30% for DS2-3 and 0-40% for DS4-5).

In each plot is reported the linear regression equation that binds the errors provided by the two approaches, according to the following notation:

$$err_{j,DS}^{MLE} = A \times err_{j,DS}^{LSE} \quad (12)$$

We can note that A coefficient (ratio between the MLE error and the LSE one), ranging from 0.98 to 1.02, is very close to the 1, regardless of the DS, confirming the similarity between the two models.

Once deafened that there are no big differences, in the following elaboration only MLE approach has been used. In fact, such approach in one hand (1) provides on average the same error as LSE model; in the other hand (2) in the assumption of multinomial likelihood function allows to derive fragility curves also starting from very small sample. In fact, such approach is able to consider simultaneously all DSs when the optimization is performed, searching for the better values of median and logarithmic standard deviation. It means that also if the number of buildings exhibiting a certain DS is very low, the regression model is able to provide the corresponding curve, based on the assumption of multinomial distribution of the likelihood function.

7.3.2 Critical review of obtained fragility trends

In the follow, only the results provided by MLE regression model have been analysed. In fact, (1) only small differences (in term of fragility curves, predicted DPMs and error) between the two considered approaches have been detected; thus, the fragility trends are substantially common to the two approaches. (2) The few differences in terms of error highlight that on average a larger error is generated when LSE approach is used. So, the analysis of the fragility trends has been presented only with reference to the lognormal parameters obtained by means of MLE regression model.

Thus, in Figure 81 lognormal parameters (namely, median PGA at each DS and the logarithmic standard deviation) of Table 29 have been graphically represented, distinguishing as a function of vertical structure, horizontal structure and construction age. In particular, the first column of plots is related to BQ masonry, whereas the second one to the GQ masonry. Each horizontal structural type is denoted by a different symbol (reported in the legend). Lastly, the construction age is reported in the abscissa axis. Each row of plots refers to a different lognormal parameter (from median PGA at DS1 to median PGA at DS5 and logarithmic standard deviation β , in that order).

Starting from BQ classes, we can note that:

- at lower DSs (namely, DS1 and DS2) the same hierarchy between horizontal structural types and construction ages identified in terms of mean damage (Section 6.3) and vulnerability curves (Section 6.4) has been confirmed also in terms of median PGA. Thus, median PGA increases going from vaults to rigid slabs and going from buildings constructed before 1919 to those built thereafter.
- For the remaining DSs (i.e., from DS3 to DS5) the hierarchy between horizontal structural types changes, resulting the semi-rigid (rather than rigid) slab the less fragile typology, especially for buildings constructed in 1962-1971 period.
- The logarithmic standard deviation mostly ranges between 0.56-0.88. The only “outlier” is β value for BQ-S class built in 1962-1971 period, that exceed 1.

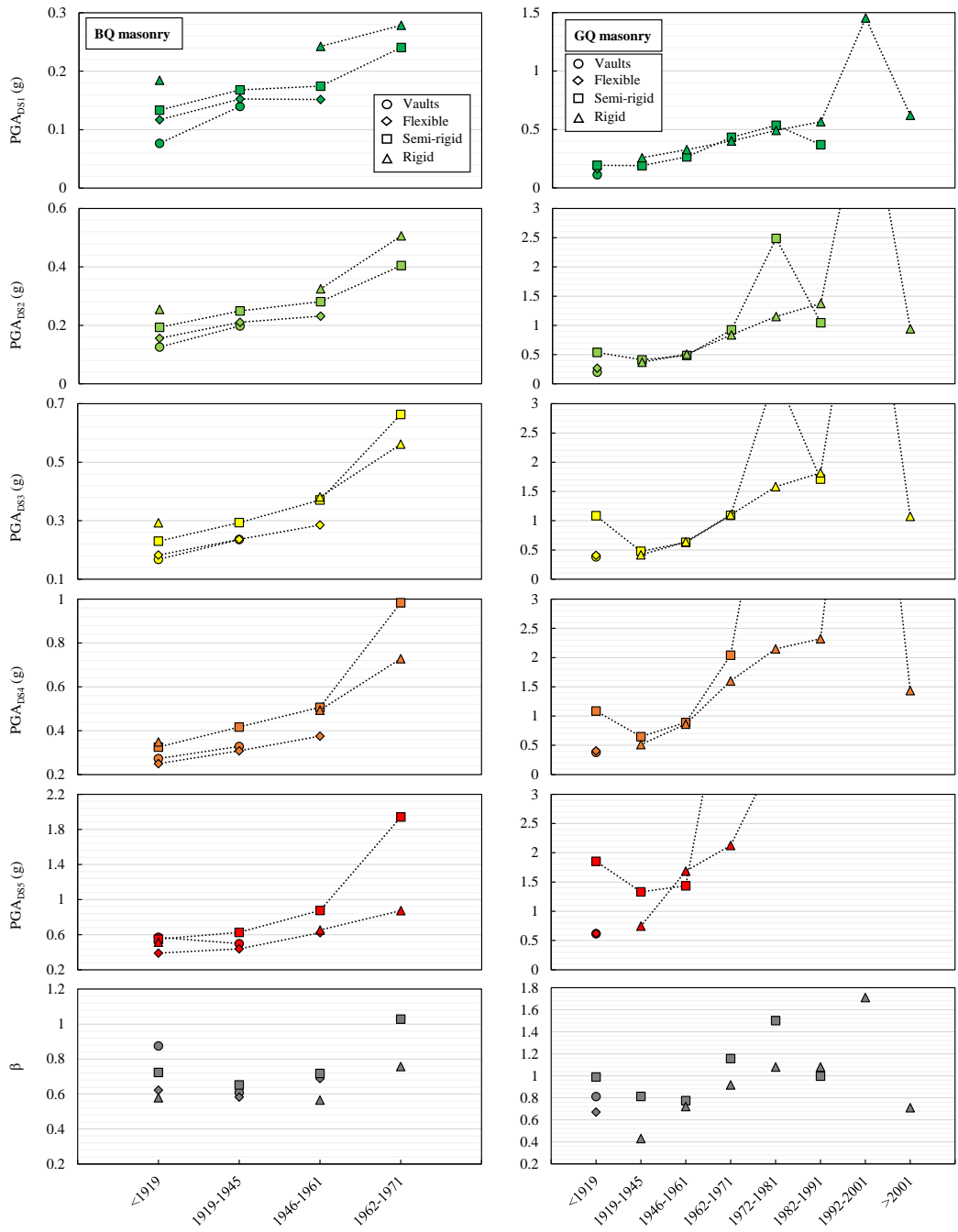


Figure 81. Lognormal parameters for as-built classes.

For what concerns GQ classes, despite the general similarity between obtained median PGAs of semi-rigid and rigid classes, some unexpected trends (especially in terms of construction age) are shown in Figure 81. In particular:

- already for the lower DS (namely, DS1 and DS2), an irregular trend in terms of construction age is observed for GQ-R class built in the most recent periods (i.e., 1982-1991; 1992-2001; >2001). In fact, median PGA gradually increases up to 1982-1991 period, showing an average increase of about 22% for each period. Then there is a significant increase (157%) in 1992-2001 period, and lastly a remarkable decrease (57%) in the last period. Such unexpected trend is even more evident for higher DSs, providing extremely high variations of median PGA.
- Similar considerations can be done considering GQ-S classes built in 1962-1971, 1972-1981 and 1982-1991 periods. As matter of fact, also for such class median PGA (from DS2 to DS5) first gradually increases with construction age, then remarkable variations are observed for 1972-1981 and 1982-1991 periods.
- GQ-R class built in 1919-1945 period shows a very lower median PGA at DS5 respect to GQ-S built in the same period, despite such classes are characterized by almost the same mean damage (Section 6.3) and vulnerability curves (Section 6.4).
- Moreover, GQ-S class built before 1919 seems to be more fragile than the same classes constructed in the following. Actually, such dubious trend has been obtained also in terms of mean damage (Section 6.3) and vulnerability curves (Section 6.4).
- GQ-V and GQ-F classes (available only for <1919 period) show a very similar median PGA at each DS.
- The logarithmic standard deviation mostly ranges between 0.67-1.16. The only “outliers” are β values for GQ-S class built in 1972-1981 period and GQ-R class built in 1992-2001 period, that largely exceed 1.2, and GQ-R class built in 1919-1945 period, which is much lower than 0.6.

7.3.3 Conditioned MLE regression model

It should be noted that the analysed lognormal parameters are basically the outcomes of a numerical procedure (i.e., *maximum likelihood estimation*) that provides the optimum solution among the infinite possible ones. Such regression model is based on the assumption that the optimum solution is that with maximum likelihood value. As above explained, MLE procedure searches the optimum solution (i.e., the six lognormal parameters, $\theta_{DS1}, \theta_{DS2}, \theta_{DS3}, \theta_{DS4}, \theta_{DS5}, \beta$), maximizing the likelihood function, herein assumed multinomial one.

In doing so, the obtained values could be influenced by the number of iterations or also by the assumed tolerance. In particular, the optimum solution could differ from the actual one because the maximum number of iterations has been attained before to find it, or also because too large tolerance has been assumed. Thus, it is relevant to assume a high number of iterations and a quite strict tolerance: in this work, 10000 iterations and a tolerance equal to 10^{-8} have been considered.

Nevertheless, it could happen that a different combination of the six lognormal parameters ($\theta_{DS1}, \theta_{DS2}, \theta_{DS3}, \theta_{DS4}, \theta_{DS5}, \beta$) provides almost the same optimization (namely, a very high likelihood value) and, simultaneously, also the expected hierarchy between classes.

Thus, in order to derive the optimum solution that also complies the trends derived in terms of mean damage (Section 6.3) and vulnerability curves (Section 6.4), hierarchy constraints have been introduced in the regression model.

In particular, the constraints have been applied on the median parameters, ensuring the same hierarchy in terms of structural typology and construction age derived by means of vulnerability curves. Clearly, if the median values change, also the corresponding logarithmic standard deviation provided by the optimization procedure changes.

In Figure 82 and Figure 83, the lognormal parameters obtained under such assumptions (i.e., “*conditioned*” MLE model) have been compared with those previously derived by means of “*unconditioned*” MLE model, distinguishing between BQ and GQ as-built classes.

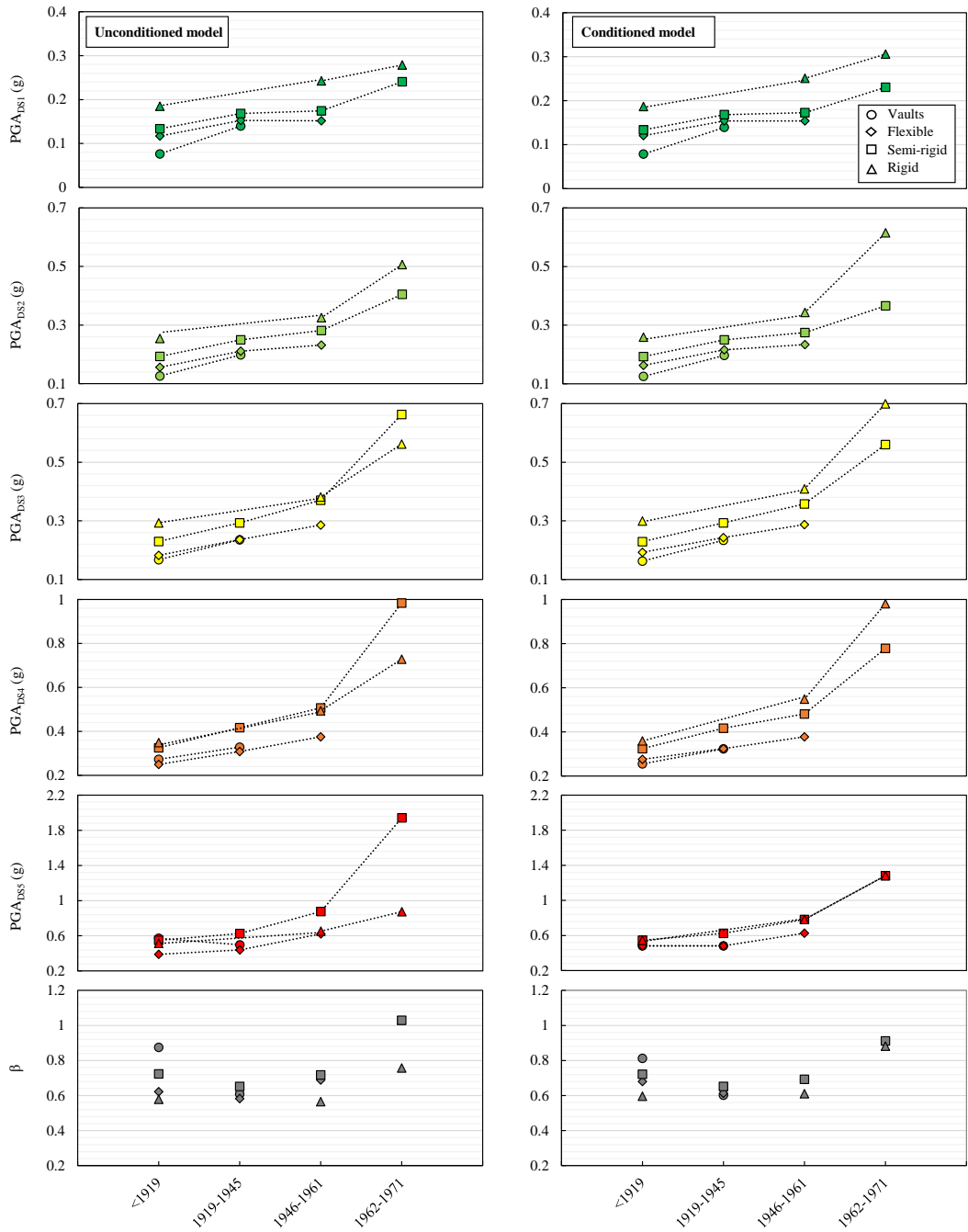


Figure 82. Lognormal parameters for as-built BQ classes, according to *unconditioned* and *conditioned* models.

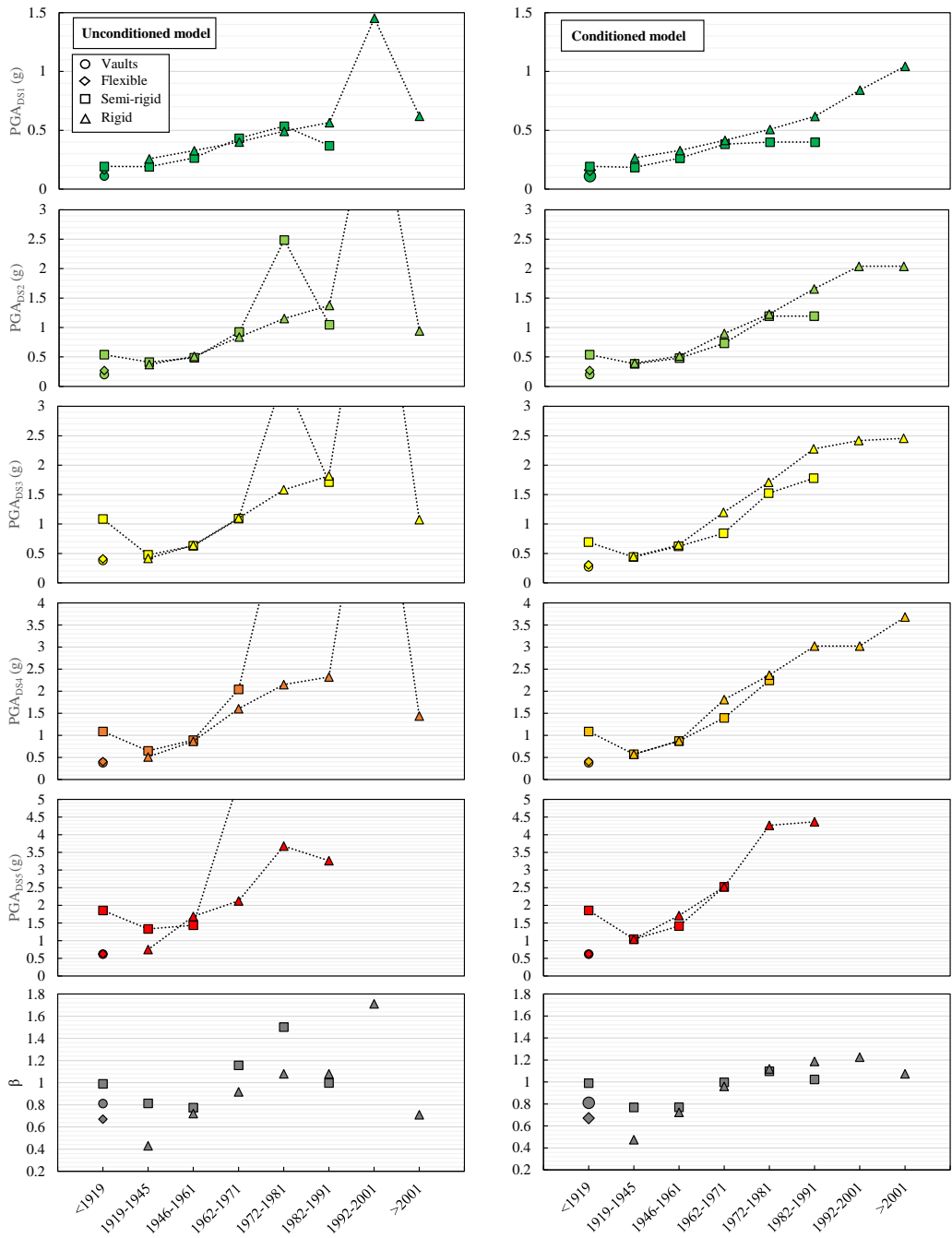


Figure 83. Lognormal parameters for as-built GQ classes, according to *unconditioned* and *conditioned* models.

For what concerns BQ classes (Figure 82), the constraints on median values lead to:

- clearly, median PGA values denoted by the same hierarchy observed on vulnerability curves in terms of construction age and horizontal structural type.
- logarithmic standard deviation for all classes ranges between 0.6 and 0.91. Thus, the constraint on median PGAs also affects the β values, leading to a reduction (respect to the *unconditioned* model) especially for BQ-S class built in 1962-1971 period.

Similarly, for what concerns GQ classes (Figure 83), the constraints on median values allow to:

- overcome the issue about the presence of large variations in the median PGA values varying the period of construction (especially for GQ-S classes built between 1972 and 1981, and for GQ-R classes built between 1992 and 2001).
- Again, the constraint on median PGAs also affects the β values. In fact, the range of variation of β results narrower, going from 0.43-1.71 (for *unconditioned* model) to 0.47-1.23 (for *conditioned* one).
- No constraint in terms of construction age has been applied on GQ-S buildings constructed before 1919, because also the corresponding mean damage (Section 6.3) and vulnerability curve (Section 6.4) seem to not respect such hierarchy.

Lognormal parameters of all (i.e., BQ + GQ) as-built classes obtained under such assumptions (so-called *Conditioned* MLE model), shown in Figure 82 and Figure 83, are summarized in Table 30 and Table 31, as a function of masonry quality, construction age, and horizontal structural type. Overall, the *conditioned* MLE model constrains in an explicit way the median PGA values at each DS, introducing indirectly a constraint also for β value to find the optimum solution. In particular, such explicit constraints based on obtained damage/vulnerability trends of Chapter 6 allow to restrict the β variability range, resulting particularly favourable because narrower β range allows to avoid or at least limit the presence

of crossing curves (Porter, 2018). Clearly to ensure no crossing curves and an ordinal hierarchy between curves, constant β values (Kircher et al., 2006; FEMA, 2012; Karababa and Pomonis, 2011; Coburn and Spence, 2003; Del Gaudio et al., 2019) should be imposed not only for all DSs but also for all building's classes.

Therefore, to check the eventually presence of crossing curves, the comparison between curves has been done for each given DS, as a function of the period of construction and the horizontal structural type.

In particular, Figure 84 compares fragility curves of all BQ classes built in the same period, varying the horizontal structural type; whereas Figure 85 compares the curves of a given BQ structural class varying the construction age.

Similarly, Figure 86 and Figure 87 provide the same comparison for GQ classes, considering (in Figure 86) only the horizontal structural typologies available for several periods of construction (i.e., GQ-S and GQ-R) and (in Figure 87) discarding the periods after 1981 (being herein available only the GQ-R structural class).

Table 30. Lognormal parameters (median and logarithmic standard deviation) for each as-built BQ building class, according to *conditioned* MLE approach.

Building Class		Conditioned MLE technique						
		θ_{DS1} (g)	θ_{DS2} (g)	θ_{DS3} (g)	θ_{DS4} (g)	θ_{DS5} (g)	β	
BQ	<1919	V	0.08	0.13	0.16	0.25	0.48	0.81
		F	0.12	0.16	0.19	0.28	0.48	0.68
		S	0.13	0.19	0.23	0.32	0.54	0.72
		R	0.19	0.26	0.30	0.36	0.54	0.60
		V	0.14	0.20	0.23	0.32	0.48	0.60
	1919-45	F	0.15	0.22	0.24	0.32	0.48	0.61
		S	0.17	0.25	0.29	0.42	0.63	0.65
		F	0.15	0.23	0.29	0.38	0.63	0.69
	1946-61	S	0.17	0.27	0.36	0.48	0.78	0.69
		R	0.25	0.34	0.41	0.55	0.78	0.61
	1962-71	S	0.23	0.37	0.56	0.78	1.28	0.91
		R	0.31	0.62	0.70	0.98	1.28	0.88

Table 31. Lognormal parameters (median and logarithmic standard deviation) for each as-built GQ building class, according to *conditioned* MLE approach.

Building Class		Conditioned MLE technique					β
		θ_{DS1} (g)	θ_{DS2} (g)	θ_{DS3} (g)	θ_{DS4} (g)	θ_{DS5} (g)	
GQ	V	0.11	0.20	0.27	0.38	0.62	0.81
	<1919 F	0.16	0.27	0.31	0.41	0.62	0.67
	S	0.19	0.54	0.69	1.09	1.85	0.99
	1919-45 S	0.19	0.38	0.44	0.57	1.04	0.77
	R	0.27	0.39	0.45	0.57	1.04	0.47
	1946-61 S	0.27	0.48	0.62	0.87	1.41	0.77
	R	0.33	0.51	0.64	0.87	1.71	0.72
	1962-71 S	0.38	0.73	0.84	1.39	2.52	1.00
	R	0.42	0.90	1.20	1.81	2.52	0.96
	1972-81 S	0.40	1.19	1.52	2.24	-	1.10
	R	0.51	1.23	1.71	2.36	4.27	1.12
	1982-91 S	0.40	1.19	1.78	-	-	1.02
	R	0.62	1.66	2.28	3.02	4.36	1.19
	1992-2001 R	0.84	2.04	2.42	3.02	-	1.23
	>2001 R	1.05	2.04	2.46	3.68	-	1.07

It should be noted that no crossing curves are mainly observed for BQ classes (Figure 84; Figure 85) at least in the considered PGA range (0-0.5 g), despite the different β logarithmic standard deviation (ranging from 0.60 to 0.91). Only in a small number of cases (namely, BQ-R at DS1 and BQ-V at DS5 in Figure 84), some crossings are observed.

For what concerns GQ classes (Figure 86; Figure 87), the curves related to GQ-R class built in 1919-1945 period intersect the remaining ones. In particular, in Figure 86 the curves of such class at lower DSs (namely, DS1 and DS2) intersect ones related to the remaining construction ages. Similarly, in Figure 87 it can be observed the presence of crossing curves at each DS between GQ-R and GQ-S classes built in 1919-1945 period. It should be noted that GQ-R-1919-1945 is the only class (among all GQ ones) with a very low β value (i.e., 0.47), whereas for all the remaining GQ classes the logarithmic standard deviation ranges between 0.67 and 1.19 (see Table 31). Thus, such crossing curves could be due to different β value.

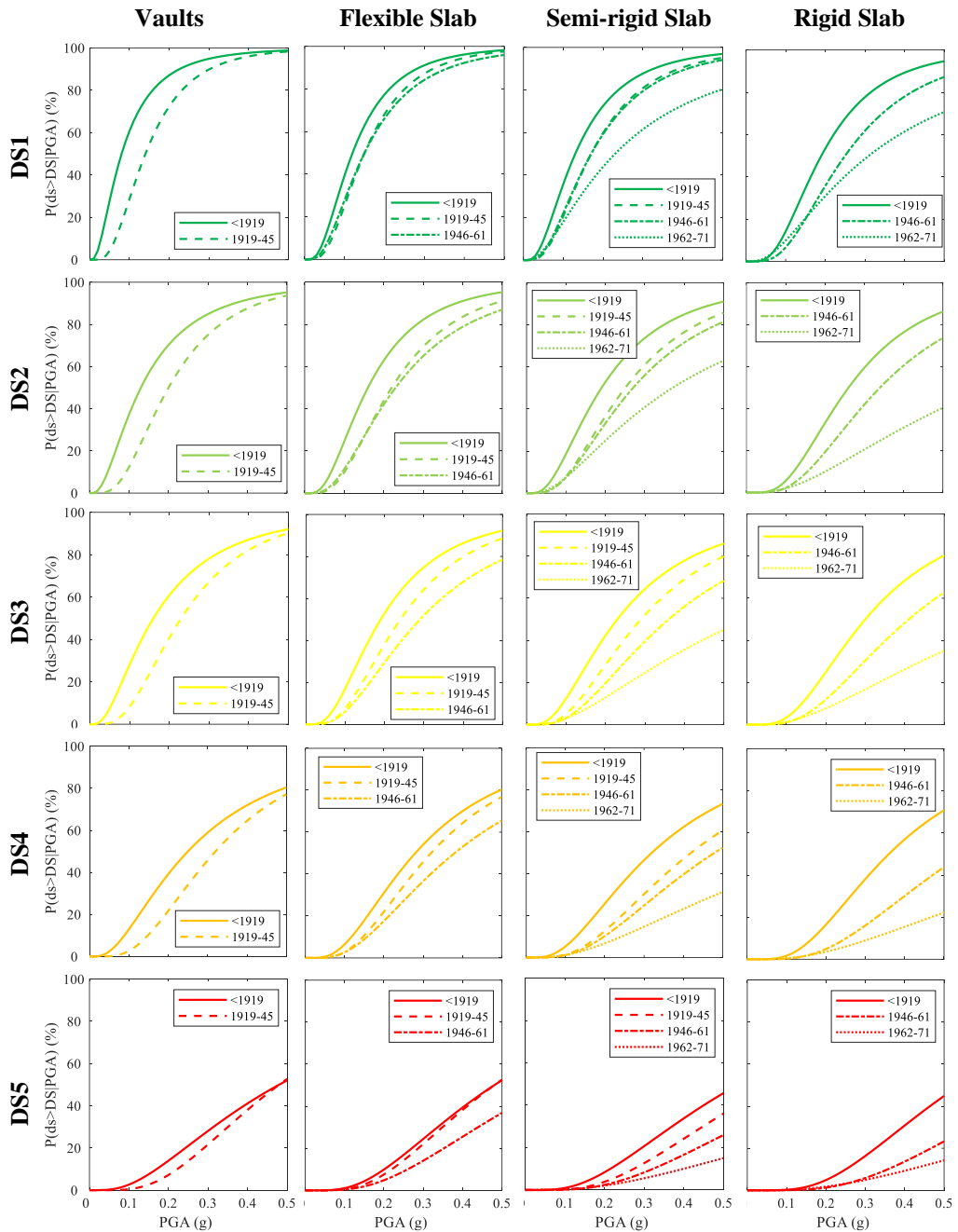


Figure 84. Comparison between fragility curves of BQ classes, given the DS and the construction age, as a function of horizontal structure.

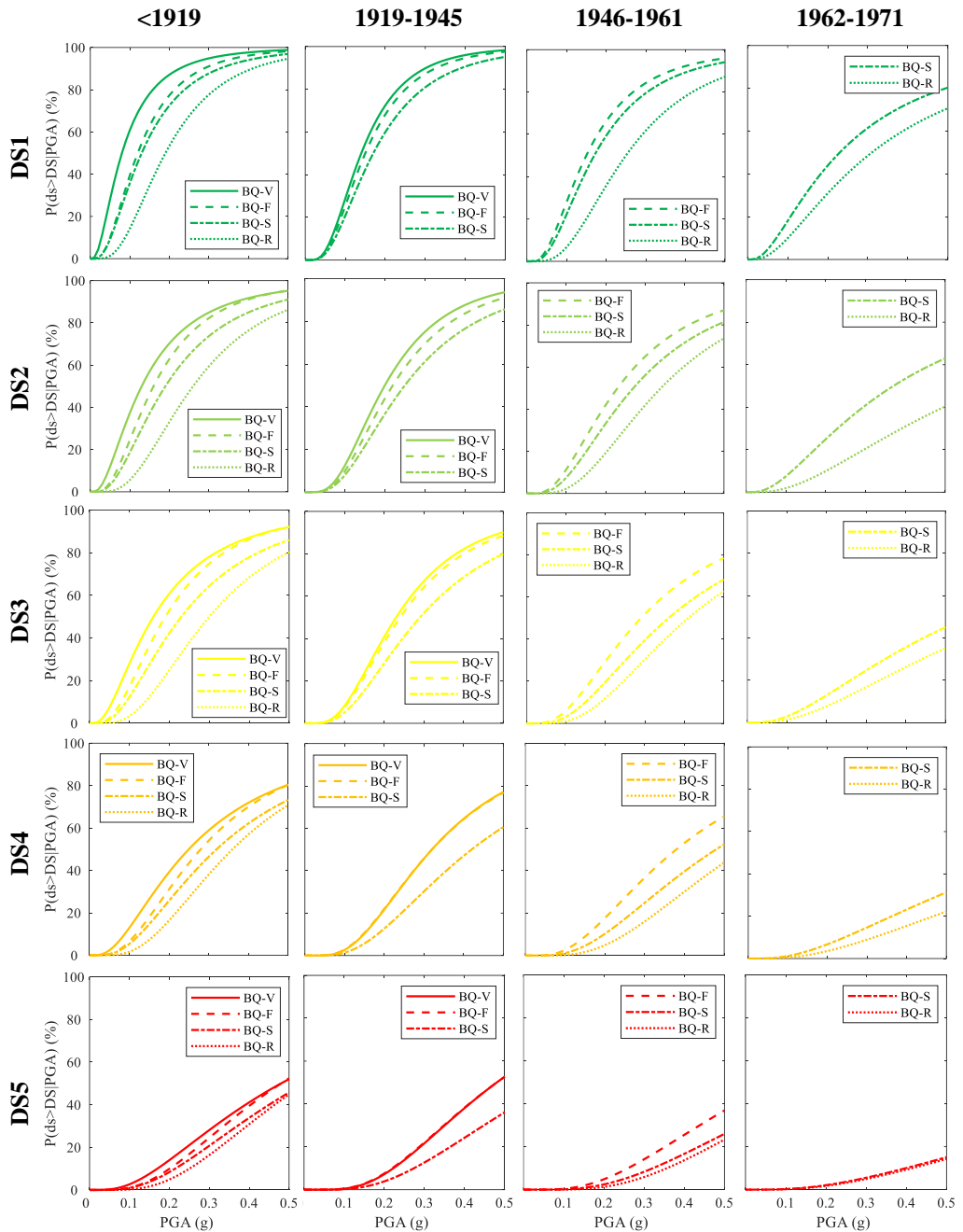


Figure 85. Comparison between fragility curves of BQ classes, given the DS and the horizontal structure, as a function of construction age.

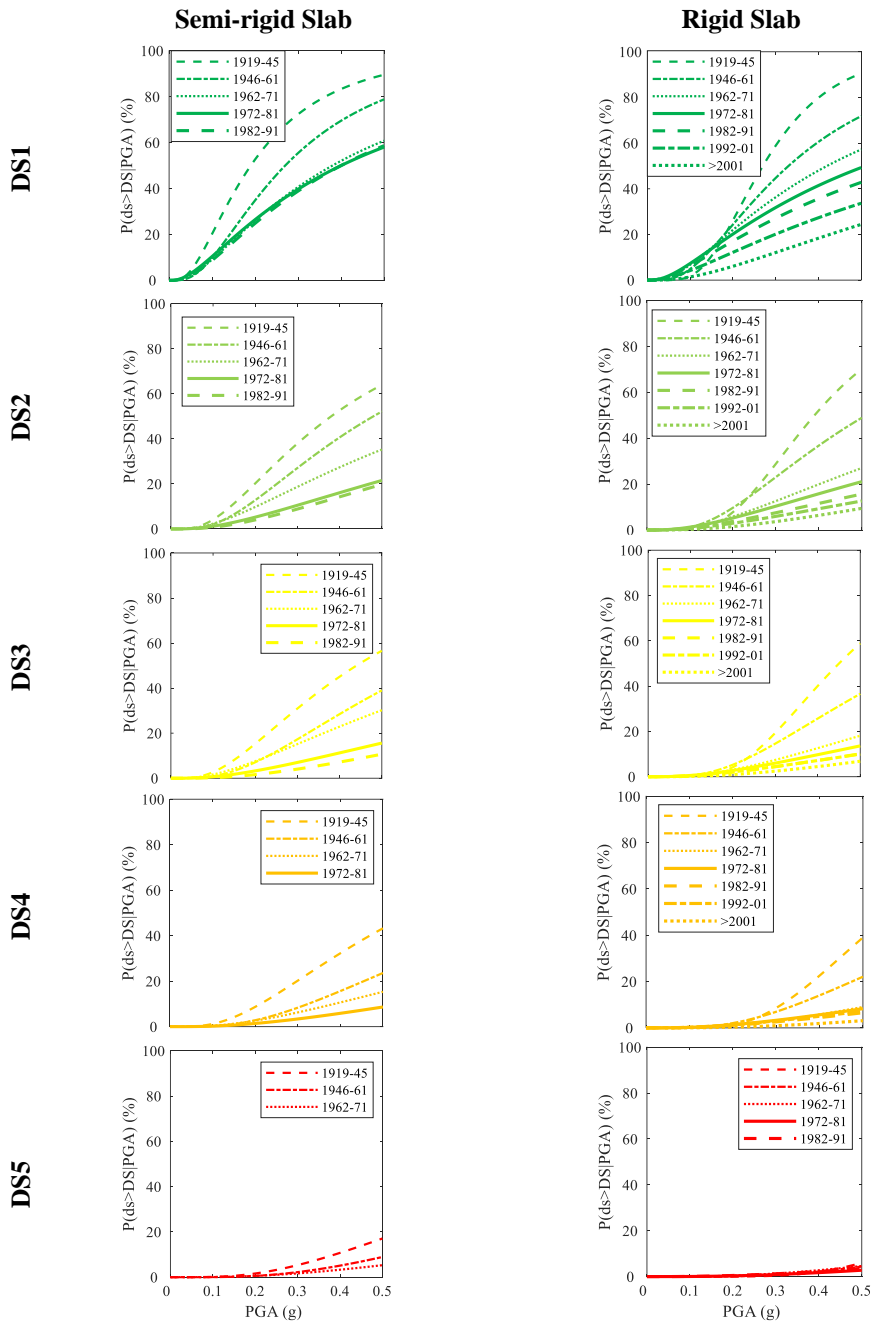


Figure 86. Comparison between fragility curves of GQ classes, given the DS and the construction age, as a function of horizontal structure.

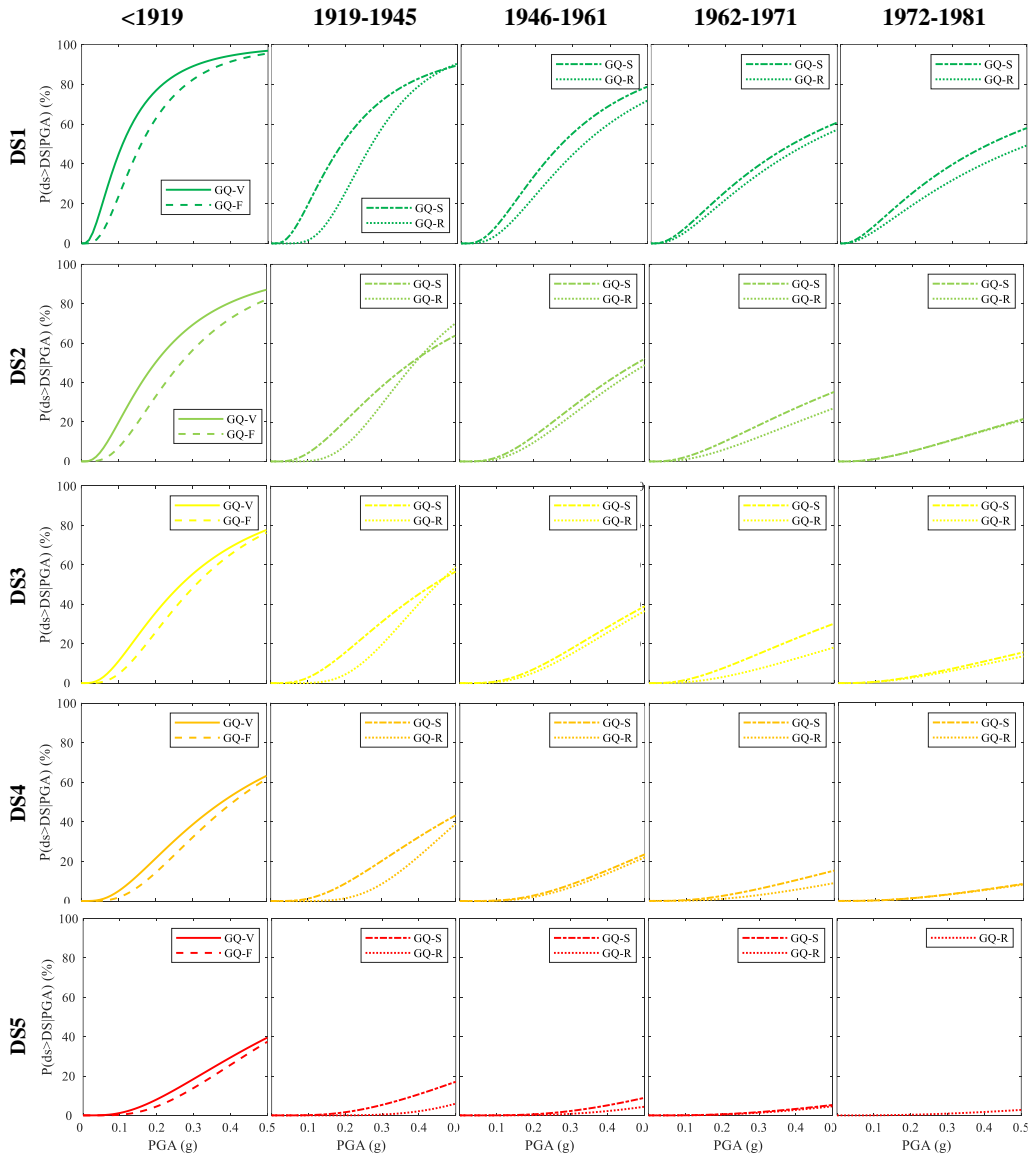


Figure 87. Comparison between fragility curves of GQ classes, given the DS and the horizontal structure, as a function of construction age.

7.3.4 *Conditioned*(β) MLE regression model

As above mentioned, only a constant β logarithmic standard deviation value (imposed not only for all DSs but also for all building's classes) can ensure no crossing curves between building's classes, allowing an ordinal hierarchy between curves. In the previous paragraph, where the so-called *conditioned* model has been applied, some crossing curves (mainly, GQ-R and GQ-S classes built in 1919-1945 period) are obtained.

Thus, in addition to the two previously analysed models (namely, *Unconditioned* and *Conditioned* MLE models), a third approach, so-called *Conditioned*(β) model, is herein introduced to overcome the presence of crossing curves. Basically, starting from the *Conditioned* MLE model, a further constraint is introduced in the fitting procedure, assuming a constant logarithmic standard deviation (Kircher et al., 2006; FEMA 2012; Karababa and Pomonis 2011; Coburn and Spence 2003; Del Gaudio et al., 2019) for all classes with the same masonry quality.

In Figure 88, Figure 89, and Figure 90, fragility curves obtained according to the three considered regression models are compared, given the building class and the DS. Lognormal parameters for the *Unconditioned* and *Conditioned* models have been above provided (Table 29 for the first one; Table 30 and Table 31 for the second one), whereas those related to the *Conditioned*(β) model are shown in Table 32. It should be noted that a major part of differences between the curves derived under different assumptions is about DS5, typically the less populated one. Basically, the constraints introduced in the *Conditioned* and *Conditioned*(β) MLE models mostly affect the curve's shape, when the corresponding observed data (i.e., the number of buildings in a given DS) is quite limited. Conversely, very little differences can be observed for the most populated classes, especially at lower DSs.

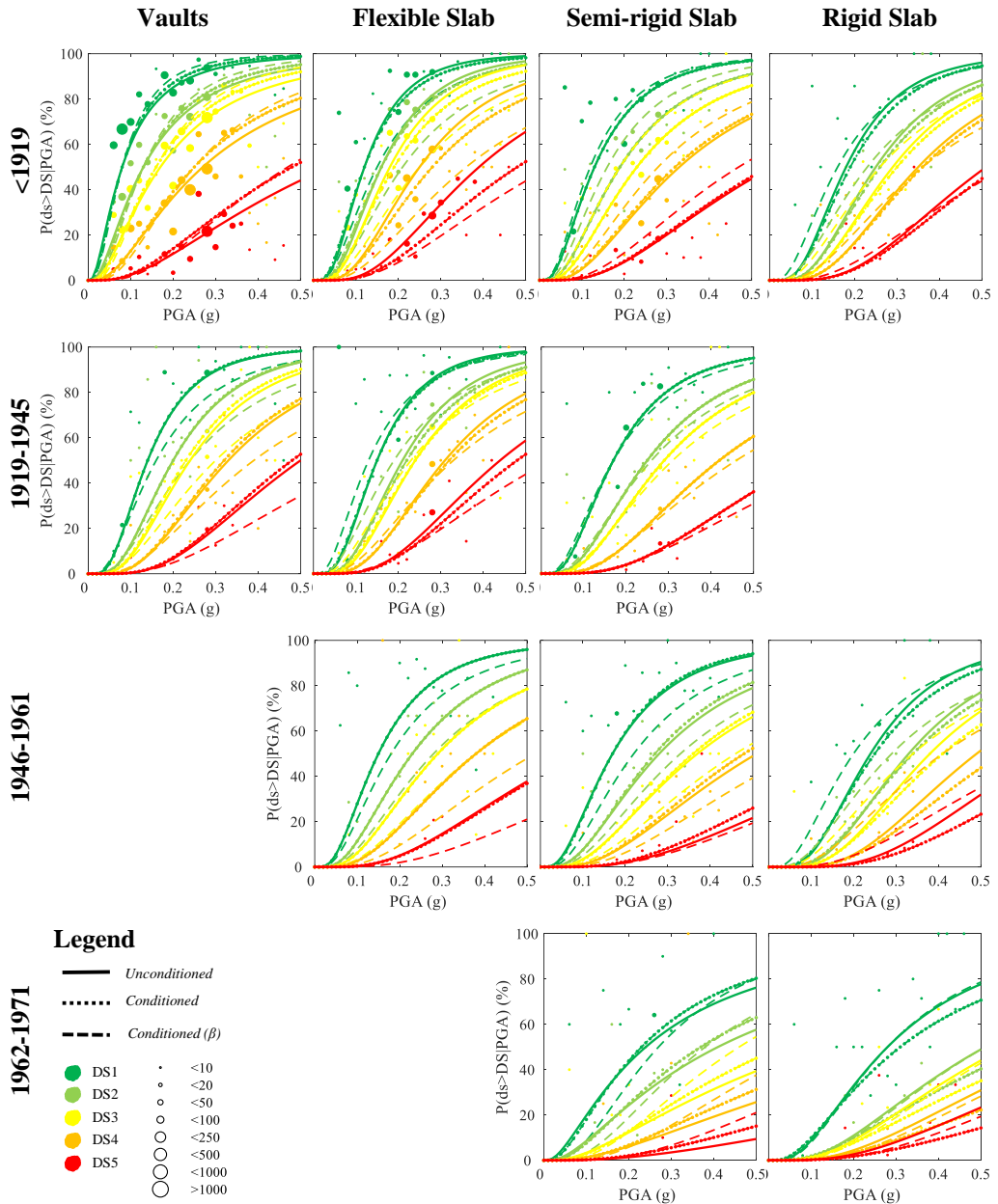


Figure 88. Fragility curves for all BQ classes given the construction age and the horizontal structures, according to the three considered models.

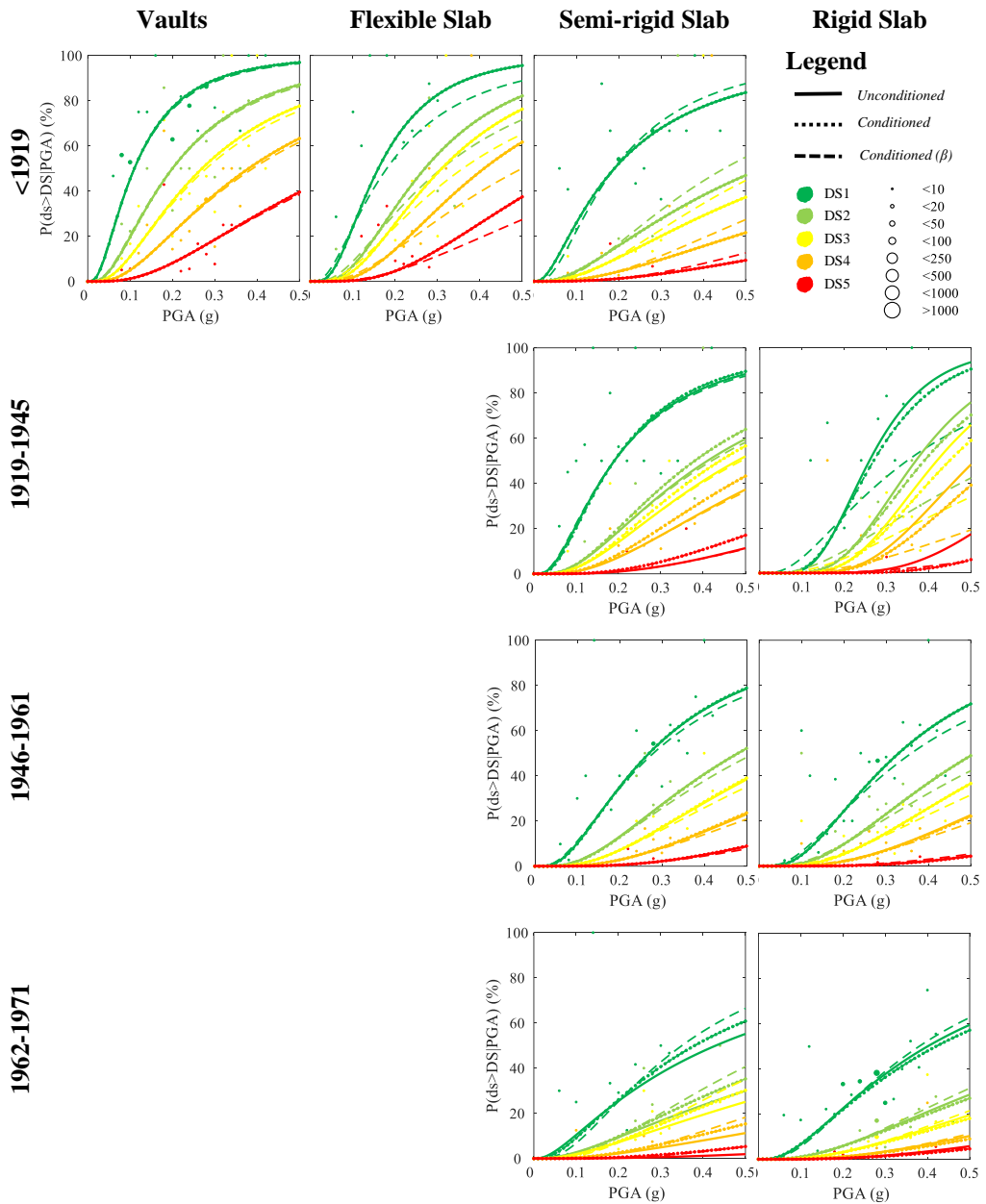


Figure 89. Fragility curves for GQ classes (built until 1971) given the construction age and the horizontal structures, according to the three considered models.

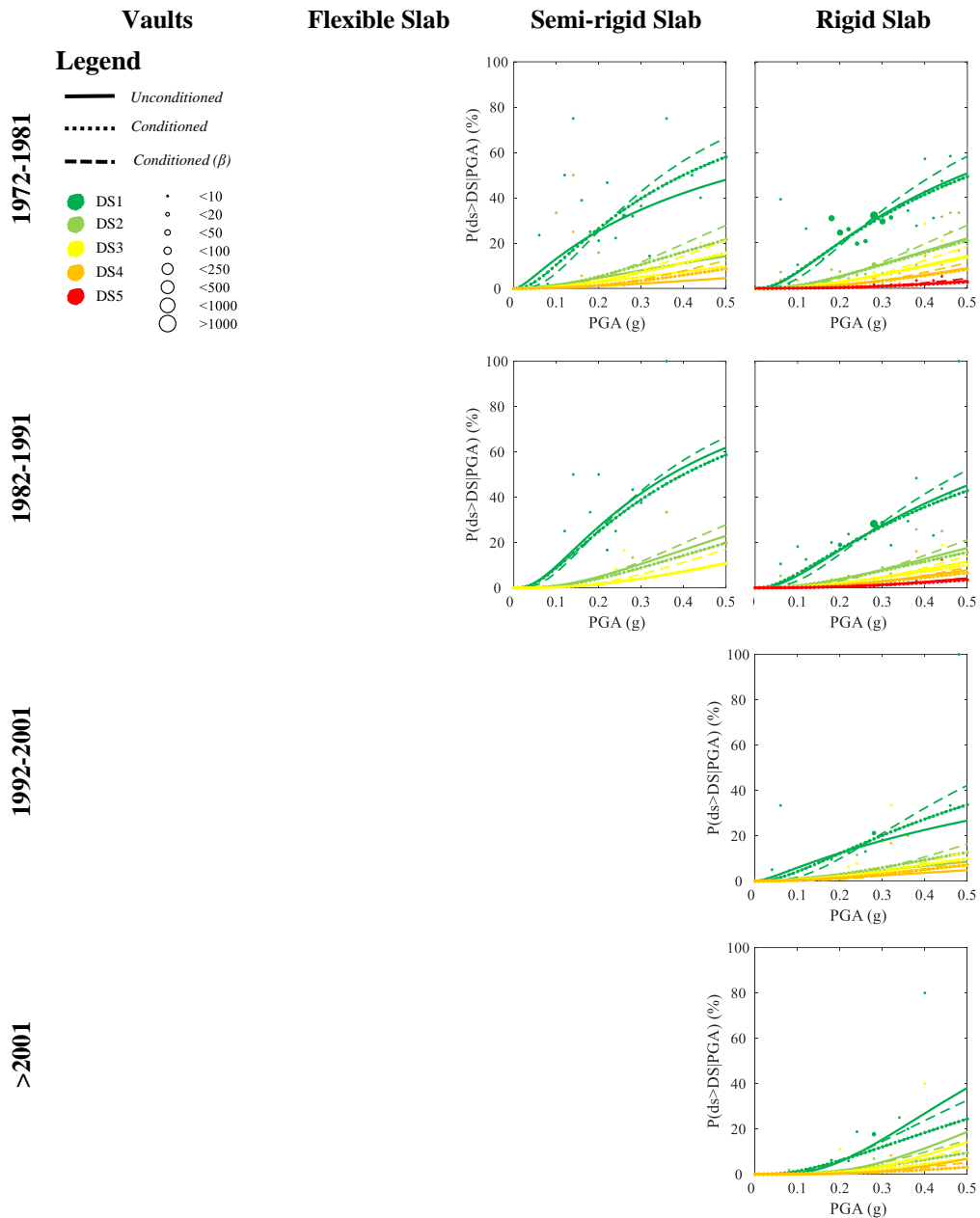


Figure 90. Fragility curves for GQ classes (built after 1971) given the construction age and the horizontal structures, according to the three considered models.

Table 32. Lognormal parameters (median and logarithmic standard deviation) for each as-built building class, according to *Conditioned* (β) MLE model.

Building Class		<i>Conditioned</i> (β) MLE technique					β
		θ_{DS1} (g)	θ_{DS2} (g)	θ_{DS3} (g)	θ_{DS4} (g)	θ_{DS5} (g)	
BQ	<1919	V	0.08	0.13	0.16	0.25	0.47
		F	0.12	0.16	0.19	0.28	0.47
		S	0.13	0.19	0.23	0.33	0.56
		R	0.20	0.29	0.34	0.41	0.66
	1919-45	V	0.15	0.21	0.25	0.36	0.56
		F	0.16	0.23	0.26	0.36	0.56
		S	0.17	0.26	0.31	0.46	0.72
	1946-61	F	0.16	0.24	0.30	0.39	0.67
		S	0.18	0.28	0.38	0.52	0.90
		R	0.27	0.38	0.46	0.63	0.90
	1962-71	S	0.22	0.33	0.46	0.61	0.94
		R	0.28	0.51	0.57	0.76	0.94
GQ	<1919	V	0.11	0.2	0.28	0.39	0.64
		F	0.18	0.31	0.36	0.5	0.83
		S	0.19	0.45	0.56	0.83	1.31
	1919-45	S	0.19	0.42	0.49	0.67	1.4
		R	0.35	0.59	0.71	1.04	1.93
	1946-61	S	0.28	0.52	0.69	0.99	1.66
		R	0.36	0.59	0.75	1.04	1.93
	1962-71	S	0.35	0.61	0.69	1.07	1.93
		R	0.38	0.75	0.97	1.38	1.93
	1972-81	S	0.35	0.82	0.98	1.32	-
		R	0.42	0.82	1.06	1.38	2.1
	1982-91	S	0.35	0.82	1.11	-	-
		R	0.48	0.98	1.24	1.54	2.1
	1992-2001	R	0.59	1.14	1.29	1.55	-
	>2001	R	0.73	1.19	1.39	1.95	-

Among the two considered conditioned models (namely, *Conditioned* and *Conditioned*(β)), the first one provides on average curves most similar to those of *unconditioned* model. Such result is due to the fact that for many building's classes the hierarchy between median PGA values is respected already in the

unconditioned model. Thus, the constraint on median PGAs is effective only for a limited number of classes, causing different curves (respect to the *unconditioned* model) only for these latters. Conversely, the constant β value (in the *Conditioned*(β) model) for all classes denoted by the same masonry quality, is a constraint effective for all building's classes. In this case, the major differences respect to the *unconditioned* model are related to the classes with high β variation between the two models.

Comparing lognormal parameters of Table 29 (*Unconditioned* model) with those of Table 32 (*Conditioned*(β) model), we can note that the higher β variation is about GQ-R(1919-1945) class, going from 0.43 to 0.84, leading to significant differences in the corresponding curves (see Figure 89).

7.3.5 Mean error evaluation

Lastly, in order to quantify the difference between the three considered (*unconditioned*, *conditioned*, *conditioned*(β)) models and then the influence of each assumption (i.e., constraint on median PGA and constant β value), again the error between observed and predicted DPMs are evaluated for each building's class, given the i^{th} DS and the j^{th} PGA value, according to the above explained equation (11), referred to here:

$$err_{i,j} = \frac{|E_{i,j} - O_{i,j}|}{\sum_{i=1}^{N_{DS}} O_{i,j}} = \frac{\left| \left(\logncdf(PGA_j, \mu_{DS_i}, \beta_{DS_i}) - \logncdf(PGA_j, \mu_{DS_{i+1}}, \beta_{DS_{i+1}}) \right) \cdot N_{PGA_j}^{OBS} - N_{DS_i, PGA_j}^{OBS} \right|}{N_{PGA_j}^{OBS}} \quad (11)$$

$err_{i,j}$ is the difference in absolute terms between predicted ($E_{i,j}$) and observed ($O_{i,j}$) numbers of buildings subjected to j^{th} PGA value and belonging to DS_i , divided by the observed number of buildings subjected to the same PGA value ($N_{PGA_j}^{OBS}$). Basically, such error is the difference between the expected and the observed ($N_{DS_i, PGA_j}^{OBS} / N_{PGA_j}^{OBS}$) occurrence frequency of each DS. In Figure 91 the observed and predicted DPMs of BQ-V(<1919) class are shown, by way of example.

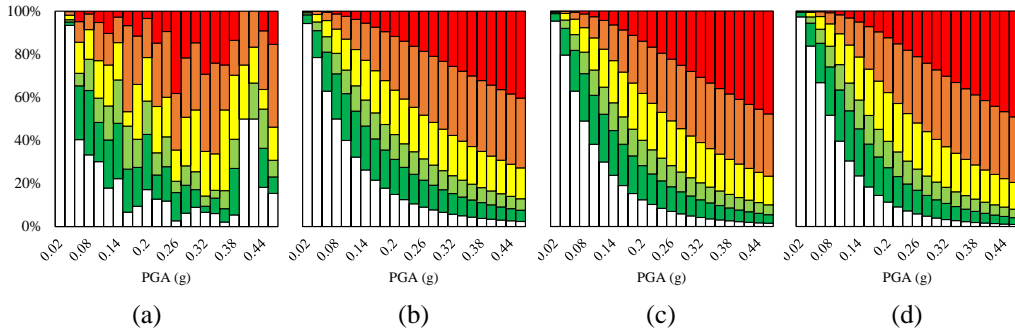


Figure 91. Observed (a) DPMs of BQ-V(<1919) class and those predicted by (b) *unconditioned*, (c) *conditioned*, and (d) *conditioned*(β) MLE models.

Clearly, the trend described by observed DPMs (Figure 91(a)) are not perfectly regular, increasing the PGA value. However, one can recognize the increasing percentage of higher DSs, increasing the intensity measure value. Such general trend is provided also by predicted DPMs (Figure 91(b-d)). Comparing the three predicted distributions, we can note that:

- *Conditioned* model overestimates the number of buildings at higher DSs (especially at DS5) for high PGA values, respect to the *Unconditioned* model;
- *Conditioned*(β) model slightly overestimates the number of buildings in DS0 for lower PGA values, respect to the *Conditioned* model;
- Thus, the major differences are observed between *Unconditioned* and *Conditioned*(β) model.

In Figure 92, the mean value of $err_{i,j}$ for each given DS is provided, for the considered class, using different colors for the three regression models (i.e., blue for *unconditioned* model, orange for *conditioned* one, grey for *conditioned*(β) model). Mean error exceeds 10% only at DS0 and DS5, regardless to the regression model. In fact, comparing the predicted DPMs with observed ones, the most evident difference is related to high PGA values, where all regression models overestimate the number of buildings in DS5, underestimating the number in DS0.

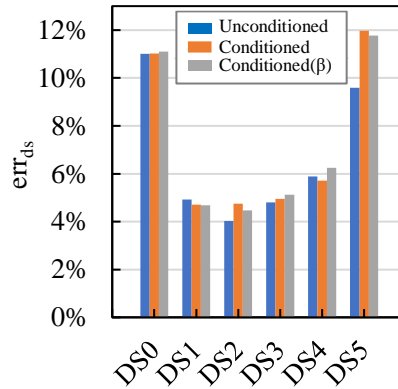


Figure 92. Mean error for BQ-V(<1919) class, according to the three considered regression models.

Despite the introduction of constraints in the *conditioned* and *conditioned(β)* models, almost the same error is provided by the three models, except at DS5. In fact, as above highlighted, both the conditioned models cause a further overestimation of buildings in DS5 (for higher PGA values), respect to the *unconditioned* model.

In the Appendix A, the mean error given the DS, herein explained with reference to the BQ-V(<1919) class, is provided for all as-built classes. The error variation between *unconditioned* model and the two conditioned ones is quite limited, reaching at most a few percentage points. In particular, the *conditioned* model leads to a maximum increment of error equal to 2% (see Appendix A); whereas *conditioned(β)* model can cause an increase of mean error up to 4%.

Thus, the greater part of the error (namely, part common to all considered models) is related to use of MLE regression model, whereas the (limited) variations in the error between the three considered models are due to the specific assumptions of each of them. Clearly, the introduction of constraints in the conditioned models causes variations (typically increase at lower DSs) in the mean error respect to the *unconditioned* one, with major variations for *Conditioned(β)* model, because more constrained than the *Conditioned* one. Nevertheless, such variations are quite limited, being the DPMs predicted by the three models quite similar each other's.

7.3.6 Influence of damage conversion rules

Fragility curves obtained in the previous paragraphs are basically the final output of the procedure explained in Figure 75. Such procedure allows to describe for a given building class, the seismic fragility first in a discrete form by means of DPMs, and then also in a continuous form (i.e., fragility curves), using a fitting technique. Clearly, the entire procedure is based on the assumption that the damage of each building belonging to the considered building class is known, being defined in a univocal way. In particular, it is assumed that the damage observed after the earthquake on vertical structures (reported in the AeDES form) can be converted in a damage description consistent with the European Macroseismic scale (Grünthal, 1998). Such conversion between damage of vertical structures and damage related to the entire building is herein based on damage conversion rules of Rota et al., 2008 (Table 19).

Clearly, the choice of the damage metric (i.e., the conversion rule to go from damage provided by the survey form for a given structural element to the building damage consistent with EMS-98 scale) is a crucial issue and could significantly influence the shape of the following fragility curves. Thus, it deserves to be further investigated, considering other proposals available in the literature.



Figure 93. EMS'98 scale damage levels (Grünthal, 1998) for masonry buildings.

Damage levels provided by Grünthal, 1998 for masonry buildings are (Figure 93): D0, no damage; D1, negligible or slight non-structural damage; D2, moderate damage (slight structural damage and moderate non-structural damage); D3, from substantial to heavy damage (moderate structural damage and heavy non-structural damage); D4, very heavy damage (heavy structural damage and very heavy non-structural damage); D5, total collapse (very heavy structural damage). Such description is related to the entire masonry building. Conversely, survey form used after the earthquake provides the damage observed on several structural and non-structural elements.

As highlighted in the Chapter 6, only the damage observed on vertical structures is considered in the present work to describe the building's damage, because the maximum damage is mostly attained by these structures (rather than horizontal or roof ones). In Table 33, damage conversion rules introduced by Rota et al., 2008 are summarized, associating to each damage description of the AeDES form (composed by damage level and its extent) the corresponding value consistent with the macroseismic scale.

It should be noted that such conversion does not consider the possible presence of more damage levels simultaneously. Conversely, it considers only the maximum damage level among observed ones. By way of example, Rota et al., 2008 classifies as DS4 all buildings in which less than 1/3 of vertical structures shows D4-D5 damage, regardless of the damage observed on the remaining 2/3.

In Table 33, in addition to these rules, also the proposal of Dolce et al., 2019 is provided. One can note that the main difference between the two considered damage metrics is about the damage description deriving from a multi-choice criterion. In fact, going back to the previous example, the damage level consistent with EMS-98 is assigned by Dolce et al., 2019, taking into consideration not only the maximum observed damage (i.e., D4-D5 on 1/3 of the vertical structures), but also the damage of the remaining portion. So, if at least 1/3 of the remaining elements shows for example D2-D3 damage, DS4 is assigned, otherwise DS3.

Table 33. Damage conversion rules by Rota et al., 2008 and Dolce et al., 2019.

	Damage Level (AeDES form)				Damage State (Rota et al., 2008)	Damage State (Dolce et al., 2019)
	D4 - D5	D2 - D3	D1	No Damage		
				✓	0	0
			< 1/3		1	1
			1/3 - 2/3		1	1
			> 2/3		1	1
Damage extension (AeDES form)		< 1/3			2	2
		< 1/3	< 1/3		2	2
		< 1/3	1/3 - 2/3		2	2
		< 1/3	> 2/3		2	2
		1/3 - 2/3	< 1/3		3	3
		1/3 - 2/3	1/3 - 2/3		3	3
		1/3 - 2/3			3	3
		> 2/3			3	3
		> 2/3	< 1/3		3	3
	< 1/3				4	3
	< 1/3		< 1/3		4	3
	< 1/3		1/3 - 2/3		4	3
	< 1/3		> 2/3		4	3
	< 1/3	< 1/3			4	3
	< 1/3	< 1/3	< 1/3		4	3
	< 1/3	1/3 - 2/3			4	4
	< 1/3	> 2/3			4	4
	1/3 - 2/3				4	4
	1/3 - 2/3		< 1/3		4	4
	1/3 - 2/3		1/3 - 2/3		4	4
	1/3 - 2/3	< 1/3			4	4
	1/3 - 2/3	1/3 - 2/3			4	5
	> 2/3				5	5
	> 2/3		< 1/3		5	5
	> 2/3	< 1/3			5	5

In Table 33, the bold type is used to highlight the differences between the two considered metrics. Basically, the conversion of Rota et al., 2008 overestimates the number of buildings in DS4 compared to that of Dolce et al., 2019, underestimating slightly the buildings in DS5 and remarkably those in DS3.

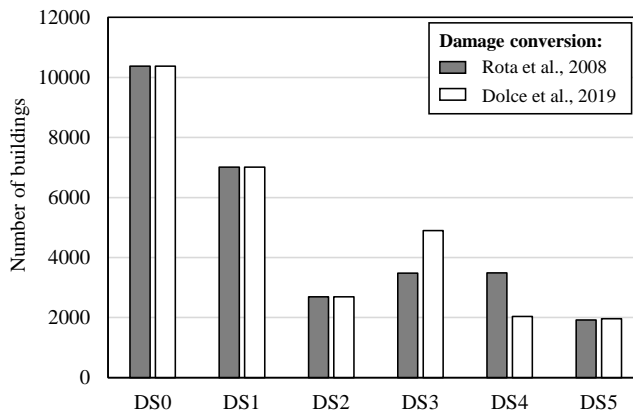


Figure 94. Number of buildings in each damage states according to Rota et al., 2008 and Dolce et al., 2019 conversion rules.

Such result is confirmed by Figure 94, where the number of buildings in each damage states according to the two considered damage metrics is provided. We can note that the number of buildings in the first damage states (from DS0 to DS2) is the same for both the conversion rules, whereas very slight differences are observed at DS5. Thus, the actual difference between the two conversion rules is clustered in the DS3-DS4 damage states, being that of Rota et al., 2008 the most conservative one.

In Figure 95, mean damage has been evaluated for each as-built building class using Dolce et al., 2019 conversion rules (white symbols), making a comparison with the corresponding values obtained by means of Rota et al., 2008 conversion (grey symbols). Each plot is related to a given horizontal structure (i.e., vaults, flexible-, semi-rigid-, and rigid-slabs); different vertical structures (i.e., good or bad quality masonries) are indicated with different symbols (rhombus and circle, respectively), and the period of construction is reported on the x-axis.

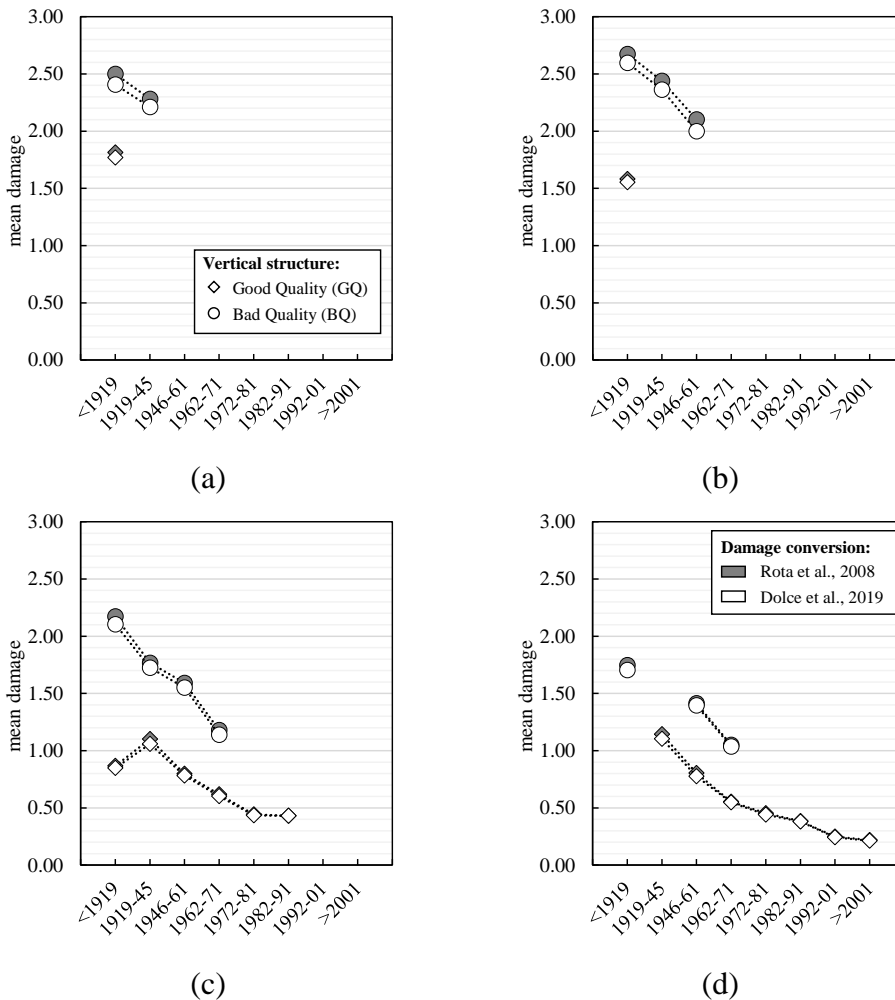


Figure 95. Mean damage of as-built classes (a- vaults; b- flexible slabs; c- semi-rigid slabs; d- rigid slabs) according to Rota et al., 2008 and Dolce et al., 2019 conversion rules.

As expected, Rota et al., 2008's conversion provides the greater values of mean damage, because of its overestimation of DS4 (and underestimation of DS3). However, the difference in terms of mean damage is not the same for all building classes, being greater for BQ classes. Moreover, such differences decrease increasing the period of construction and going from vaults to rigid slabs. Thus, the lower the vulnerability of the building class, the lower the

difference of mean damage between the two considered conversion rules. Such result is due to the fact that most vulnerable classes (namely, those characterized by high values of mean damage) are those with more buildings in the higher damage states, and as above explained the difference between the two metrics is mainly about the DS3-DS4. Basically, the higher the weight of higher DSs, the higher the difference of mean damage between the two metrics.

However, mean damage is the weighted average of the observed damage, thus the differences due to the adopted metric are quite small, reaching just 5%. A similar argument is related to the corresponding vulnerability curves, being also these latter an average representation of the damage. Conversely, higher differences are expected on fragility curves because each of them is related to a given DS.

In Figure 96, Figure 97 and Figure 98, fragility curves of as-built classes are shown. Such curves have been derived according to *Conditioned(β)* model, using both the considered damage conversion rules (dashed lines for Rota et al., 2008, and solid lines for Dolce et al., 2019). Comparing the lognormal parameters shown in Table 34 (obtained using the damage metric of Dolce et al., 2019) with those of Table 32 (Rota et al., 2008), we can note that the logarithmic standard deviation β and the median PGA values at the lower DSs are substantially the same, despite the different damage conversion rules.

Clearly, it is expected that only fragility curves related to the last two DSs change between Rota et al., 2008 and Dolce et al., 2019 metrics, being the obtained β the same for both the conversion rules. However, the greater difference is about the curve at DS4, given the conversion scheme of Table 33. Coherently with the results in terms of mean damage, the probability of exceeding DS4 is higher if the damage conversion of Rota et al., 2008 is used: in fact, the higher such probability the higher the number of buildings in DS4, being the curve at DS3 the same.

Therefore, the use of different damage conversion rules affects the obtained fragility curves. In the present paragraph, the proposal of Dolce et al., 2019 has been examined, reaching the following conclusions:

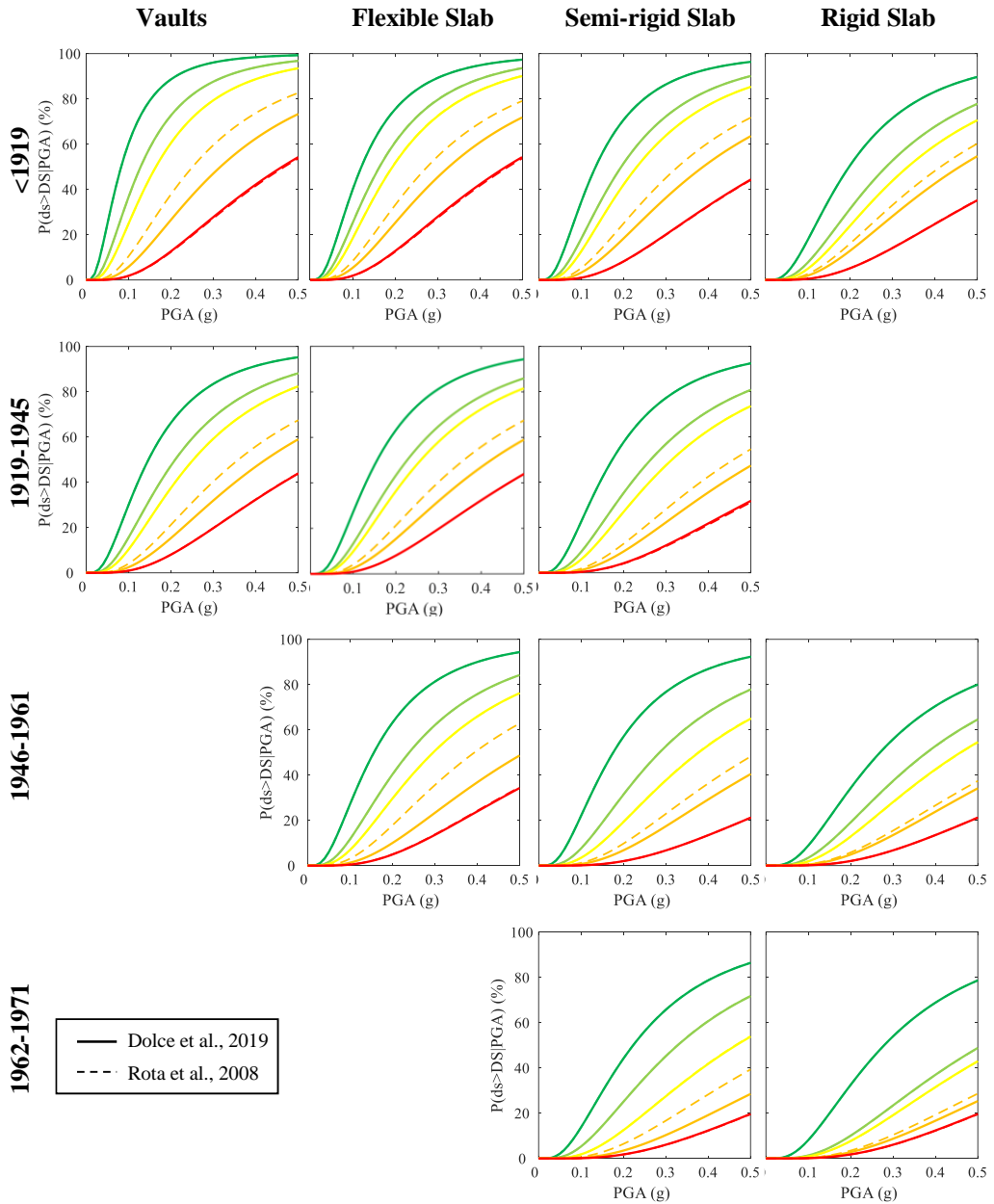


Figure 96. Fragility curves for all BQ classes given the construction age and the horizontal structures, according to Rota et al., 2008 and Dolce et al., 2019 conversion rules.

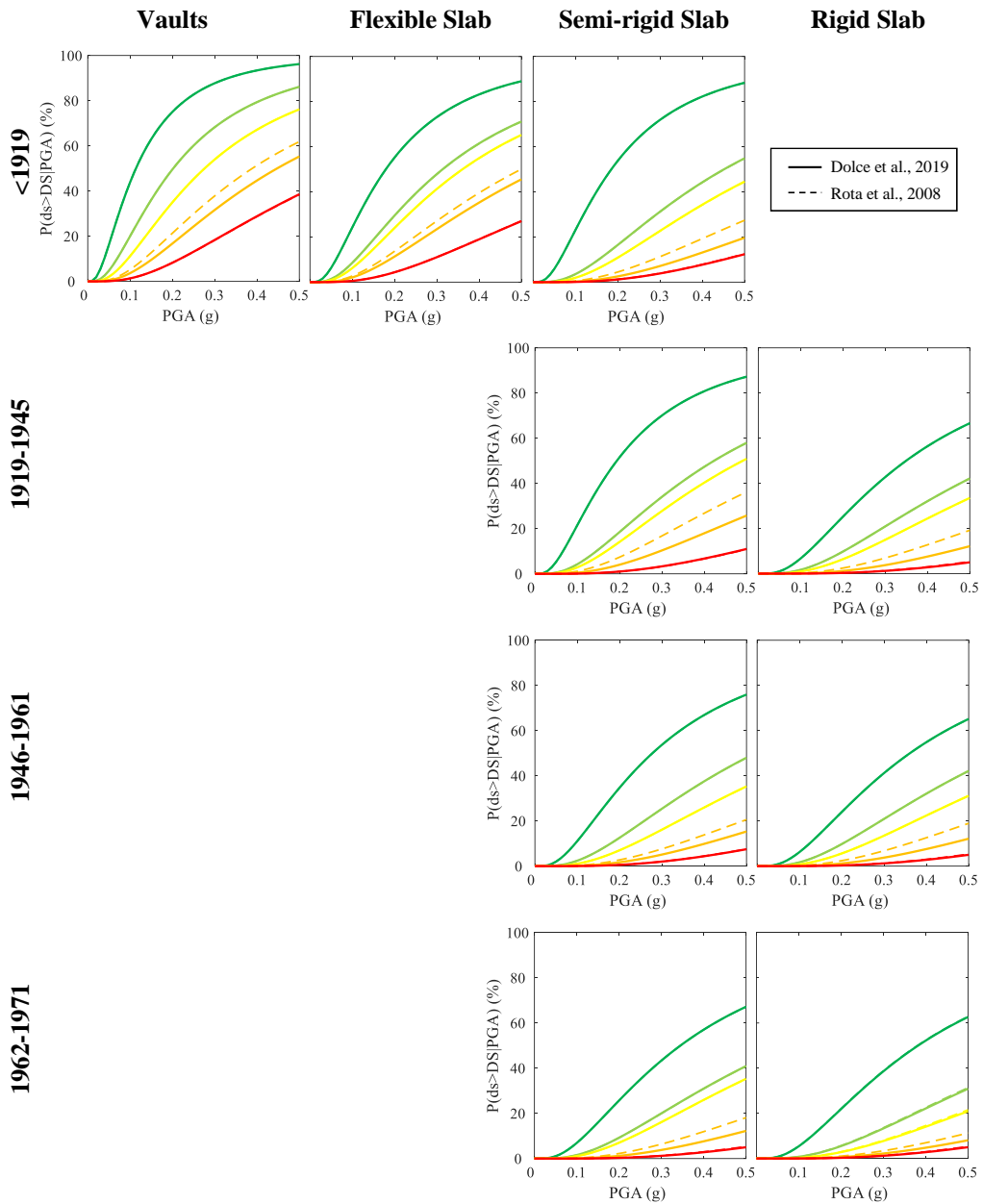


Figure 97. Fragility curves for GQ classes (built until 1971) given the construction age and the horizontal structures, according to Rota et al., 2008 and Dolce et al., 2019 conversion rules.

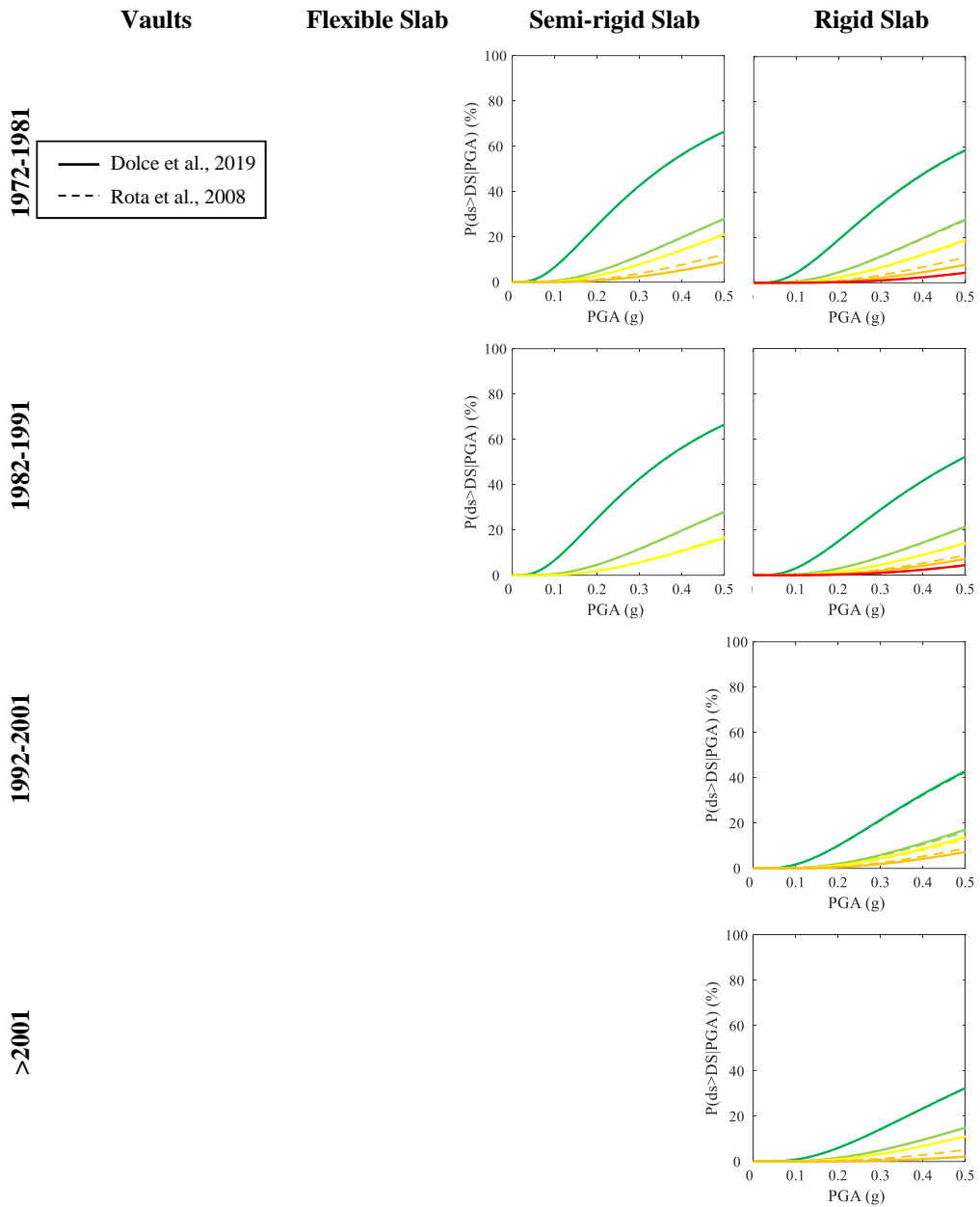


Figure 98. Fragility curves for GQ classes (built after 1971) given the construction age and the horizontal structures, according to Rota et al., 2008 and Dolce et al., 2019 conversion rules.

Table 34. Lognormal parameters (median and logarithmic standard deviation) for each as-built building class, according to damage conversion rules of Dolce et al., 2019.

Building Class		Conditioned (β) MLE technique					β	
		θ_{DS1} (g)	θ_{DS2} (g)	θ_{DS3} (g)	θ_{DS4} (g)	θ_{DS5} (g)		
BQ	<1919	V	0.08	0.13	0.16	0.32	0.46	0.73
		F	0.12	0.16	0.19	0.33	0.46	
		S	0.13	0.19	0.23	0.39	0.55	
		R	0.20	0.29	0.34	0.46	0.66	
	1919-45	V	0.15	0.21	0.25	0.42	0.56	
		F	0.16	0.23	0.26	0.42	0.56	
		S	0.17	0.26	0.31	0.52	0.71	
	1946-61	F	0.16	0.24	0.30	0.51	0.67	
		S	0.18	0.28	0.38	0.60	0.90	
		R	0.27	0.38	0.46	0.67	0.90	
	1962-71	S	0.22	0.33	0.47	0.76	0.94	
		R	0.28	0.51	0.57	0.81	0.94	
GQ	<1919	V	0.11	0.20	0.28	0.45	0.64	0.83
		F	0.18	0.31	0.36	0.55	0.83	
		S	0.18	0.45	0.56	1.02	1.31	
	1919-45	S	0.19	0.42	0.49	0.86	1.39	
		R	0.35	0.59	0.71	1.33	1.97	
		1946-61	S	0.28	0.52	0.69	1.17	
	R		0.36	0.59	0.75	1.33	1.97	
	1962-71	S	0.34	0.61	0.69	1.32	1.97	
		R	0.38	0.76	0.98	1.61	1.97	
	1972-81	S	0.35	0.81	0.98	1.55		
		R	0.42	0.81	1.04	1.62	2.07	
	1982-91	S	0.35	0.81	1.13			
		R	0.48	0.97	1.22	1.69	2.07	
	1992-2001	R	0.58	1.10	1.24	1.69		
	>2001	R	0.73	1.19	1.39	2.70		

(1) the shape of the curves does not change if Rota et al., 2008 or Dolce et al., 2019 rules are used; but (2) the median PGA at DS4 decreases using the rules of Dolce et al., 2019 rather than those of Rota et al., 2008.

7.4 FRAGILITY CURVES FOR RETROFITTED CLASSES

In the present Section, the same analysis above performed on non-retrofitted buildings has been extended also to retrofitted ones. Thus, starting from the *Unconditioned* MLE model, further two regression models have been considered, first constraining the median PGA values and then, also the logarithmic standard deviation. The aim of the *conditioned* model is to improve the numerical solution provided by the MLE regression by means of expected hierarchy between building classes, based on the results of Chapter 6. Instead, the *Conditioned*(β) model has been introduced to avoid any crossing curves between building's classes.

As shown in the Chapter 5, the greater part of retrofitted buildings is denoted by bad quality and/or irregular layout (BQ class) and has been originally built before 1919. Thus, as for mean damage and vulnerability curves evaluation (Chapter 6), also the fragility assessment has been performed only on BQ buildings constructed before 1919 and then retrofitted, distinguishing in four structural typologies (i.e., vaults, flexible-, semi-rigid- and rigid-slabs, all denoted by bad quality masonry).

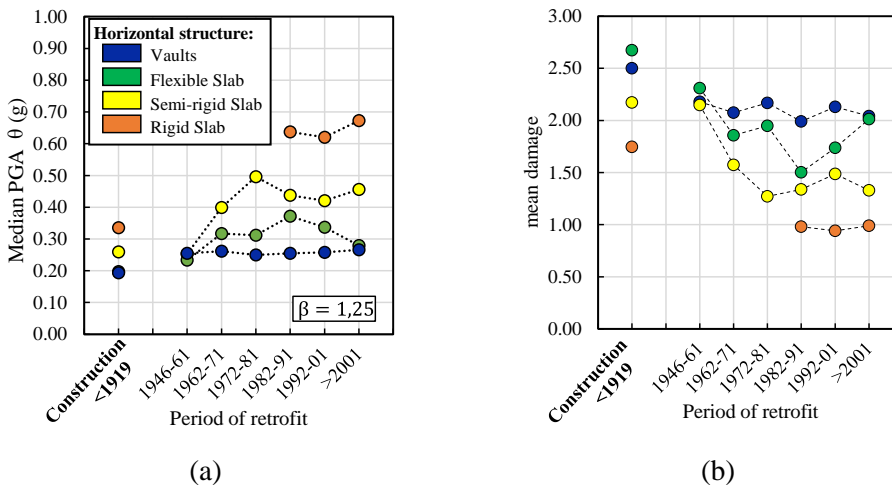


Figure 99. Median PGA (a) and mean damage (b) values for retrofitted BQ classes built before 1919 as a function of retrofit age and horizontal type (see Chapter 6 for more details).

However, fragility curves have been derived considering only two retrofit ages (i.e., <1980 and >1980). The selection of such time intervals as period of retrofit is justified by some aspects: (i) the great variability shown by the retrofitted buildings after 1981 with flexible and semi-rigid slabs in terms of mean damage (see Figure 99(b)) and vulnerability curves (see Figure 99(a)); (ii) the implications due to the intense production of technical codes focused on retrofit strategies of masonry buildings after the 1980 Irpinia and the 1984 Abruzzi earthquakes (in particular, D.M. 2/7/1981 n.593 and D.M. 24/01/1986, see Section 3.4.3 for more details). Moreover, (iii) the very high number of buildings retrofitted starting from 1980s (see Figure 100) could be due to the increasing attention toward the existing building stock, especially after the earthquakes occurred during such period.

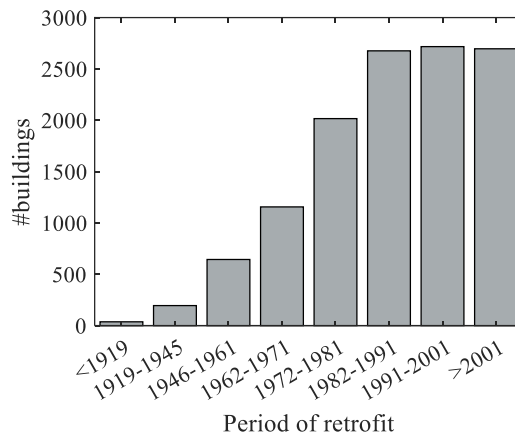


Figure 100. Number of retrofitted buildings (sited in the municipality where a building-by-building survey has been done after 2009 L'Aquila earthquake) varying the period of retrofit.

Thus, 8 retrofitted building classes are considered in the fragility assessment, combining the above mentioned four structural typologies with the two periods of retrofit. Nevertheless, as shown in the previous Chapters (namely, Chapter 5 and Chapter 6), only few buildings with rigid slabs built before 1919 have been subjected to retrofit intervention before 1980s. Thus, for such structural class,

only buildings retrofitted after 1980 have been analysed, according to vulnerability assessment (summarized in Figure 99).

7.4.1 Fragility curves according to *Unconditioned*, *Conditioned* and *Conditioned(β)* models

In Figure 101 and Table 35-Table 36-Table 37, fragility curves and the related lognormal parameters (i.e., medians, θ_{DSi} , at each DS and logarithmic standard deviation, β) according to the three considered regression (*Unconditioned*, *Conditioned* and *Conditioned(β)*) models are provided, for the available 7 retrofitted building classes.

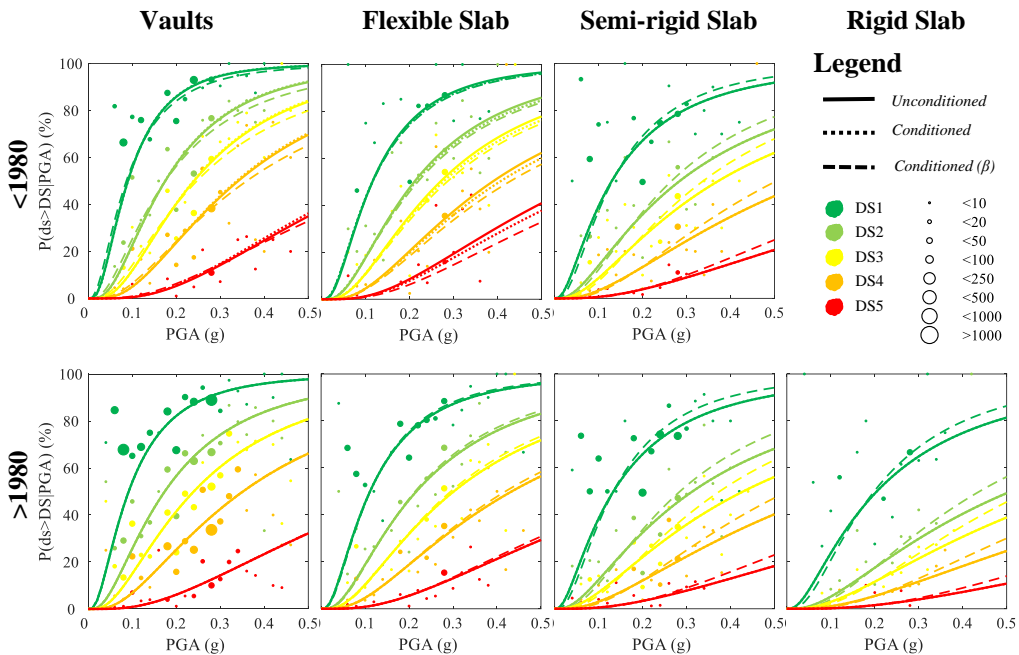


Figure 101. Fragility curves for BQ retrofitted classes built before 1919, given the retrofit age and the horizontal structures, according to the three considered models.

As explained in the previous Section (related to the as-built classes), the “degree of constraint” of considered models increases going from *Unconditioned* to *Conditioned(β)* model. In fact, the assumptions on which the models are based are:

- *Unconditioned* model: MLE regression model has been used, assuming a multinomial likelihood function and a cumulative lognormal functional form described by six parameters (namely, the median values θ_{DSi} and a common logarithmic standard deviation β for all DSs).
- *Conditioned* model: starting from the assumptions of *Unconditioned* model, a constrain on median PGA values has been imposed, ensuring the same hierarchy between horizontal structures obtained by means of damage/vulnerability assessment (summarized in Figure 99). In particular, mean damage and median PGA of vulnerability curves of Figure 99 describe a clear trend as a function of the horizontal type. Basically, mean damage in each retrofit age decreases increasing the slab stiffness, namely going from vaults to rigid slab. Similarly, the corresponding median PGA values (derived from vulnerability curves) increase, increasing the slab stiffness. Thus, the same hierarchy among horizontal structures is imposed in the present model in terms of median PGA values at each DS.
- *Conditioned(β)* model: starting from the assumptions of *Conditioned* model, a further constrain has been introduced, imposing a common logarithmic standard deviation for all above defined retrofitted classes. The aim of such assumption is to avoid the possible presence of crossing curves among considered building classes. Clearly, the output of the previous two regression models (see, Table 35 and Table 36, respectively for *Unconditioned* and *Conditioned* model) are six lognormal parameters (namely, the median values θ_{DSi} and a common logarithmic standard deviation β for all DSs) for each building class, resulting in 42 (7 classes x 6 parameters) lognormal parameters. Conversely, for the *Conditioned(β)* model, we obtain an overall number of lognormal parameters equal to the number of building classes multiplied by 5 (namely, the θ_{DSi} value at each DS for all classes), plus 1 (that is the common logarithmic standard deviation), resulting in 36 (7 classes x 5 θ_{DSi} parameters + common β value) lognormal parameters. These latter are reported in Table 37.

Table 35. Lognormal parameters (median and logarithmic standard deviation) for each retrofitted (BQ built before 1919) building class, according to *unconditioned* model.

Building Class			Unconditioned MLE technique					
			θ_{DS1} (g)	θ_{DS2} (g)	θ_{DS3} (g)	θ_{DS4} (g)	θ_{DS5} (g)	β
<1919 BQ	<1980 (R)	V	0.09	0.18	0.24	0.34	0.67	0.74
		F	0.12	0.21	0.27	0.39	0.60	0.81
		S	0.13	0.28	0.37	0.58	1.10	0.96
	>1980 (R)	V	0.09	0.17	0.24	0.35	0.74	0.84
		F	0.11	0.22	0.30	0.43	0.80	0.87
		S	0.13	0.31	0.43	0.64	1.22	0.99
		R	0.20	0.51	0.66	0.99	1.73	1.00

Table 36. Lognormal parameters (median and logarithmic standard deviation) for each retrofitted (BQ built before 1919) building class, according to *conditioned* model.

Building Class			Conditioned MLE technique					
			θ_{DS1} (g)	θ_{DS2} (g)	θ_{DS3} (g)	θ_{DS4} (g)	θ_{DS5} (g)	β
<1919 BQ	<1980 (R)	V	0.09	0.17	0.24	0.34	0.65	0.74
		F	0.11	0.21	0.28	0.40	0.65	0.83
		S	0.13	0.28	0.37	0.58	1.10	0.96
	>1980 (R)	V	0.09	0.17	0.24	0.35	0.74	0.84
		F	0.11	0.22	0.30	0.43	0.80	0.87
		S	0.13	0.31	0.43	0.64	1.22	0.99
		R	0.20	0.51	0.66	0.99	1.73	1.00

Table 37. Lognormal parameters (median and logarithmic standard deviation) for each retrofitted (BQ built before 1919) building class, according to *conditioned(β)* model.

Building Class			Conditioned(β) MLE technique					
			θ_{DS1} (g)	θ_{DS2} (g)	θ_{DS3} (g)	θ_{DS4} (g)	θ_{DS5} (g)	β
<1919 BQ	<1980 (R)	V	0.09	0.18	0.25	0.36	0.73	0.84
		F	0.12	0.22	0.28	0.43	0.73	
		S	0.13	0.27	0.34	0.50	0.88	
	>1980 (R)	V	0.09	0.17	0.24	0.35	0.73	
		F	0.11	0.21	0.30	0.42	0.76	
		S	0.13	0.29	0.38	0.53	0.93	
		R	0.20	0.44	0.55	0.78	1.24	

Comparing lognormal parameters obtained by means of *Unconditioned* and *Conditioned* models, one can observe a very little difference. Basically, going from the *Unconditioned* model to the *Conditioned* one, only parameters of BQ-V and BQ-F classes retrofitted before 1981 slightly change. Such result is due to the fact that a major part of median PGA values provided by *Unconditioned* model is already consistent with the expected trend.

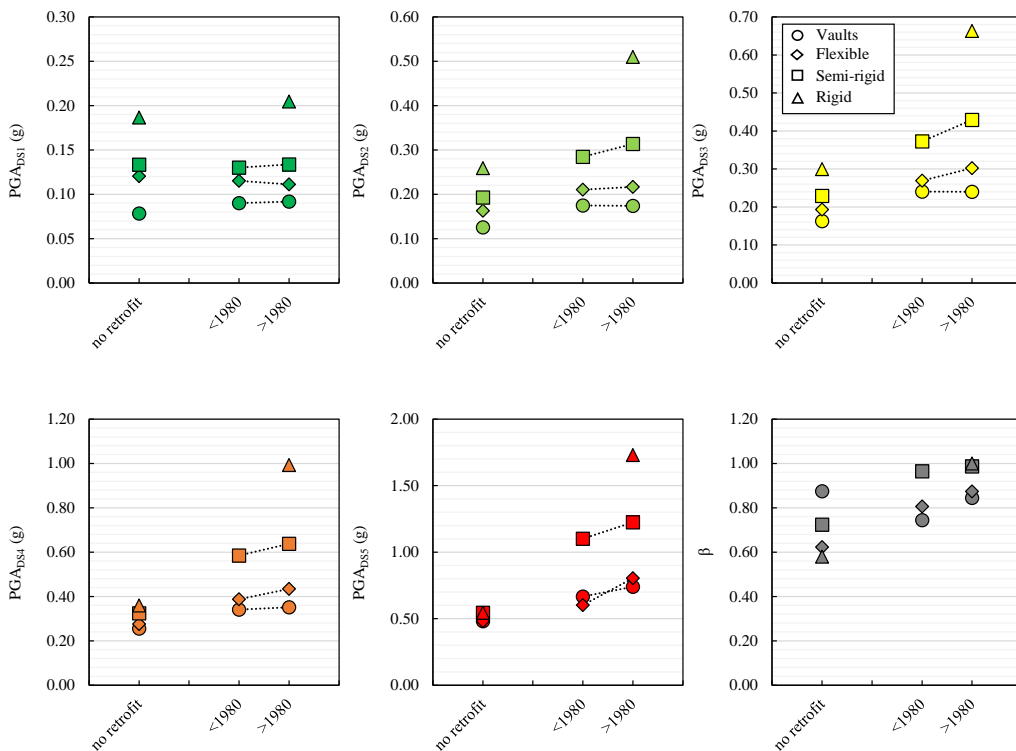


Figure 102. Lognormal parameters for retrofitted BQ classes built before 1919, according to *Unconditioned* model.

In Figure 102, lognormal parameters obtained using the *Unconditioned* model are shown, for each considered structural class. It should be noted that median PGA values mainly increase going from vaults to rigid slabs, except for buildings with vaults and flexible slabs retrofitted before 1980, at DS5. Thus, the constraint on median PGA values in the *Conditioned* model is effective only for such

classes, without affecting the remaining parameters. Clearly, to equal lognormal parameters correspond overlapped fragility curves: in Figure 101 in fact, curves provided by *Unconditioned* and *Conditioned* models are mainly overlapped, except for BQ-V and BQ-F classes retrofitted before 1980 for which very slightly differences are observed. Moreover, as highlighted in the previous Section on non-retrofitted buildings, also the logarithmic standard deviation could change, if corresponding median PGAs change, because of optimization technique. In this case, β value change only for BQ-F class (retrofitted before 1980), going from 0.81 to 0.83.

Conversely comparing lognormal parameters obtained by means of *Unconditioned* and *Conditioned*(β) models, slightly differences are observed for all considered building classes, except BQ-V one retrofitted after 1981. As above mentioned, *Conditioned*(β) model is the most constrained one among the three considered models, because the constraint on the constant β value affects all classes. Clearly, the difference between *Unconditioned* and *Conditioned*(β) curves (see Figure 101) increase, increasing the variation of β value. In the *Unconditioned* model, the logarithmic standard deviation β ranges from 0.74 (BQ-V class retrofitted before 1980) to 1 (BQ-R class retrofitted after 1980), whereas the common β value of the *Conditioned*(β) model is equal to 0.84. Thus, the greater variation (about 19%) of β value is observed for BQ-R class retrofitted after 1980. Conversely, for BQ-V class retrofitted after 1980 (the most populated class among all available ones) no variation in the β value is observed, being equal to 0.84 already in the *Unconditioned* model. So, the corresponding fragility curves provided by the three considered models are exactly the same, resulting overlapped curves (see Figure 101).

7.4.2 Mean error evaluation

Starting from the obtained fragility curves, “expected” DPMs can be derived according to the procedure explained in Figure 79 and then, a comparison with the observed ones can be done. The synthetic parameter used in this Thesis work to compare expected and observed DPMs is the mean error given the DS, according to the Equation 11.

As above explained, such error measure derives from the difference between expected and observed occurrence frequency of a given (i^{th}) DS under a given (j^{th}) seismic intensity measure (i.e., $err_{i,j}$). Thus, the mean error is basically the mean value of all $err_{i,j}$ terms for a given DS (namely, the mean of all $err_{\overline{DS},j}$ terms with j ranging from 1 to the number of available PGA values).

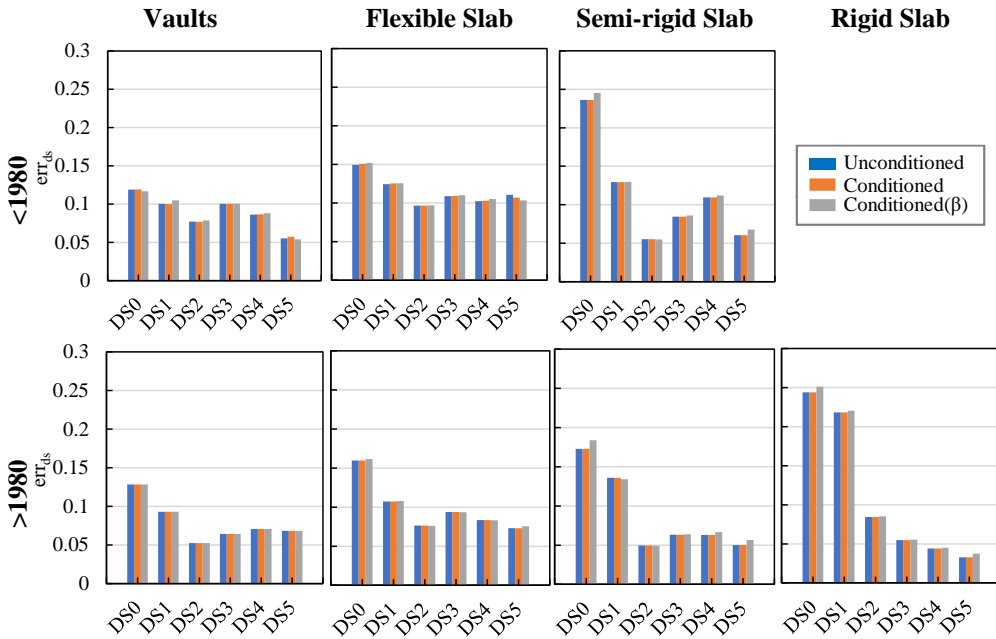


Figure 103. Mean error for retrofitted classes, according to the three considered regression models.

In Figure 103, mean error has been evaluated with reference to the seven retrofitted building classes, according to the three considered regression models. Clearly, the mean error for BQ-V class retrofitted before 1980 is the same, regardless to the used model, because each of them provides the same lognormal parameters (as shown in Table 35-Table 36-Table 37). In other words, no error variation among the three considered models has been observed, because no variation in the output lognormal parameters has been obtained, using the three models. Similarly, variations in the mean error between *Unconditioned* and *Conditioned* models are observed only for those classes for which the median

PGA constraint is effective (namely, for BQ-V and BQ-F classes retrofitted before 1980). Conversely, slightly variations in the error provided by *Unconditioned* and *Conditioned*(β) models are identifiable for each building class, except for the above mentioned BQ-V class retrofitted before 1980. Moreover, the greater the variations of logarithmic standard deviation going from the *Unconditioned* to the *Conditioned*(β) model, the greater the variation of mean error between *Unconditioned* and *Conditioned*(β) models. In fact, in Figure 103, the major differences are observed for classes with semi-rigid and rigid slabs, for which β value goes from 0.96 (BQ-S classes retrofitted before 1980), 0.99 (BQ-S classes retrofitted after 1980) and 1.00 (BQ-R classes retrofitted after 1980) of the *Unconditioned* model to 0.84 for the *Conditioned*(β) one.

It is quite clear that the mean error is mainly due to the adopted fitting procedure (i.e., MLE technique with multinomial likelihood function), rather than to the specific assumptions on lognormal parameters progressively introduced. In practical terms, the difference between DPMs predicted by means of *Unconditioned*, *Conditioned*, or *Conditioned*(β) models is negligible respect to the difference between observed and predicted DPMs. This latter, as shown in Figure 91 for as-built classes, is mainly due to the fact that observed DPMs are quite irregular (especially in the less populated PGA bins), whereas predicted DPMs describe a regular (monotonic) trend, increasing the seismic intensity measure value.

7.4.3 Analysis on effectiveness of retrofit intervention

In the previous paragraph, it has been shown that the error in the predicted DPMs negligibly changes, if *Unconditioned*, *Conditioned*, or *Conditioned*(β) model is used. Thus, in the present paragraph, lognormal parameters (in particular, the median PGA values) obtained using *Conditioned*(β) model are analysed in order to study the influence/effectiveness of retrofit interventions. In Figure 104, median PGA values of each considered (as-built and retrofitted) classes have been shown, varying the period of construction or the period of retrofit.

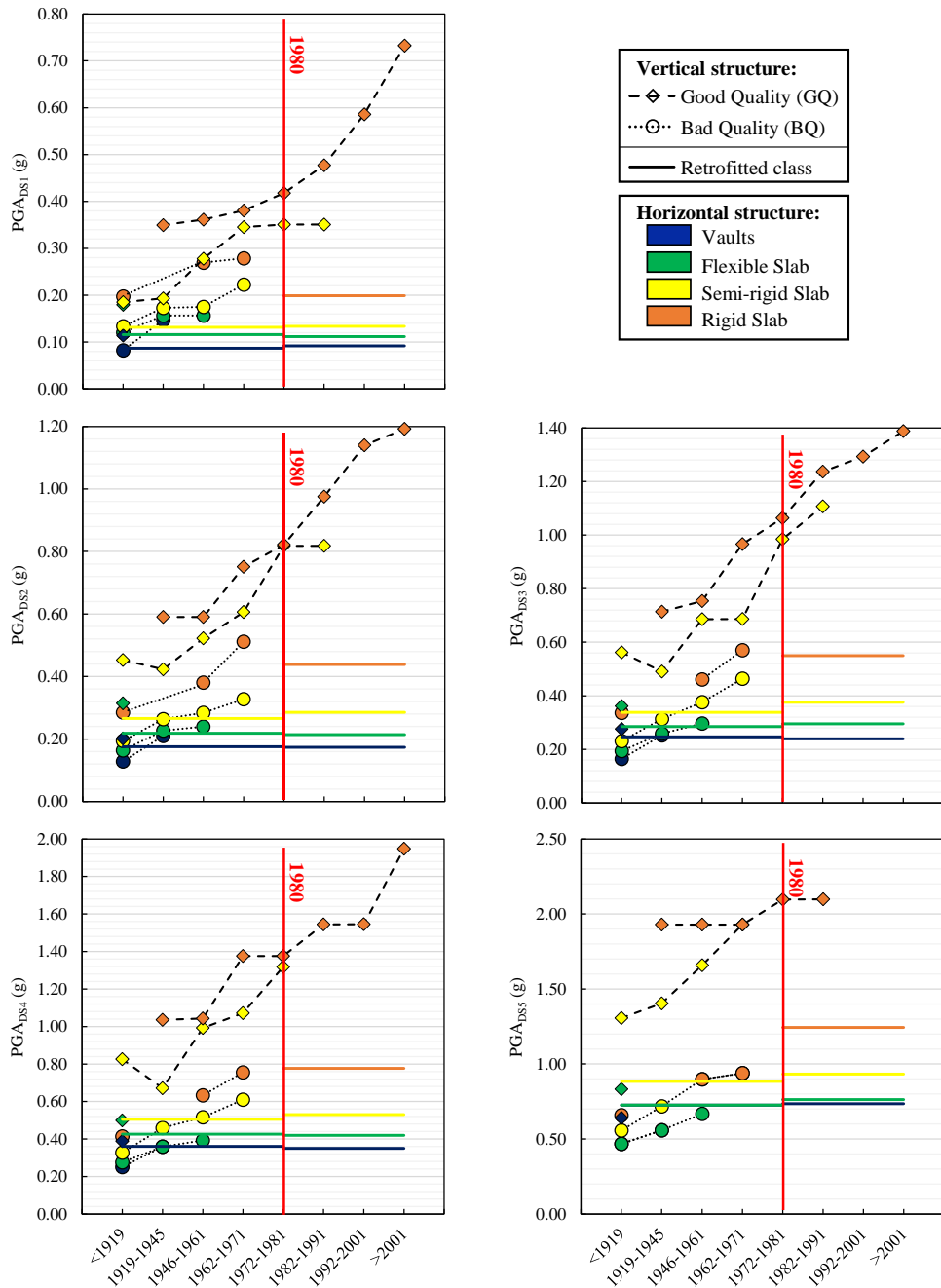


Figure 104. Median PGA values for each as-built and retrofitted classes, according to *Conditioned*(β) model.

In particular, each plot of Figure 104 refers to a given DS, providing (on the y-axis) the median PGAs of all building classes at the same damage state. In each plot, BQ and GQ as-built classes are denoted by different markers (i.e., circle for BQ and rhombus for GQ) and lines (i.e., dotted for BQ and dashed for GQ). Solid lines are used for retrofitted classes (namely, BQ buildings originally built before 1919 and then retrofitted before or after the 1980s). Moreover, each horizontal structural type is marked in a different color. Time intervals on the x-axis are the periods of construction for as-built classes, and the period of retrofit for retrofitted ones. Note that for retrofitted buildings, only two periods of retrofit (<1980 and >1980) have been considered: thus, median PGA values for such classes are represented by piecewise-constant lines, with discontinuity in correspondence of 1980 year.

As above explained, little difference in the mean error is obtained if *Unconditioned*, *Conditioned*, or *Conditioned(β)* model is used. So, in Figure 104 it was decided to compare median values obtained by means *Conditioned(β)* model, given the very little variation of logarithmic standard deviation β among all considered classes. Basically, (1) all as-built classes with the same masonry quality and all retrofitted classes are described by the same β (respectively, 0.73 and 0.84 for as-built BQ and GQ classes and 0.84 for retrofitted ones). So, a comparison between median values can be done with the same β for all classes belonging to as-built BQ, as-built GQ or retrofitted BQ group of classes. Actually, (2) β of retrofitted BQ classes is the same of as-built GQ ones (0.84) and slightly changes respect to the one of as-built BQ classes (0.73).

Some general trends, regardless to the DS, can be derived from Figure 104:

- greater median PGA is observed for GQ classes respect to the BQ ones, given the period of construction and the horizontal structural type, despite no constraint has been imposed between BQ and GQ classes.
- Median PGA of retrofitted classes is less than the one of as-built GQ classes, given the horizontal structural type. It means that structural interventions performed on buildings denoted by bad quality and/or irregular layout (originally constructed before 1919) not are able to ensure

the same seismic performance of a building with good quality (even if quite ancient). Only for BQ-V retrofitted class the median PGA at DS5 overcome that of GQ-V as-built class built before 1919.

- Surprisingly very little difference is observed between buildings retrofitted before or after the 1980, given the structural typology. Based on such results, it seems that no influence on the retrofit interventions has been due to the enactment of code regulations starting from the 1980s. However, it should be noted that the present evaluation has been performed regardless of the kind of structural intervention (unfortunately not available data). Each subset could contain different kinds of interventions, which influence cannot be precisely isolated due to the achieved level of knowledge. Thus, such unexpected result could be due to the presence of several (and different) retrofit techniques or also to a different widespread of a certain retrofit technique over the time.

Moreover, Figure 104 shows that the higher the DS the higher the influence of the retrofit intervention. In practical terms, retrofit interventions performed over the time have been allowed to increase the median PGA especially at higher DSs. In fact, comparing the median PGA values of BQ classes built before 1919 and then retrofitted with those BQ not retrofitted built in the same period, we can note that:

- about the same median PGA at DS1 is shown both by retrofitted and non-retrofitted buildings (with the same horizontal structure), confirming that the aim of such interventions was not avoiding the hair-line cracks in the masonry walls or the fall of small pieces of plaster.
- An increase (ranging from 30 to 60%) of median PGA is observed at DS2-3. The major increase is related to the buildings with the most rigid horizontal structures (i.e., BQ-S and BQ-R). Such increase could be due to interventions such as the securing of chimneys, roof tiles or non-structural components (partitions or gable walls).

- A significant increase (ranging from 40 to 90%) of median PGA is observed at DS4-5. Again, the major increase is related to the buildings with the most rigid horizontal structures (especially BQ-R ones). Such increase could be due to interventions on anchorage details, which make the difference between a more effective intervention or not (Indirli et al. 2013; Rossetto et al., 2011; Azzaro et al., 2011), avoiding the overturning of masonry walls.

7.5 REFERENCES

- [1] Amiri G.G., Jalalian M., Amrei S.A.R. (2007). Derivation of vulnerability functions based on observational data for Iran. *Proceedings of International Symposium on Innovation & Sustainability of Structures in Civil Engineering*.
- [2] Ang A.H., & TANG W. H. (2007). *Probability concepts in engineering*. Wiley. (ISBN: 978-0-471-72064-5)
- [3] Azzaro R., Barbano M. S., D'Amico S., Tuvè T., Scarfi L., Mostaccio A., 2011. The L'Aquila 2009 earthquake: an application of the European Macroseismic Scale to the damage survey in the epicentral area. *Bollettino di Geofisica Teorica ed Applicata*, 52(3), 561-581.
- [4] Baggio, C., Bernardini, A., Colozza, R., Corazza, L., Della Bella, M., Di Pasquale, G., Papa, F., 2007. Field manual for post-earthquake damage and safety assessment and short term countermeasures (AeDES). European Commission—Joint Research Centre—Institute for the Protection and Security of the Citizen, EUR, 22868.
- [5] Charvet I, Ioannou I, Rossetto T, Suppasri A, Imamura F (2014) Empirical fragility assessment of buildings affected by the 2011 Great East Japan tsunami using improved statistical models. *Nat Hazards* 73:951–973.
- [6] Coburn, A., & Spence, R. (2003). *Earthquake protection*. John Wiley & Sons.
- [7] D'Amato M, Laguardia R, Di Trocchio G, Coltellacci M, Gigliotti R. Seismic Risk Assessment for Masonry Buildings Typologies from L'Aquila 2009 Earthquake Damage Data. *Journal of Earthquake Engineering* 2020; 00(00): 1-35. DOI: 0.1080/13632469.2020.1835750.

- [8] Decreto Ministeriale 2 Luglio 1981. Normativa per le riparazioni ed il rafforzamento degli edifici danneggiati dal sisma nelle regioni Basilicata, Campania e Puglia. **(in Italian)**
- [9] Decreto Ministeriale 24 Gennaio 1986. Norme tecniche relative alle costruzioni antisismiche. **(in Italian)**
- [10] Del Gaudio C., De Martino G., Di Ludovico M., Manfredi G., Prota A., Ricci P. and Verderame G.M.; 2017: Empirical fragility curves from damage data on RC buildings after the 2009 L'Aquila earthquake. *Bull. Earthquake Eng.*, 15, 1425-1450.
- [11] Del Gaudio C., De Martino G., Di Ludovico M., Manfredi G., Prota A., Ricci P., Verderame G.M., 2019. Empirical fragility curves for masonry buildings after the 2009 L'Aquila, Italy, earthquake. *Bulletin of Earthquake Engineering*. <https://doi.org/10.1007/s10518-019-00683-4>.
- [12] Del Gaudio, C., Di Ludovico, M., Polese, M. et al. Seismic fragility for Italian RC buildings based on damage data of the last 50 years. *Bull Earthquake Eng* 18, 2023–2059 (2020). <https://doi.org/10.1007/s10518-019-00762-6>
- [13] Del Gaudio, C., Scala, S.A., Ricci, P., Verderame G.M., 2021. Evolution of the seismic vulnerability of masonry buildings based on the damage data from L'Aquila 2009 event. *Bull Earthquake Eng* (2021). <https://doi.org/10.1007/s10518-021-01132-x>
- [14] Federal Emergency Management Agency (FEMA) (2012) Hazus-MH 2.1 technical manual: earthquake model
- [15] Grünthal M., 1998. European Macro-seismic Scale. *Cahiers du Centre Européen de Géodynamique et de Séismologie*, Vol. 15. European Macro-seismic Scale 1998. European Center for Geodynamics and Seismology. (in French)
- [16] Indirli M., S. Kouris L.A., Formisano A., Borg R.P., Mazzolani F.M., 2013. Seismic damage assessment of unreinforced masonry structures after the Abruzzo 2009 earthquake: The case study of the historical centers of L'Aquila and Castelvechio Subequo. *International Journal of Architectural Heritage*, 7(5), 536-578.
- [17] Ioannou, I., Rossetto, T., & Grant, D. N. (2012, September). Use of regression analysis for the construction of empirical fragility curves. In *Proceedings of the 15th world conference on earthquake engineering*, September.

- [18] Karababa, F.S., Pomonis, A., 2011. Damage data analysis and vulnerability estimation following the August 14, 2003 Lefkada Island, Greece, Earthquake. *Bull Earthquake Eng* 9, 1015–1046. <https://doi.org/10.1007/s10518-010-9231-5>
- [19] Kircher, Charles A., Robert V. Whitman, and William T. Holmes. "HAZUS earthquake loss estimation methods." *Natural Hazards Review* 7.2 (2006): 45-59.
- [20] Lallemand, D., Kiremidjian, A., & Burton, H. (2015). Statistical procedures for developing earthquake damage fragility curves. *Earthquake Engineering & Structural Dynamics*, 44(9), 1373-1389.
- [21] Porter K (2018) A beginner's guide to fragility, vulnerability, and risk. University of Colorado Boulder. <http://spot.colorado.edu/~porterka/Porter-beginnersguide.pdf>
- [22] Rossetto T., Ioannou I., Grant D.N., 2013. Existing empirical fragility and vulnerability functions: Compendium and guide for selection, GEM Technical Report 2013-X, GEM Foundation, Pavia, Italy.
- [23] Rossetto T., Peiris N., Alarcon J.E. et al., 2011. Field observations from the Aquila, Italy earthquake of April 6, 2009. *Bull Earthquake Eng* 9, 11–37 (2011). <https://doi.org/10.1007/s10518-010-9221-7>.
- [24] Rossetto, T. and Elnashai, A. (2003) Derivation of Vulnerability Functions for European-Type RC Structures Based on Observational Data. *Engineering Structures*, 25, 1241-1263. [http://dx.doi.org/10.1016/S0141-0296\(03\)00060-9](http://dx.doi.org/10.1016/S0141-0296(03)00060-9)
- [25] Rosti A., Del Gaudio C., Di Ludovico M., Magenes G., Penna A., Polese M., Verderame G.M., 2020a. Empirical vulnerability curves for Italian residential buildings. *Bollettino di Geofisica Teorica ed Applicata*, 61(3).
- [26] Rosti A., Del Gaudio C., Rota M., Ricci P., Di Ludovico M., Penna A., Verderame G.M., 2020b. Empirical fragility curves for Italian residential RC buildings. *Bull Earthquake Eng* (2020). <https://doi.org/10.1007/s10518-020-00971-4>.
- [27] Rosti A., Rota M., Penna A., 2020c. Empirical fragility curves for Italian URM buildings. *Bulletin of Earthquake Engineering*.
- [28] Rota M., Penna A., Strobbia C.L., 2008. Processing italian damage data to derive typological fragility curves. *Soil Dynamics and Earthquake Engineering*, 933-947.
- [29] Sabetta F., Goretti A., Lucantoni A., 1998. Empirical Fragility Curves from Damage Surveys and Estimated. 11th European Conference on Earthquake Engineering © 1998 Balkema, Rotterdam, ISBN 90 5410 982 3.

- [30] Scala S.A., Del Gaudio C., Verderame G.M., 2022. Influence of construction age on seismic vulnerability of masonry buildings damaged after 2009 L'Aquila Earthquake (**under review**)
- [31] Zuccaro G, Perelli FL, De Gregorio D, Cacace F (2020) Empirical vulnerability curves for Italian masonry buildings: evolution of vulnerability model from the DPM to curves as a function of acceleration. Bull Earthq Eng. [https:// doi. org/ 10. 1007/ s10518- 020- 00954-5](https://doi.org/10.1007/s10518-020-00954-5)

CONCLUSIONS

In this study, the evolution of seismic vulnerability has been investigated using the post-earthquake data related to masonry buildings, collected after 2009 L'Aquila seismic event. To foster such analysis, first an in-dept study of the Italian seismic classification, following the occurrence of the strongest earthquakes and analysing the evolution of normative contents, has been done (Chapter 3).

Over the last century, several strong earthquakes hit the Italian territory, highlighting the inadequacy of the current seismic classification and the enacted normative prescriptions. In fact, the main changes in the seismic classification (and in the normative contents) have been done after the major seismic events of the last century, going from the 1908 Messina earthquake (Royal Decree, R.D. n.193 of 18 April 1909) to the 2002 Molise earthquake (Ordinance of the President of the Council of Ministers, OPCM n. 3274 of 20 March 2003). Thus, a timeline of the major Italian earthquakes of the last century is firstly provided. Then, the seismic classification of the entire national territory adopted after these events is described, detecting the most relevant normative contents about the definition of seismic loads, structural details and retrofit interventions on masonry buildings.

However, the earthquake's occurrence was not only the base on which the seismic classification has been updated over the years, allowing to detect seismic-prone areas. In fact, the analysis of post-earthquake damage allowed to

identify those structural-geometric details able to affect the seismic behaviour negatively or positively. For example, it was understood that the seismic behaviour of masonry buildings is best when those are equipped with tie rods and/or tie beams, improving the so-called box behaviour. Conversely, the presence of pushing structures (such as vault without suitable chains) has been recognized as a vulnerability factor, able to negatively affect the whole building's behaviour under seismic loads.

Therefore, the analysis of post-earthquake damage (Chapter 4) is a valuable source of information about the building's behaviour under seismic loads. With this in mind, the Italian DPC (*Dipartimento della Protezione Civile*, Department of Civil Protection), with the support of Eucentre Foundation (European Centre for Training and Research in Earthquake Engineering), provided an online platform, called Da.D.O. (*Database del Danno Osservato*, Database of Observed Damage) (Dolce et al., 2019), which allows the access to a large database of buildings, collected during the visual inspections done right after the main earthquakes occurred in Italy in the last 50 years. Such large amount of data is particularly useful in the vulnerability and/or fragility studies of the existing building stock, allowing to detect, for example, a relation between the damage attitude and the building's features. The analysis of this data could be a support to identify the most vulnerable building's typologies, directing possible policies of seismic risk mitigation.

Obviously, the data resulting from different seismic events (namely, adopting different survey forms developed over the years) are not immediately comparable with each other. Moreover, the survey campaign could be conducted following different criteria, reaching different degree of completeness, especially between the areas farthest and nearest to the epicenter. All these issues (together with other ones, such as the adopted building's taxonomy or the sample size) could affect the data's use or introduce bias in the vulnerability/fragility assessment, if not properly addressed.

Building taxonomy has been selected inspired by a fair compromise between the need to consider all the parameters available from the in-situ survey campaign and the obtainment of reliable and homogeneous sample. Among all the

parameters a selection based on only 5 parameters has been adopted, namely the structural typology, the quality layout of masonry, the presence/absence of retrofit interventions, the construction age (and seismic classification) and on the horizontal structural type.

A time-consuming data processing (Chapter 5) was performed to avoid damage overestimation due to the un-representativeness of sample sited far away from the epicenter, where partial survey was done, at the risk of systematically neglecting major part or even the totality of un-damaged buildings. To this aim, only the municipalities completely inspected were used to account for the positive evidence of damage. Then municipalities slightly or completely not inspected were added to the former, assumed as completely un-damaged, to account for negative evidence of damage. Both of them, *damaged* and *undamaged* database, were combined together for vulnerability and fragility analysis performed in this study. Data characterization of *damaged* database was fulfilled taking advantage of the Da.D.O. platform, whereas *undamaged* database typified based on census data (ISTAT 2011), laboriously manipulated taking advantage of statistical analysis on the *damaged* database for all available parameters.

Damage analysis of Chapter 6 was done considering 5+1 damage grades (related to the whole building) based on the conversion of damage observed on vertical structures in sight of the classification of European Macroseismic Scale. Vulnerability curves were derived assuming a lognormal statistical model and peak ground acceleration as intensity measure, through a minimization procedure (i.e., *LSE technique*) of the distance between predicted and observed mean damage.

These results have been exploited to analyse the influence of main vulnerability factors, i.e. quality and layout of vertical structures, type of horizontal structures, construction age, some of which already been analysed in previous studies, with a systemic and organic approach applied to an unprecedented amount of post-earthquake data offered by the Da.D.O. online platform.

The findings of this study lead to the following conclusions about masonry buildings not subjected to structural retrofit interventions:

- the masonry quality/layout confirmed its strong impact on vulnerability. In fact, buildings with good quality masonry layout (for example those constituted by natural and/or artificial bricks), have a systematically smaller vulnerability if compared to bad quality buildings (for example those constituted by pebbles or rubble stones). The rationale of these results can be explained by the significant vulnerability of BQ buildings with respect to both out-of-plane, with possible disaggregation of the wall, and in-plane actions, due to the low resistance of materials and of friction strength due to the irregular layout of stones. Conversely, buildings GQ buildings show a strong resistance to both the in-plane and the out-of-plane actions.
- A key role is also played by the slab stiffness given the vertical structures. Firstly, the results have shown a very similar vulnerability among buildings equipped with vaults and flexible slabs and between buildings equipped with semi-rigid and rigid slabs. Furthermore, it was observed that for buildings with flat horizontal structures the smaller the slab flexibility the greater vulnerability, decreasing the capability of guaranteeing a proper connection between masonry walls parallel and orthogonal to seismic actions, greatly emphasizing the criticalities due to the masonry quality/layouts also. In fact, the more flexible slabs, for example wooden floors with a simple wood plank or brick elements, unlike the more rigid slabs, for example those made of concrete joists and hollow clay bricks with an upper reinforced concrete slab, have not a sufficient rigidity to transfer the out-of-plane actions to all the walls, thus not allowing a rigid floor redistribution of seismic forces.
- Lastly, a decreasing trend in vulnerability was also observed increasing the construction age, which effects have been very few analysed in the recent literature. This trend clearly depicts the evolution of damage through the years for masonry building struck by 2009 L'Aquila earthquake and can be basically ascribed to the improvements in the building construction and to the enhancement in the quality of materials, together with the continuous enactment of increasingly stringent code prescriptions.

The main conclusions regarding the effectiveness of retrofit interventions that could be drawn from the comparison between mean damage values and vulnerability curves are as follows:

- It was higher with higher slab stiffness, probably because such effectiveness is more evident when a box-like behaviour is ensured (rigid slabs) and is limited when a partial or global overturning due to the absence of effective horizontal elements or devices have a greater probability of occurrence (flexible slabs).
- It showed a reduced trend as a function of period of retrofit, probably due to the improvement in construction practice and to the increasing attention to anchorage details.

The outcomes shown in Chapter 6 represented a concrete beginning for further investigations on fragility analysis of masonry buildings, exploiting the sturdy analysis on impact of different vulnerability factors herein investigated, i.e. taking into consideration in the definition of taxonomy the effect of parameter whose effects are often not considered, such the construction age. Then, fragility curves were derived assuming a lognormal statistical model, through two regression procedures: lognormal parameters are obtained, in the first case (*LSE technique*) minimizing the distance between the observed and the expected cumulative damage distributions. In the second case (*MLE technique*), the same parameters are derived, maximizing a multinomial likelihood function. Thus, fragility curves have been derived according to the two approaches, quantifying the difference between the corresponding predicted DPMs and the observed ones by means of the error $err_{i,j}$ for a given (j^{th}) PGA value and a given (i^{th}) DS. Once deafened that there are no big differences in the obtained error if LSE or MLE approach is used, in the following elaboration only MLE approach has been used. In fact, such approach in one hand (1) provides on average the same error of LSE model; in the other hand (2) in the assumption of multinomial likelihood function allows to derive fragility curves also starting from very small sample. In fact, such approach is able to consider simultaneously all DSs when the optimization is performed, searching for the better values of median and logarithmic standard

deviation. It means that also if the number of buildings exhibiting a certain DS is very low, the regression model is able to provide the corresponding curve, based on the assumption of multinomial distribution of the likelihood function.

Starting from such fitting approach (so-called “*unconditioned*” model), further two regression models have been considered, first constraining the median PGA values (“*conditioned*” model) and then, also the logarithmic standard deviation (“*conditioned*(β)” model).

Basically, the constraint of median PGA values allows to derive the optimum solution of the fitting procedure that also complies the trends derived in terms of mean damage and vulnerability curves. In particular, the constraints have been applied on the median parameters, ensuring the same hierarchy in terms of structural typology and construction age derived by means of vulnerability curves. Then, a third approach (so-called *Conditioned*(β) model) is introduced to overcome the presence of crossing curves. Basically, starting from the *Conditioned* model, a further constraint is introduced in the fitting procedure, assuming a constant logarithmic standard deviation for all classes with the same masonry quality.

Lastly, in order to quantify the difference between the three considered (*unconditioned*, *conditioned*, *conditioned*(β)) models and then the influence of each assumption (i.e., constraint on median PGA and constant β value), again the comparison between the corresponding DPMs have been done, using the mean error. It should be noted that:

- variations in the mean error between *Unconditioned* and *Conditioned* models are observed only for those classes for which the median PGA constraint is effective. Conversely, slightly variations in the error provided by *Unconditioned* and *Conditioned*(β) models are identifiable for each building class, being the β constraint effective for all considered building's classes.
- Moreover, the greater the variations of logarithmic standard deviation going from the *Unconditioned* to the *Conditioned*(β) model, the greater the variation of mean error between *Unconditioned* and *Conditioned*(β) models.

- However, mean error is mainly due to the adopted fitting procedure (i.e., MLE technique with multinomial likelihood function), rather than to the specific assumptions on lognormal parameters progressively introduced.
- In practical terms, the difference between DPMs predicted by means of *Unconditioned*, *Conditioned*, or *Conditioned*(β) models is negligible respect to the difference between observed and predicted DPMs. This latter is mainly because observed DPMs are quite irregular (especially in the less populated PGA bins), whereas predicted DPMs describe a regular (monotonic) trend, increasing the seismic intensity measure value.

The findings disclosed in Chapter 6 and Chapter 7 can certainly foster forthcoming approaches dealing with fragility analysis in heuristic approaches. In fact, starting from vulnerability curves, fragility curves could be obtained with the assumption of a continuous damage distribution (for example binomial or beta), using fragility curves herein proposed as reference in the validation phase.

Moreover, the entire vulnerability and fragility assessment herein conducted based on damage data collected after the L'Aquila 2009 earthquake could also be extended to other post-earthquake databases to characterize the seismic vulnerability of masonry buildings in areas with different seismic history and/or different evolution of seismic normative contents. In this view, post-earthquake data collected after the devastating Irpinia 1980 earthquake or the dramatic Molise 2002 event (also available on the Da.D.O. platform), could be used to characterize the seismic behaviour of masonry buildings sited in municipalities seismically classified in more recent periods. Clearly, the adoption of a different database leads to the necessity to address further issues: for example, after Irpinia 1980 earthquake the field campaign was performed with a different survey form (respect to the AeDES one), providing a different building's description (for example, information about the presence/absence of retrofit interventions is not available). Conversely, after 2002 Molise seismic event, building-by-building survey was performed only in few municipalities, resulting in a quite small database (especially if compared with the L'Aquila 2009 one).

Moreover, further investigations could be about retrofitted buildings. In fact, as above highlighted, the survey form allows gaining information on the period when structural interventions are executed, beyond the original period of construction. Thus, the survey form for buildings subjected to structural interventions contains a double filled field regarding period, the oldest referring to its construction and the most recent referring to its retrofit. Obviously, this information is typically obtained by inspectors through a direct interview reliably granted by the owner. Additionally, the information on type of interventions, among injections or unreinforced coating, reinforced masonry or masonry with reinforced coating, other or unidentified strengthening, is also reported in the survey form. Nonetheless, in almost all cases (about 98%) this information was not filled by surveyor after L'Aquila 2009 earthquake. Probably the rapidity required by emergency condition together with the way the inspections were conducted (only visual) did not allow the surveyors to precisely determine the kind of structural intervention, although they were aware that there had been. The lack of such information did not allow to precisely characterize the seismic vulnerability and/or fragility of these classes, since each subset could contain different kinds of interventions. Nevertheless, such issue could be at least partially overcome using further data sources (such as interviews to local engineers or town council technicians).

Further studies could be about the influence of the adopted statistical treatment of observed data. In fact, as explained in the Section 5, data completeness has been guaranteed using the so-called *mixed* approach. Thus, the considered study database is composed by (1) *damaged* buildings sited in municipalities with completeness ratio equal or greater than 91%, and (2) *undamaged* buildings sited in municipalities with completeness less than 10%. In doing so, municipalities with ratio between 10% and 91% are excluded, discarding an important number of buildings. Thus, the proposed approach could be further investigated in the future, considering the comparison with other methodologies available in the literature to understand how it impacts the resulting shape of fragility curves. For example, the number of buildings herein

discarded could be increased to the number of Census data, assuming all undetected structures as undamaged.

As highlighted in the Section 7.3.6, an important issue in the proposed methodology is the choice of damage metric (i.e., the conversion rule to go from damage provided by the survey form for a given structural element to the building damage consistent with EMS-98 scale). This aspect is relevant and could significantly influence the shape of the following fragility curves, and it deserves to be further investigated in the future. Beyond the damage conversion rules proposed by Rota et al., 2008 and Dolce et al., 2019, other proposals available in the literature could be examined, exploring their effect on fragility curves shape.

Lastly, the outcomes of the present study could be used for the validation of mechanical-analytical methods. In these latter, differently from empirical methods, the relationship between seismic intensity and expected damage is provided by a model with direct physical meaning. The use of an algorithm to evaluate the structural vulnerability allows to take into account directly and transparently, in a detailed way, the various characteristics of the considered building class. In the other hand, such kind of procedure needs of a higher computational effort, compared with empirical methods.

In general, methods for the assessment of seismic vulnerability of a given building class should represent the best compromise between reliability and reasonable demand of computational effort. In this view, simplified analytical models could represent a very satisfying solution, being simultaneously based on simplified mechanical assumptions, and calibrated on the observed data.

In particular, mechanical procedures with different degree of simplification are largely used in the literature. Among those, the POST (i.e., *PushOver on Shear-Type*, Del Gaudio et al., 2017) methodology, originally conceived for R.C. buildings, could be re-calibrated based on the empirical results herein discussed, allowing the fragility assessment also for masonry buildings.

REFERENCES

- [1] Del Gaudio, C., Ricci, P., Verderame, G. M., & Manfredi, G. (2017). Urban-scale seismic fragility assessment of RC buildings subjected to L'Aquila earthquake. *Soil Dynamics and Earthquake Engineering*, 96, 49-63.
- [2] Dolce, M., Speranza, E., Giordano, F., Borzi, B., Bocchi, F., Conte, C., ... & Pascale, V. (2019). Observed damage database of past Italian earthquakes: the Da. DO WebGIS. *Bollettino di Geofisica Teorica ed Applicata*, 60(2).
- [3] Rota, M., Penna, A., & Strobbia, C. L. (2008). Processing Italian damage data to derive typological fragility curves. *Soil Dynamics and Earthquake Engineering*, 28(10-11), 933-947.

AUTHOR'S PUBLICATIONS

1. Del Gaudio, C., Scala, S. A., Ricci, P., & Verderame, G. M. (2019). “*The influence of retrofit intervention on vulnerability of masonry buildings from post-earthquake damage data of the last 50 years*”, 415-427. In Atti del XVIII Convegno ANIDIS L'ingegneria Sismica in Italia: Ascoli Piceno, 15-19 settembre 2019.
2. Scala, S., Del Gaudio, C., Ricci, P., Verderame, G.M., and Prota A. (2020). “*The effect of retrofit intervention on empirical vulnerability curves of Italian masonry buildings,*” in 17th World Conference on Earthquake Engineering (Sendai).
3. Scala, S., Ricci, P., Del Gaudio, C., Gómez-Martínez, F., and Verderame, G.M. (2020). “*Simplified Analytical Methodologies for Seismic Fragility Assessment of RC Buildings with Infills,*” in 17th World Conference on Earthquake Engineering (Sendai).
4. Del Gaudio, C., De Risi, M. T., Scala, S. A., & Verderame, G. M. (2020). “*Seismic Loss Estimation in Pre-1970 Residential RC Buildings: The Role of Infills and Services in Low–Mid-Rise Case Studies*”. *Frontiers in Built Environment*, 188.
5. Del Gaudio, C., Scala, S. A., Ricci, P., & Verderame, G. M. (2021). “*Evolution of the seismic vulnerability of masonry buildings based on the damage data from L'Aquila 2009 event*”. *Bulletin of Earthquake Engineering*, 19(11), 4435-4470.

6. De Risi, M. T., Scala, S. A., Del Gaudio, C., & Verderame, G. M. (2021). *“Seismic performance assessment of as-built and retrofitted R.C. buildings considering the influence of infills: pre- ‘70 low-mid rise case-studies”*, in 8th International Conference on Computational Methods in Structural Dynamics and Earthquake Engineering (Athens, 28 - 30 June 2021).
7. Scala S.A., Del Gaudio C., Verderame G.M. (2022). *“Influence of construction age on seismic vulnerability of masonry buildings damaged after 2009 L’Aquila Earthquake”* (**under review**).

APPENDIX A

Fragility curves of Chapter 7 have been derived, according to three different models, each of them based on different assumptions:

- *Unconditioned* model: MLE regression model has been used, assuming a multinomial likelihood function and a cumulative lognormal functional form described by six parameters (namely, the median values θ_{DSi} and a common logarithmic standard deviation β for all DSs).
- *Conditioned* model: starting from the assumptions of *Unconditioned* model, a constrain on median PGA values has been imposed, ensuring the same hierarchy between building's classes obtained by means of damage/vulnerability assessment.
- *Conditioned(β)* model: starting from the assumptions of *Conditioned* model, a further constrain has been introduced, imposing a common logarithmic standard deviation for all building classes. The aim of such assumption is to avoid the possible presence of crossing curves among considered building classes.

In order to quantify the difference between the three considered (*unconditioned*, *conditioned*, *conditioned(β)*) regression models and then the influence of each assumption (i.e., constraint on median PGA and constant β value), the error between observed and predicted DPMs are evaluated for each

building's class, given the i^{th} DS and the j^{th} PGA value, according to following equation:

$$err_{i,j} = \frac{|E_{i,j} - O_{i,j}|}{\sum_{i=1}^{N_{DS}} O_{i,j}} = \frac{\left| \left(\logncdf(PGA_j, \mu_{DS_i}, \beta_{DS_i}) - \logncdf(PGA_j, \mu_{DS_{i+1}}, \beta_{DS_{i+1}}) \right) \cdot N_{PGA_j}^{OBS} - N_{DS_i, PGA_j}^{OBS} \right|}{N_{PGA_j}^{OBS}}$$

$err_{i,j}$ is the difference in absolute terms between predicted ($E_{i,j}$) and observed ($O_{i,j}$) numbers of buildings subjected to j^{th} PGA value and belonging to DS_i , divided by the observed number of buildings subjected to the same PGA value ($N_{PGA_j}^{OBS}$). Basically, such error is the difference between the expected and the observed ($N_{DS_i, PGA_j}^{OBS} / N_{PGA_j}^{OBS}$) occurrence frequency of each DS.

In the following, the mean value of $err_{i,j}$ (namely, the mean of all $err_{\overline{DS},j}$ terms with j ranging from 1 to the number of available PGA values) given the DS is provided, for the considered as-built class, using different colors for the three regression models (i.e., blue for *unconditioned* model, orange for *conditioned one*, grey for *conditioned(β)* model).

In particular, Figure 105 and Figure 106 are related to BQ as-built classes, whereas Figure 107 and Figure 108 to GQ as-built ones. In the figures, each row provides the error related to a different DS; whereas each column refers to a different horizontal structures (i.e., vaults, flexible-, semi-rigid- and rigid-slabs). Moreover, the period of construction is reported on x-axis.

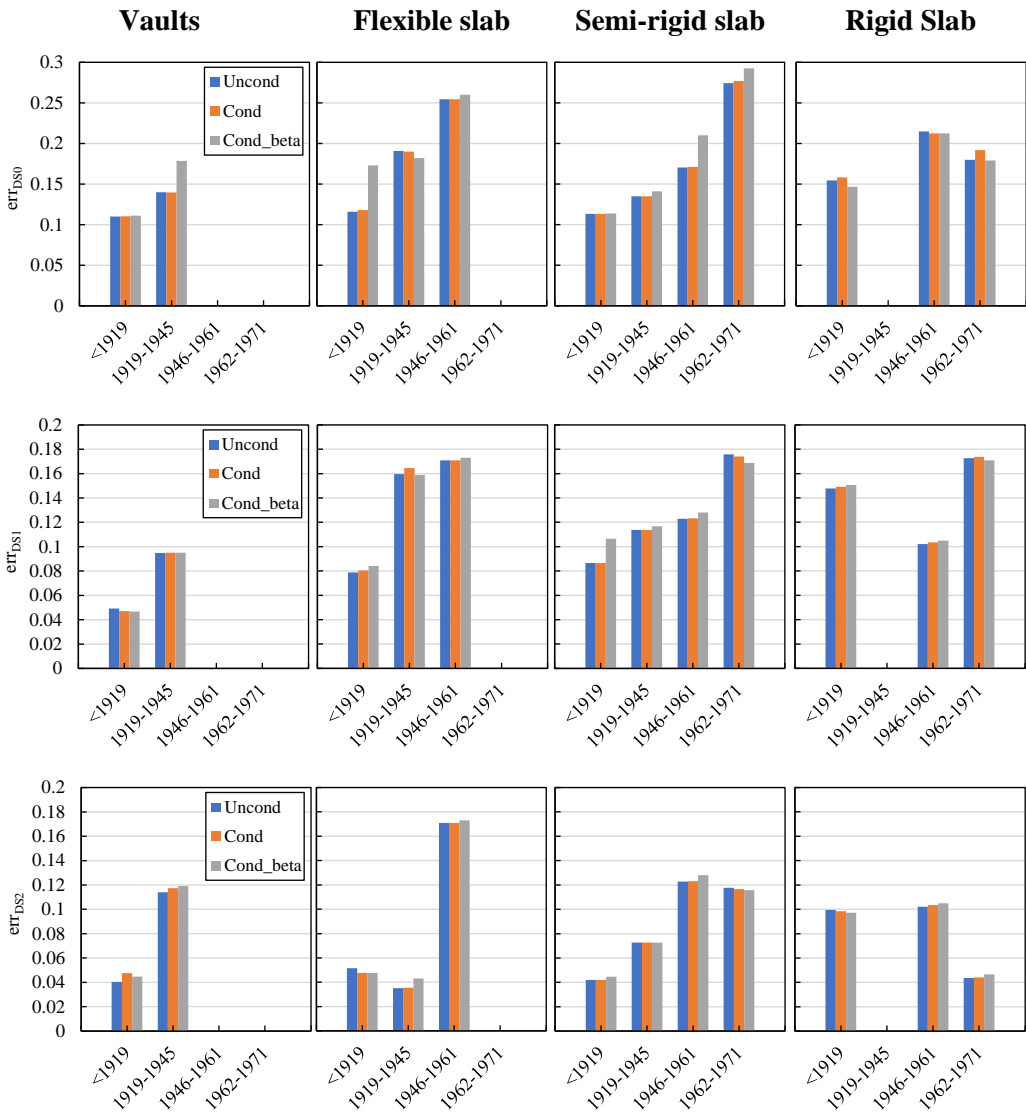


Figure 105. Mean error given the DS (going to DS0 to DS2) for BQ as-built classes varying the period of construction.

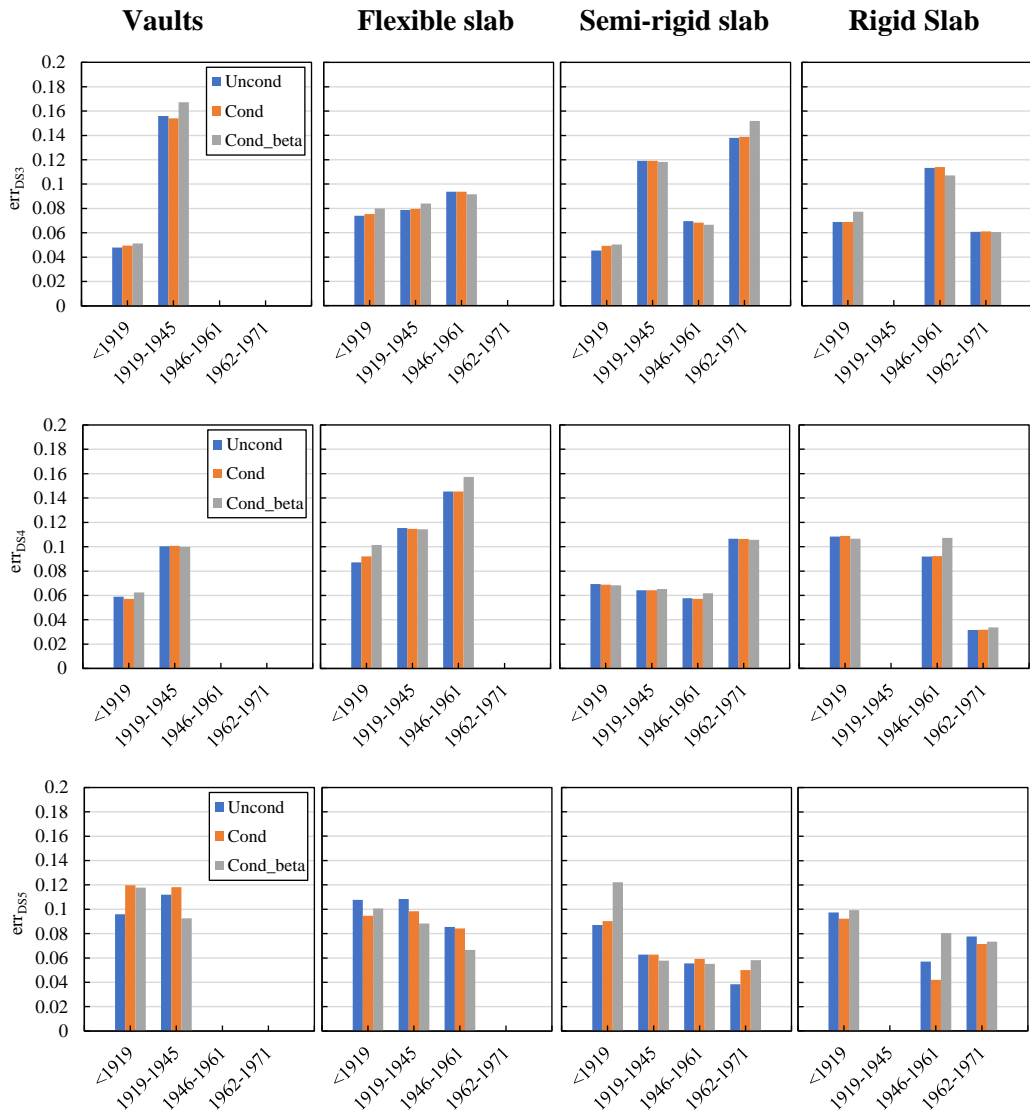


Figure 106. Mean error given the DS (going to DS3 to DS5) for BQ as-built classes varying the period of construction.

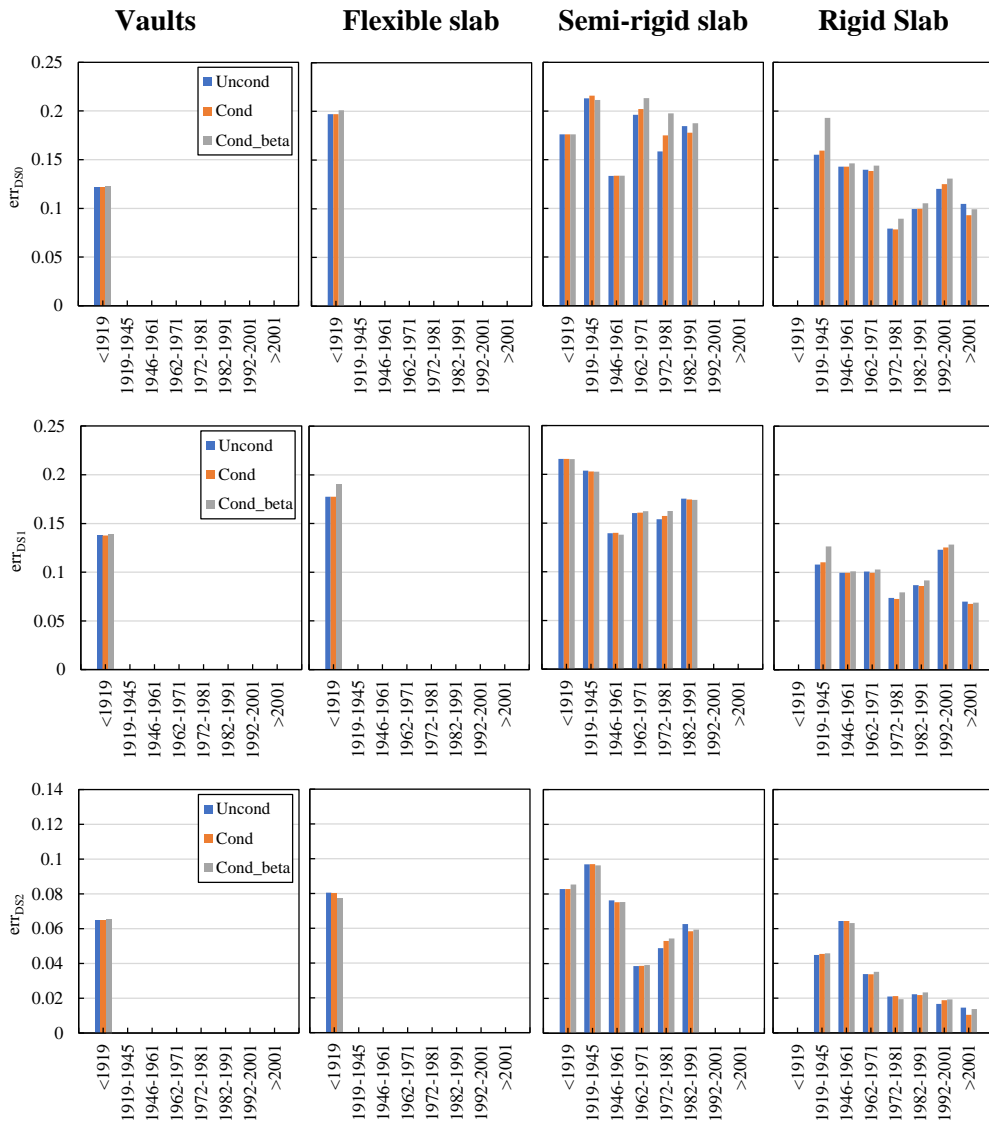


Figure 107. Mean error given the DS (going to DS0 to DS2) for GQ as-built classes varying the period of construction.

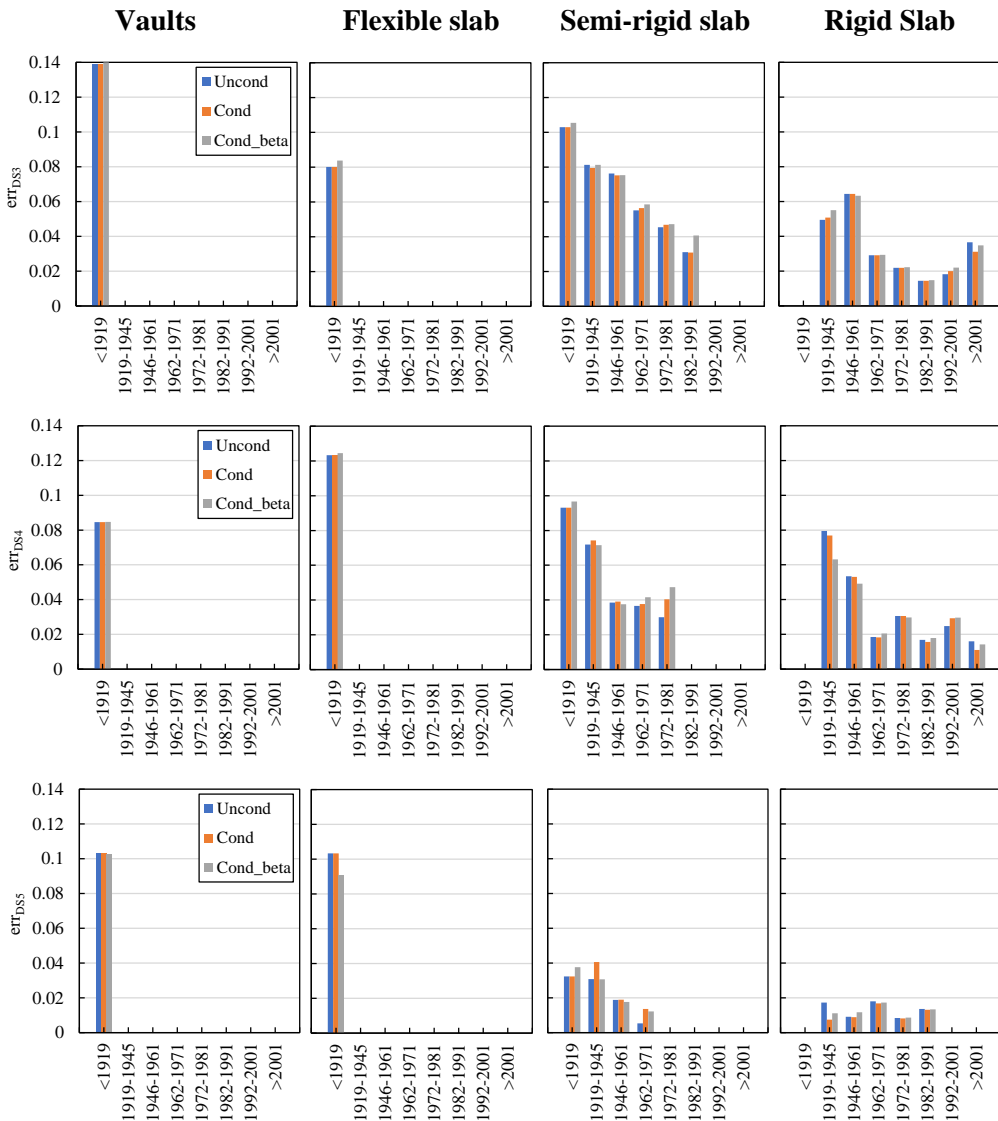


Figure 108. Mean error given the DS (going to DS3 to DS5) for GQ as-built classes varying the period of construction.

